DETERMINING THE CAPABILITY OF A VEGETATION COVER TO LIMIT EFFLUENT LEACHING FROM A WASTE IMPOUNDMENT

Gary Duwayne Morgan

Submitted in partial fulfilment of the requirements for the degree of
MSc in Hydrology

School of Bioresources Engineering and Environmental Hydrology
University of KwaZulu-Natal
Pietermaritzburg
South Africa

June 2009

ABSTRACT

A final cover on a waste impoundment is the main physical barrier between the waste impoundment and the environment designed to protect against physical, chemical and biological factors isolating the waste from the atmospheric environment. Since the early 1990's regulators in the United States have started accepting vegetation covers in lieu of the prescriptive covers. Currently in South Africa, data that provide field performance comparisons of alternative vegetation covers are few or non-existent; hence a research program was undertaken by an industrial corporation in South Africa to determine the potential use of vegetation covers. In proposing a practical way forward, the Company (AECI Limited) reached an understanding with the Regulators that a vegetated evapotranspiration (ET) cover, would be acceptable provided that its performance in limiting surface water infiltration (and subsequent leaching) could be quantitatively demonstrated.

The overall object of this research was to determine the capability of vegetation cover to limit effluent leaching from a waste impoundment. Analysis of the following sub-objectives were required to address and give answers to this study (1) determine, as accurately as possible a climatic water balance on the vegetation covers, (2) determine the geohydrological properties of the material of the waste impoundment, (3) determine the fate of the water i.e. proportion reused via evapotranspiration as opposed to the proportion infiltrating the waste body beneath the root zone and (4) determine the leaching potential below the waste.

The study identifies and evaluates the climatic (above ground) and geohydrological (sub-surface) parameters used to estimate the water balance of the materials for a waste impoundment. The study then utilizes these parameters at the respective sites in a finite-element model, called the HYDRUS-2D model, to simulate the water balance of the material. The simulated water balance results were then compared against collected field data, which provide the evidence of the efficiency of a vegetation cover to limit effluent from the impoundment.

PREFACE

The work described in this dissertation was carried out in the School of Bioresources Engineering and Environmental Hydrology, University of KwaZulu-Natal, Pietermaritzburg, from March 2003 to August 2006, under the supervision of Professor S. A. Lorentz.

These studies represent original work by the author and have not otherwise been submitted in any form for any degree or diploma to any university. Where use has been made of the work of others it is duly acknowledged in the text.

Signed: …… Date: ……
G.D. Morgan (author)

Signed: …… Date: ……
S. A. Lorentz (supervisor)

ACKNOWLEDGEMENTS

I would like to express my sincere appreciation and gratitude to my supervisor, Professor S.A. Lorentz, for providing invaluable assistance and vast knowledge throughout the duration of this study. Special thanks goes to members of the School of Bioresources Engineering and Environmental Hydrology, Mr. C.J. Pretorious for assistance and patience with field instrumentation, Mr. S.L.C Thornton-Dibb for his assistance with programming, Mr P. Goba for his assistance in the laboratory and various other aspects of analysis, Mr. M. Jilli for his assistance in collecting samples and laboratory analysis. The School of Bioresources Engineering and Environmental Hydrology, for providing the resources and working environment making this study possible. My family for all the support, prayer and encouragement throughout the duration of my studies. To my friends, for all the encouragement, support and good times shared during my studies.

TABLE OF CONTENTS

LIST OF FIGURES

LIST OF TABLES

ACRONYMS

AFC: Alternative final cover

BET: Bowen ratio evapotranspiration measurements

BTX: Benzene, Toluene, Xylenes

DCE: 1,2-Dichloroethene

DWAF: Department of Water Affairs and Forestry

EPA: Environmental Protection Agency

ET: Evapotranspiration

ET_o: Potential Evapotranspiration

FAO: Food and Agriculture Organisation

MR: Minimum Requirements

PCE: Tetrachloroethene

RCRA: Resources Conservation and Recovery Act

TCE: Trichloroethene

TCE: Trichloroethylene

VC: Vinyl chloride

SYMBOLS

G	soil heat flux density [MJ/m^2/day]
u_2	wind speed at 2 m height [m/s]
γ	psychometric constant [kPa/^{o}C]
n	unitless parameter related to the pore connectivity or tortuosity
R_n	net radiation at the crop surface [MJ/m^2/day]
T	mean daily temperature at 2m height [^{o}C]
e_s	saturated vapour pressure [kPa]
e_a	vapour pressure [kPa]
$e_s - e_e$	saturated vapour pressure deficit [kPa]
Δ	slope of vapour pressure curve [kPa/^{o}C]
ΔS	change in the volume of water held in storage per unit area (mm)
P	volume of precipitation per unit area (mm)
D	volume of water draining out the bottom of the waste site per unit area (mm)
K_c	crop coefficient
θ_s	water content at saturation
θ_r	residual water content
m	equal to 1-1/n [-]
Ks_{ij}	saturated hydraulic conductivity of material between port i and j
Δl_{ij}	length of porous medium between port i and j [mm]
h_c	height of capillary rise [L]
γ	surface tension between water and air [M/T^2]
r	pore or capillary radius (equivalent to the matric potential) [L]
ρ_w	density of water [M/L^3]
$K(h)$	unsaturated hydraulic conductivity [L/T]
h	water pressure [L]
h	pore water matric pressure head [L]
θ	volumetric water content [L^3/L^3]
K	unsaturated hydraulic conductivity [L/T]

α	coefficient in the soil water retention function [1/L]
θ_r	residual water content [L^3/L^3]
θ_s	saturated water content [L^3/L^3]
α	inverse of air-entry value [-]
S_p	potential uptake rate [L/T]
L_R	depth of the root zone [L]
L_m	maximum rooting depth [L]
L_0	initial rooting depth [L]
$f_r(t)$	root growth function
r	growth rate [L/T]
$\alpha\,(h)$	function of the soil matric pressure head $(0 \le \alpha \ge 1)$ [-]
A	total cross sectional area of the column [mm]
$H_{i\ or\ j}$	total hydraulic head at the port i or j [mm]
K_s	saturated hydraulic conductivity [L/T]
l	pore connectivity parameter [-]
n	pore-size distribution index [-]
Q	volumetric outflow rate [mm/h]
S	root uptake sink term [$L^3/(L^2T)$]
S_e	effective water content [-]
t	time [T]
T_p	potential transpiration rate [L/T]
x	spatial coordinate with positive value upward [L]
z	vertical spatial coordinate with positive value upward [L]

1. INTRODUCTION

South Africa generates enormous quantities of waste and with the rapid population growth and envisaged vast industrial development this problem will be further exacerbated. Ideally, emphasis should be focused on waste minimisation, as it is a function of environmental responsibility. According to the *White Paper on Environmental Management Policy for South Africa,* Notice 1096 of 1997, this will be emphasised in future legislation. However, waste management options such as prevention, minimisation or recovery are not always possible. Thus effective waste disposal must be controlled in the most environmentally acceptable and cost-effective way. Waste impoundments or landfills are considered to be controlled systems where these wastes can be effectively disposed. It is estimated that 95% of waste generated in South Africa is disposed of in waste containment systems or landfills (DWAF, 1998a). With the large quantities of waste at containment sites, pollution is inevitable, resulting in chemicals entering the environment and contaminating soil and water resources. Soil and water polluted with hazardous contaminants pose major environmental and health problems that need an effective and affordable technological solution (Ensley, 2000).

The term 'waste containment or landfilling' refers to the deposition of waste on land, subsequently involving appropriate engineering, creating a mandatory physical separation between the wastes, the surface water and groundwater regimes (DWAF, 1998a). The final cover is the main physical barrier between the waste impoundment and the environment designed to protect against physical, chemical and biological factors isolating the waste from the atmospheric environment. Prescriptive design for waste impoundment covers recommended by the United States Environmental Protection Agency (EPA) is a principal barrier layer. Specifically, the principle goals identified for all final waste covers are:

- *Isolating wastes:* if water is successfully controlled, then most of the important pathways for contaminant movement into the environment are cut off (Weand *et al.*, 1999). Exposed waste allows direct contact with potential receptors. Final waste covers thus serve to isolate the waste material from human and ecological receptors.
- *Minimization infiltration:* Water that percolates through the waste may dissolve contaminants and form leachate, which can pollute both soil and groundwater as it travels from the site (Hauser *et al.*, 2001). Under current South African regulations the

goal is prevention of water ingress into, flow through, and discharge out of the bottom of the waste impoundment.

- *Controlling landfill gases:* The release of toxic gases can create a potential hazard to human and ecological receptors in the vicinity of the waste impoundment.

According to the South African Department of Water Affairs and Forestry, DWAF, (1998a) final waste covers in South Africa have the same governing principles. It would be fitting to conclude the South African legislation mirrors the Resources Conservation and Recovery Act (RCRA) of the United States. However, integrity of the final waste cover is subject to numerous problems including desiccation cracking which, regardless of climate or site geology, result in failure (Mulder and Haven, 1995). Evidence shows that the performance of prescriptive waste covers decreases with time. Thus the water moving through a final cover into the underlying waste contributes to environmental problems caused by leachate leaking from the waste impoundments (Caldwell and Reith, 1993).

Regulators in the United States have thus been open to accepting alternative vegetation covers as alternative waste impoundment covers in lieu of the prescriptive covers. These governing authorities need acceptable field data, demonstrating that an alternative cover will perform as well as a prescriptive cover. Furthermore, regulators need to develop confidence that design tools (models) reliably predict cover performance, which is indicated by the prediction of a water balance.

In South Africa, there is currently little data that provides either field performance comparisons or studies of the accuracy of available design tools for vegetative cover. A research program was undertaken by an industrial corporation (AECI Limited) in South Africa to assess and evaluate the performance of an alternative cover system. Preliminary work undertaken by AECI Limited, in 2000 revealed that the upper 1 m or so of the materials in the waste impoundment had been transformed and had formed a substrate capable of supporting life. The unique combination of climate, vegetation and porous media also indicated a potential for use of alternative (to physically engineered) means for surfacing the site. In deciding a practical way forward, AECI Limited, reached an understanding with the Regulators (DWAF) that such an alternative, named an evapotranspiration (ET) cover, could be considered provided that its performance efficiency in controlling surface water

percolation (and subsequent leaching) could be demonstrated quantitatively (Lorentz, 2003). Water balance and vegetation aspects were monitored by the company from the beginning of 2002 and continued through to 2006. Soil hydraulic properties were measured in the laboratory and field. Numerical simulations of the water balance were conducted for various sites on the waste impoundment to assess and gain insight into the alternative cover performance. Performance of the cover was based on the ability to minimize the movement of water through the profile at different sites. Three sites were selected to assess and determine the water fluxes to the groundwater from the waste impoundment at the study area. The outflow seepage rate or flux is the criterion used by regulators and cover design engineers to determine the overall adequacy of the cover. Thus the site with the lowest flux to groundwater was deemed to be the best performer of the alternative cover, whilst the site that yields the highest flux would be the worst performer.

The overall objective of this research was to evaluate and thus test the hypothesis: A vegetated cover is able to limit effluent leaching from a waste impoundment. Analysis of the following sub-objectives would be required to address the hypothesis;

1. Determine a climatic water balance on the vegetation covers;
2. Determine the geohydrological properties of the waste material;
3. Determine the fate of the water i.e. amount reused via evapotranspiration as opposed to the effluent from the waste body beneath the root zone; and
4. Determine the leaching potential below the waste.

1.1 Structure of Thesis

Chapter 1: This chapter includes an introduction to the topic, summarising the importance of the research and outlining the research objectives.

Chapter 2: This chapter provides a literature review of the design of waste covers and the various process components associated with different vegetation cover systems. Also presented are the relevant inherent qualities for the different covers and provides a regulatory background as to how different final covers could be used.

Chapter 3: Provides some background to the study site and the rehabilitation strategy for the final vegetation cover on the study site.

Chapter 4: Identifies the above-ground and climatic variables and describe how these variables were analysed for their use in the modelling of the study site. This chapter also evaluates the calculated variables which will be used in the model.

Chapter 5: Describes the geohydrological information needed to conduct the study and the specific methods for their determination. This information provides the subsurface input parameters for the model used in this study.

Chapter 6: This chapter describes HYDRUS-2D software which is the principle tool used during the investigation. The appropriateness of the HYDRUS-2D model in terms of the relevant equations used in the model is presented.

Chapter 7: A description and a parametric sensitivity analysis of the HYDRUS-2D model are outlined.

Chapter 8: This chapter sets out to explain the modelling exercises in the context of available literature, actual field data or any assumption that may have been made on the simulated water use and on the simulated water balances specific to the site.

Chapter 9: Simulated results are presented and compared against the collected field data. This chapter provides evidence of the efficiency of the vegetation cover by discussing the simulated results.

Chapter 10: Conclusions and Recommendations are presented in this chapter.

2. LITERATURE REVIEW

In the United States, land disposal of waste is governed under the Resources Conservation and Recovery Act (RCRA). The two principle types of landfills are hazardous solid waste and municipal solid waste, which are regulated under the RCRA Subtitle "C" and "D" respectively.

In an attempt to define the details of design methodology, the Environmental Protection Agency (EPA) published a design guidance document (EPA, 1991). This design document recommends that waste impoundment closures for RCRA Subtitle "C" (hazardous facilities) incorporate the following layers in the cover profile illustrated in (Figure 2.1). The top layer cover is 60 cm thick consisting of native soil for vegetation growth. Below this layer a 30 cm drainage layer of sand or synthetic material with a minimum hydraulic conductivity of $1x10^{-2}$ cm/s is required. A geomembrane layer is placed below the drainage layer. At the very bottom of the cover is the barrier layer comprising 60 cm of native soil compacted to achieve a maximum hydraulic conductivity of $1x10^{-7}$ cm/s (EPA, 1983). The compacted soil layers are difficult to construct and it is recommended that this layer be typically installed in a wet condition to achieve a low saturated hydraulic conductivity. These compacted layers include one or more barrier layers made of compacted clays, geomembranes, or geosynthetic clay. Thus a capillary barrier is formed by placing a fine clay material over a coarser soil material. The capillary barrier is formed from the difference in pore structure which results in an interface as a result of the change in pore sizes between the layers of fine and coarse material. The capillary force causes the layer of fine clay overlaying the coarser soil to hold more water than if there was no change in particle size between layers. Therefore the water is held in the fine clay material until it approaches saturation near the interface (Stormont, 1997).

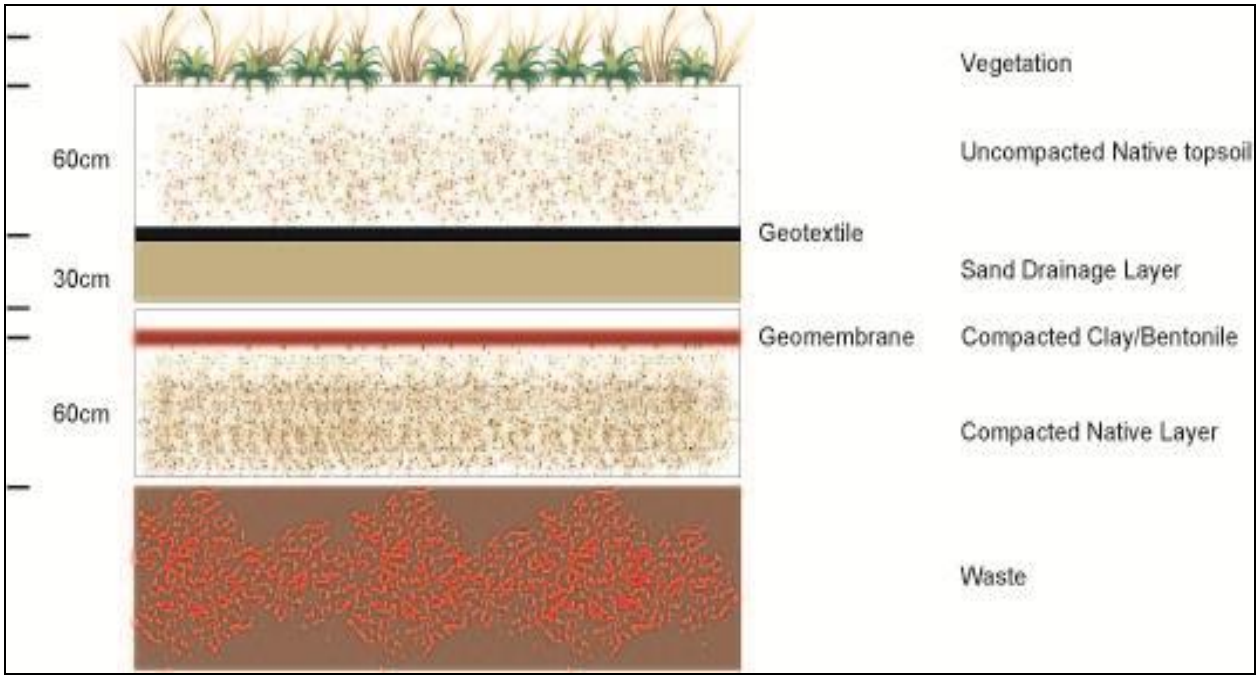

Figure 2.1 RCRA subtitle "C" (after Dwyner et al., 2000). The various layers incorporated in the cover comprise native topsoil, a geotextile layer, sand, geomembrane layer and native soils.

Although the concept of using these low permeability clay materials is sound, in practice, however, this methodology has proven to be problematic to achieving the goal of waste isolation. The barrier will fail if water accumulates in the fine clay layer or the desired large change in pore size is missing in places. This will result in lateral flow along the interface and subsequent leaking. Suter *et al.*, (1993) reviewed failure mechanisms for compacted soil covers and concluded, "natural physical and biological processes can be expected to cause clay barriers to fail in the long term."

Unlike these conventional cover system designs that use materials with low hydraulic permeability (barrier layers), vegetation covers use water balance components to reduce percolation (EPA, 2003). Thus vegetation covers are designed to work with the forces of nature rather than attempting to reduce or eliminate infiltrating water with an impermeable barrier.

2.1 Alternative final covers

Alternative final covers (AFCs) are considered a relatively new concept in South Africa and though well understood in some parts of the world, particularly the United States, they are still considered an innovative technology in developing countries such as South Africa. The AFC which is also referred to in this thesis as an evapotranspiration cover (ET), or phytoremediation cover has not been officially written into any South African policy or regulations. It will take a few years for the equivalent alternative of a conventional cover to have the back up of field data, performance assessment, modelling and written regulations. Thus for regulators such as Department of Water Affairs and Forestry (DWAF) to be accepting and approve AFCs, they will need to understand the engineering and the science behind alternative covers to evaluate them and subsequently apply flexibility in the regulations associated with AFCs (ITRC, 2003).

A vegetative cap is defined in the introduction to phytoremediation EPA, 2000 as "A long term, self sustaining system of plants growing in and/or over materials that pose environmental risk; a vegetative cap may reduce that risk to an acceptable level and generally requires minimal maintenance." Thus the ET cover is a practical, self sustaining and easily maintained biological system that will remain effective over extended periods of time at low cost.

Two types of vegetative covers have been identified:

An evapotranspiration (ET) cover

A evapotranspiration (ET) cover is a cover comprising soil and plants engineered to maximise the available storage capacity of the soil, the evapotranspiration rates and transpiration processes of plants, and minimise water infiltration into the waste below. The soil is a monolithic layer with adequate thickness to retain water until it is removed by evaporation and transpiration mechanisms. Risk reduction relies on the isolation of contaminants and the reduction of leachate formation and migration (Hauser and Gimon, 2004).

A phytoremediation cover

A phytoremediation cover is a cover consisting of soil and plants selected to reduce infiltration and to aid in the degradation of underlying waste. The vegetative cover provides for hydraulic control, degradation, and volatilisation, and is used for the uptake of water and for the treatment of soil, sludge and sediments. Risk reduction relies on the isolation of contaminants and the reduction of leachate formation and migration, and the degradation of contaminants (EPA, 2000). Phytoremediation is the name given to a set of technologies that use plants to remediate contaminated sites. Phytoremediation uses living plants for *in situ* remediation of contaminated soil, sludges, sediments, and groundwater through contaminant removal, degradation, or stabilization. Phytoremediation can be used to remediate various contaminants including metals, pesticides, solvents, explosives, hydrocarbons and landfill leachate. It utilizes a variety of plant biological processes and the physical characteristics of plants to aid in the site remediation (ITRC, 1999)

2.2 Plant processes

"Natural processes occurring in plants include water and chemical uptake, metabolism within the plant, exudate release into the soil that leads to contaminant loss and physical and biochemical impacts of plant roots. In order for a chemical to be taken up into the plant, it must be in solution where the water is absorbed from the soil solution into the outer tissue of the root. Contaminants in the water can move through the epidermis to and through the Casparian strip, and then through the endodermis, where they can be sorbed, bound, or metabolised. Chemicals or metabolites passing through the endodermis and reaching the xylem are then transported in the transpiration stream or sap. The compounds might react with or partition into plant tissue, be metabolised, or be released to the atmosphere through stomatal pores." (Pivetz, 2001).

In plants the uptake and translocation of organic compounds are dependent on key parameters that influence sorptive behaviour, such as their solubility, polarity, molecule weight and hydrophobicity/solubility-water partitioning coefficient (Lyman *et al.*, 1992). After uptake of the pollutant/foreign compound its chemical structure is changed by plant enzyme reactions, which increase the polarity (and thus solubility) of the compound. This occurs through the addition of functional groups such as hydroxyl groups $(OH)^-$. Conjunction is the next process, where plant biomolecules such as amino acids and glucose are added to further polarize the

pollutant/foreign compound. After conjunction has occurred the polarized compound is far less toxic and is easier to transport along aqueous channels in the plant. The pollutant/foreign compound polymerizes in a lignin-like manner which is a complex structure, which is sequestered (metabolized) in the plant. Once an organic chemical is translocated, the plant may store the chemical and its fragments in new plant structures via lignification (covalent bonding of chemical or its fragments into lignin of the plant), or it can volatilize, metabolise, or mineralise the chemical completely to carbon dioxide and water. Chlorinated aliphatic compounds such as trichloroethylene (TCE) have been reported to be mineralised to CO_2 and less toxic metabolites such as trichloroethanol, trichloroacetic acid, and dichloroacetic acid (Newman *et al.*, 1997).

Phytoremediation thus requires an understanding of the soil, roots and micro-organism interactions that need to occur, the plants selected, and what needs to be done to ensure plant growth. Screening studies will be important in selecting the most useful plants for the actual field situation requirements. Phytoremediation requires an initial commitment of resources and time, but has the potential to provide in the long term a lower-cost, environmentally acceptable alternative solution to conventional remedial technologies at appropriate sites (Schnoor and Dee, 1997).

Phytoremediation encompasses various processes that can lead to contaminant degradation (breakdown of harmful contaminant to less harmful chemical), removal from soil (through accumulation or dissipation in the plant itself), or immobilization (ensuring contaminant remains *in situ*). Different forms of phytoremediation may apply to specific types of contaminants or contaminated media, thus there are a number of different forms of phytoremediation (Pivetz, 2001).

2.2.1 Phytoextraction

Phytoextraction is contaminant uptake by roots with subsequent accumulation in the aboveground portion of a plant, generally to be followed by harvest and ultimate disposal of the plant biomass. This process is applied to metals, metalloids and radionuclides, as these are generally not further degraded or changed in form within the plant. This does not generally apply to organic contaminants, as these can be metabolised, changed or volatised (Pivetz, 2001).

2.2.2 Phytostabilisation

The remediation of contaminated sites with hazardous chemicals/waste often involves excavation or stabilisation with chemicals that will bind the hazardous chemicals/waste. These practices, which are based on civil engineering works, are environmentally invasive and expensive. One developing alternative remediation technique is phytostabilisation, also called *in-place inactivation* or *phytorestoration* (Berti and Cunningham, 2000).

Phytostabilisation is thus the use of vegetation to contain soil contaminants *in situ*, through modification of the chemical, biological and physical conditions of the soil. Phytostabilisation builds on a broad base of knowledge and experience in fundamental soil chemistry, through the modification of the chemical, biological, and physical conditions in the soil. Contaminant transport in the soil, sediments, or sludges can be reduced through adsorption and accumulation by roots, adsorption onto roots, precipitation, complexation, or metal valence reduction in soil within the root zone, or binding into humic (organic) matter through the process of humification (Pivetz, 2001).

2.2.3 Rhizodegradation

Rhizodegradation, also called enhanced rhizosphere biodegradation is the enhancement of naturally occurring breakdown of contaminants in the soil. Increasing the soil organic carbon, bacteria, mycorrhizal fungi, basically the factors that encourage the degradation of organic chemicals in soil ultimately can detoxify the organic contaminants. (Schnoor and Dee, 1997).

The presence of roots will often increase the size and variety of microbial populations in the soil surrounding the root. For example significantly higher populations of total heterotrophs, denitrifiers, pseudomonades, BTX (benzene, toluene, xylenes) degraders, and atrazine degraders were found in rhizosphere soil around hybrid poplar trees than in non-rhizosphere soil. The increased diversity of microbial populations is due to stimulation by plant exudates, compounds produced by plants and released from plant roots. These root exudates also contain readily biodegradable organic macromolecules, thus allowing a wide range of organic contaminants to be candidates for rhizodegradation, such as petroleum hydrocarbons, chlorinated solvents, pesticides and polychlorinated biphenyls (Jordahl *et al.*, 1997).

2.2.4 Phytodegradation

Phytodegradation is the uptake, metabolising, and degradation of contaminants within the plant (ITRC, 1999). The plants are capable of degrading organic contaminants through the metabolic processes described in the sub-category of section 2.2 Plant Processes.

2.2.5 Phytovolatisation

Phytovolatisation is the uptake of a contaminant by a plant, and the subsequent release of a volatile daughter product of the contaminant. Thus for the phytoremediation to be successful, the degradation product or daughter form should be less toxic. Phytovolatisation is primarily a contaminant removal process, transferring the contaminant from the groundwater or soil water to the atmosphere. The subsequent transferring of the contaminant through the plant to the leaves allow the contaminant to be altered to the less toxic form (Pivetz, 2001). An example includes the reduction of highly toxic mercury species to less toxic elemental mercury. However, the major disadvantage of this method is the difficulty of measuring the by-products of these metabolic plant processes. Phytovolatisation can also occur with organic contaminants, such as TCE, generally in conjunction with other phytoremediation processes (EPA, 2000).

2.2.6 Hydraulic Control

The United States EPA's "Introduction to Phytoremediation" addresses two types of vegetative caps: the evapotranspiration cover, which is designed to maximize the storage capacity, evaporation, and transpiration; and a phytoremediation cover, which is designed to minimize infiltration and to contribute to the degradation of underlying waste (EPA, 2000). Hydraulic control (or hydraulic plume control) is the use of vegetation to influence the movement of groundwater and soil water, through the uptake and consumption of large volumes of water. Hydraulic control may influence and potentially contain movement of a groundwater plume, reduce infiltration and leaching, and ideally induce upward flow of water from the water table through the vadose zone (Pivetz, 2001).

Phreatophytes are deep-rooting plants, which are capable of obtaining a significant amount of the water from the zone of saturation or capillary fringe. Phreatophytes are capable of tapping into shallow water tables and are thus suited to perform hydraulic control (EPA, 2000). Hydraulic pumping can occur when the tree roots take up large amounts, thus counteracting

slow flow through the soil and prevent lateral migration of the contaminants within a groundwater zone. Application of phreatophytes in achieving hydraulic control involves drawing down water tables or reversing groundwater gradients. The water uptake is a result of transpiration rates, which is determined by the climatic conditions and season. Since these are seldom constant, the monitoring of the system is important to ensure the overall infiltration does not exceed the evapotranspiration that could lead to the migration of the contaminant. Thus hydraulic control will likely require site-specific observations of water levels, flow patterns and water uptake rates. The major advantage of hydraulic control is that the other processes such as rhizodegradation, phytodegradation and phytostabilisation can take place (Pivetz, 2001).

As with many technologies, AFCs are not always the best possible solution for all landfills. They have advantages and disadvantages and below are certain aspects identified by the EPA, 2000.

Potential advantages:

- cost is a major advantage;
- shorter post-closure maintenance than for traditional caps are envisaged by reducing surface erosion and establishing a self-sustaining ecosystem;
- aesthetically pleasing;
- reduced long-term stewardship liabilities;
- waste de-watering can be achieved at the same time attain passive hydraulic gradient control;
- vegetative covers have the potential to enhance the biodegradation of contaminants in soils and
- vegetation may encourage aerobic microbial activity in the root zone, which could discourage formation of anaerobic landfill gases or degrade them.

Potential disadvantages:

- designs for one vegetative cover will differ to another as a result of being climate-specific, thus universally applicable designs are not possible as designs will differ as a result of soil and climate-specific differences;
- contaminants may be taken up by plants thus potential adverse effects could occur with animal consumption;

- an effective vegetation cover is preceded by a long lag time, thus it may be necessary to ensure strategies are in place preventing contaminant migration and
- downward flow to underlying waste or groundwater could consequently be increased by decaying roots resulting in larger macropores in the soil.

2.3 Site Specific Aspects for Alternative Final Covers

There are certain factors that need to be considered before a vegetation cover can be selected as an alternative cover. These include:

- *Contaminant concentrations:* For degradation to occur, the plant roots need to be in contact with the contaminated waste and contaminant concentrations should not be at phytotoxic levels.
- *Root depth:* The effective depth of contaminant degradation for the phytoremediation cover is the root depth of the plants.
- *Plants:* Ideally, the vegetation selected for the system should be a mixture of native plants and consist of warm and cool season species.
- *Soil conditions:* Soils most suitable for a vegetative cover have a high water storage capacity. The soils should therefore be a mixture of clays and silts. Soils with rapid drainage are to be avoided.
- *Climatic conditions:* Climatic variables such as precipitation, type, intensity, temperature and humidity should be evaluated. Areas with high precipitation rates require more water to be transpired or stored in the soil.
- *Ground and surface water:* Water tables that are relatively high may result in soils with less available water storage capacity, if evaporation and transpiration processes are not sufficient.
- *Regulatory acceptance:* Regulatory standards have not yet been developed specifically for alternative covers and installations must be approved on a site-by-site basis. A vegetative cover must demonstrate equivalent performance with generic cover designs. In the USA, these specifications are detailed in the Design and Construction of RCRA/CERCLA Final Covers – EPA/625/4-91/025; and Technical Guidance from RCRA/CERCLA Final Covers – EPA/OSWER Draft.

2.4 Regulatory Flexibility and Goals for Alternative Cover Systems

Regulatory flexibility and goals such as the protection to human health, the protection of the environment are considered the most important. More recently the EPA has adopted the policies that are meant to improve remediation and encourage the use of innovative designs. Thus the opportunity for alternative landfill covers has been created. This section identifies regulations and guidance related to final landfill covers and particular regulatory flexibility that can be referenced when using alternative final covers within South Africa.

2.4.1 Regulatory Flexibility

The Resources Conservation and Recovery Act (RCRA) is the controlling federal law for hazardous and municipal solid waste landfills in the United States. According to the Code of Federal Regulations (CFR) Title 40 Subchapter I, Parts 260-279 contain the regulations governing the management of hazardous waste facilities. There are several points indicated in CFR Section 264.110 with regard to applicability that alternative regulatory requirements could be used to supersede the more specific prescriptive regulations (63 Federal Register 56733, Oct. 22, 1998). Section 264.111 focuses on the management of potential risks associated with a hazardous or solid waste unit without specifying prescriptive regulatory requirements. Basically alternative requirement that will protect human health and environment are negotiable by the regulators and the waste unit operators. Section 264.111(d) clearly affords the opportunity for the use of "alternative requirements" protective of human health and the environment. Clearly opportunity arises for the Regional Administrators to consider alternative covers.

The two primary objectives defined by the EPA's minimum technical requirements (EPA 1987, 1991) are:

- to minimise leachate formation by keeping liquids out of the landfill;
- to detect, collect and remove the leachate that is generated.

Motivation for implementing the innovative technologies such as the alternative covers in South Africa can be related to the following factors:

- The remediation approach must address legal obligations, particularly the 'duty of care' provisions in the National Water Act (Act 36 of 1998) and the National Environmental Management Act (Act 107 of 1998). Interventions that offer the opportunity to decrease environmental liabilities in the long-term are, therefore, the imperative.
- Entombment of waste is viewed as a high-risk option from a long-term liability point of view, because it does not serve to reduce the source of the problem, but to contain it. Hence, in the event of the containment system failing, waste sites will be exposed to the same level of potential liability as currently exists. This is not a sound business risk management approach. Accordingly, interventions that promote a 'living system' are considered preferable, as these provide opportunity to reduce source contaminant levels.
- Cost effectiveness is an important decision-making factor, as the company must (as would any business) aim to apply its available financial resources responsibly.
- International experience and acceptability are also considerations, particularly as regards technological developments with respect to long-term risk management and reduction.

(DWAF, 1998b) provides the required guidelines for disposal of Hazardous Wastes in the "Minimum Requirements for the Handling, Classification and Disposal of Hazardous Waste". The objectives of the Minimum Requirements for the disposal of Hazardous Waste are to:

- prevent water pollution and ensure sustained fitness for use of South Africa's water resources;
- attain and maintain minimum waste management standards in South Africa, so as to protect human health and the environment from possible harmful effects caused by the handling, treatment, storage and disposal of wastes;
- effectively administer and provide a systematic and nationally uniform approach to the waste disposal process;
- endeavour to make South African waste management practices internationally accepted and
- provision is not for the use of a vegetative cover in the Minimum Requirements, although the design criteria indicated are to (i) maximise run-off of precipitation, and (ii) minimise infiltration.

Performance criteria for lining and capping hazardous sites that should be met are:

- the steady-state infiltration rate must not exceed 0.5 m/year or $1.5x10^{-6}$ cm/s;
- the outflow rate at the base of the waste body must not exceed 0.03 m/year or $1x10^{-7}$ cm/s.

In this chapter the various aspects of phytoremediation were addressed that would aid in the clean up of a waste impoundment. The process of phytoremediation including phytoextration, phytostabilisation, rhizodegradation, phytodegradation, phytovolatisation and hydraulic control were reviewed to give a holistic understanding into the processes occurring. The site specific aspects or conditions were evaluated for the use of alternative cover systems to be successful. This chapter finally identified regulations and guidance related to final landfill covers and particular regulatory flexibility that can be referenced when using alternative final covers for South Africa in the future.

Given the performance requirements, an evapotranspiration cover is considered to be meeting the spirit of the Minimum Requirements. The most important consideration for evaluating the evapotranspiration cover against the Minimum Requirements is the outflow from the base of the waste body, since it is key in determining movement of pollution into groundwater and the environment. Again, these performance criteria will almost certainly be revised as a result of successful research or studies as more information becomes available. These minimum requirements do not account for the increasing storage capacity within the waste impoundment with drying due to evapotranspiration.

3. BACKGROUND TO STUDY

"The Vumbuka Reserve, previously called the North West Waste Site is the waste disposal area for a chemical manufacturing facility, located within the Umbogintwini Industrial Complex, which is approximately 25 km to the South of Durban. The area of the Complex extends some 27 ha and has been in operation since 1907. A diverse range of chemical products including paints, explosives, herbicides, pesticides and chlorine have been manufactured at the complex. The disposal of these chemical wastes as a result of these operations has occurred for some 90 years until its decommissioning in 1998 and since that time AECI Limited has been in the process of rehabilitating the site" (Lorentz and Morgan, 2006).

The Vumbuka Reserve comprises of effluent precipitation settling dams (referred to as the Dams Area 1, 2, 3-4, 5 and 6) and an area where a large number of drums containing chlorinated hydrocarbons were stacked and subsequently covered (Drums Area). The Dams Area which covers an area of 20 ha and contains more than 1 000 000 tons of waste material of which up to an estimated 20 m is saturated slimes. Plant effluent in the form of lime slurry containing dissolved calcium chloride and saturated with dissolved and free phase organic reactants was pumped into the Dams. The Drums Area which covers some 7 ha contains in excess of some 50 000 tons of waste, about half of which is chlorinated hydrocarbon based sludge. The area also comprises of disused mercury sludge dams. The areas are illustrated in (Figure 3.1) and have different chemical signatures thus required different remedial strategies (Duthe and Cameron-Clarke, 2004).

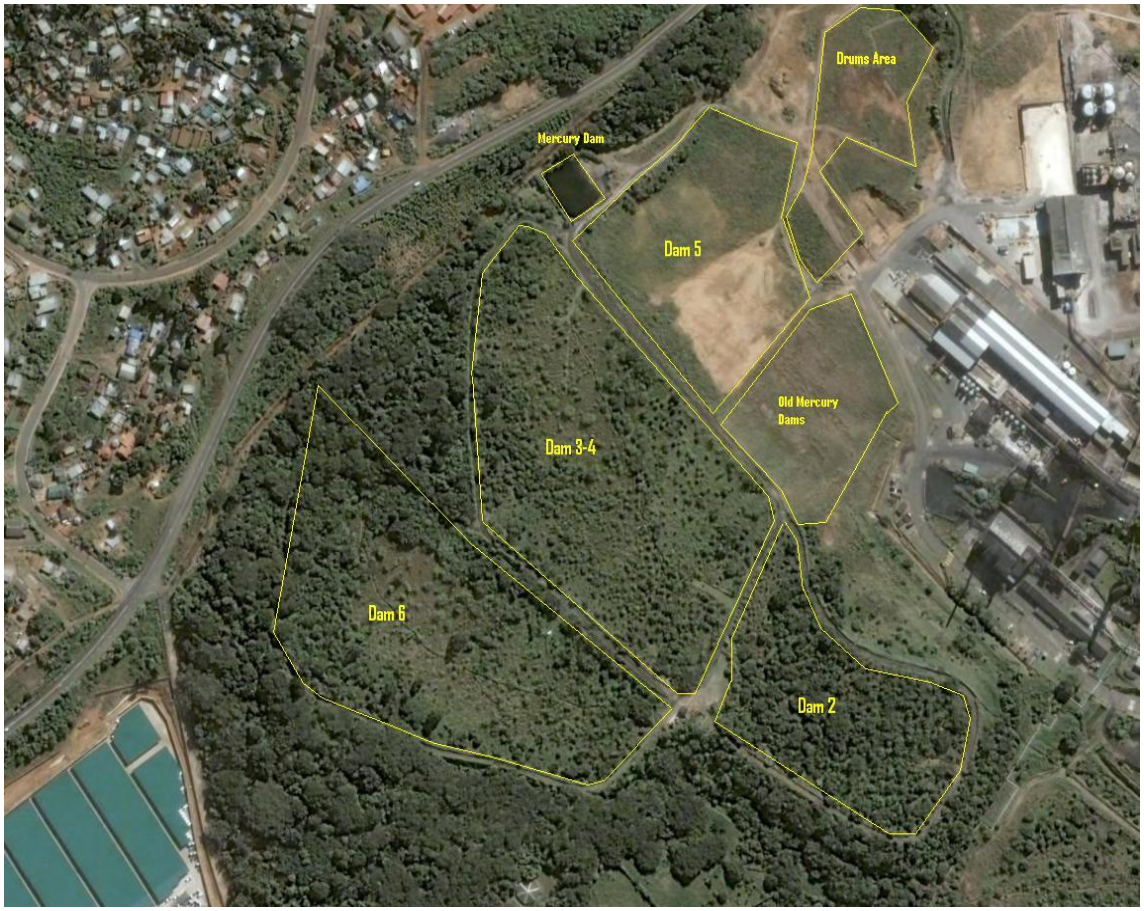

Figure 3.1 Aerial view of the study site presenting the Dams, Drums area and Mercury Dams.

The aerial photo of the study site shows clear evidence of the vegetation cover on the Dams Areas. Dam 2 has the most dense vegetation canopy, which comprise mainly trees and grass. Dam 3-4 and Dam 6 comprise mixed species of woody shrubs/grasses, while the tree species are younger and less dense compared to Dam 2. The respective Dams are covered by various vegetation species, including Grass *(Cynodon nlemfuensis)*, common wild Fig tree *(Ficus thonningii)*, Bugweed *(Solanum mauitianum)*, Pigeon Wood *(Trema orientalis)* and mixed woody shrubs/grasses. For the purpose of the study, monitoring was performed at various locations on the Dams to compare the movement of water through the waste material in the root zone. The monitoring would effectively determine the influence of the roots on water fluxes. For experimental purposes other sites were also prepared on the Dams, including a Bare site, where the vegetation was completely removed exposing a patch of material approximately (6 m x 6 m), a Covered site where a patch of soil was completely covered with an impermeable plastic cover (6 m x 6 m), and a Grass site. In total ten sites were monitored on the Dams, to gain understanding and compare difference of root zone fluxes.

3.1 Chemicals in the Vumbuka Reserve

The legislation DWAF, (1998a) stipulates that the Dams need to be lined if it is to contain hazardous waste. Prior to the establishment of the Dams the site was used for the disposal of burnt pyrite (calcine) from sulphuric acid manufacture in the 1900s. In the late 1960s, the effluent Dams were constructed but the design, acceptable at that time, was not according to current DWAF requirements for disposal of waste. The Dams are not lined. There is great concern of the potential migration of contaminants to the neighbouring areas, which are inhabited by both formal and informal residential settlements. Historical information relating to the deposition of the slimes estimated that the materials consisted largely of:

- ferric oxide and ferric sulphide;
- calcium sulphate;
- ash (from a power station);
- calcium carbonate;
- calcium chloride solution with chlorinated hydrocarbons;
- tars still residue;
- non-mercurial brine sludge;
- ferric hydroxide;
- mercury (elemental and as oxide) and
- smaller volumes of arsenic trioxide, vanadium pentoxide, biocides and herbicides, hydrazine, corvic sludge, methyl methacrylate and phosphates.

The main chemicals of concern were identified as chlorinated hydrocarbons which include ethenes (tetrachloroethene (PCE), trichloroethene (TCE), 1,2-dichloroethene (DCE) and most hazardous daughter products from the breakdown of these compounds, such as vinyl chloride (VC) are of concern. Other potential concerns are elemental metals and oxides, atrazine, diazinon and hexachlorobutadiene (Duthe and Cameron-Clarke, 2004).

3.2 Geology

Druzynski and Duthe, (2003) formulated a conceptual illustration of the underlying geology from information of previous work, available literature and field studies. The Vumbuka Reserve area is almost entirely covered by sediments of the Berea Formation. These form a very thick ridge consisting of dune sands and sandy clays adjacent to the Indian Ocean.

Underlying the unconsolidated sediments of the Berea formation are fractured rocks of the Dwyka Group, Tillite. This very dense, hard, non-porous matrix is very well jointed with preferential weathering occurring at these joints. The Natal Group Sandstone, being a very dense matrix is the oldest of the geological units, extents all the way from the Dams Area inland. The three dimensional conceptual mesh illustration of the geology is presented in (Figure 3.2) showing the underlying Berea Formation, Dwyka Group and the much older Natal Group. The two geological cross sections are presented in (Figure 3.3) with trends of the N-S and E-W directions. These depict the Natal Group in extent of the northern western boundary of the Dams area. This also shows the inclusion of the Lower Ecca Group, Shale to the north east of the Dams. The waste materials in the Dams are lime slurries and sludges, interspersed with sands and clays and containing organic and inorganic chemicals in excessive concentrations. The waste materials are silty sized upon drying, but can be described as clay sized or sand sized (Druzynski and Duthe, 2003).

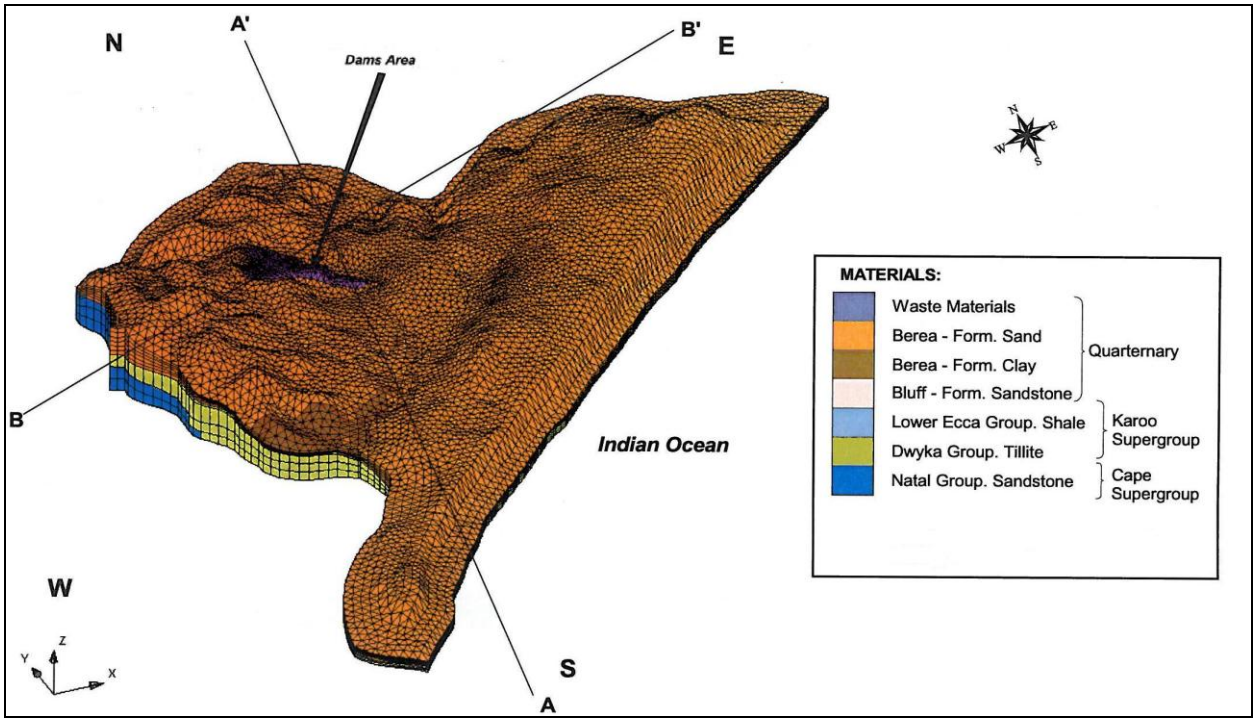

Figure 3.2 3D Mesh of conceptual geology of the study area (Druzynski and Duthe, 2003).

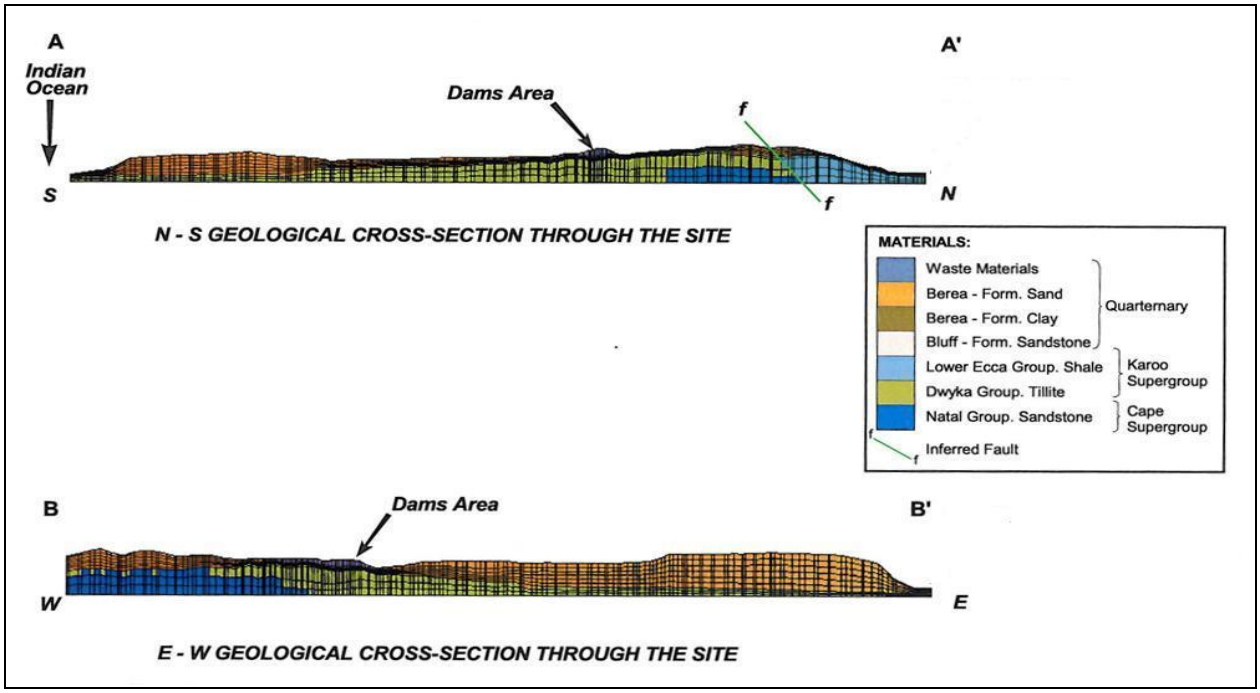

Figure 3.3 Geological cross-sections through the study area (Druzynski and Duthe, 2003).

3.3 Hydrogeology

Studies undertaken have indicated that there are three regional aquifers, with the boundaries much greater than the Dams Area (Druzynski and Duthe, 2003). The main aquifer systems that have been identified are:

- Berea Formation sands and clays contain a significant amount of groundwater that is recharged by precipitation and also by recharge occurring from the Dwyka Tillite and Natal Group Sandstone aquifers,
- Dwyka Group Tillite is a poor medium for groundwater, however by virtue of its very dense matrix, it is extensively fractured thus allows for preferential flow paths and,
- Natal Group Sandstone by virtue of being the oldest geological unit impacted by the Dams Area plays an important part in the groundwater recharge to the overlying aquifers. This medium is very low in porosity, but will have more fracturing due to age, thus may have the preferred conduits for groundwater flowing beneath the Dams Area.

A perched water table has also been identified to exist within the Dams, as a result of the materials being extremely fine and having a high surface area. The waste materials have extremely low hydraulic properties and thus extremely low flows within the material. Parts of the Dams Area are underlain by clays, which may locally separate the waste materials from the subsurface aquifers, thus contribute to the perched aquifer that is found within the waste materials. Investigations on groundwater have revealed contamination migration into two of the three aquifers, namely the Berea Formation aquifer and the Dwyka Tillite aquifer. Due to the underlying geology being partially consolidated dune sands (Berea Formation), overlaying fractured rock formations (Dwyka Tillite and Natal Sandstone) the potential for migration of contaminants from the Vumbuka Reserve is a major concern. “There is evidence that the Vumbuka Reserve has impacted on groundwater and there is thus a potential for exposure to informal residential settlements. Fortunately risks posed are not considered unduly high, as water supply to both the formal and informal communities is reticulated” (Duthe and Cameron-Clarke, 2004).

3.4 Rehabilitation strategy

It is envisaged that the final land use of the Dams Area will be a nature reserve, named Vumbuka Nature Reserve, with controlled access. The overall strategy for the rehabilitation of the Dams comprises an integrated hydraulic containment system, a managed evapotranspiration cover and surface water controls to maximize surface water runoff. These measures fall well within the generic principles for the sustainability of the evapotranspiration covers. One of the requirements by DWAF is that the land must be rehabilitated to its natural state, or to a predetermined and agreed standard or to land which conforms to the concept of sustainable development. Another requirement is that monitoring should be carried out continuously especially with regard to infiltration control. Infiltration control will be to limit the amount of water entering at the surface, which would result in percolation through the waste material (DWAF, 1998c). With regard to rehabilitation of a Hazardous Waste site in South Africa, the generic framework of processes for the rehabilitation to closure is illustrated in (Figure 3.4).

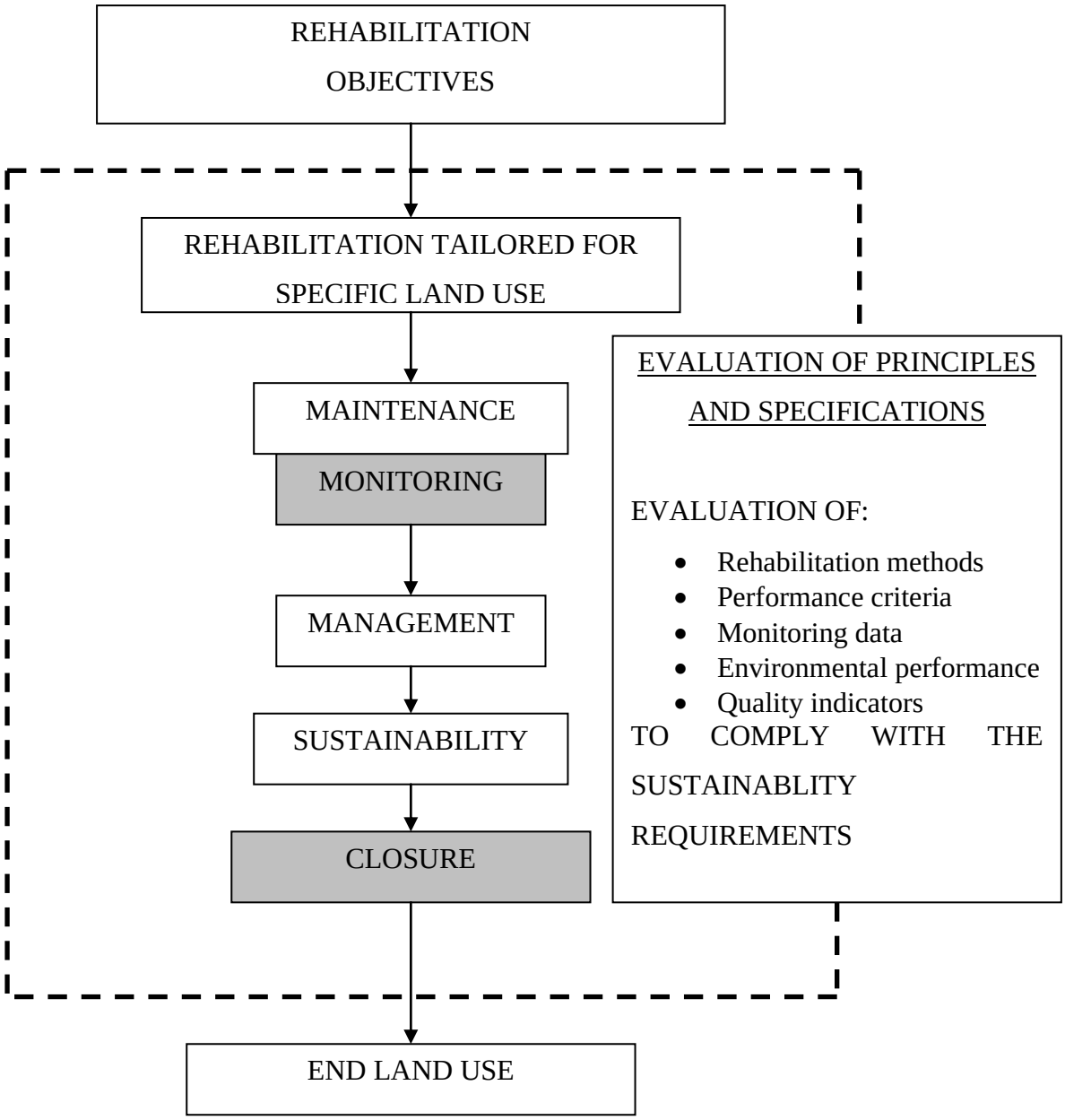

Figure 3.4 The Generic framework of processes from the Rehabilitation to Closure (DWAF, 1998c).

As stated in the evapotranspiration covers chapter, rehabilitation objectives have well-established criteria in place for water control measures and water quality requirements. Unfortunately there is a lack of information with respect to the rehabilitation methods, management systems and monitoring criteria. There are also no specifications with respect to the waste quality and vegetation standards. Therefore it is essential to define the function that the rehabilitated Dams must fulfil with respect to the end-land use.

An overall and a very basic procedure for the rehabilitation of the Dams using evapotranspiration covers would comprise the following:

- Defining all impacts (erosion, pollution, odour etc).
- Limitations and risks associated with the identification of constraints
    - Natural (rainfall, floods, temperature, etc)
    - Physical (slope length, slope gradient, aspect, texture, water holding capacity, etc)
    - Chemical (pH, toxicity, nutrient balance etc.)
    - Biological (vegetation, organic matter, micro-organism activity, etc)
    - Economical (resources distribution and allocation)
- Solution/method statement – using supportive information (data basis, theory, research, models, technology) to obtain innovative solutions.
- Validation – testing the solutions against the legislation requirements and the requirements of sustainable management.
- The capacity to implement the strategy.

Maintenance, monitoring and management programs should be developed with a sustainable end-land use in mind. The objectives of these programs need to be supportive to the rehabilitation and closure phases to comply with the obligations and requirements. Sustainability is a measure of the likelihood that a particular land use will remain physically, economically and socially appropriate to that particular location for a significant period. For this particular program, success in terms of sustainability would ultimately only need maintenance to the vegetation cover. Maintenance would only be required with regard to ensuring control of the vegetation, yet guarantee the cover has developed to the extent all objectives that have been set out are achieved. Success would be achieved when the rainfall into the waste material is less than the evaporation over a period. This will simply reduce the potential for storage in the system, which will ultimately eradicate seepage. The success of a vegetation cover system is determined by monitoring and understanding the meteorological variables. These are explained in the meteorological variables section (Chapter 4).

4. METEOROLOGICAL VARIABLES

In terms of the climate monitoring, rainfall and actual evaporation rate are the driving forces for determining whether the water balance will be effective in limiting impacts on the groundwater regime. Thus rainfall was measured directly with two rain gauges located on Dams. The potential evaporation was determined by an empirical equation. Actual evapotranspiration of the vegetation were determined through sap flow measurements and Bowen ratio measurements on the Dams and for the modelling calculated from the potential evaporation by application of an appropriate crop coefficient. The location and type of instrumentation on the Dams are illustrated in (Figure 4.1).

Figure 4.1 Layout of the instrumentation for monitoring on Dams 2 and Dams 3-4.

4.1 Long term climatic conditions

The long term climatic data for the study area can be derived using the meteorological data from the Durban International Airport record (1960 – 2004), which is 9 km to the North. These average monthly totals for the Durban International data are presented in (Table 4.1). The total rainfall for the year is approximately 1 000 mm, where most of the rains occur in the summer months.

Table 4.1 Average monthly totals for the Durban International Airport

	Jan	Feb	Mar	Apr	May	Jun	Jul	Aug	Sep	Oct	Nov	Dec
Max Daily Temp (^{o}C)	27.8	28.2	27.8	26.1	24.6	23.2	22.7	23.0	23.4	24.1	25.4	26.9
Min Daily Temp (^{o}C)	21.1	21.3	20.3	17.6	13.8	10.7	10.5	12.6	15.3	16.9	18.4	20.0
Rain (mm)	137.4	115.0	115.2	77.0	50.7	27.0	48.2	50.6	69.9	99.3	109.6	109.1
Humidity % 08h00	76	78	79	78	76	74	74	75	74	74	74	75
Humidity % 14h00	69	69	68	65	60	53	53	60	66	68	70	70
Humidity % 20h00	83	82	83	82	81	79	77	79	81	82	83	83

4.2 Rainfall

Rainfall was measured with an automatic rain gauge on the Dam 2 site, providing a record from March 2000 to December 2005. Rainfall data for the same monitored period was also obtained from a rain gauge at Durban International Airport, (rain gauge number W_0240808). These two rainfall records were then used to compare corresponding rainfall events. A second automatic rain gauge, associated with an automatic recording weather station on Dam 2 was used to measure the rainfall from February 2002 to December 2004. This site's rain gauge was subsequently used for filling in missing data from the original automatic rain gauge, which would stop recording as a result of low battery power and technical failure. In addition the data were used to verify the corresponding rainfall events. A complete record at the Dam 2 site for the period February 2002 to December 2005 was derived for the water balance simulation. A comparison of the cumulative rainfall records from the airport and the Dam 2 rain gauge are depicted in (Figure 4.2).

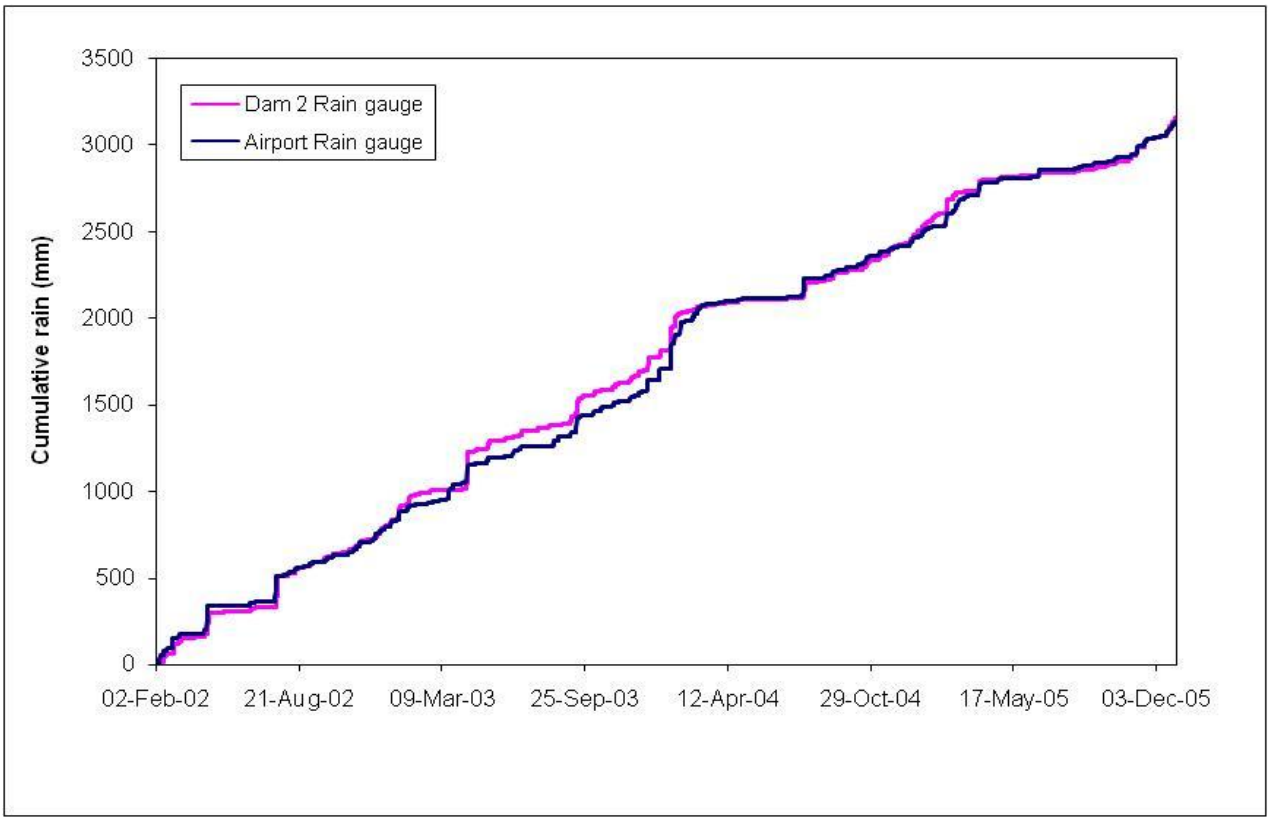

Figure 4.2 Cumulative rainfall recorded for the Durban International Airport and at Dam 2.

The daily accumulative rainfall from Dam 2 and the airport compared well for monitored period, thus acceptable rainfall data could be used with confidence in an appropriate model.

4.3 Evaporation

Water evaporates from the soil and plant surfaces and transpires through the plant to satisfy an atmospheric demand. The combination of these processes i.e. evaporation from the surface and transpiration from the plants is termed evapotranspiration. Potential evaporation (ET_o) is a measure of the ability to remove water from the surface through the processes of evapotranspiration and assuming non-limiting water conditions (Clark *et al.*, 1989). Actual evaporation (ET) is the quantity of water that is actually removed from the surface through evapotranspiration. No single method of ET_o determination is likely to be ideal for all circumstances. Depending on the availability of data, common methods may infer potential ET through a direct measure of evaporation from a Class A-pan or an indirect estimate using an empirical equation, for example, the Penman - Monteith equation.

There are two parts to the evaporation discussion. In the first part, the method and computation for determining the estimates of daily ET_o is explained. In the second part, the relationship between Penman – Monteith estimates and Class A-pan data are assessed.

4.4 Data and method of computation of Penman – Monteith equation

The Food and Agriculture Organisation (FAO) methodology is considered the international standard for predicting crop water requirements (Allen, 1998). Reference crop evapotranspiration refers to ET from a uniform green crop surface, actively growing, of uniform height, completely shading the ground, under well-watered conditions. There are four methods that are recommended by the Food and Agriculture Organisation. The Penman method only requires radiation, but has the potential of being erratic in arid climates. The Blaney–Criddle method requires temperature parameters only, which are empirical and require local calibration to achieve satisfactory results. Pan evaporation methods clearly predict the microclimatic conditions; since the study area is small A-pan data for the use of comparison could prove to be useful. Any of the selected methods used for estimating ET_o depends on the availability of data (Smith, 1992).

Sufficient data were available for calculating ET_o using the Penman – Monteith method, thus this method could be used in this study as presented in (Equation 4.1).

$$ET_o = \frac{0.408\Delta(R_n - G) + \gamma \frac{900}{T + 273} u_2 (e_s - e_a)}{\Delta + \gamma(1 + 0.34u_2)} \qquad 4.1$$

where

ET_0 is the potential evaporation [mm/day],

R_n is the net radiation at the crop surface [MJ/m^2/day],

G is the soil heat flux density [MJ/m^2/day],

T is the mean daily temperature at 2m height [^{o}C],

u_2 is the wind speed at 2 m height [m/s],

e_s is the saturated vapour pressure [kPa],

e_a is the vapour pressure [kPa],

$e_s - e_e$ is the saturated vapour pressure deficit [kPa],

Δ is the slope of vapour pressure curve [kPa/^{o}C], and

γ is the psychometric constant [kPa/^{o}C].

With Δ the slope of the saturation vapour pressure curve in kPa /^{o}C

$$\Delta = \frac{4098 e_s}{(T_a + 273.3)^2} \qquad 4.2$$

and G the soil heat flux (MJ/m^2/day) calculated from the current day's (DOY) and previous day's (DOY-1) average air temperature (T_{avg}).

$$G = 0.38[T_{avg}(DOY) - T_{avg}(DOY - 1)] \qquad 4.3$$

where

$$T_{avg} = \frac{(T_{\max} + T_{\min})}{2} \qquad 4.4$$

γ is the psychrometer constant (kPa/^{o}C) and is calculated as:

$$\gamma = \frac{0.00163 P_a}{\lambda} \qquad 4.5$$

with λ the latent heat of vapourisation (MJ/kg)

$$\lambda = 2.501 - 2.361 \times 10^{-3} T_{avg} \qquad 4.6$$

The weather parameters were measured at 15 min intervals using the automatic weather station on Dam 2. However, it was decided that daily estimates of these parameters would be derived, since daily estimates were available for comparison from the Durban International Airport. The disadvantage of calculating ET_o at the daily time step is the loss of intra-daily variation. The principle weather parameters considered are presented below and once again these parameters were compared to the parameters measured at the Durban International Airport. Thus the airport estimates could be used as a means to verify daily estimates and as a surrogate for missing data or where the data were suspect. Missing data or suspect data from the weather station was associated to battery failure and corrosion related problems to electrical components within the weather station. The weather station was powered by a solar radiation panel, which powered the unit during daylight but during the night the unit was powered by battery. If the battery was low, data would be missing for the duration of non

light hours. The station would start recording when the sun emerged in the morning. The associated electrical problems were a direct consequence of the humid conditions at the site, which would corrode components. This would result in recorded data being suspect and therefore had to be compared against the data from Durban International Airport.

4.5 Net radiation

Net radiation provides the largest source of energy available for the vapourisation of water to water vapour and this is reflected in the Penman – Monteith equation. Since net radiation is the most important variable in the ET_o estimation, great care was taken during the calculation of the daily values for this variable. The net radiation at the weather station was measured in terms of power (W/m^2) whereas for the Penman – Monteith equation, values of energy ($MJ/m^2/day$) are required. The net power can be converted into daily net energy (MJ/m^2) by integrating the power over the length of the day from dawn to dusk (Blight, 2002) and converting to energy units using (Equation 4.7).

1 Joule = 1 Watt*1 s 4.7

According to Schulze, (1997) the energy from net radiation should be within the range 4 - 36 MJ/m^2 for the Durban region. The comparison between daily net radiation data for the Dams and Durban International Airport are illustrated in (Figure 4.3) and reveal the estimates of daily net radiation to be within this range and are thus considered acceptable. The recorded data values smaller are considered to be outliers. The difference in the daily net radiation values could be the result of factors such as location. Altitude and distance from the sea would influence factors such as cloud cover and this would be the reason for the differences in daily net radiation.

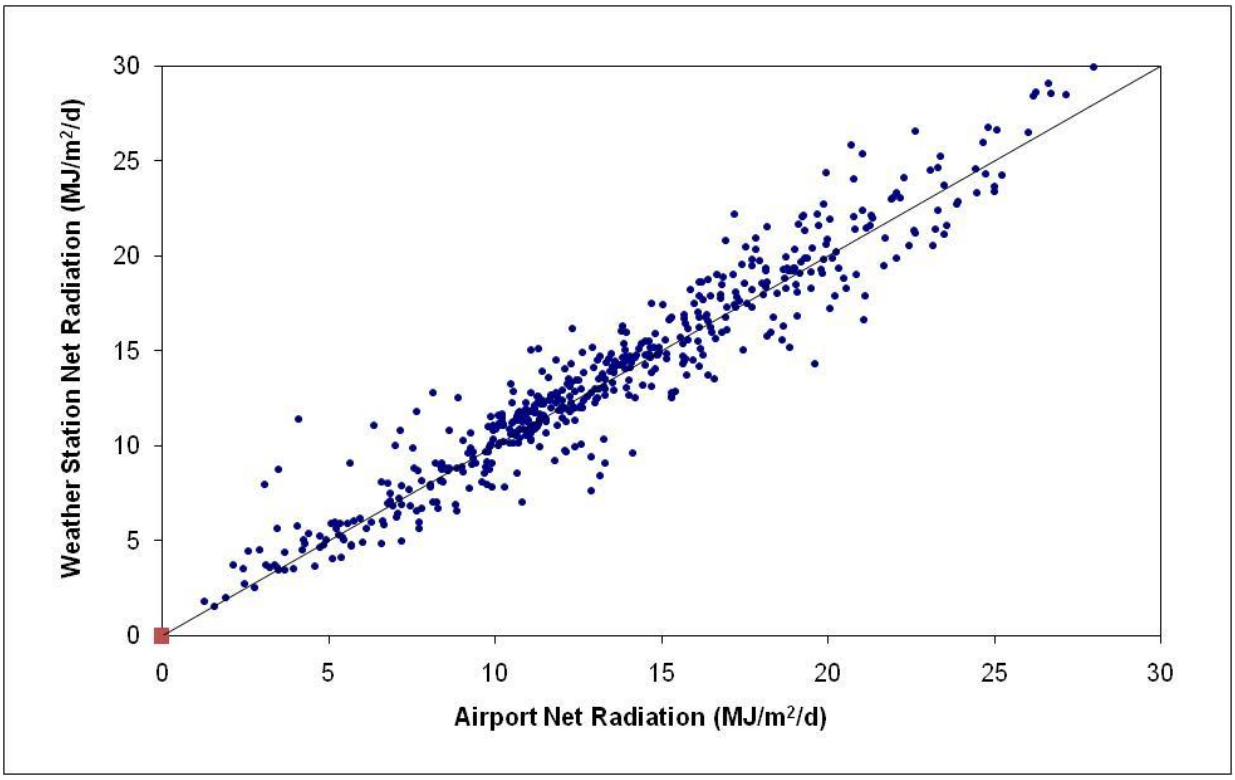

Figure 4.3 Comparison of daily net radiation for the weather station against Durban International Airport.

The correlation coefficient (r^2), for the data presented equals 0.919. The missing daily net radiation values for the Dams could thus be calculated using the correlation equation.

4.6 Temperature

The air temperature above the earth's surface is controlled by the net radiation and the heat emitted from the surface. The rate of evapotranspiration is influenced by surrounding air, since it transfers energy to the crop. Evapotranspiration would be higher in sunny warm weather (higher temperatures) than in cloudy and cool weather (lower temperatures) (Allen, 1998). The temperature variables needed for Penman – Monteith equation were the maximum, minimum and the average daily temperatures. The respective highest and lowest temperatures of the day were extracted from the recorded weather station data on the Dams. Comparison of the highest daily temperatures for the weather station against the Durban International Airport is presented in (Figure 4.4) and had an (r^2) equal to 0.936. These are close when compared, since the highest daily temperature would be during the hours of midday when the weather station was powered by the solar radiation panel. If there were any

problems related to low battery it would not affect this high temperature record. Comparison of the lowest daily temperatures is presented in (Figure 4.5) and had an (r^2) equal to 0.894. The lowest daily temperature would be during the night time and considering periods when the weather station was not recording throughout the night due to low battery. The lowest temperature on record would be the early morning or late afternoon, which would be a few degrees higher than the actual lowest temperature. This would explain the lower (r^2) for the daily low temperatures. Missing daily high and low temperatures for the weather station were calculated using the respective correlation equations.

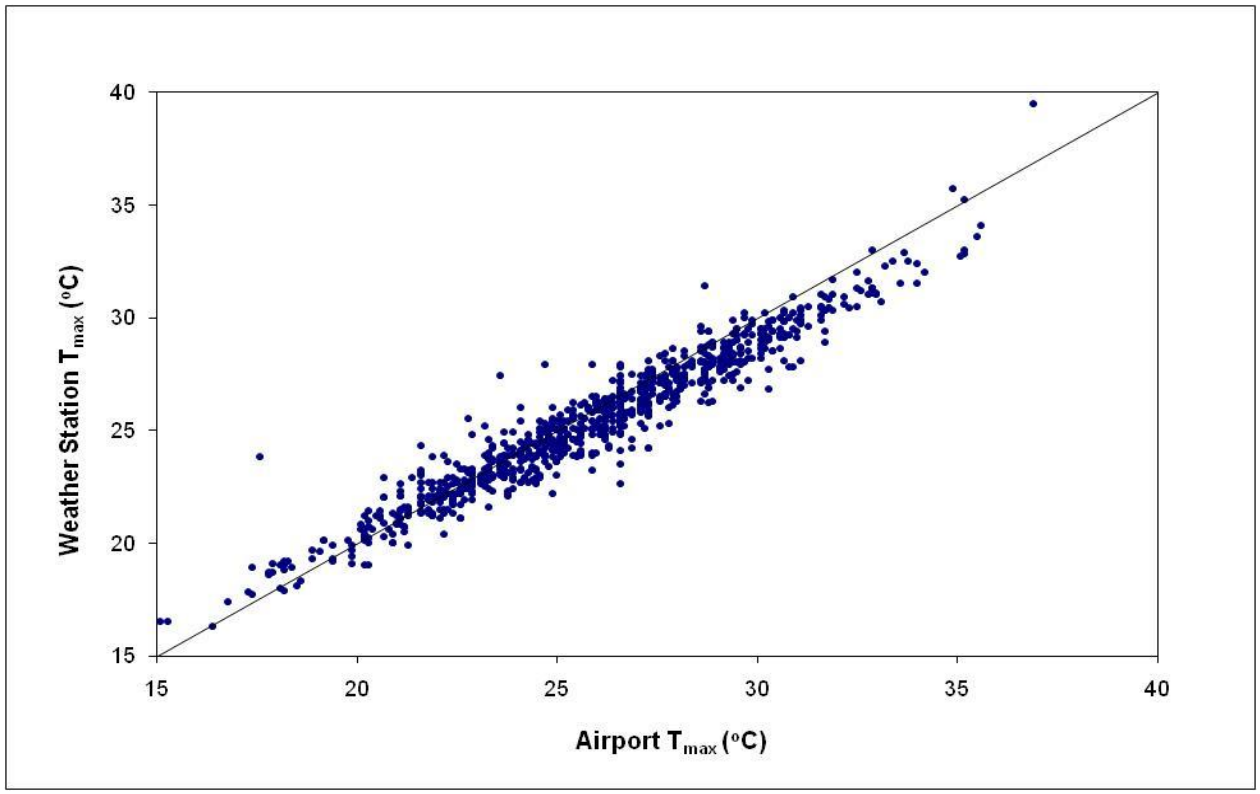

Figure 4.4 Comparison of daily high temperature for the weather station against Durban International Airport.

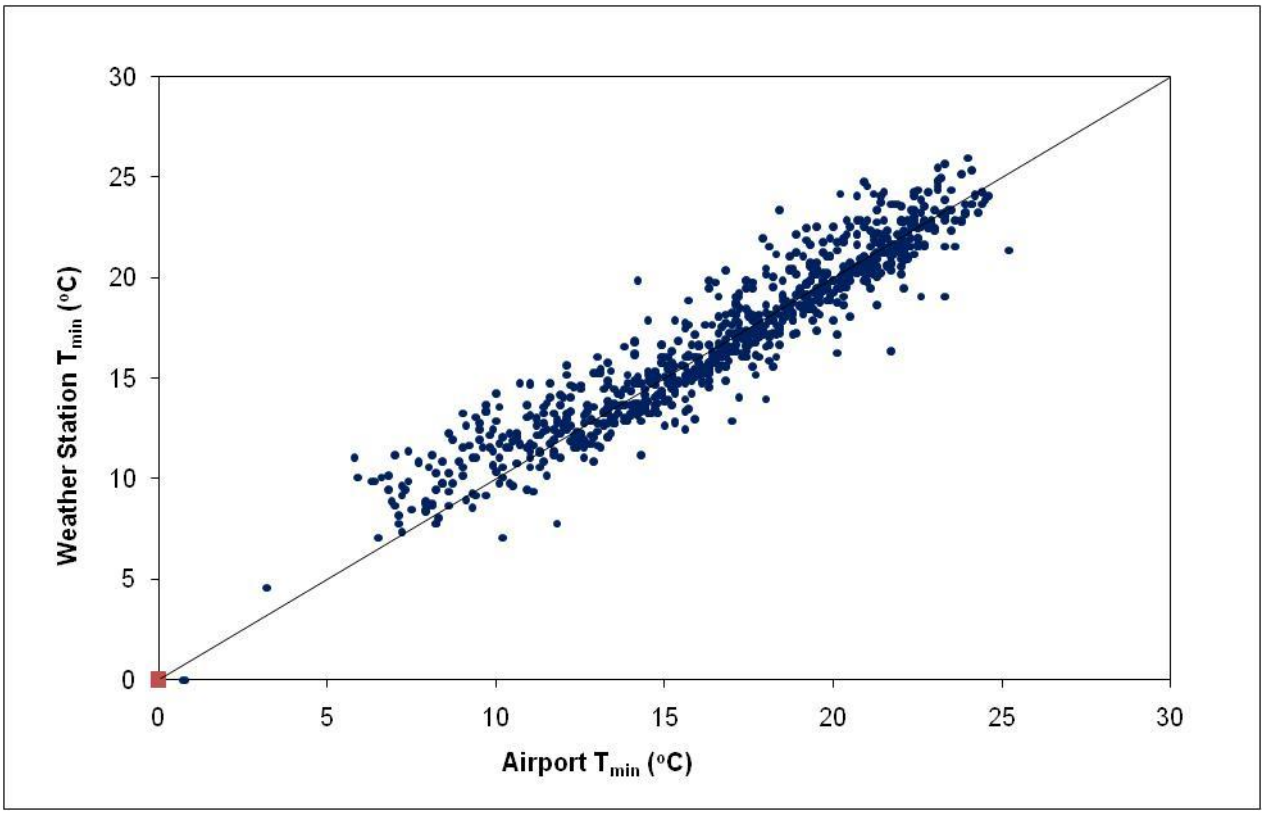

Figure 4.5 Comparison of daily low temperature for the weather station against Durban International Airport.

4.7 Ambient relative humidity

While the net radiation and the air temperature are the main driving forces for vapourisation of water. The removal of vapour is also largely determined by the water vapour pressure at the evapotranspiring surface and the surrounding air. The daily maximum and minimum relative humidity data were extracted from the weather station record. (Figure 4.6) and (Figure 4.7) compare the ambient relative humidity for the Dams against the ambient relative humidity data from the airport.

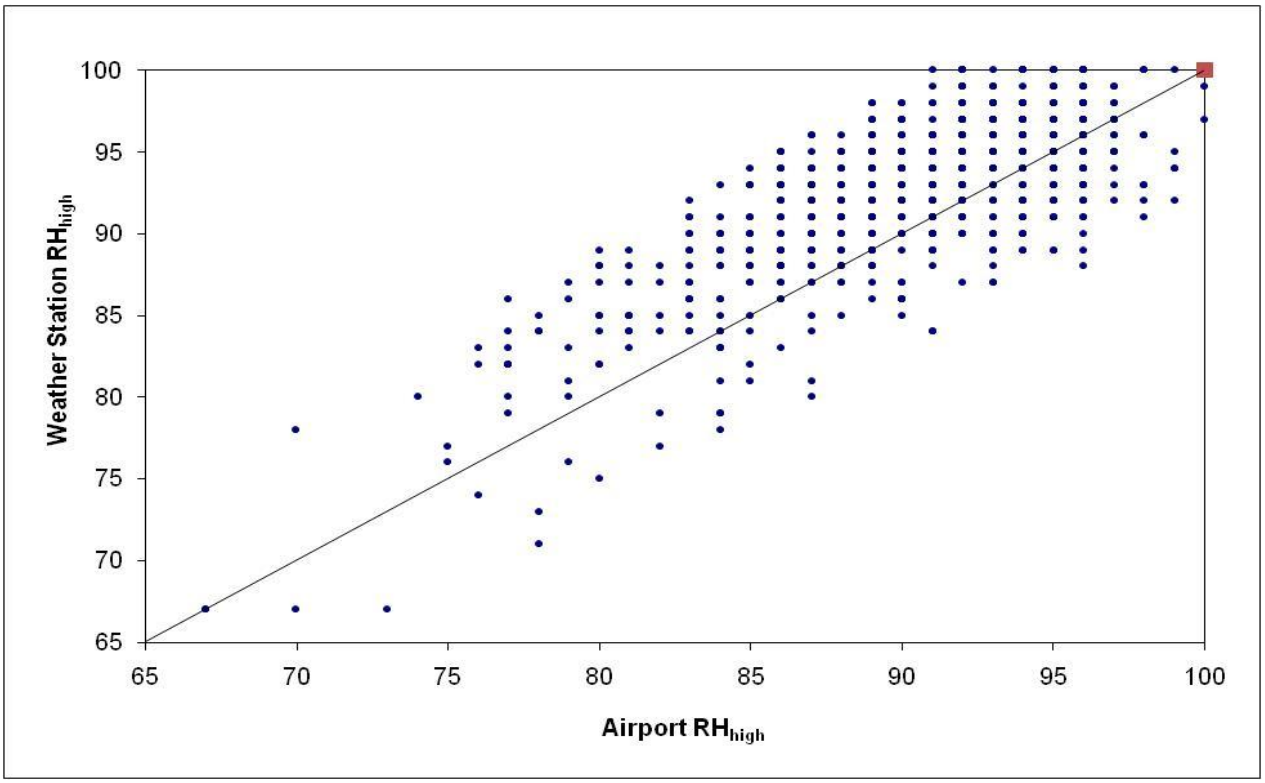

Figure 4.6 Comparison of the daily maximum humidity for the weather station against Durban International Airport.

The correlation of the daily maximum humidity for the weather station against Durban International Airport had a coefficient (r^2) equal to 0.610. The difference may be the result of locality between the two sites and the sensors that are used to record the humidity at the respective sites. The correlation of the daily minimum humidity for the weather station against Durban International Airport had a coefficient (r^2) equal to 0.936. Missing values for the weather station were calculated using the respective correlation equations.

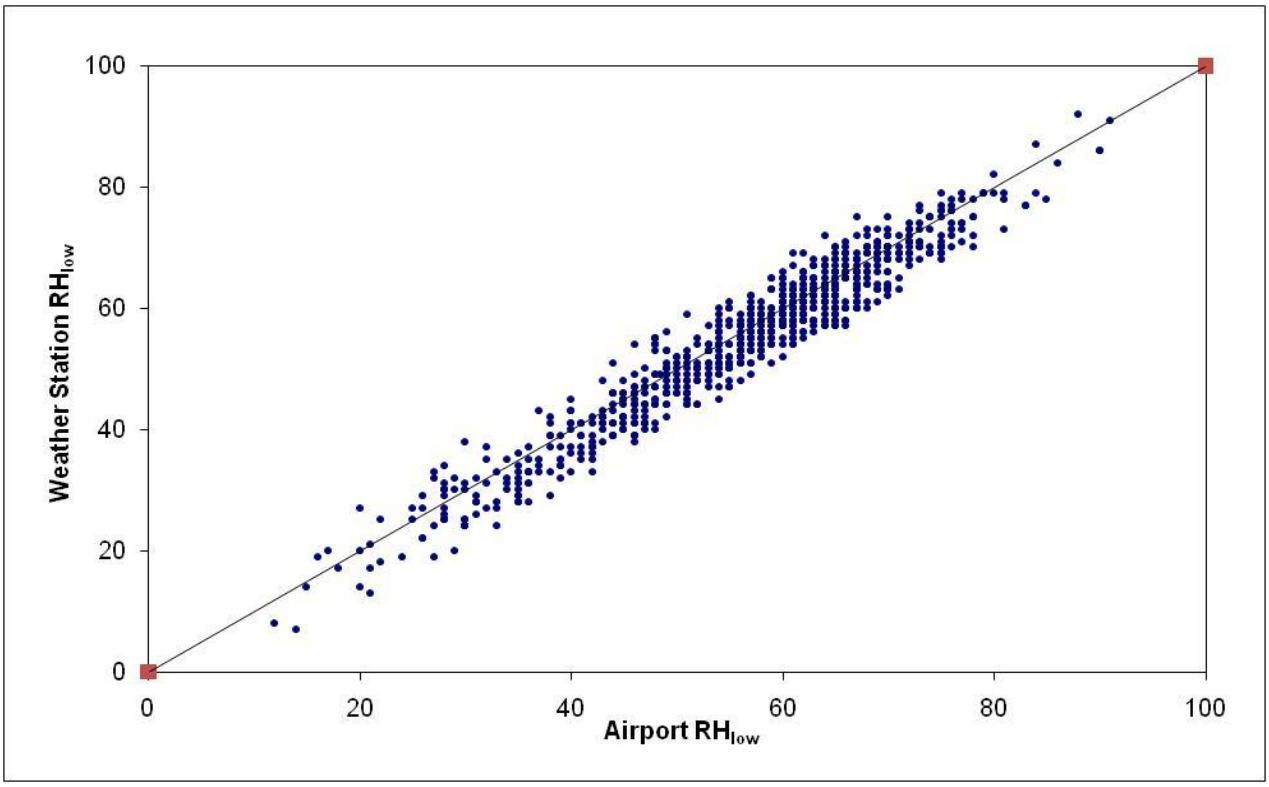

Figure 4.7 Comparison of the recorded low humidity for the Durban International Airport and the weather station on the Dam 2.

4.8 Wind velocity

When water evaporates, the air above the evaporating surface gradually becomes saturated. Wind aids in the removal of this saturated air, replacing it with drier air (depends on the up-field wind conditions). Windy conditions allow for the air above the surface to continuously be replaced with drier air. Under these circumstances, more water vapour can be taken up (Allen, 1998). As operations at the Dams were undertaken under humid conditions, the wind replaces the saturated air with slightly less saturated (humid) air. Consequently, the wind velocity affects the evapotranspiration to a far lesser extent than the net radiation, temperature and ambient relative humidity. In fact (Blight, 2002) demonstrated in experiments under humidified conditions, that even with considerable increased wind velocities there was no significant increase in evapotranspiration. In fact, transpiration from vegetation may even decrease with increasing wind velocity due to closure of the stomata to conserve water (Blight, 2002). For the purpose of this study the missing wind velocity values were simply replaced with a wind velocity of 2 m/s. Other factors for this decision were the distance

between the airport and the Dams. The higher elevation of the Dams Area and closer distance to the sea would result in the Dams having potentially higher wind velocity of the two sites.

The water balance components of the Dams comprise input by rainfall and output by evapotranspiration as well as fluxes to the groundwater. The difference between the input and output is the changes in the storage within the Dams material expressed in (Equation 4.8).

$$\Delta S = P - ET - D \qquad 4.8$$

where

- ΔS is the change in the volume of water held in storage per unit area (mm),
- P is the volume of precipitation per unit area (mm),
- ET is the volume of water lost through evaporation (climate and porous media dependent) and transpiration (species dependent) per unit area (mm), and
- D is the volume of water draining out the bottom of the waste site per unit area (mm).

The precipitation component of the water balance was obtained from the meteorological data. Thus in order to complete the water balance for the Dams the evaporation component needed to be evaluated.

4.9 Monthly Potential Evaporation and Monthly Rainfall

The comparison of the monthly rainfall and monthly potential evaporation for the period of 2002 to 2005 indicates a large capacity for the use of the vegetation as a cover (Equation 4.9). The average ratio of ET_o to rainfall for this period was:

$$ET_o/P = 4700/3158 \qquad 4.9$$

$$= 1.48$$

This simple average ratio comparison of ET_o and rainfall would show that the potential evaporation is greater, however the cause of concern would be times when the rain would be higher thereby increasing the potential for high seepage volumes. This comparison of the monthly rainfall and monthly potential evaporation is illustrated in the (Figure 4.8). As indicated by the red arrows the maximum rainfall months that could be of major concern occurred during July 2002, April 2003, September 2003 and January 2004 respectively. During these months the rainfall exceeds the ET_o and extreme rainfall events will be worth noting to assess the vegetation cover and impacts on the groundwater.

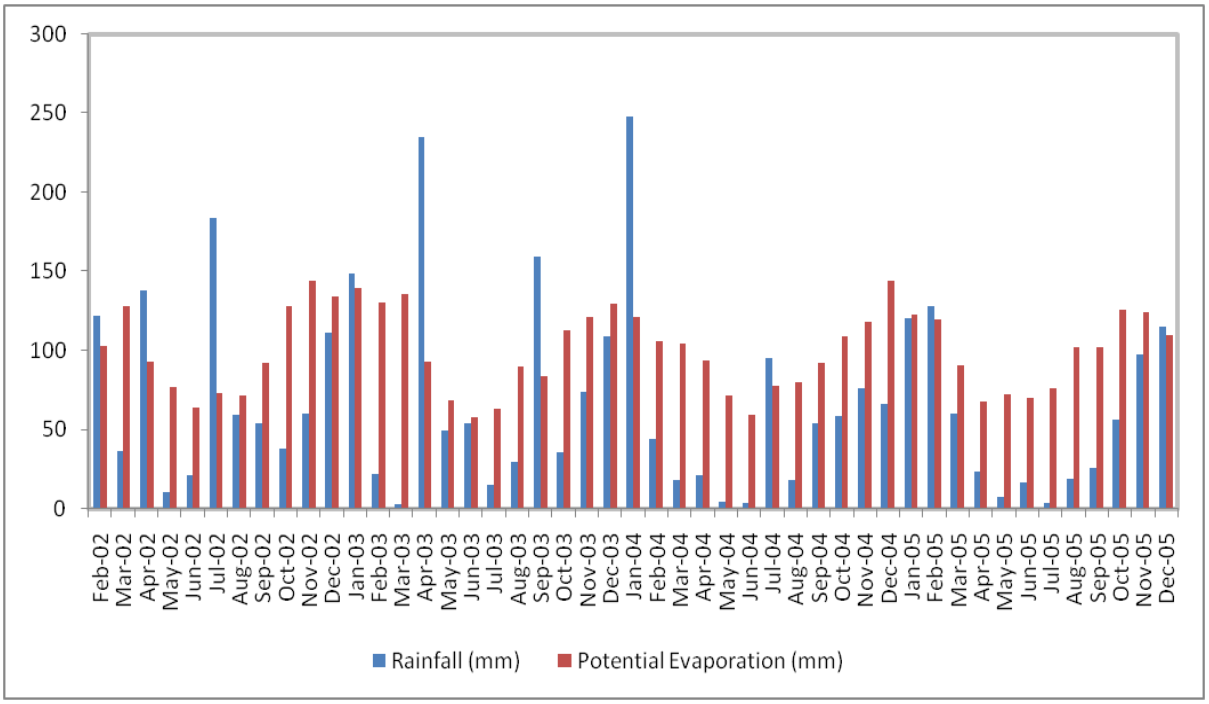

Figure 4.8 Monthly comparison of the rainfall and reference potential evaporation.

4.10 A-pan evaporation

Data from Class A-pan evaporation were used as a basis for assessing the estimated potential evaporation calculated from the Penman – Monteith equation. The A-pan is a conventional and popular method used for the estimation of ET_o. The A-pan is, however, sensitive towards micro-climatic conditions, especially its management, the soil heat flux and vegetation cover around the pan (Smith, 1992). Reading for the Class A-pan, which was situated on the Dams site, were taken every two to three days.

Calculated potential evaporation estimates were compared against the measured A-pan evaporation. The amount of water evaporated from the A-pan over a period was divided by the duration of the period to give the average rate of evaporation. A-pan readings were recorded every two or three days, thus the total water evaporated from the A-pan was divided by the days from the last reading. For example if the last reading was 3 days ago and the measurement of 24 mm evaporated, a average daily rate of 8 mm was considered to have evaporated per day. This was not a very accurate way to determine average daily evaporation rate, since the evaporation for a particular day may actually be higher or lower than the calculated daily values. Other inaccuracies with the A-pan readings result from its physical dimensions and exposure to the atmosphere render its readings unrepresentative. According to Bosman, (1990), screening of the A-pan, which was the case for the A-pan on the Dams, evaporation losses are suppressed by 5-15%. Thus it would be expected that the estimated ET_o via the Penman-Monteith equation would be higher than the measured A-pan values. A difference of 20% was calculated for the period (Figure 4.9) of February to October 2002.

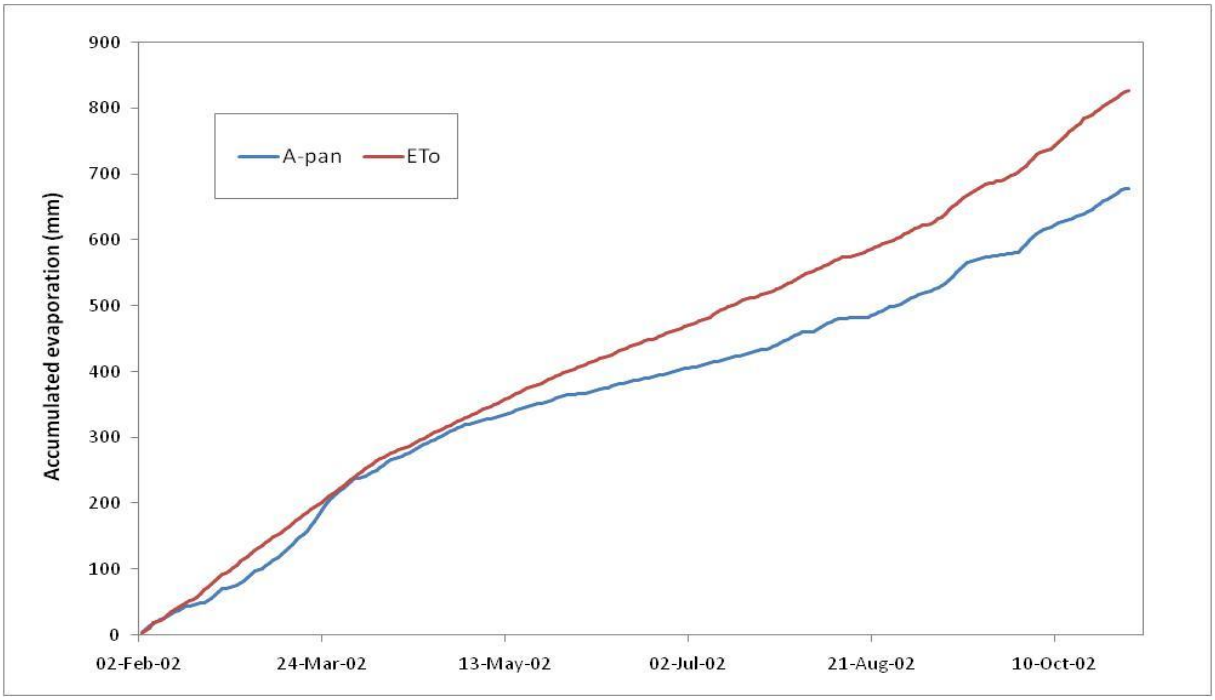

Figure 4.9 Comparison of the accumulated A-pan against accumulated ET_o for 2002.

4.11 Actual Evaporation using Sap flow experiments on Dam 2

A means of measuring the evapotranspiration (ET) is required to assess the water balance of the vegetation cover of the Dams. Actual ET determination is more difficult and requires direct measurements. Techniques used to estimate ET on the Dam 2 were derived from sap flow measurements of the various tree species and ET measurements on Dam 3-4 were derived from Bowen ratio energy techniques on the mixed vegetation. The sap flow estimation experiments were performed by the School of Applied Environmental Sciences at the University of Natal, Environmentek, CSIR, C/O Agrometeorolgy. The following results and discussion of the sap flow measurements was the work performed by the Everson (2003).

The sap flow measurements studies were designed to record transpiration rates at different times of the year for three different tree species on Dam 2. The tree species have a greater potential for transpiration on the Dams, simply for factors of the rooting physiology within the Dams. The technique measures sap flow rates within the tree stems using the heat-pulse velocity. This technique is based on the principle of releasing short pulses of heat into the outer, sapwood portion of the tree stem and recording how quickly the heat is carried by the rising sap to the fixed measurement point of heat release. Thus probes, one of releasing heat at pre-determined intervals, and the other recording the temperature of the sap are positioned around the tree stem. The conclusion of the study is that careful measurements are made on the various sapwood characteristics (moisture content, density, sapwood area, etc) and a final sap flow is calculated for the tree. This can then be expressed in mm units of and equivalent depth of water by dividing the litres per tree by the area occupied by the tree canopy. The sap flow measurements were made on three tree species on Dam 2. The species were:
Bugweed *(Solanum maurtianum),*
Pigeonwood *(Trema orientalis)* and
Fig *(Ficu natalensis).*
Useful results were derived from two species, i.e. Bugweed and Pigeonwood. However, for the Fig tree the presence of latex exuded at the wound would interfere with recordings, thus measurements could not be concluded.

The following results were concluded by Everson, (2003) from the sap flow experiments. During the summer volumetric water use values of 60-80 L/day were derived for the larger species of Pigeonwood and for the Bugweed values of 20-30 L/day. However, due to the larger canopy of the Pigeonwood the uptake rate in mm/day is less for the Pigeonwood than for the Bugweed species. The experiments also indicated a drop in water use for the Bugweed in mid June as a reaction to stress due to drought conditions. The drop in water use was less evident in the Pigeonwood species. This was attributable to the shallower root system of the Bugweed species.

The sap flow results from the Pigeonwood tree species are illustrated in (Figure 4.10) and results of the Bugweed are illustrated in (Figure 4.11). The sap flow measurements derived for the summer months was 2 mm/day and winter months had sap flow rates of 0.5 mm/day. The measurements do not include the interception losses and the ET from the understory.

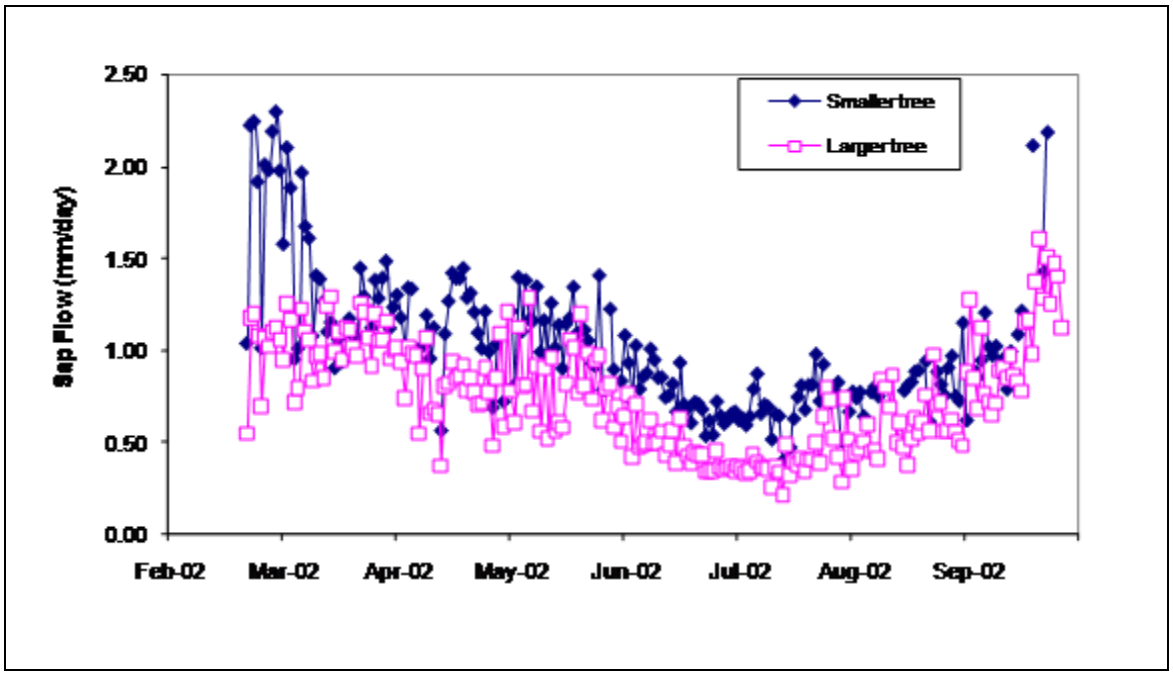

Figure 4.10 Sap flow rate from large and small Pigeonwood tree species

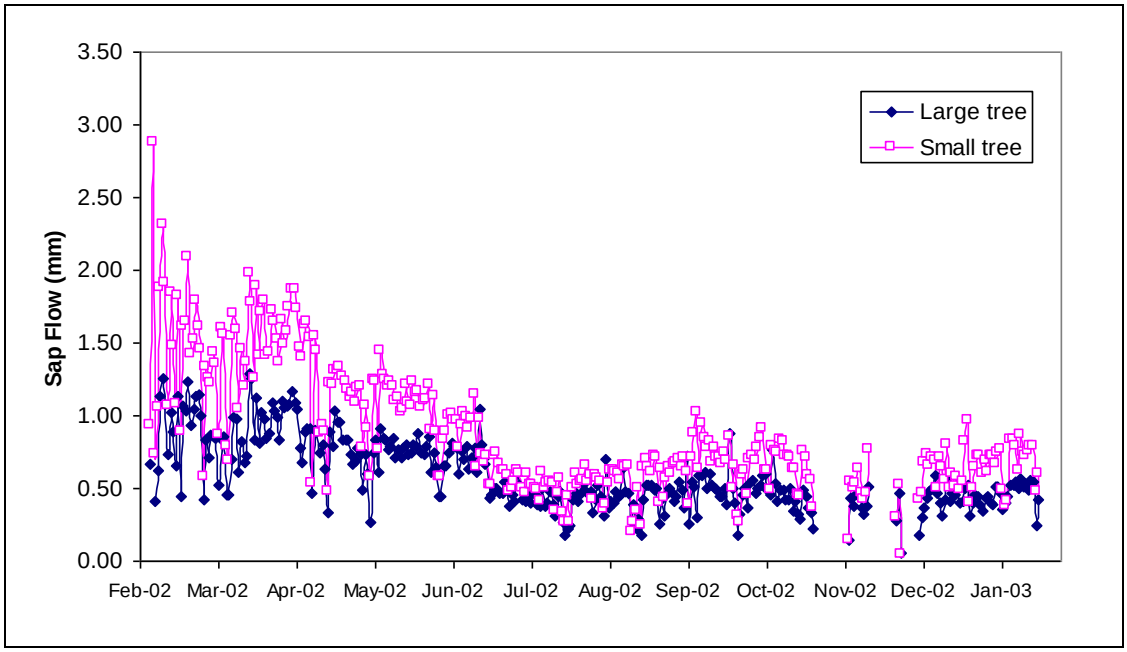

Figure 4.11 Sap flow rate from large and small Bugweed tree species.

Actual evaporation can be calculated from the potential evaporation estimate by considering an appropriate crop coefficient (K_c) as expressed in (Equation 4.10).

$$ET = ET_o \times K_c \qquad 4.10$$

where K_c is the crop coefficient,

ET is the actual evaporation, and

ET_o is the potential evaporation.

The ET for the Fig tree and the Bare site was calculated by application a crop coefficient for the respective sites as presented in (Table 4.2) for the Fig tree and (Table 4.3) for the Bare site. The crop factor estimates for the Fig tree were derived from the sap flow experiments performed on Dam 2. The crop coefficient estimates for the Fig tree site would be expected to be higher if compared to the measurements derived from the other tree species. The Fig tree has a deeper and wider root system, larger tree stem, larger *LAI* and do not lose the leaves during the winter months.

Table 4.2 Estimated monthly crop coefficients derived for the Fig tree.

Description	Jan	Feb	Mar	Apr	May	Jun	Jul	Aug	Sept	Oct	Nov	Dec
Fig tree	0.75	0.75	0.75	0.75	0.75	0.75	0.75	0.75	0.75	0.75	0.75	0.75
Understory	0.1	0.1	0.1	0.1	0.1	0.1	0.1	0.1	0.1	0.1	0.1	0.1

Table 4.3 Estimated monthly crop coefficients derived for the Bare site.

Description	Jan	Feb	Mar	Apr	May	Jun	Jul	Aug	Sept	Oct	Nov	Dec
Bare site	0.7	0.7	0.7	0.7	0.7	0.7	0.7	0.7	0.7	0.7	0.7	0.7

4.12 Bowen ratio experiment of Dam 3-4

Estimates of the ET on Dam 3-4 were measured using Bowen ratio energy balance techniques. The Bowen ratio energy balance method requires measurements of net irradiance, soil heat flux density and the mean air temperature and water vapour pressure differences. The net irradiance and soil heat flux density are used to establish the available energy. The Bowen ratio experiments were performed by the School of Applied Environmental Sciences at the University of Natal, Environmentek, CSIR, C/O Agrometeorolgy. The following results and discussion of the Bowen ratio measurements was the work performed by the Everson (2003). Soil heat flux plates, together with averaging thermocouples are used to calculate the soil heat flux density at the soil surface. The buried soil heat flux plates sense the soil heat flux density at the soil surface. Two pairs of averaging thermocouples, buried at 20 and 60 mm, are used to calculate the heat stored above the soil heat flux plates for the soil temperature increase. The heat stored in the soil is calculated from the change in soil temperature and the specific heat capacity of the soil. The specific heat capacity of the soil is a function of the bulk density of the soil, the specific heat of dry soil, and the specific heat of the water and the soil water content The Bowen ratio system is equipped with instrumentation for measuring and calculating of the average air temperatures and vapour pressures. The Bowen ratio estimates of actual evapotranspiration (BET) experiment was conducted on Dam 3-4 for the period February to December 2002. Experiment measurements of the evapotranspiration i.e. vegetation transpiration and soil water evaporation were made above recently planted indigenous trees, mixed with weedy, early colonising species as illustrated in (Figure 4.12).

Figure 4.12 Bowen ratio experiment on the Dam 3-4.

The crop factor estimates for the vegetation were derived by assessing of the Bowen ratio experiment data performed on Dam 3-4. The monthly crop coefficients presented in (Table 4.4) were derived from the experiments performed on the mixed woody species on Dam 3-4.

Table 4.4 Monthly crop coefficients used in the modelling exercise.

Description	Jan	Feb	Mar	Apr	May	Jun	Jul	Aug	Sept	Oct	Nov	Dec
Shrubs/grass	0.63	0.63	0.6	0.45	0.4	0.3	0.3	0.3	0.4	0.6	0.63	0.63
Understory	0.15	0.15	0.17	0.2	0.25	0.3	0.3	0.3	0.25	0.2	0.15	0.15

Bowen ratio measurements were compared to the derived ET estimates, which were calculated from the potential evaporation estimate and considering the monthly crop coefficient. The comparison of the Bowen ratio evapotranspiration measurements (BET) against the estimated ET is illustrated in (Figure 4.13).

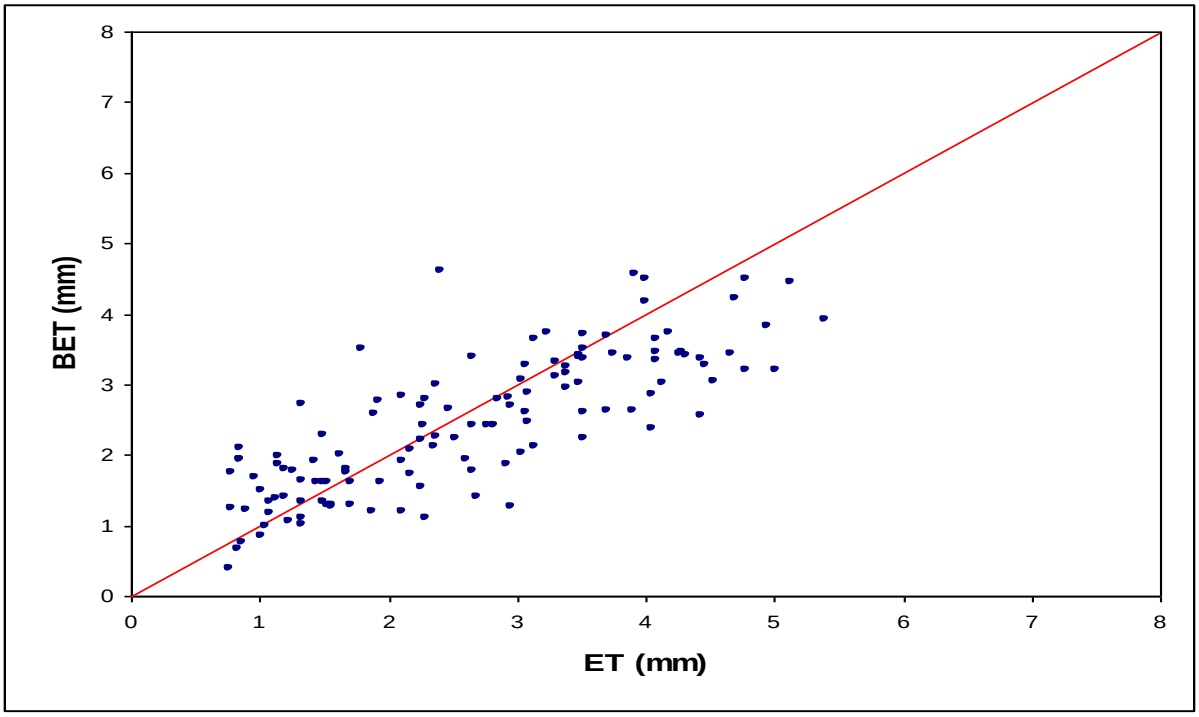

Figure 4.13 Comparison of the measured Bowen ratio evapotranspiration measurements, (BET), against the estimated actual evapotranspiration.

If the success of the water balance was based on the difference between input and output of the above ground parameters, this study would not deem necessary and the only concerns would probably be the major rainfall events. But the system in its entirety is more complex, thus the major component of this study should consider the processes that occur in the subsurface. These are investigated further in material characteristics chapter of this study.

5. MATERIAL CHARACTERISTICS

Groundwater recharge is frequently estimated from elementary meteorological information such as that provided in Chapter 4. Despite decades of research efforts on the individual processes, such methods can hardly be relied on for an accurate water balance study. Thus, in order to adequately quantify the groundwater recharge, sufficient information of the porous media hydraulic characteristics and the dynamics of the interstitial water are required. There are numerous techniques for measuring and monitoring these subsurface variables. The specific instruments and techniques used in this study were developed and tested in the hydrological processes laboratory in the School of Bioresources Engineering and Environmental Hydrology at the University of Natal (Lorentz *et al.*, 2001).

Previous studies of the waste material from the Dams indicated extremely low hydraulic conductivity. As a result of the extreme fine nature and high surface area, bond water to their surface and as a result have an exceptionally high water retention capacity. This evidently would result in a perched water table within the Dams, which extremely low flow occurs in the horizontal and vertical direction (Druzynski and Duthe, 2003). Analysis of waste material from selected locations and depths on the experimental site were analysed to determine their hydraulic characteristics. It is important to understand that dumping over the years occurred in layers, thus heterogeneity of the material should primarily occur vertically. Soil geohydrological information at different sites on the respective Dams would be similar with respect to material characteristics at a specified depth.

Soil geohydrological information required is detailed in the subsections 5.1 to 5.5 and comprises:

- Gravimetric water content survey
- Texture and soil particle size distribution;
- Water retention information;
- Saturation hydraulic conductivity;
- Unsaturated hydraulic conductivity characteristic.

5.1 Gravimetric Water Content

Porosity is defined as the ratio of volume of voids to the total volume of the waste material. The effective porosity defines the volume of water that a given volume of bulk porous medium can contain. Water content reflects the volume of the void space that is filled with water, relative to the bulk porous medium. Water content values were measured down the profile in Dam 2 at the Bare, Fig tree, and Bugweed sites. The water content was determined by drying samples at 105^{o}C to calculate the mass of water in the sample. The water content results are presented in Appendix A. The water contents were low in the first 2 m of the profile, ranging from approximately 0.18 to 0.35, but were high (ranging from approximately 0.6 to 0.9) throughout the rest of the profile as illustrated in (Figure 5.1), which superimposes an equilibrium status retention characteristic curve (Lorentz and Morgan, 2006) on the data. This curve was derived by assuming the water table depth below the surface to be at 15 m. The soil water tension in the material above that, at equilibrium, would be the elevation above the 15 m depth. This elevation (or tension) was applied to each water retention characteristic of the appropriate material at each elevation, yielding a water content, which is plotted as the equilibrium water content line.

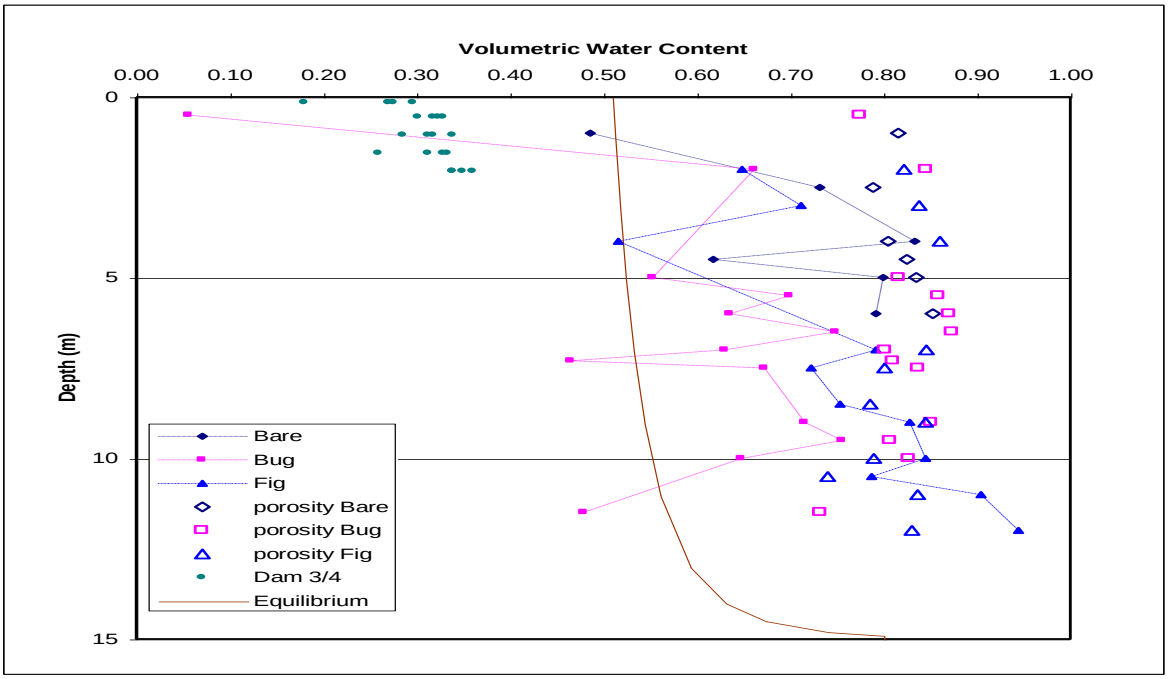

Figure 5.1 Water content and porosity down the profile with a superimposed equilibrium water retention characteristic (Lorentz and Morgan, 2006)

Based on the historical information described in Chapter 3, relating to the materials deposited in the Dams, it would be expected that the particle size would be much smaller than that of clay. Deposited materials some slurry's, may respond different to that of soils with regard to characteristics of water retention and hydraulic properties. The textural analysis of the material would prove important in this study.

5.2 Textural analysis and waste material particle size distribution

The particle size distribution often referred to as the texture of the soil (porous medium), may be defined as the relative proportions of sand, slit and clay size particles. The particle size distribution influences the soil behaviour e.g. infiltration of water, hydraulic conductivity, water retention characteristics, its ability to aggregate and propensity for crusting after successive wetting and drying (Gee and Or, 2002). The different particles in a soil sample are classified into groups of the various sizes on the basis of their effective diameter as follows:

sand 2.0 – 0.05 mm (coarse sand 2.0 – 0.5 mm, medium sand 0.5 – 0.25 mm and fine sand 0.25 – 0.05 mm)

silt 0.05 – 0.002 mm

clay < 0.002 mm

Two procedures, sieving and sedimentation, were used to measure the size of the individual soil particles. The sample to be characterized is first pre-treated with a Calgon solution, which aids in dispersing aggregates and allows them to settle faster. The residue is then air dried before being passed through a series of coarse screens of specified openings. Only material particles that are smaller than that specified opening will pass through. The remaining material that cannot pass through the sieve openings are characterized indirectly by sedimentation procedures using the hydrometer method. Results for the particle size distribution analysis are presented in Appendix B**.** Analysis of these results show materials to be in the range of fine sands to silts. It is imperative to note that although these materials are characterised according to the soils particle size distribution, they are not soils and thus may in effect have different characteristics.

5.3 Water Retention Characteristics

Soil hydraulic properties are required in order to model transport of water in the vadose zone. The ability of a porous media to retain and transmit water is characterized by the relationships between water content, (θ), matric pressure head, (h), and the hydraulic conductivity, (K). The most substantial challenges for experimental and theoretical investigations of fluid flow in unsaturated porous media, result from the extremely nonlinear behaviour of the hydraulic properties as a function of saturation and the highly irregular nature of pore geometry (Leij and van Genuchten, 1997). The aim of this section is to provide a perspective of saturated and unsaturated hydraulic characterization and measurement used in the study of the Dams material. Determining the water retention and hydraulic conductivity characteristics in the laboratory usually disturbs the sample and is thus not a good reflection of actual field conditions. However, for this part of the analysis a specialized auger was developed to retain the structure of the undisturbed sample. The auger allowed for a steel inner core to be inserted into the head of the auger, thus allowing for an undisturbed material sample to be extracted. These inner core samples were then tightly wrapped in plastic prior the laboratory analysis.

The material water retention characteristics were derived using the outflow cell and pressure pot techniques to define the desorption characteristics. These techniques are developed to measure water content in soil as a function of capillary pressure. The points of the water retention characteristic are determined by monitoring equilibration of the capillary pressure

rather than equilibration of the liquid volumetric content. This experimental method is described in detail by Lorentz *et al.*, (2001). Effective saturation, (S_e) (often referred to as the reduced water content) is usually represented by the van Genuchten, 1980 equation below.

$$S_e = \frac{\theta - \theta_r}{\theta_s - \theta_r} = \left(\frac{1}{1 + (\alpha h)^n} \right)^m \qquad 5.1$$

where θ_s is the water content at saturation,

θ_r is the residual water content,

α is a parameter inversely related to the air entry value or matric potential required to empty the largest soil pore of water [1/L],

n is a unit less parameter related to the pore connectivity or tortuosity,

m is equal to 1-1/n and is unit less,

m, n are parameters that affect the slope or, together with,

α the location of the inflection point on the retention curve.

The mathematical curve (van Genuchten characteristic) is then fitted to the data points for the increasing values of capillary pressure head (h). (Figure 5.2) to (Figure 5.4) depict examples of the fitted van Genuchten curve to the data points of the outflow cell and pressure pot experiments and these defined parameters are used in the modelling simulations. The remainder of the curves for other sites are illustrated in Appendix B. Analysis of the van Genuchten curves characterizes the material as being of high porosity and high retention capacity. The material retains interstitial water, since relatively high volumetric water contents (> 0.4) prevail at high (h) and this retention is evident from the steep drainage curve.

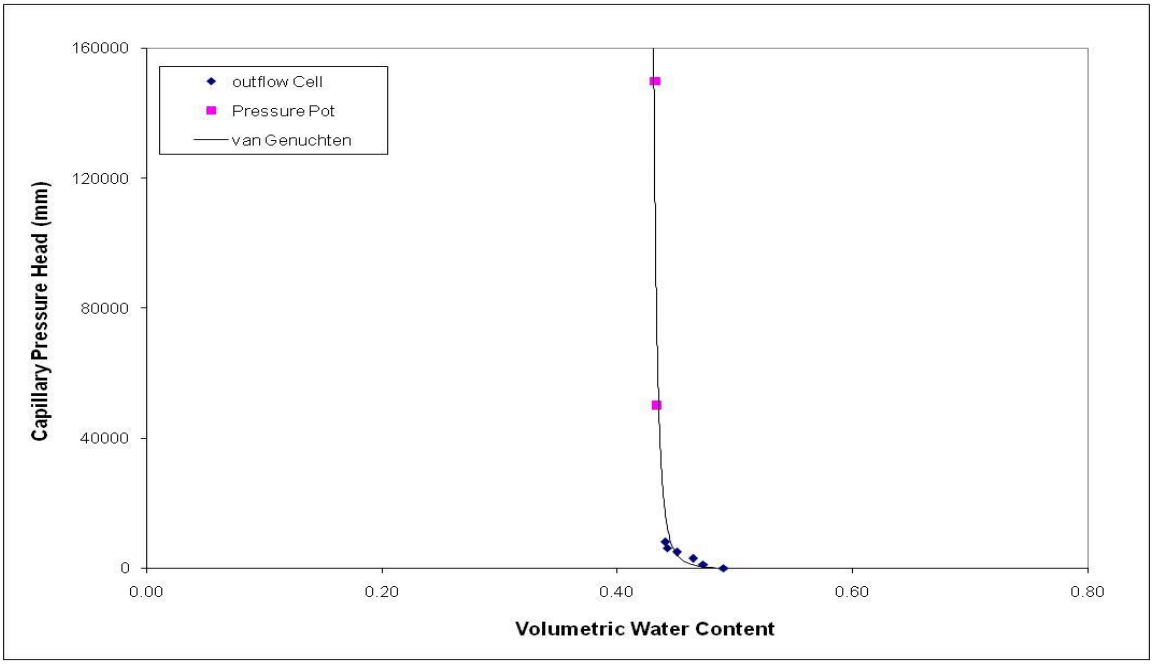

Figure 5.2 Waste material water characteristic of the Fig site material at depth 3 500 mm

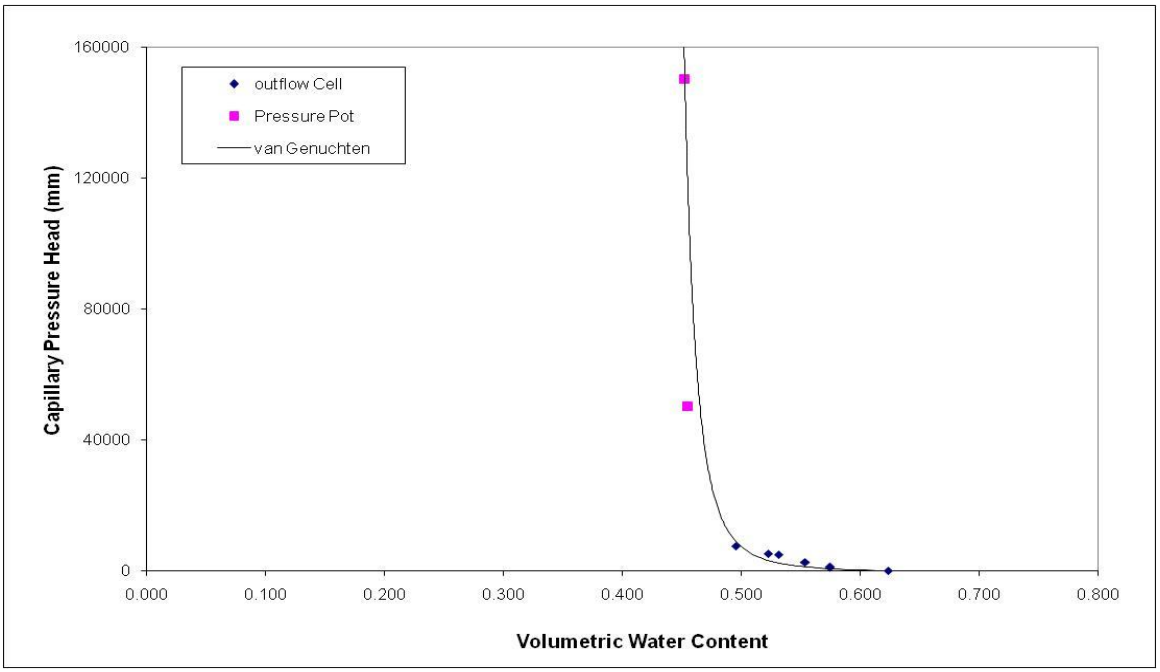

Figure 5.3 Waste material water characteristic of the Fig site material at depth 8 000 mm

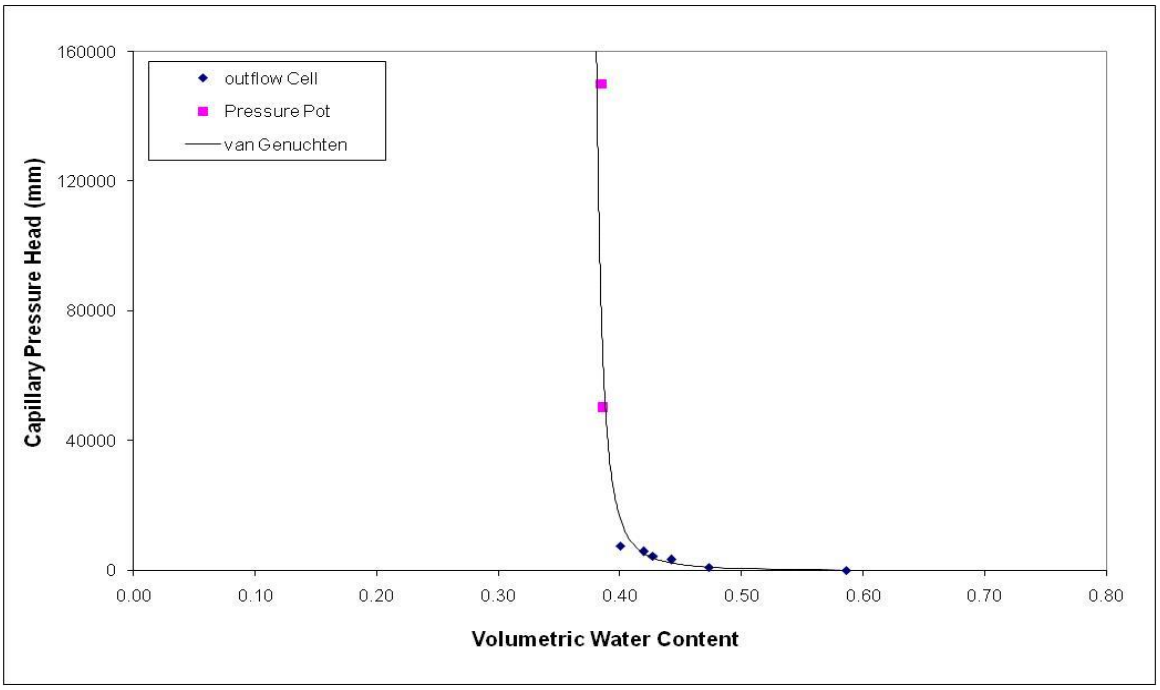

Figure 5.4 Waste material water characteristic of the Fig site material at depth 2 500 mm

5.4 Saturated Hydraulic Conductivity

The saturated hydraulic conductivity characteristics were measured in the laboratory for various depths of the waste material. These are illustrated in (Figure 5.5) for the Fig tree site and (Figure 5.6) for the Bugweed site. Saturated hydraulic conductivity was measured by means of a permeameter, by applying Darcy's Law across the permeameter pressure ports. Lorentz *et al.*, (2001) describe this experiment in detail using Darcy's Law as follows:

$$Ks_{ij} = \left(\frac{\Delta l_{ij}}{H_i - H_j} \right) \times \left(\frac{Q}{A} \right) \qquad 5.2$$

where Ks_{ij} is the saturated hydraulic conductivity of material between port *i* and *j*,

Δl_{ij} is the length of porous medium between port *i* and *j* [mm],

$H_{i\ or\ j}$ is the total hydraulic head at the port *i* or *j* [mm],

Q is the volumetric outflow rate [mm/h], and

A is the total cross sectional area of the column [mm].

The saturated hydraulic conductivity varies throughout the profile, with no observable trend down the profile. Variability with regard to colour, hardness and moisture of the material at varying depth is as a result of the different materials discarded over time. Values of the saturated conductivity varied in range from less than 1 mm/h to 91 mm/h.

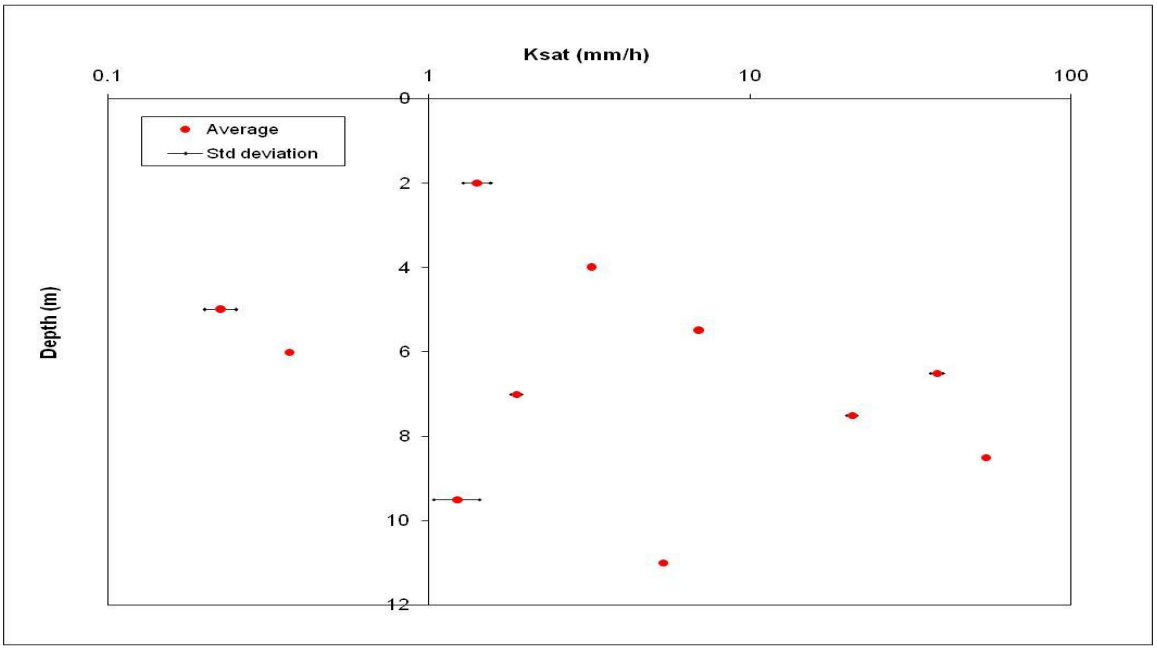

Figure 5.5 Saturated hydraulic conductivity at the Fig site

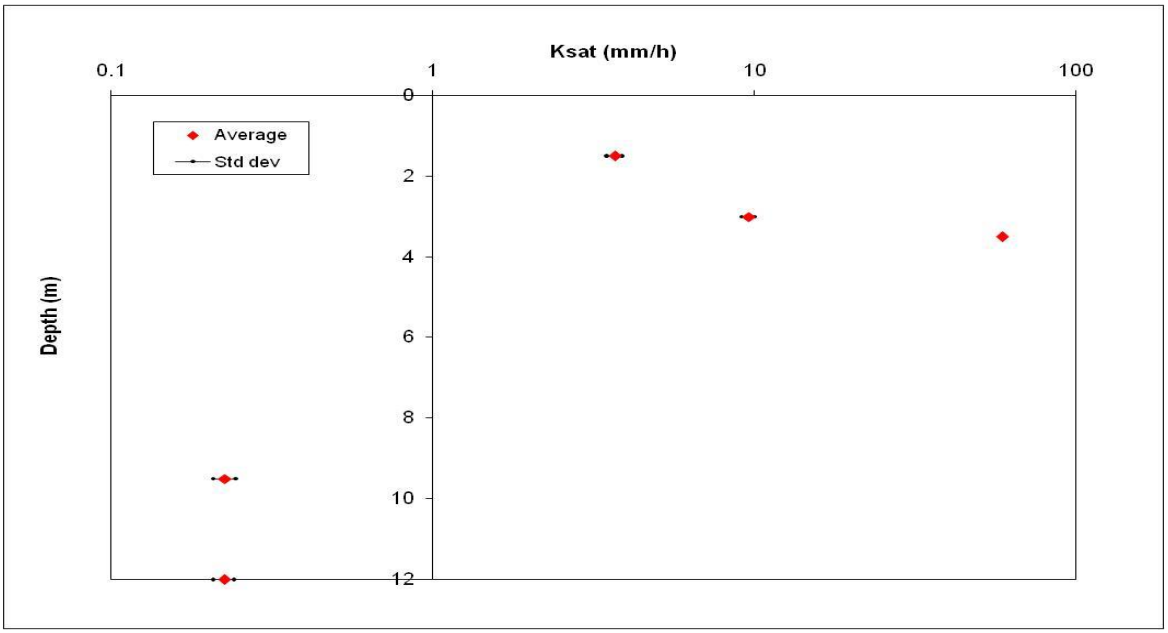

Figure 5.6 Saturated hydraulic conductivity at the Bugweed site

5.5 Unsaturated Hydraulic Conductivity

The unsaturated hydraulic conductivity characteristics were determined for near surface materials *in situ* with tension infiltrometers. Together with a ponded double ring infiltrometer test, the macropore conductivities can be observed, relative to conductivities with a small tension. The tension infiltrometers allow control of water supply pressures (h) at values less than zero at the soil surface. As defined under capillarity theory, the more negative the water pressure, the smaller the soil pores that will remain water-filled and thus conduct water (Perroux and White, 1988). This relationship is described by the capillary rise equation (Hillel, 1998):

$$h_c = \frac{2\gamma \cos\alpha}{rg\rho_w} \qquad 5.3$$

where h_c is the height of capillary rise [L],

γ is the surface tension between water and air [M/T^2],

α is the contact angle between the water and the pore wall,

r is the pore or capillary radius (equivalent to the capillary potential) [L], and

ρ_w is the density of water [M/L^3].

Flow in the unsaturated porous media has traditionally been described by the Richards equation. Based on the Buckingham-Darcy flux equation, this approach assumes a one-dimensional vertical flow in a homogenous medium.

$$\frac{\partial\theta}{\partial t} = \frac{\partial}{\partial z}\left[K(h)(\frac{\partial h}{\partial z} + 1) \right] \qquad 5.4$$

where θ is the volumetric water content [L^3/L^3],

t is time [T],

$K(h)$ is the unsaturated hydraulic conductivity [L/T],

h is the water pressure [L], and

z is vertical spatial coordinate with positive value upward [L].

The hydraulic characteristics required to calculate flow and transport in the porous media are saturated and unsaturated conductivity. The experimental method is described in much detail

by Ankeny *et al.*, (1991), which uses a sequence of tension infiltrometer measurements taken at steady-state water flow for increasing tensions (0 to progressively more negative) on the same soil surface. This rapid field technique is capable of determining soil infiltration and shallow subsurface water movement in the unsaturated zone. They derived linear functions for the fluxes measured at each pressure head from the Wooding, (1968) solution for steady-state infiltration from a shallow circular pond (soil surface area). Results from experiments undertaken at the Fig tree site are illustrated in (Figure 5.7) and Grass site results are illustrated in (Figure 5.8). The results show with the increase in the capillary pressure head there is a decrease in the hydraulic conductivities. The tests also show that the near surface hydraulic conductivities are higher at both sites. These results also are an indication that the higher porosities are in the upper layer of the material. The water is capable of moving more easily through material in the upper layer. Water moves at slower rate in the deeper levels of the material profile.

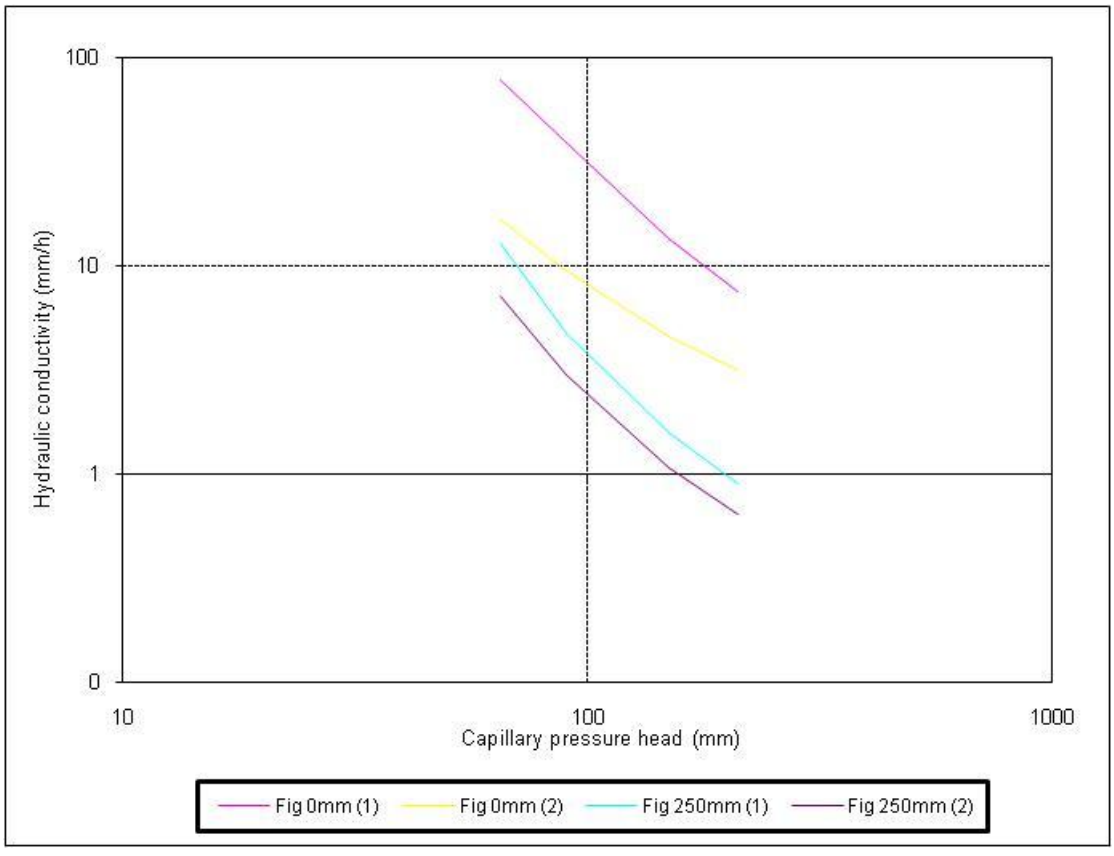

Figure 5.7 Unsaturated hydraulic conductivity at the Fig site (0-250 mm)

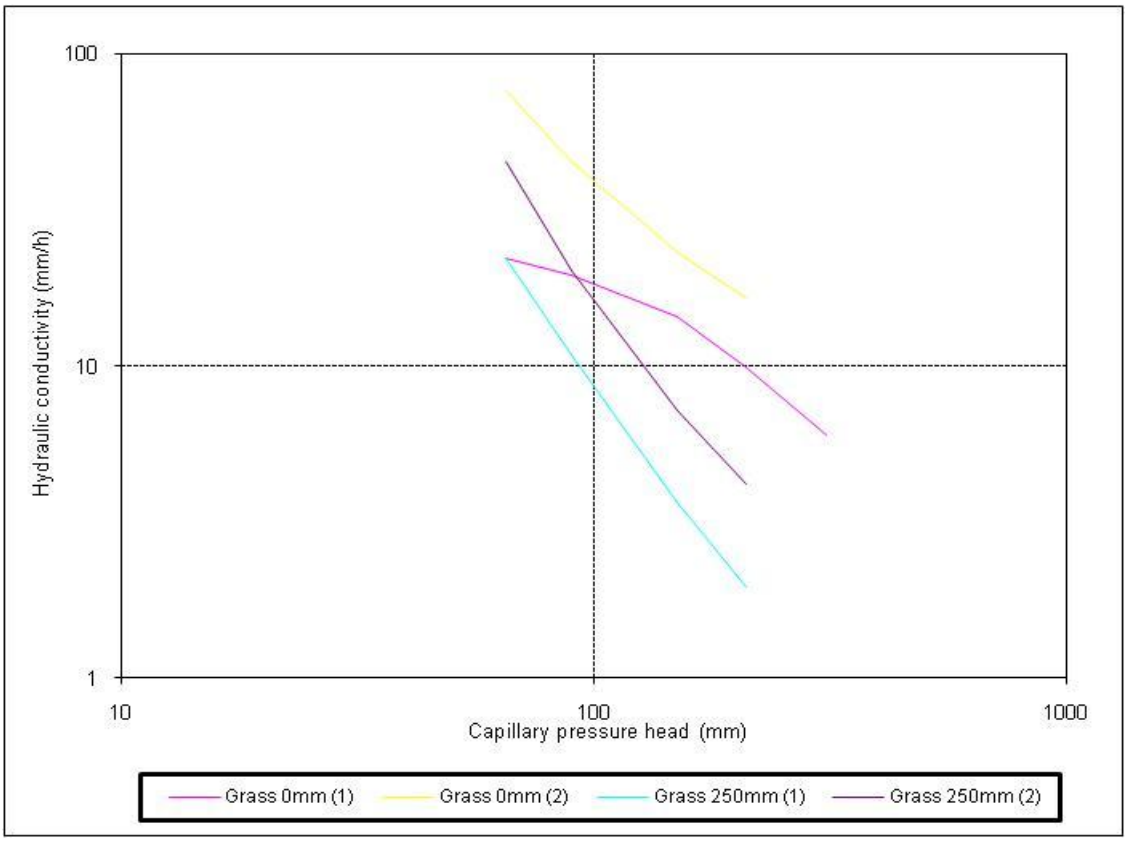

Figure 5.8 Unsaturated hydraulic conductivity at the Grass site (0-250 mm)

5.6 Root zone monitoring

Tensiometers were used to measure material water pressure in the operational range from 0 – 1000 mbar. Tensiometers can also be used to measure positive pressure in soils that are saturated and thus can act as piezometers for monitoring perched water tables. Tensiometers have the advantage in that they provide a direct measure of the water potential. They require a continuous water column that extends from the measurement point to the pressure transducer located at the surface. An example of how the position of the tensiometers would be placed in the soil is illustrated in (Figure 5.9). As illustrated by a schematic of the root zone they would dry the material out increasing the moisture storage capacity.

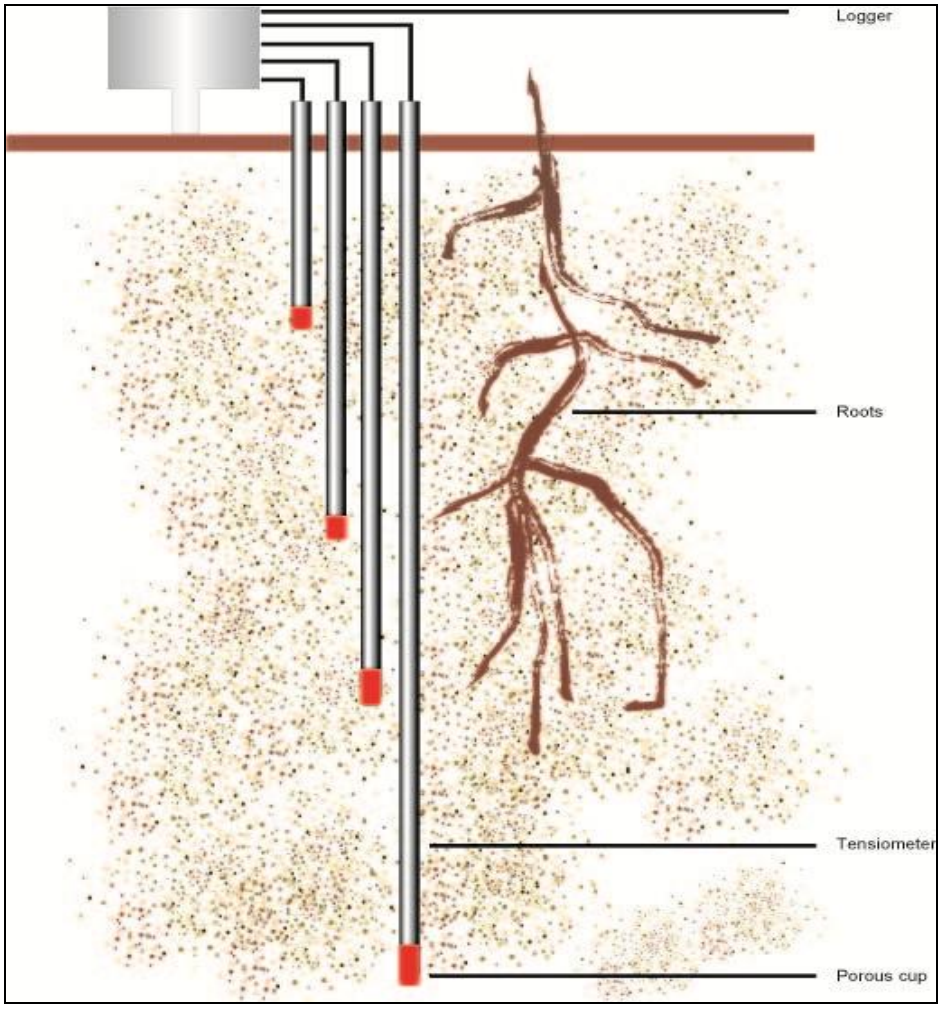

Figure 5.9 Schematic of the root zone and the components of the tensiometers.

The tensiometers positioned at different depths down the profile would measure the tensions, which would be related to dryness. (Figure 5.10) shows an increase in the matric pressure as the material dries. The tensions in the upper surface of the upper profile show more changes in the matric head with drying and wetting during rainfall events. It is these tensions from the tensiometers at the varying depths that are used to determine the fluxes in the materials. This will be done by the use of a model to simulate the measured tensions in the material.

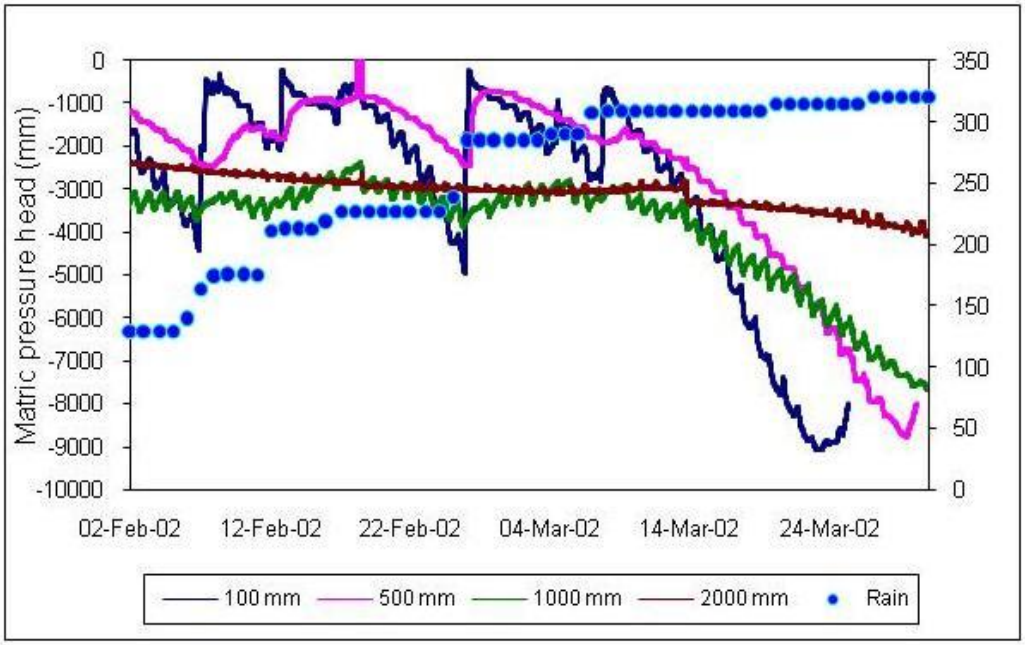

Figure 5.10 Monitored tensiometer data for the root zone. Illustrating the matric pressure head (mm) at 100 mm, 500 mm, 1000 mm and 2000 mm down the material profile.

5.7 Advanced tensiometer – Deep profile monitoring

The vaporization of water in the water column limits the depth of emplacement of tensiometers to depths of 8 m and has precluded the use of tensiometers to estimate fluxes at greater depths. Hubbell and Sisson, (1998) have overcome this problem by developing the advanced tensiometer. A version of the advanced tensiometer, developed at the SBEEH of the University of KwaZulu-Natal, formed an important component of this study as these tensions would be used as a means to determine the seepage at the base of the waste impoundment. The advanced tensiometer consists of two parts, a permanently installed porous cup assembly with PVC casing that extends to the land surface and a removable electronic pressure transducer as depicted in (Figure 5.11). The advanced tensiometer results would ultimately determine the success of the vegetation cover, since material fluxes at the 8 m depths could be measured. By positioning the transducer close to the ceramic cup, the water column up to the land surface is removed, thus eliminating thermally associated problems. The advanced tensiometer is thus connected directly to the ceramic cup. An o-ring is placed at the end of an inner PVC tube around the transducer, ensuring direct contact with the water in the ceramic cup and no leaks. Replenishment of the advanced tensiometers was

done by removing the inner PVC tubing, pouring water down the outer PVC casing, then gently pushing the inner tubing with the o-ring into the ceramic cup.

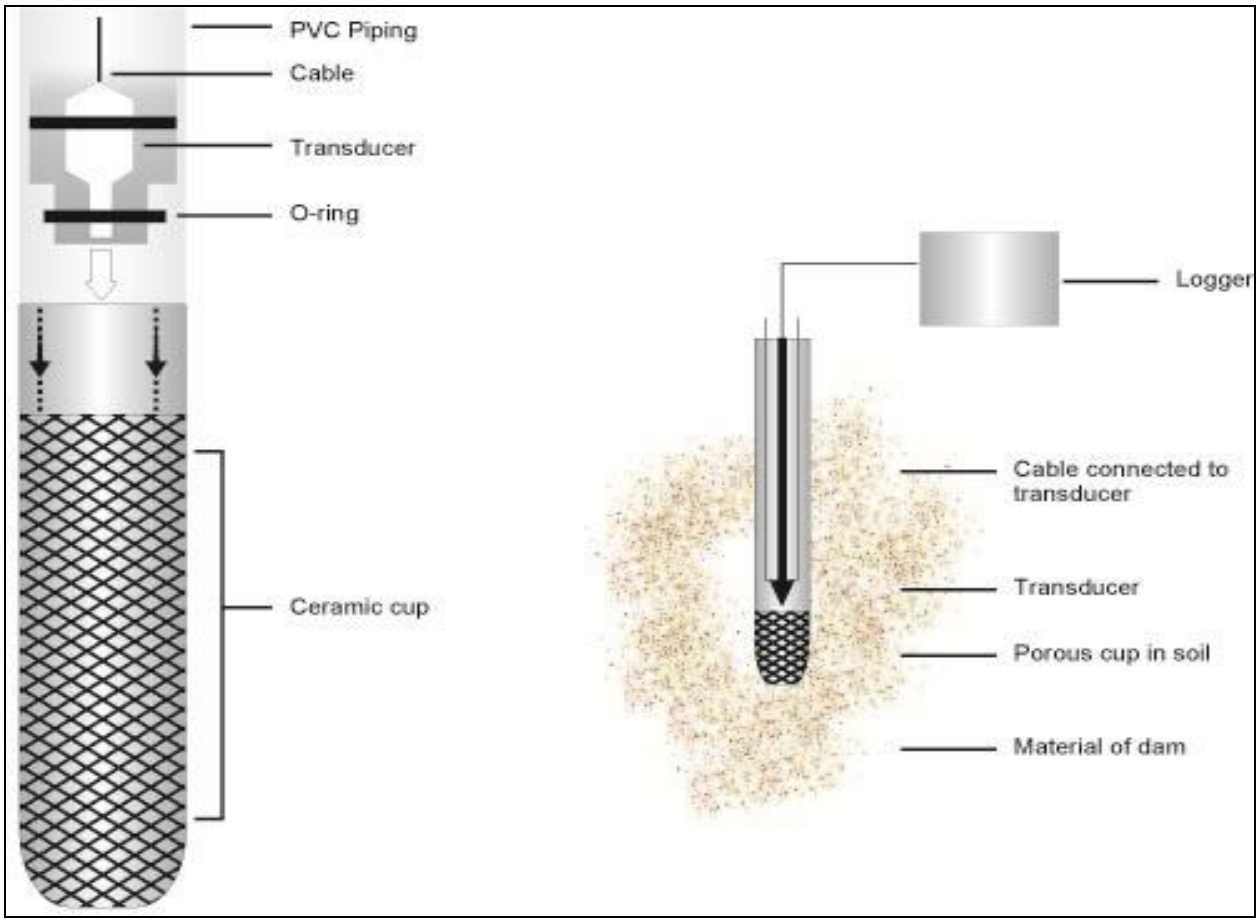

Figure 5.11 Schematic of advanced tensiometer showing the ceramic cup, transducer and outer PVC piping.

The pressure transducers were calibrated before they were tested with a leak test and a simulated field conditions test.

5.7.1 Leak test

The aim of this test was to determine whether there could be any leak at the o-ring of the tensiometer. Suction on the ceramic cup from the material tension will allow the o-ring to be pulled down onto the ceramic, thus not allowing any air to escape. For the test, the ceramic end was connected to a pump, which allowed a suction to be pulled on the transducer. The transducer was set at 2.0 V when there is no tension and would drop with suction on the transducer. The tension on the transducer was applied and monitored for a period of four

days. The result of this experiment is illustrated in (Figure 5.12). The voltage remained relatively constant in the approximate range 0.85 V. The variation in the voltages can be attributed to noise.

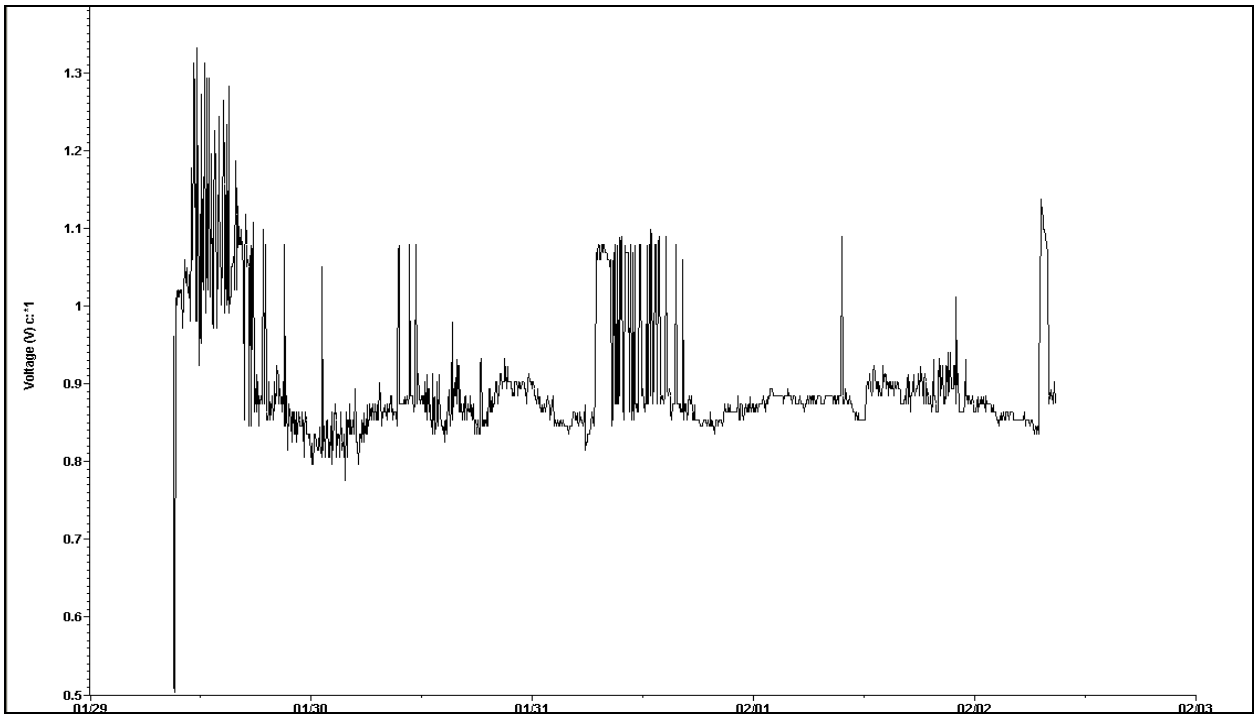

Figure 5.12 Monitored voltage for the leak test over a period of four days.

5.7.2 Field simulation test

Material from the Dams was set into a glass jar approximately 240 mm high and 110 mm in diameter. The ceramic of the advanced tensiometer was set into the material 100 mm deep. The material in the jar was dried or wetted and the voltages were recorded at five-minute intervals. The result of the experiment is illustrated in (Figure 5.13). The experiment was implemented in systematic manner as follows. Initially the material sample was placed in the sun, where very little drying out occurred. As illustrated in the leakage experiment a decrease in the voltage indicates drying out of the material. The jar was then placed in an oven and the temperature was set to 30^{o}C (indicated by 1). There was a significant drying out of the material over a period of a day. The temperature was further increased to 60^{o}C (indicated by 2) and drying out of the material was increased further. At this point of the experiment, water was added into the jar (indicated by 3) to determine the effect of wetting. The effect of water was an immediate reduction of tension in the material. The voltage returning back to 2.0 V

illustrates saturated conditions as the advanced tensiometers were set to 2.0 V for no tension exerted on the transducer. The material was then placed in the oven at 60^{o}C, with extensive drying of the material, cracking occurred in the material. It was suspected that contact was lost between the material and the ceramic of the advanced tensiometer (indicated by 4). Water was then added to the material (indicated by 5) but at a slower rate. It is clear from the voltages that the material was still very dry. The simulation of field conditions had proven that there was potential use of the advanced tensiometer in the field.

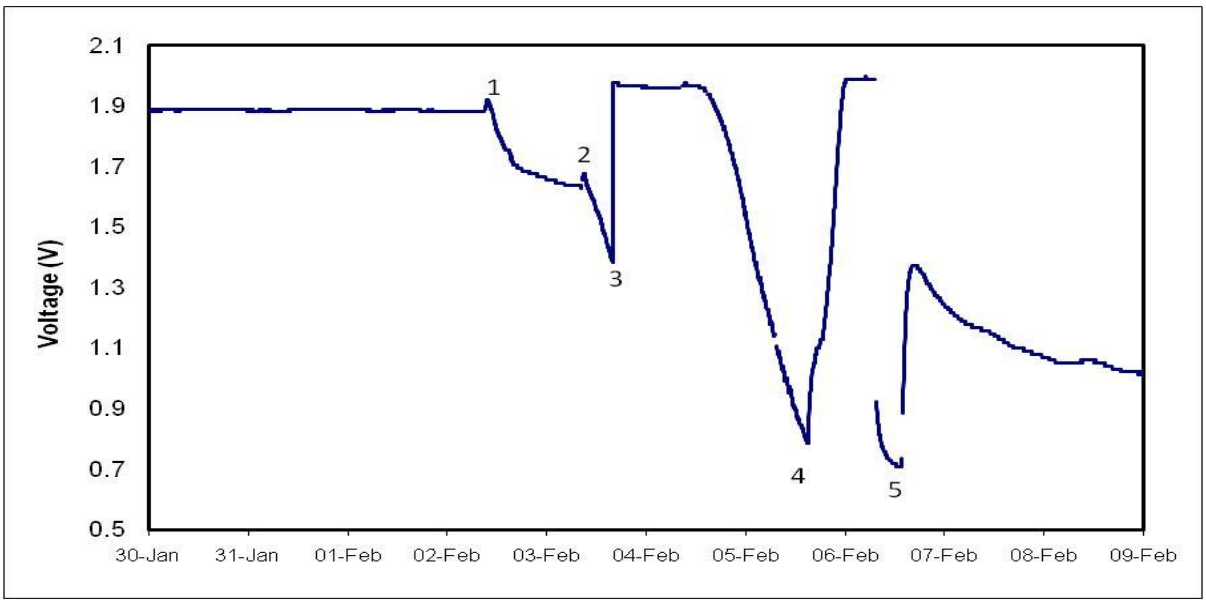

Figure 5.13 Test for simulation of the field conditions.

The advanced tensiometers were placed in the material of the dams by augering holes into the material of the dams and then the outer casing with the ceramic were pushed into the holes to the specified depths of 6 to 8 m. Water was then poured into the ceramic and the transducer was then pushed into the ceramic housing. A major problem associated with the installation of the transducer into the ceramic occurs as a result of the depths at which the transducer is installed below the surface. Personnel cannot see the connection and cannot feel the pressure exerted during the connecting process. Thus extreme caution had to be exercised during the connection of the transducer to the ceramic as large positive pressures exerted from the water during the connecting of the transducer to the ceramic, would burst the sensor in the pressure transducer.

In this chapter the geohydrological information that would directly impact seepage from the waste impoundment was assessed. These included the water content, textural material particle size distribution, water retention characteristics, saturated and unsaturated hydraulic conductivity. Instrumentation and monitoring methods for determining the material moisture were assessed as these collective factors are used to determine the fluxes. These factors were assessed as they are used in the HYDRUS-2D model for simulations of the water balances. In the following chapter the HYDRUS-2D model together with the equations governing the model are discussed.

6. THE HYDRUS-2D MODEL

The HYDRUS-2D model (Šimunek *et al.*, 1999) was the principle tool used to determine the water balances at the observation sites on the Dams. The HYDRUS-2D model is a finite-element model, which numerically solves the Richards' equation for saturated-unsaturated water flow. Richards equation for one dimensional flow requires knowledge of the soil hydraulic functions, i.e., the soil water retention curve, $\theta(h)$, describing the relationship between water content (θ) and the pressure head (h), and the unsaturated hydraulic conductivity function, *K(h)*, defining the hydraulic conductivity (*K*) as a function of (*h*). The flow equation incorporated in HYDRUS-2D is coupled with a sink term, (*S*), to account for water uptake by the plant roots (Šimunek *et al.*, 1999).

$$\frac{\partial \theta}{\partial t} = \frac{\partial}{\partial x}\left[K\left(\frac{\partial h}{\partial x} + \cos\alpha \right) \right] - S \qquad 6.1$$

where
- h is the pore water matric pressure head [L],
- θ is the volumetric water content [L^3/L^3],
- t is time [T],
- x is vertical spatial coordinate with positive value upward [L],
- S is the root uptake sink term [$L^3/(L^2T)$],
- K is the unsaturated hydraulic conductivity [L/T], and
- α is the coefficient in the soil water retention function [1/L].

HYDRUS-2D solves for water content using the van Genuchten equation in which the pressure head is negative (Šimunek *et al.*, 1999).

$$\theta(h) = \begin{cases} \theta_r + \dfrac{\theta_s - \theta_r}{\left[1 + |\alpha h|^n\right]^m} & h < 0 \\ \theta_s & h \geq 0 \end{cases} \qquad 6.2$$

where
- θ is the volumetric water content [L^3/L^3],
- θ_r is the residual water content [L^3/L^3],
- θ_s is the saturated water content [L^3/L^3],
- n is a pore-size distribution index [-], and

α is the inverse of air-entry value [-].

The hydraulic conductivity is solved as a function of the water content in HYDRUS-2D using the equation of Mualem, 1976.

$$K(h) = K_s S_e^l \left[1 - \left(1 - S_e^{\frac{1}{m}} \right)^m \right]^2 \qquad 6.3$$

where $m = 1 - 1/n$, $n > 1$

K_s is the saturated hydraulic conductivity [L/T],

l is the pore connectivity parameter [-], and

S_e is the effective water content [-], given by

$$S_e = \frac{\theta - \theta_r}{\theta_s - \theta_r} \qquad 6.4$$

The parameters (α), (n) and (1) in HYDRUS-2D are considered to be empirical coefficients affecting the shape of the hydraulic functions.

The Feddes *et al.*, (1978) model for root water uptake as a function of soil matric potential, (in the form of the matric pressure head), is the option in HYDRUS-2D for defining the sink term (S).

$$S(h) = \alpha(h) S_p \qquad 6.5$$

where

$$S_p = \frac{1}{L_R} T_P \qquad 6.6$$

where

$$L_R(t) = L_m f_r(t) \qquad 6.7$$

where

$$f_r(t) = \frac{L_0}{L_0 + (L_m - L_0)e^{-rt}} \qquad 6.8$$

where $\alpha(h)$ is a function of the soil matric pressure head ($0 \leq \alpha \geq 1$) [-],

S_p is the potential uptake rate [L/T],

T_p is the potential transpiration rate [L/T],

L_R is the depth of the root zone [L],

L_m is the maximum rooting depth [L],

L_0 is the initial rooting depth [L],

$f_r(t)$ is the root growth function, and

r is the growth rate [L/T] (Šimunek *et al.*, 1999).

The HYDRUS-2D model solves the nonlinear Richards (1954) equation using numeric iteration with user-defined discretization of the soil profile into nodes (depths) at which hydraulic properties (hydraulic capacity, hydraulic conductivity, and water content) are evaluated. Time discretizations for numerical computation solution intervals are set by the user. The model uses upper and lower boundary conditions (matric pressure head, drainage, flux), climate (precipitation, potential evaporation, and potential transpiration), and soil-texture-dependent hydraulic properties as the primary variables controlling soil-water flow. Root density distribution and vegetation type control the root uptake (Šimunek *et al.*, 1999). The van Genuchten equation is the option used to define the soil hydraulic conductivity and water retention functions.

The performance of the ET cover is governed by a complex set of interacting processes. Mathematical models may describe the individual processes, but due to the interactions among processes, the individual mathematical processes need to be integrated into single working model. ET cover evaluation thus requires a model that incorporates all of the important elements. Some models are good research or scientific investigation tools, but are not sufficiently complete to serve all the aspects of assessing waste impoundment remediation. Evaluation of available models pertinent to ET covers are described in detail by (Hauser *et al.*, 2001). For a model's performance to be considered suitable, one needs to understand and evaluate exactly what is to be achieved. For the purpose of this study the

HYDRUS-2D model was selected as it produces good estimates of water movement within the soil profile. However, it does not estimate mixed plant communities or directly estimate surface runoff.

6.1 Modelling Approach

The HYDRUS-2D model was configured to simulate the observations of soil water matric pressure head from the tensiometers on the Dams. Intensive analysis of data from the monitoring sites on the Dams revealed some records to be broken or unreliable, thus it was concluded that three sites would be selected due to criteria of data quality and length of data records. The HYDRUS-2D model was set up for three of the sites on the Dams and since the objective for the study is to answer the hypothesis of whether a vegetated cover is able to limit effluent leaching out the base of the Dams material. Analysis of the possible differences in water fluxes at the threes sites would answer the hypothesis.

During the initial simulations of these sites it was noted that changes in certain model parameters affected the simulations in different ways. The waste material became drier much faster, for example, if the pore size distribution index was increased. In this example the increase in the pore size distribution index allowed the material to act more as a loamy soil rather than a clayey soil. A further increase of the pore size distribution index gives the material the drainage characteristics of a sandy soil rather than a loamy soil. This explains the change in drainage from the waste material with the change in the pore size distribution index or the air entry pressure head, which is related to the largest drainable pore size. Thus a sensitivity analysis of rates of wetting or drying was considered to derive generalised behaviour changes with the parameters in the model.

7. SENSITIVITY ANALYSIS

The objective of the sensitivity analysis was to identify the model parameters that would be of importance during water flow simulation. The sensitivity analysis comprised making changes to the soil hydraulic parameters and examining the subsequent changes in the simulation output. Small changes in an input parameter, resulting in relatively large output changes are indicative of the parameter's sensitivity. Thus the modelling could be made simpler if a parameter hierarchy and effect could be identified. The sensitivity of a parameter can be placed higher on the sensitivity hierarchy depending on its effects or how much the parameter changes the tension (matric pressure head) response and in what way. A preliminary screening of parameter response permitted the selection of a small set of parameters for the sensitivity analysis. The parameters selected for the analysis were the saturated hydraulic conductivity (K_s), saturated water content (θ_s), residual water content (θ_r), matric potential required to empty the largest soil pore water (α) and pore size distribution index (n).

The unsaturated soil hydraulic properties are general highly nonlinear functions of the matric pressure head. Thus in HYDRUS-2D, soil hydraulic characteristics are modified to add flexibility to the description of the hydraulic properties near saturation. The parameter (θ_s) in the van Genuchten's retention function is replaced by a fictitious (extrapolated) parameter (θ_m) slightly larger than (θ_s). The modified hydraulic characteristic assumes that the predicted hydraulic conductivity function is matched to a measured value of the hydraulic conductivity, (K_k) = $K(\theta_k)$, at some water content (θ_k) less than or equal to the saturated water content. Thus according to the modified parameters, $(\theta_k) \le (\theta_s)$ and $(K_k) \le (K_s)$. This simply means when water is ponded or the supplied water exceeds the (K_k), the (K_s) value will be effective and when at an unsaturated water content the (K_k) value will be effective. (θ_m) is the measure of the soils macroporosity, which discharges water at supply rates greater than (K_k) i.e. (K_s). When water is ponded the macroporosity of the soil is expressed by (θ_m) and (θ_k) and although this has little or no effect on the retention curve, the effect on the shape and value of the hydraulic conductivity function is considerable. The water will drain from

the material at a lower matric pressure and will continue draining as long as the saturation range is maintained, i.e. between (θ_m) and (θ_s). Thus it can be expected that this can have a tremendous effect of the movement of water through the material. This is pertinent for fine-textured soils where (n) is relatively small 1.0< (n) <1.3 (Šimunek *et al.*, 1999).

The scenario designed for the sensitivity analysis was represented by a 1 m x 1 m single layer of typical material from the Dams. The sensitivity analysis was conducted on the water retention parameters to determine their effective influence on the matric pressure head time series. The values of the baseline water retention parameters are presented in the Table 7.1 below. Only one parameter was changed at a time to evaluate its effective sensitivity against the baseline matric pressure head time series. Thus when analysing the graphs, the parameter sensitivity can actually be measured by the change or difference from the baseline graph. The baseline parameters where that of the typical material from the Dams, since a parameter may be more or less sensitive when accompanied by a set of different parameters. The time period for the sensitivity scenario simulations was three months.

Table 7.1 Water retention parameters for the baseline scenario of sensitivity analysis.

Scenario	θ_r	θ_s	α	n	K_s	I	θ_m	θ_a	θ_k	K_k
Baseline	0.25	0.77	0.005	1.2	80	0.5	0.770	0.25	0.77	80
Analysis	0.30	0.92	0.006	1.4	96	-	0.772	-	-	-

7.1 Residual water content

The residual water content is when the water content is low or the material is considered to be dry. An increase of the residual water content (θ_r) by 20 % had no effect on the matric pressure head response as illustrated in (Figure 7.1). The residual water content would be expected to be influential during dry conditions. For this sensitivity scenario soil does not dry a great deal, thus as long as the soil is relatively wet, the change of the residual water content has very little effect on the matric pressure head response.

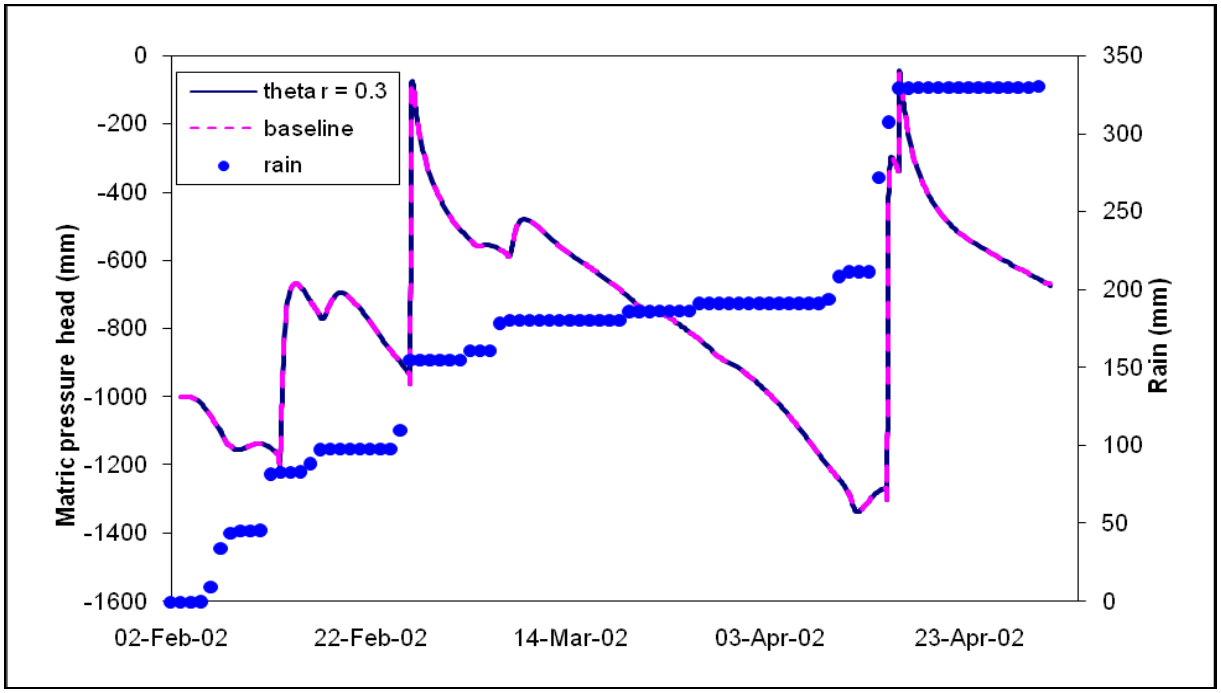

Figure 7.1 Pressure head depicting sensitivity of the residual water content, θ_r for a three month period.

7.2 Saturated water content

The saturated water content is when the water content in the material is high or the material is wet. An increase of the saturated water content (θ_s) by 20 % revealed it to be a very sensitive parameter during wetting of the soil as illustrated in (Figure 7.2). Analysis of the pressures shows that when it does rain it never wets up as much as the baseline conditions. The (θ_s) has no real effect on the drying of the soil, as the soil still dries at the same rate and to the same water content. This parameter also revealed the material to be very sensitive to even a small amount of input rain, especially when the soil is dry. The material volumetric capacity has been increased, so when it rains, the water enters the voids without increasing the matric pressure heads to the same level as they would for a material with a smaller pore volume.

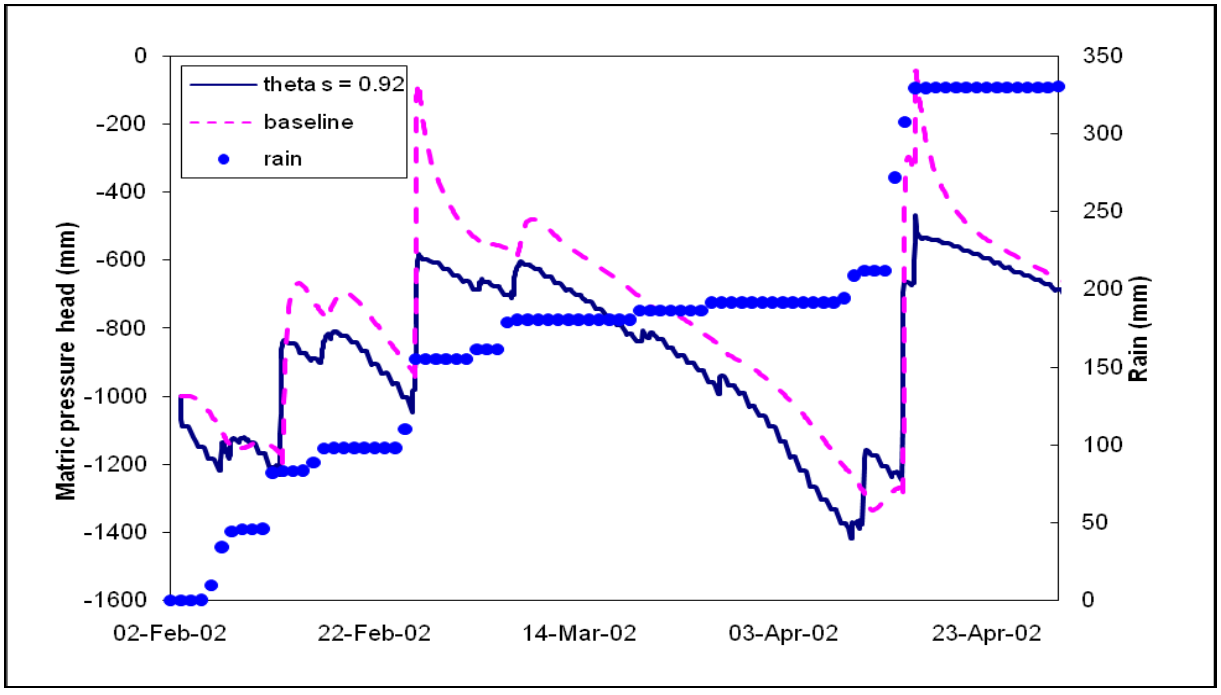

Figure 7.2 Pressure head depicting sensitivity of the saturated water content, θ_s for a three month period.

7.3 Alpha

Alpha can be explained as a measure of the inverse of the air entry pressure. Alpha affects the drying rate of the material. Analysis of the pressure heads reveals that, when the material does wet up, it wets up to the same degree as the baseline case. The illustration (Figure 7.3) shows a 20% increase of this parameter results in the rate of drying to be slightly higher than in the baseline case, since water is held more effectively in the larger pore range in the baseline case. Thus, an increase in the alpha value means a decrease in the air entry pressure, meaning an increase in the largest drainable pore size allowing more water to drain out easier at lower matric pressure head. Alpha would affect the matric pressure of the material significantly if drying occurred for an extended period of time. However, when the water is added it would wet up to the same matric pressure head.

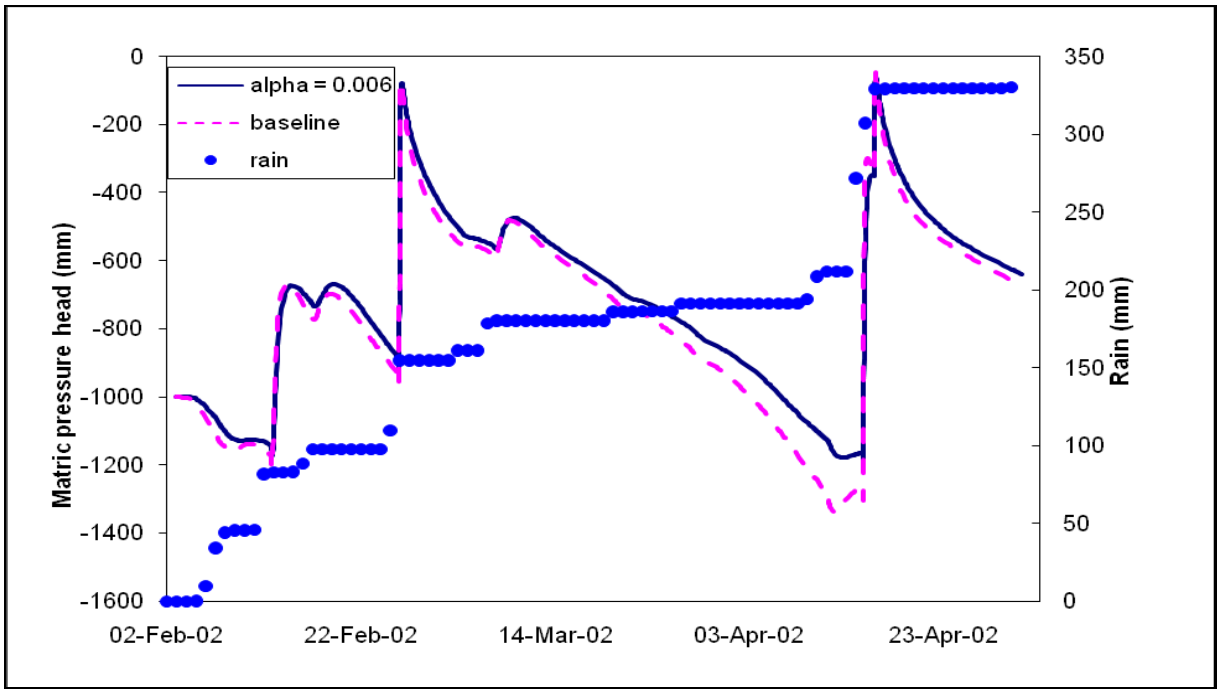

Figure 7.3 Pressure head depicting sensitivity of alpha for a three-month period.

7.4 Pore size distribution index

Analysis of the matric pressure head response reveals that a 20 % increase in the pore size distribution index, results in the profile not wetting up to the baseline level when the profile is relatively wet as illustrated in (Figure 7.4). However, when the profile is very dry, for example during the 10th of April 2002, a small increment of rain water can have a far greater effect on the reduction in tension than in the baseline case. In this case 14 mm of rain reduced the tension by 924 mm, whereas in the baseline case it was reduced by a mere 74 mm. The profile does not wet up as much when close to saturation, because the increased pore size results in water draining out the soils easier. The drainage characteristics are more directed toward characteristics of sandy soil. When close to saturation, the profile drains easier than in the baseline case because the pore size range is larger and the matric pressure in the soil is much lower. Water is thus released at a slower rate than the baseline case since it is being held in the pores. (*n*) thus has the effect of intensifying the wetting up of very dry material, but reduces the drying rate of wet soils.

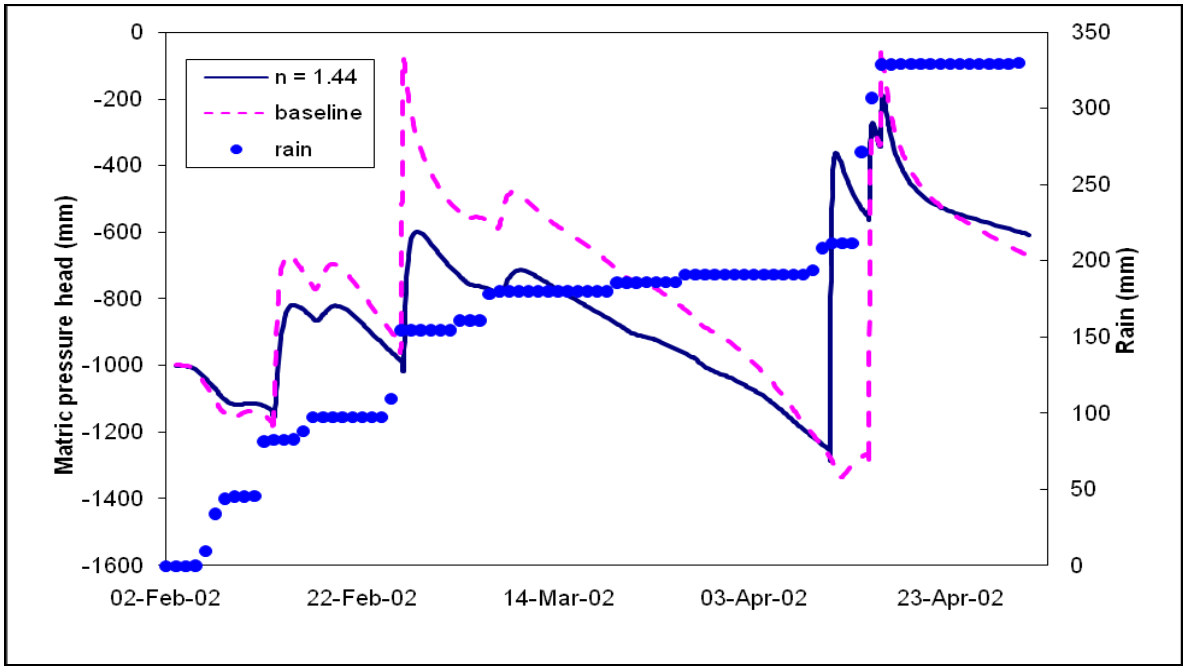

Figure 7.4 Pressure head depicting sensitivity of pore size distribution index, *n* for a three month period.

7.5 Saturated hydraulic conductivity

Hydraulic conductivity describes the ease with which the soil pores permit water movement in response to a hydraulic gradient. The parameter (K_s) describes this movement when the soil pores are completely filled with water. An increase in the saturated hydraulic conductivity caused a significant decrease of the pressure head when the soil is dry, as illustrated in (Figure 7.5). This occurred during the 10th of April 2002 where 14 mm of rain reduced the pressure by 831 mm compared to the baseline case of 78 mm. The soil with higher (K_s) wets up more with a smaller increment of water. There is no significant effect on the rate at which the material dries. Thus, if both materials start drying as a result of the same evapotranspiration demand, with no water being added, they will dry out all the same.

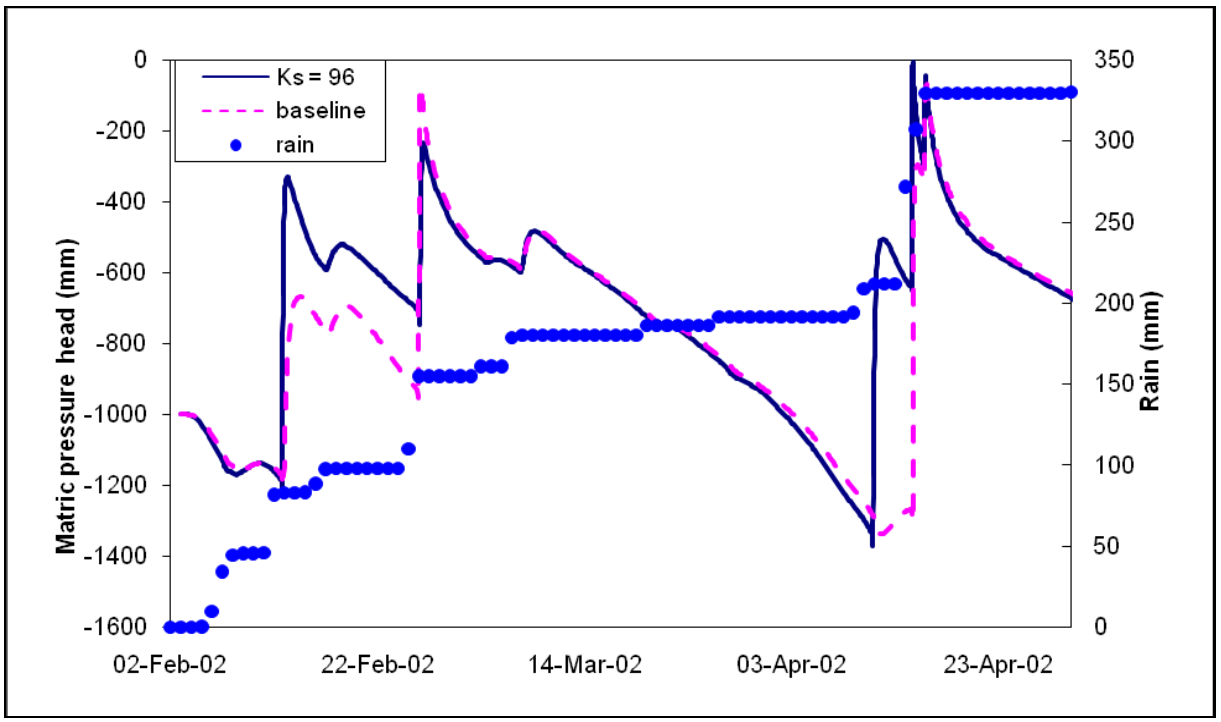

Figure 7.5 Pressure head depicting sensitivity of saturated hydraulic conductivity, *Ks* for a three month period.

7.6 Macropore flow

As described earlier in the chapters, Šimunek *et al.*, (1999) use the (θ_m) parameter to describe the macropore space when the material is saturated. This parameter in the modified van Genuchten equation establishes conditions for macropore flow and is especially significant when the water is ponded or rainfall supply rates are higher than (K_k). Water moves down through the material faster and thus the material dries out faster. The macropore space (θ_m), is an extremely sensitive parameter since a small increase of 0.002 has an effect on the matric pressure head response as illustrated in (Figure 7.6). The materials of the Dams crack when dry, thus (θ_m) would be an important parameter in the modelling exercise and even more considerable at the modelling site with roots, since roots provide a possible conduit for macropore flow. It is important to note that this parameter is sensitive only for a very small change of the parameter, thus an increase of the parameter by 1% will have no greater effect on the matric pressure head time series than that induced by an increase in the parameter of 0.002. The parameter (θ_k) plays the same role of simulating macropore flow in the modelling process, thus aids as a means for further enhancing the macropore flow phenomenon.

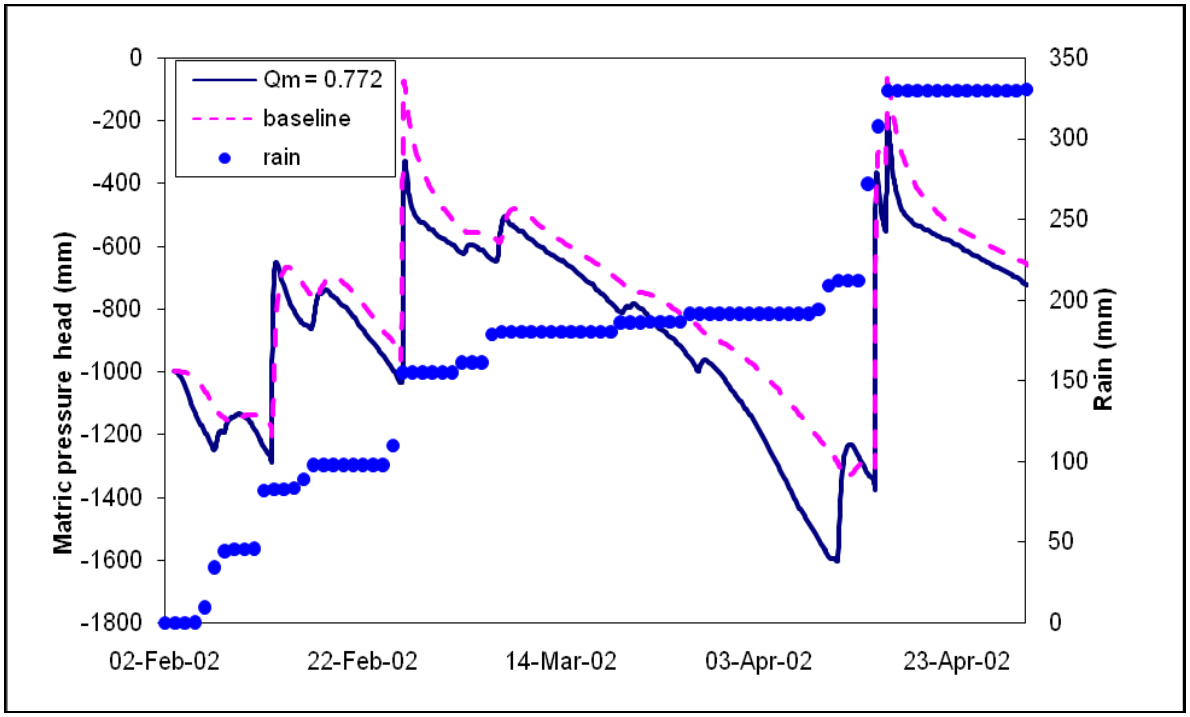

Figure 7.6 Pressure head depicting sensitivity of macropore flow, θ_m for a three month period.

The sensitivity analysis was to identify the model parameters that would be of importance with regard to the simulation of water flow. The next chapter sets out the detail of the modelling exercises in context of available literature, actual field data or any assumption that may have been made on the water use and or on the water balances. Three sites were modelled namely the Bare site and Fig tree site on Dam 2 and Nest 9 consisting of woody shrubs/grasses on Dam 3-4.

8. SIMULATED WATER BALANCE

It is important to understand that the simulated results presented in this study are the results from the HYDRUS-2D model. The respective sites were modelled as separate individual units to determine the climatic and base (seepage) water balance fluxes. The sites modelled in this study were the Bare, Fig tree and Nest 9 to determine the differences in simulated results. The following assumptions have been adopted in the HYDRUS-2D modelling of the Dams Area:

- There are no slopes on the Dams surface, thus all water that reaches the surface at the modelling sites is considered to enter the material profile.
- The sites were modelled as a 180 mm wide by 15 000 mm deep block of material, with water entering and leaving the top of the material (no horizontal flow out the sides) and seepage at the base of the block.
- The vertical profiles of each site consist of three heterogenic materials,
  first profile 165 mm deep,
  second profile 3 185 mm deep, and
  third profile 11 650 mm deep.
- The boundary conditions for the modelling simulations were as follows:
  atmospheric conditions at the surface,
  constant pressure boundary at the bottom, and
  zero flux on the sides.
- The model does not allow for change in parameters such as effects of growth, thus conservative estimates may have been assumed. This would apply to parameters such as *LAI*, rooting depths and actual evaporation.

The Bare site situated on Dam 2 consists of a 6 m x 6 m bare patch. The root water balance was first derived by calibrating the HYDRUS-2D model to the monitored tensiometer data. These were initially optimized to represent the material water status from rainfall and soil evaporation for the period of two months. The same process was followed when modelling the Fig tree site and the Nest 9 site. However, with these two sites the plant transpiration and various processes such as rainfall losses to vegetation interception were also considered in the modelling. Thus the HYDRUS-2D model was optimized for a three to four month period for

all the sites. Although this may seem to be a simple exercise, much effort was required in the optimization of the model. One would get a good result for the first profile but may find the third profile to have unacceptable errors and vice versa. Once an acceptable simulation of the responses at all three sites was achieved for the short duration simulation, the full period was used to estimate the water balance over four years. The comprehensive set of model parameters used in the simulation of HYDRUS2-D for the respective sites are presented in Appendix D. The simulated results for the three sites for the full period are illustrated in Appendix E.

This chapter aims to explain the derived input variables to HYDRUS-2D based on assumptions or theoretical basis for the processes within the model. For the modelling, the identified key processes that should be considered as being important are:

- Development of the vegetation canopy,
- Loss of water intercepted by the vegetation canopy and water use by the vegetation,
- Water use relative to a reference crop, and
- Root development and extent.

An effective managed vegetative cover will only be realised with full canopy closure on the Dams. Various vegetation species were planted and others naturally colonised the Dams. Some of the more common species are listed in the Table 8.1. The vegetation canopy of the grasses on Dam 2 is denser than the mixed woody shrubs/grasses on Dam 3-4. Due to compliance with alien species legislation, the Bugweed trees were removed in 2004 after 2 years of monitoring, thus the current vegetation on the Dams is considered native species to the area. Overall the development of the vegetation canopies for the various species is considered to be in excellent condition. The value for the canopy cover for the modelling exercises was derived from a Leaf Area Index (*LAI*). *LAI* is defined as the ratio of leaf surface area per unit ground area. During an initial water balance study undertaken by Lorentz, (2001), *LAI* measurements were measured for the species listed in Table 8.1.

Table 8.1 List of the various vegetation species and derived *LAI* values on the Dams Area.

Description	Species	*LAI [-]*
Common Wild Fig	*Ficus thonningii*	2.72
Bug Weed	*Solanum mauritianum*	2.72
Pigeon Wood	*Trema orientalis*	2.18
Grass	*Cynodon nlemfuesis*	5.40
Mixed Woody Shrubs/Grasses		2.5 (estimated)

A view under the canopy of the Fig tree is depicted in (Figure 8.1) and it is evident that the tree will provide sufficient shading to the ground surface. The canopy overall will have a measurable impact on the interception losses and will be an important factor when considering the amount of water that will reach the ground surface. The *LAI* is used for determining the interception of rainfall by the vegetation. Interception losses were estimated from the daily rainfall amounts using the Von Hoyningen-Huene method (Schulze *et al.*, 1994). This method gives estimates of daily interception loss (I_l), based on the *LAI* value and the amount of rainfall for a particular day.

$$I_l = 0.30 + 0.27P_g + 0.13LAI - 0.013P_g.LAI - 0.007LAI^2 \qquad 8.1$$

where I_l is the daily rainfall interception loss [mm],

P_g is the daily gross rainfall [mm], and

LAI is the leaf area index.

Figure 8.1 View under the canopy of the Fig tree for determining *LAI*.

The Von Hoyningen-Huene equation has, however, been found to be valid only for daily rainfall amounts up to 18 mm. Thus for the purpose of the modelling exercises it was assumed that an (I_l) saturation point was reached, which depended on the *LAI*. Daily rainfall events exceeding 18 mm would have reached that (I_l) saturation, thus no more interception would occur and all the excess rainfall would be considered as through fall (rain that reaches the ground). Since the vegetation on the Dams Area comprise trees, shrubs and grass, according to (McNaughton and Jarvis, 1983), height and canopy structure are important drivers for evapotranspiration. The relative importance of the radiation versus aerodynamic components of the vegetation depends on how well the crop is coupled with the atmosphere. Tall, sparsely spaced trees on the Dams will be well coupled and their transpiration is more dependent on the aerodynamic component than on the incoming radiation. The shorter more uniform vegetation, shrubs/grasses will be considered to be decoupled from the atmosphere by the thick boundary layer of humid air and the radiation is the primary determinant of transpiration. In addition, direct evaporation from tall trees which could be considered as being well coupled to the atmosphere can be several times greater than the open water

evaporation rates because of the additional energy available from warm, dry air blowing through the canopy, a process known as advection. It is therefore important to determine the extent that the vegetation is coupled to the atmosphere as this will have important implications for their water use and the hydrologically effective component of rainfall.

A simple procedure to predict the effects of advection in terms of the modelling exercise is to modify the crop coefficient (K_c) that is used to estimate the crop evapotranspiration from the reference evapotranspiration. If all incoming solar energy were used to evaporate water, rather than heat the air, soil and vegetation, the maximum crop coefficient would be higher. However, for the modelling exercises on the Dams Area the estimation of the ET_o is calculated from the conservative (K_c).

8.1 Root development

The root development and distribution is largely determined by the following main factors, namely the vegetation rooting characteristics (i.e, depth of roots, root density), the moisture of the material and the material characteristics. The vegetation rooting characteristics are a major factor for the root development. The rooting characteristics and patterns of the Fig trees on the Dams have a preponderance of surface roots extending away from the tree at 100 to 300 mm below surface. These near surface roots are prevalent at up to 8 m away from the Fig tree. Although the majority of roots are at the surface, distribution of finer roots do advance as far as 2 m below the surface and are distributed in a wide area below the tree. A photo of surface roots for the Fig tree is illustrated in (Figure 8.2) and the finer deeper roots are illustrated in (Figure 8.3).

Figure 8.2 Surface roots of Fig tree. The width of the path is approximately 3 m

Figure 8.3 Root depths of the Fig tree at 1.2 m (Photograph courtesy of C. J Ward, 2001).

The distribution of roots of the trees over such a wide area at the surface can also be attributed to the availability of water and management practices on the Dams. The trees have initially colonised very sparsely, allowing the root physiology to spread far from the tree. The root physiology of the woody shrubs/grasses is, of course, very different to that of the trees.

The roots for woody shrubs/grasses were observed at depths of 300 mm below the surface. The root physiology of the shrubs/grasses exceed the Fig tree roots in terms of their density. Soil moisture has been found to be a major determinant of root biomass accumulation (Lui and Dickmann, 1992). The trees and the grasses/shrubs on the Dams would be very responsive to differences in water content in the root zone. The Dams can be considered as being dry in the upper layers, thus roots of the Fig tree were observed at depths of 2.0 m to attain water.

8.2 Climatic water balance fluxes

The three sites from the Dams Area were simulated, namely the Bare site and Fig tree site on Dam 2 and Nest 9 on the Dam 3-4. The cumulative rainfall is the corrected rainfall from the rain gauges taking into account interception losses for the respective Fig tree and Nest 9 sites. These interception loss estimates were calculated from daily rainfall amounts using the Von Hoyningen-Huene method. The potential evaporation presented is calculated based on the Penman-Monteith equation. The actual evaporation (predicted) was determined in the HYDRUS-2D model for the period, February 2002 to December 2005. The simulated climatic water balance graphs are illustrated for the Bare site in (Figure 8.4) and Fig tree site in (Figure 8.5). (Figure 8.6) illustrates the simulated climatic water balance for Nest 9 for the period August 2002 to December 2005.

The cumulative actual evaporation was simulated at significantly less than the cumulative potential evaporation at the Bare site. The calculated potential evaporation is 3 400 mm, whilst the simulated actual evaporation is 2 114 mm. The cumulative rainfall for this period was 3 157 mm, which allows for an excess of 1 043 mm into the material profile. This is assessed later in the change in storage and the seepages for the Bare site. It is evident from analyzing the HYDRUS-2D simulated actual evaporation as illustrated by (Figure 8.4), that during the drier periods, evaporation is lower and the cumulative plot tends to flatten out, while during wetter periods the simulated actual evaporation cumulative plot tends to steepen. This further is demonstrated during extreme events, since at the Bare site it is from the upper most layers that the water is lost.

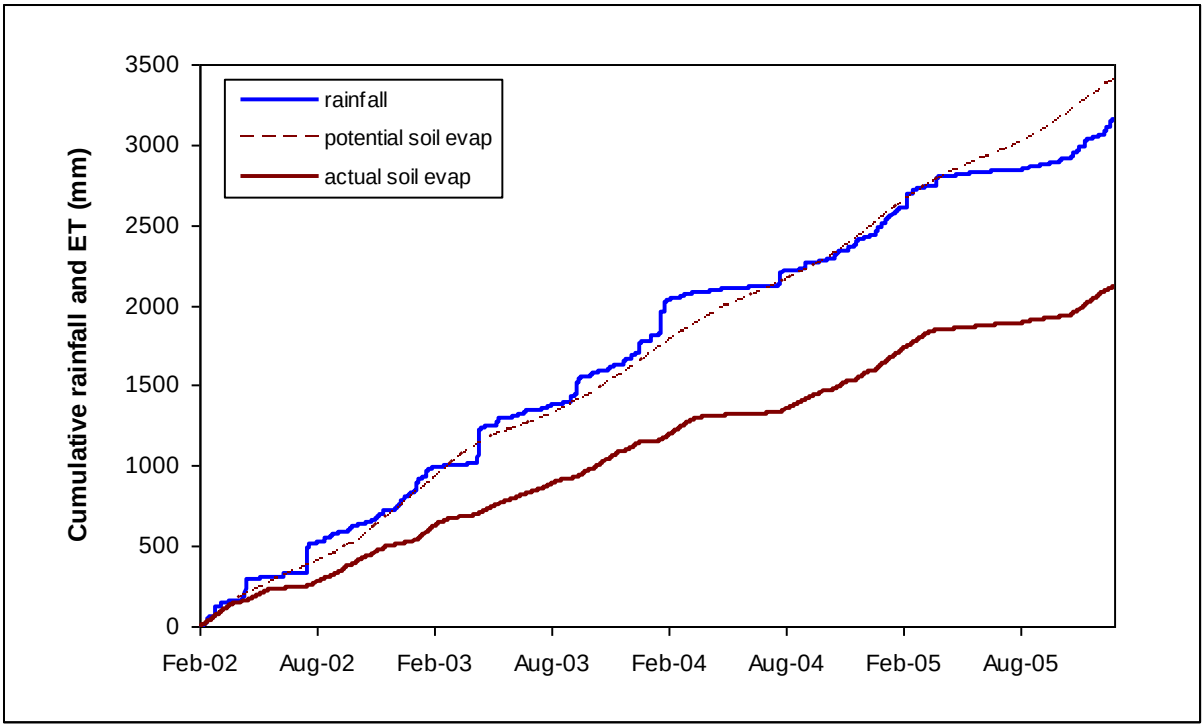

Figure 8.4 Cumulative rainfall (from rain gauges corrected for gaps), potential (from Penman-Monteith) and actual (calculated from model) evaporation at the Bare site for the observed period, February 2002 to December 2005.

For the period between February 2002 and December 2005 the rainfall amounted to 2 573 mm, excluding the intercepted losses that was calculated from the daily rainfall amounts using the Von Hoyningen-Huene method. The calculated actual evaporation was 2 542 mm, thus the total rainfall exceeds the actual evaporation (predicted) by 30 mm at the end of the period. This does not mean that it drained out of the base of the impoundment since the profile does retain large volumes of water. This 30 mm would be retained in the profile and during the drier periods could be evapotranspired. The simulated seepages are assessed later in the chapter. It is important to note that the vegetation growth was not taken into account during the modelling, as the model does not allow for growth in the modelling process. The intercepted water and the transpiration from the vegetation will be considered as being conservative estimates to account for the growth over the time period. These simulations are modelled with the parameters such as *LAI* at initial conditions from 2002.

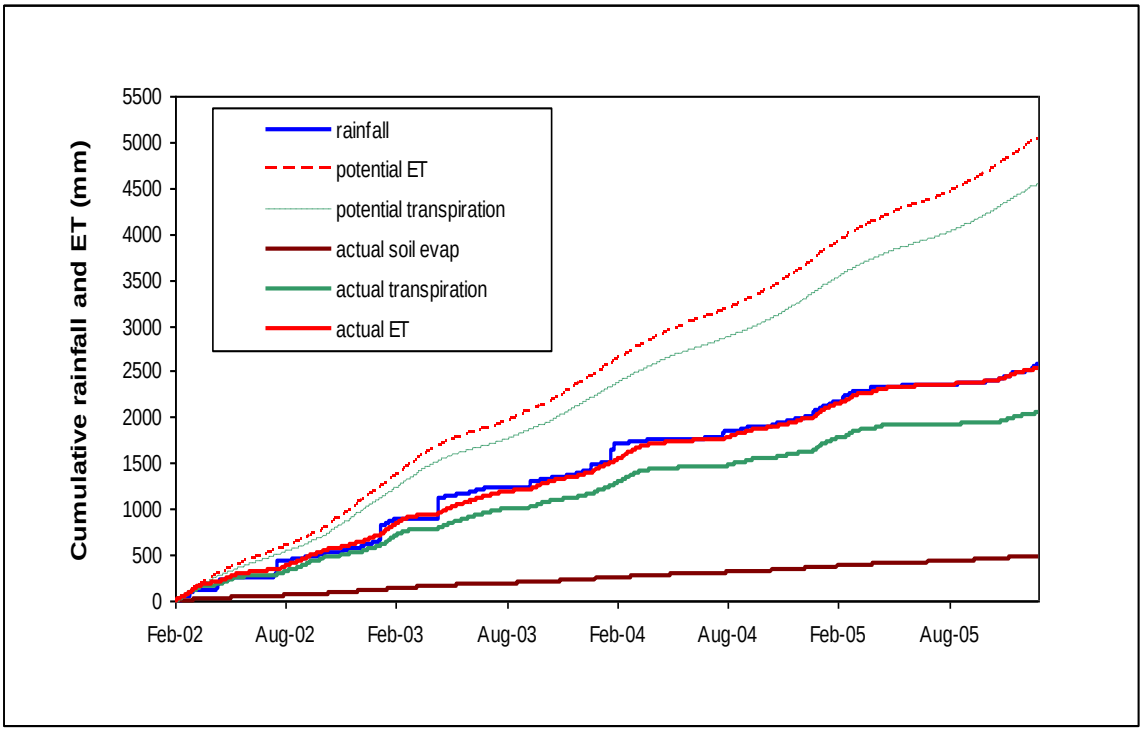

Figure 8.5 Cumulative rainfall (from rain gauges corrected for gaps), potential (from Penman-Monteith) and actual (calculated from model) evapotranspiration at the Fig tree site for the observed period, February 2002 to December 2005.

Assessment of the results for the simulated period between 22 August 2002 and December 2005 shows a cumulative rainfall of 2 117 mm, this excludes the intercepted losses that were calculated from the daily rainfall amounts using the Von Hoyningen-Huene method. The simulated evapotranspiration for this period was 2 045 mm, which would allow a total of 72 mm excess into the profile.

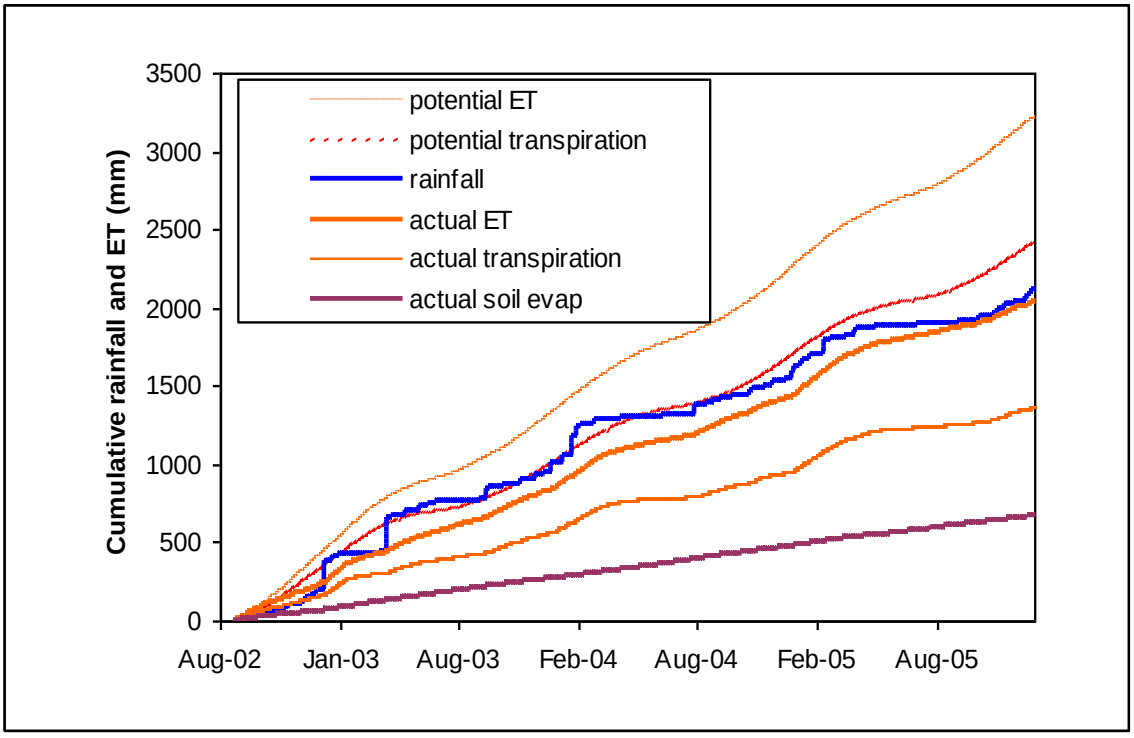

Figure 8.6 Cumulative rainfall (from rain gauges corrected for gaps), potential (from Penman-Monteith) and actual (calculated from model) evapotranspiration at the Nest 9 for the observed period, August 2002 to December 2002.

8.3 Base water balance fluxes

The advanced tensiometer experiments were to determine some measureable tensions to compare against the simulated fluxes at depths of 7 m and 8 m respectively. These advanced tensiometers were installed on Dam 2 and Dam 3-4 at the Fig tree site and near Nest 9. They were positioned in pairs, each at depths differing by 0.5 m for determining hydraulic gradients from the tensions. The advanced tensiometers demonstrated many problems as a result of their depths and thus required constant maintenance for their functioning. The prevalent problems experienced were associated with susceptible leaks or loss of tension. This would lead to very to erratic recordings as illustrated for the Fig tree site (Figure 8.7). These tensiometers had to be replenished regularly, since it was concluded that the actual tensions of the material were the immediate data after the replenishment. Assessment of the capillary pressures for the advanced tensiometer at the Fig tree site show the actual measured tensions were approximately 5 000 mm as compared to the simulated tensions being approximately 6 500 mm. The reason for the advanced tensiometer at the Fig tree site having

various periods was due to the replacement of the transducer. The period without record was due to the transducer bursting during replenishments. The outer casing was retained while and the inner tube and pressure transducer were renewed at different periods during the record.

The simulated tensions at the Fig tree site illustrated by (Figure 8.7) are not accurate and show the material to be dryer initially by a difference of approximately 2 000 mm. This may not affect the calculated seepage rates significantly because the fluxes are determined from the tensions in the soils at varying depths. The simulated tensions do however follow the observed data in terms of the decrease in head at the period of September 2003. The simulated data also follows the observed data closely near the end period.

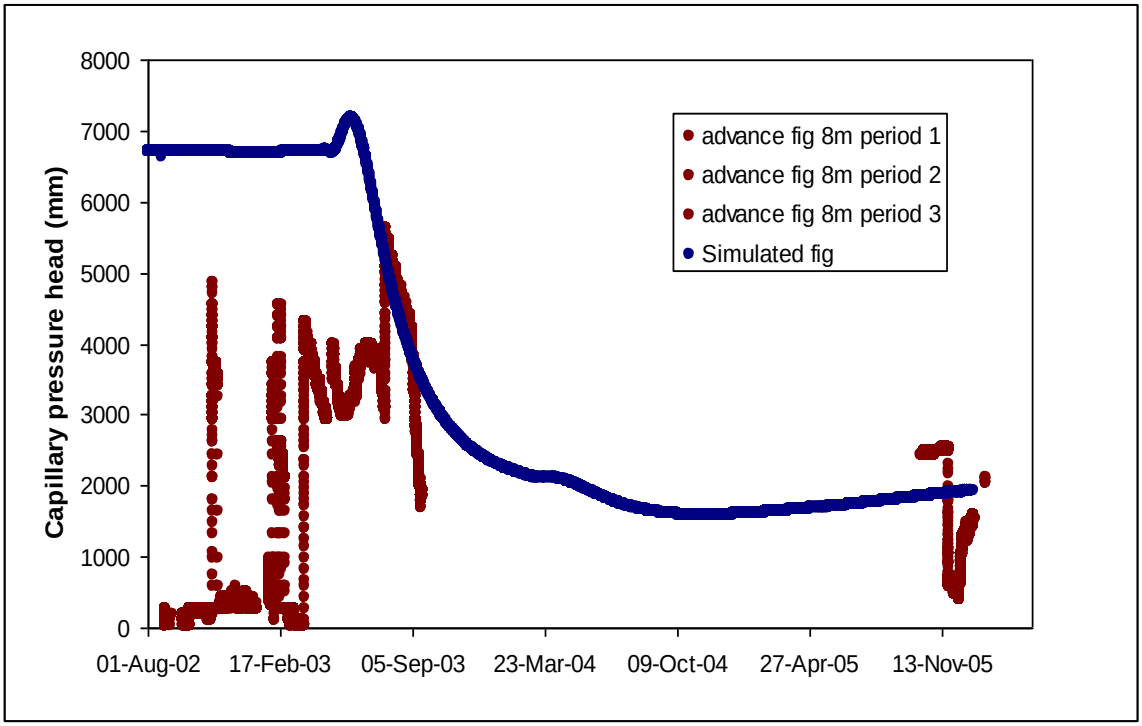

Figure 8.7 Comparison of the observed and simulated tensions 8 m below the surface at the Fig tree site.

The simulated results at the Nest 9 site are illustrated by (Figure 8.8) and follow the observed data for a short period where observed data were available.

Evidence of the efficiency of the vegetation cover comes from analysis of the change in storage and the seepage rates estimated from the simulated fluxes at 8 m below the surface.

The change in storage volume was simulated for the 15 m profile and is also shown to be evidence of the vegetation cover efficiency.

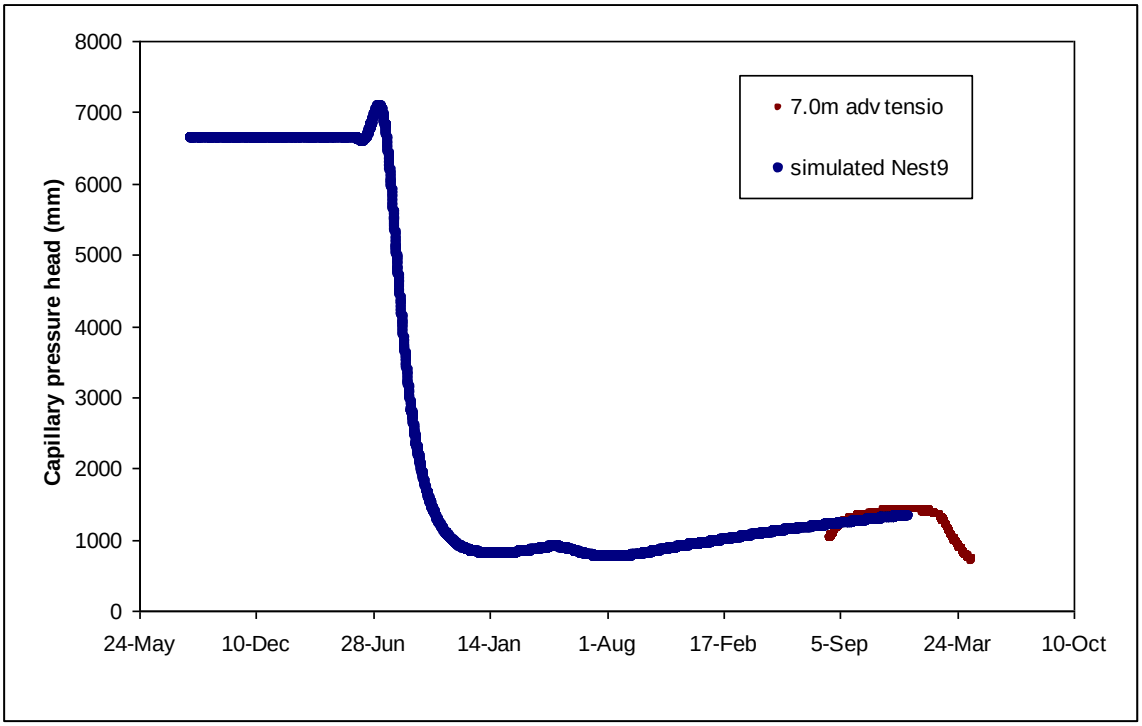

Figure 8.8 Comparison of the observed and simulated tensions 7 m below the surface for the Nest 9 site

Assessment of the seepage from the base of the impoundment starts some 9 months after the extreme rainfall event of 12-13 April 2003 at the Fig site and increases to a peak rate of 10.5 mm/y, 19 months later (September 2005). The simulated results are illustrated in (Figure 8.9). The seepage rate then begins to decrease. During the observation period, a total of 12 mm is estimated to seep from the base of the impoundment for the Fig tree site. It would have been interesting to observe the simulation further than the simulated period, since no large rainfall events occur after February 2004 and it is apparent that near the end of the simulation the seepage rate is observed to reach a maximum before decreasing. The simulated seepage rate at the Fig tree site is low and this could be attributed to the deep rooting. The roots would have the ability to dry the material profile 2 m below the surface, thus capillary properties would favour the possibility for the material to be dry. When these large rainfall events do occur it would take some time before they demonstrate their effects. The material properties would certainly favour the hypothesis that upward movement of water is possible if extremely dry conditions were to be experienced for extended periods.

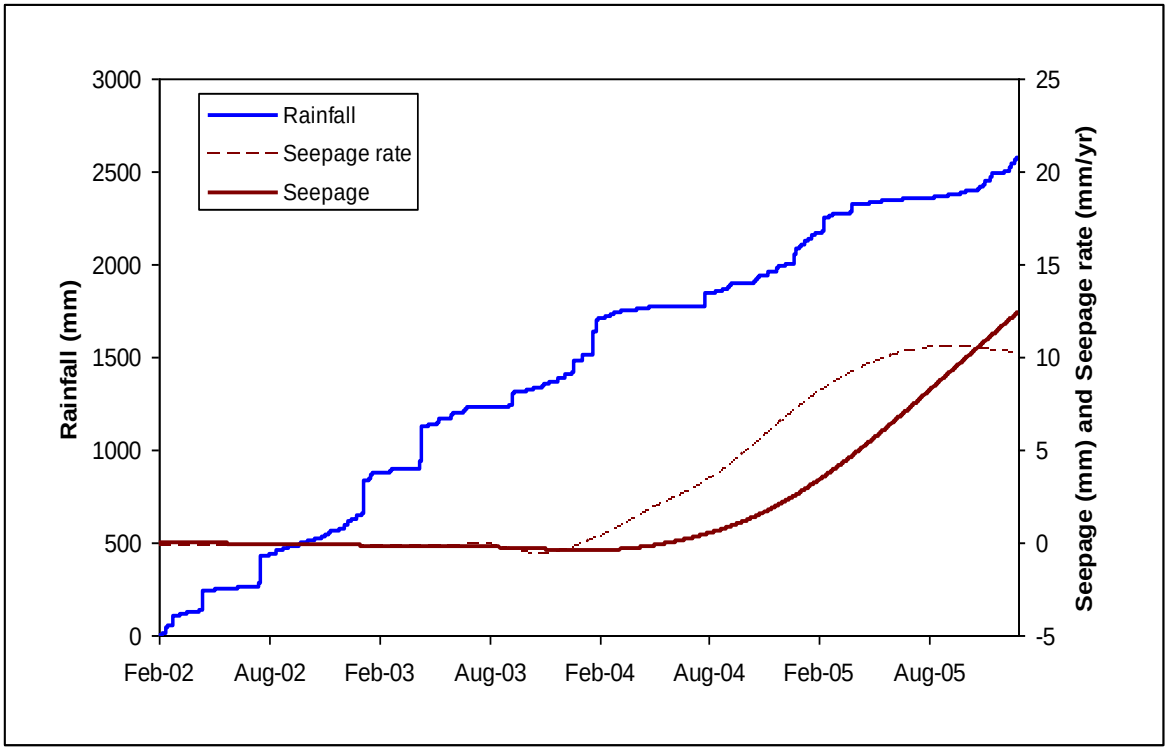

Figure 8.9 Cumulative rainfall (from rain gauges corrected), simulated seepage and seepage rate at 8 m below the surface at the Fig tree site for the observation period February 2002 to December 2005.

Analysis of the storage state for the Fig tree site is illustrated in (Figure 8.10) at the end of the observation period exceeds the storage state at the start by approximately 18 mm. The rooting depth of the Fig tree was modelled to extend to depths of 2 m, thus allowing drying of the material profile. The deeper roots are capably of drying out the material at greater depths. This is evident from the simulations where the change to low storage state is returned almost immediately after the larger rainfall events. These rather erratic jumps in the simulation are the result of the roots drying out the material profile, thus when extreme rainfall does occur their effects on the retained water are not manifested.

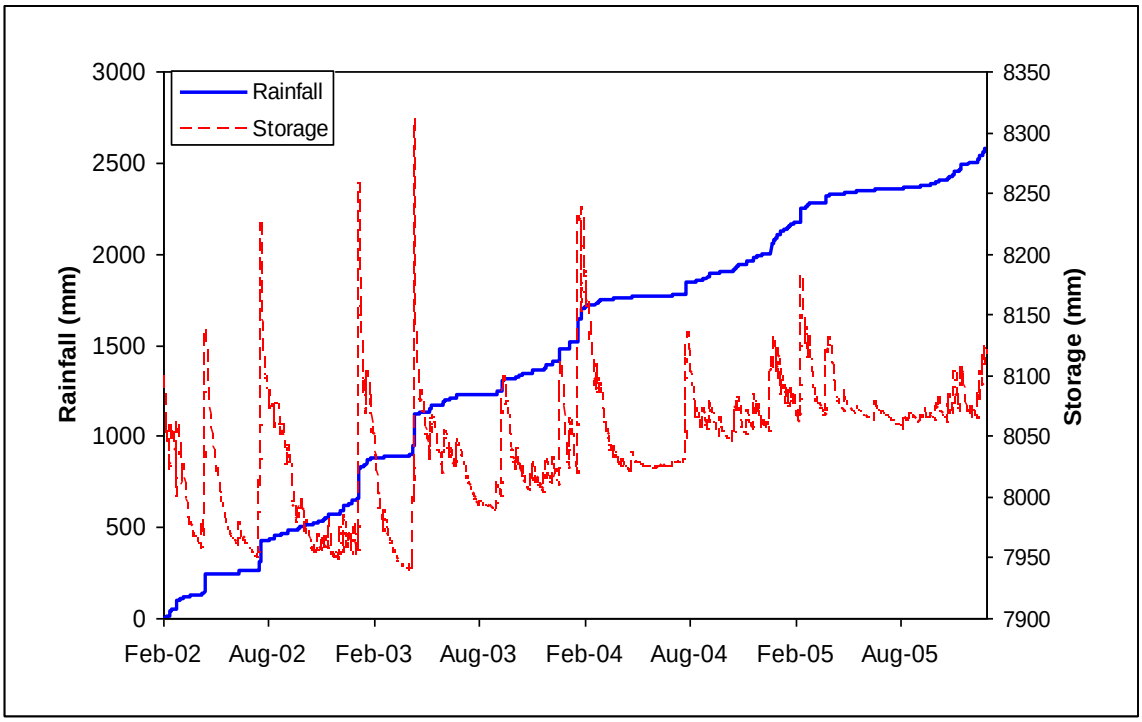

Figure 8.10 Cumulative rainfall (from rain gauges corrected) and simulated storage volume for the 15 m profile at the Fig tree site for the observation period, February 2002 to December 2005.

Assessment of the seepage from the base of the impoundment at the Nest 9 site is illustrated in (Figure 8.11). Seepage starts some 6 months after the extreme rainfall event of 12-13 April 2003 at the Nest 9 site and increases to a peak rate of approximately 70 mm/y. The seepage rate then decreases at for the rest of the simulated period. During the observation period, a total of 83 mm is estimated to seep from the base of the impoundment for the Nest 9 site. This total seepage over the observation period occurs earlier than that for the Fig tree site. The vegetation at Nest 9 does not have as deep a rooting into the material profile as the Fig tree site. Although the rooting density may be high in the upper top (300 mm) layer of the material, it does not dry out the material to the extent down the profile as that of the Fig tree site. In simpler terms the dry vertical extent is greater down the profile of the Fig tree site than the Nest 9 site, thus a greater void would occur at the Fig tree site. This would explain the increase in the seepage rate occurring much earlier after the high rainfall event of 12-13 April 2003.

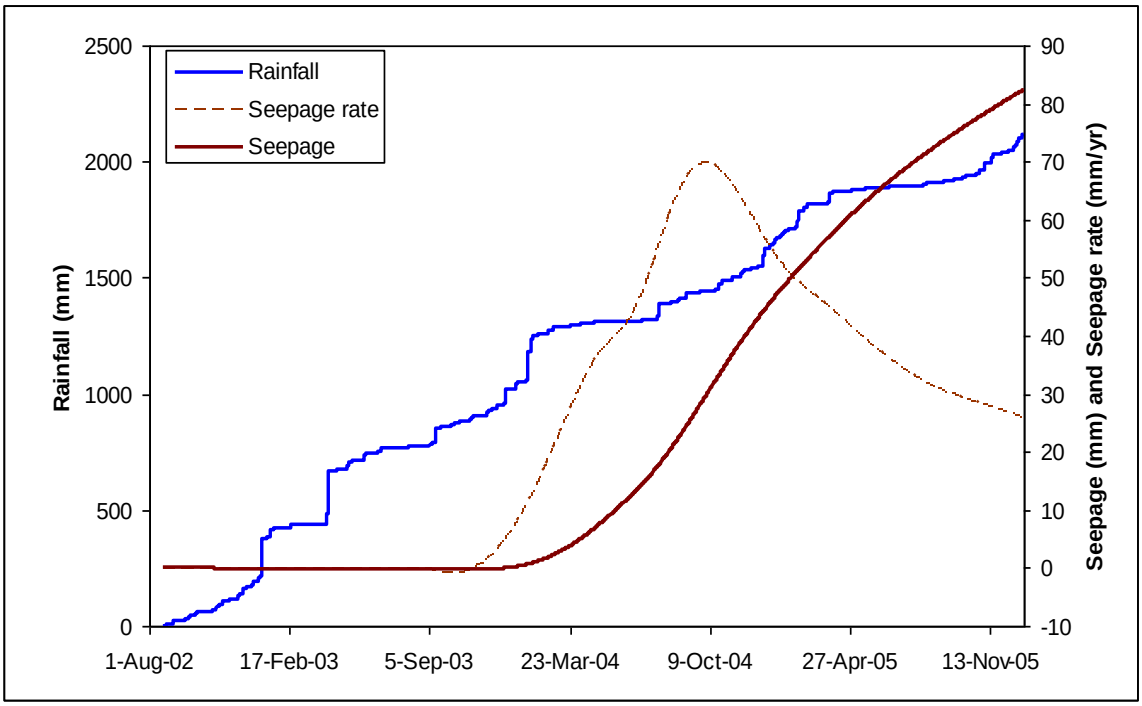

Figure 8.11 Cumulative rainfall (from rain gauges corrected), simulated seepage and seepage rate at 8 m below the surface at the Nest 9 site for the observation period, August 2002 to December 2005.

The storage state of the profile is generally higher in Nest 9 as illustrated in (Figure 8.12) than at the Fig site. The drop in storage from high rainfall events is not as immediate as at the Fig tree site. This can be attributed to the waste material properties on Dam 3-4 being different to that of Dam 2. The vegetation rooting distribution is in the top 300 mm of the profile, thus the material is not as dry down the vertical extent of the profile. The change in storage illustrates a change of -10 mm for the initial to the end of storage.

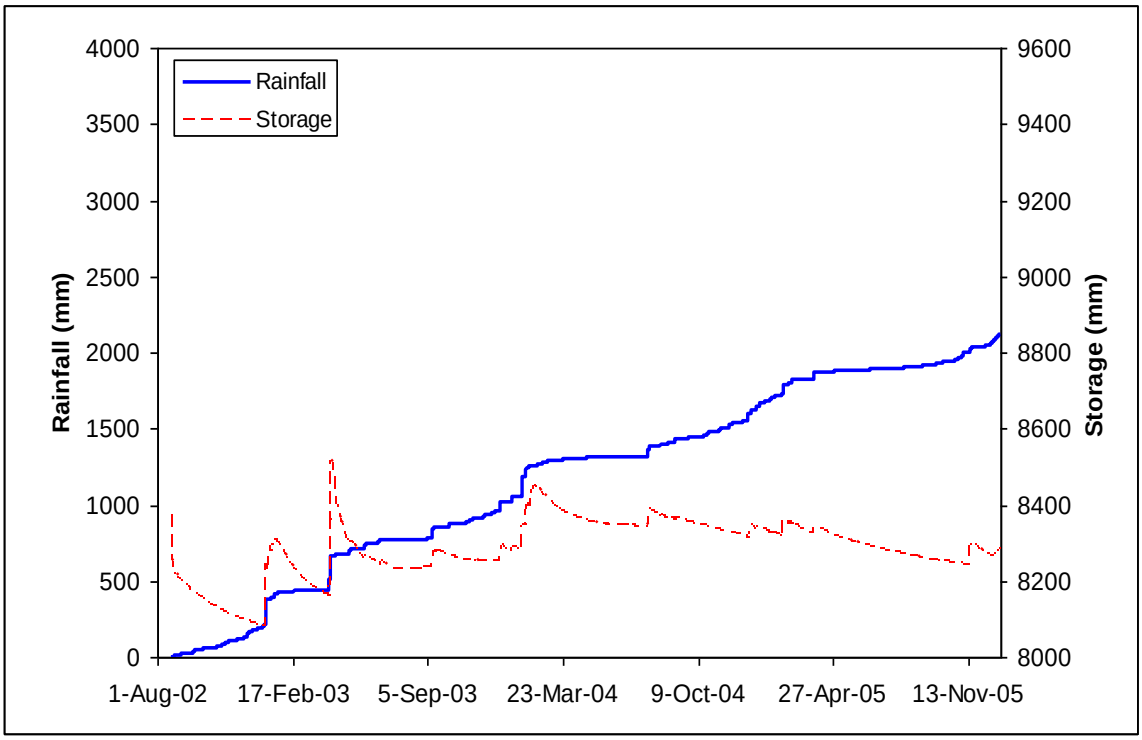

Figure 8.12 Cumulative rainfall (from rain gauges corrected) and simulated storage volume for the 15 m profile at the Nest 9 site for the observation period, August 2002 to December 2005.

Assessment of the seepage from the base of the impoundment starts some 3 months after the extreme rainfall event of 12-13 April 2003 illustrated in (Figure 8.13) for the Bare site and increased to a peak rate of 900 mm/y. Compared to the sites with vegetation (roots), the Bare site responds to the other major rainfall events, such as the 23 January 2004 and a simulated peak rate of 1400 mm/y was the result of the material profile remaining saturated from previous rainfall events. During the observation period, a total of 800 mm is estimated to seep from the base of the impoundment for the Bare site. The seepage rate decreases almost immediately after reaching a maximum after extreme rainfall events, which does not occur for any of the other simulations at the other sites. This is the result of the seepage actually moving through the material profile at the Bare site, since there are no roots, thus no evapotranspiration. The high seepage at the Bare site can again be explained by the material properties, when in the region of saturation. Water will move through the profile at high rates, because the material is saturated after extreme high rainfall.

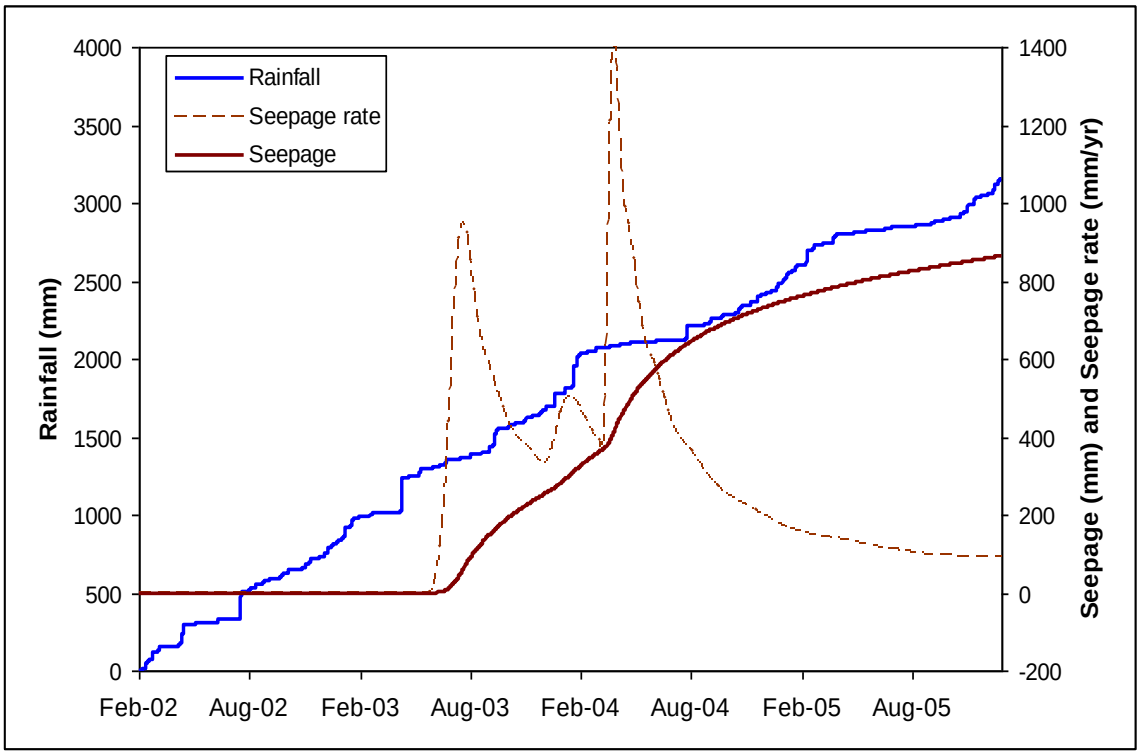

Figure 8.13 Cumulative rainfall (from rain gauges corrected), simulated seepage and seepage rate at 8 m below the surface at the Bare site for the observation period, February 2002 to December 2005.

The decrease of the storage at the Bare site is far less after extreme events illustrated by (Figure 8.14) when compared to both the Fig tree and Nest 9 sites. This is an indication of the effect the transpiration at the respective sites. The responses to the extreme event of April 2003 for Dam 3-4 (Nest 9) and the Bare site on Dam 2 are more rapid, reflecting the wetter initial condition in the profile due to the smaller transpiration and evaporation losses.

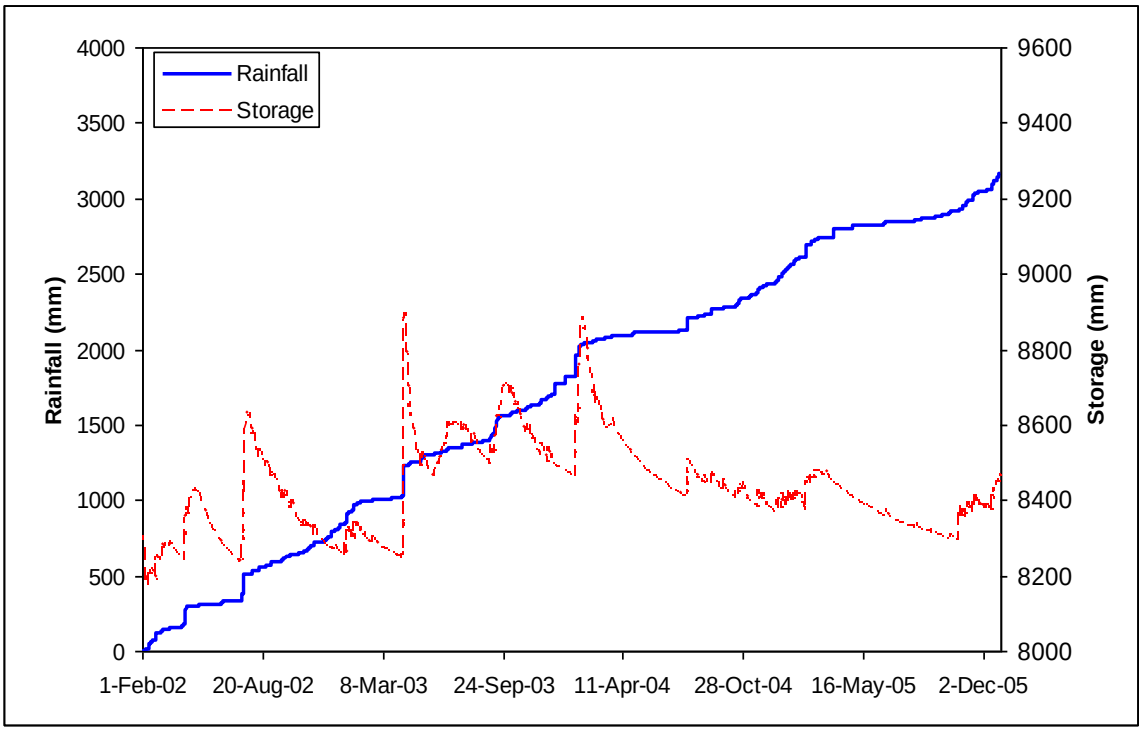

Figure 8.14 Cumulative rainfall (from rain gauges corrected) and simulated storage volume for the 15 m profile at the Bare site for the observation period, February 2002 to December 2005.

The water balance over the profile of the Dams can be expressed as:

Net rainfall + Interception = Evapotranspiration + Evaporated interception + Seepage + Change in storage (Runoff assumed = 0)

where interception is the amount of gross rainfall intercepted by the vegetation and subsequently evaporated. This water balance is summarized for each of the sites simulated in (Figure 8.15).

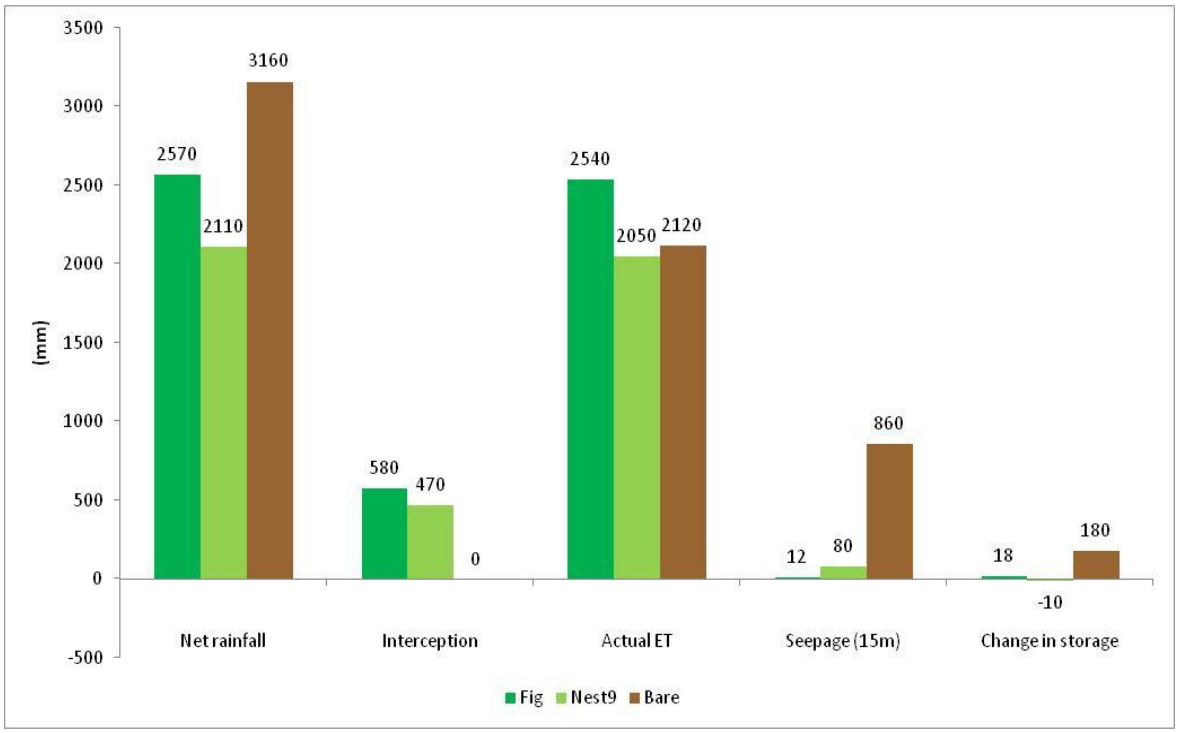

Figure 8.15 Summary of the simulated water balances over the observation periods for the respective sites.

The DWAF minimum requirements state the outflow/seepage rate at the base of the waste body must not exceed $1x10^{-7}$ cm/s. It is important to really understand the dynamics of the systems, since this requirement would certainly prove ok for a static system or a tradition impervious waste cover system. However, for the vegetation cover it is important that the understanding of the material profile be studied as a non-static system. Thus simulated monthly or annual values would be a more realistic comparison. Although an extreme event could occur that would be detrimental in terms of the seepage, a non-static approach would not account for the system possibly drying the material. Thus the event may not be as detrimental and actually be taken up in the storage capacity within the material itself. Comparison of the simulated results from the three study sites are shown in Table 8.2.

Table 8.2 Summary of the simulated performance for the respective sites.

Performance criteria	Fig Tree	Nest 9	Bare
Start date	2 February 2002	4 August 2002	2 February 2002
End date	31 December 2005	31 December 2005	31 December 2005
Total seepage (mm)	12.4	82.4	864
Seepage rate (cm/s)	2.49×10^{-8}	1.2×10^{-7}	1.7×10^{-6}
Seepage rate at peak (cm/s)	3.3×10^{-8}	2.2×10^{-7}	4.5×10^{-6}

The ability for roots to draw water out of the material together with the material characteristics is considered the major factors with regard to the subsurface conditions that establish the hypothesis. The most significant factor in this study is that roots do aid the covers performance by reducing the material water content. In the next section, electrical resistivity tomography investigations were performed to assess and give an indication of the materials water content

8.4 Electrical Resistivity Tomography

Electrical Resistivity Tomography (ERT) investigations are used to identify zones with different electrical resistivity, which can deflect differences in material densities or properties and water content. An ERT survey was performed across Dam 2 and Dam 3-4 as illustrated in (Figure 8.16) to assess the variability of water saturation in the material.

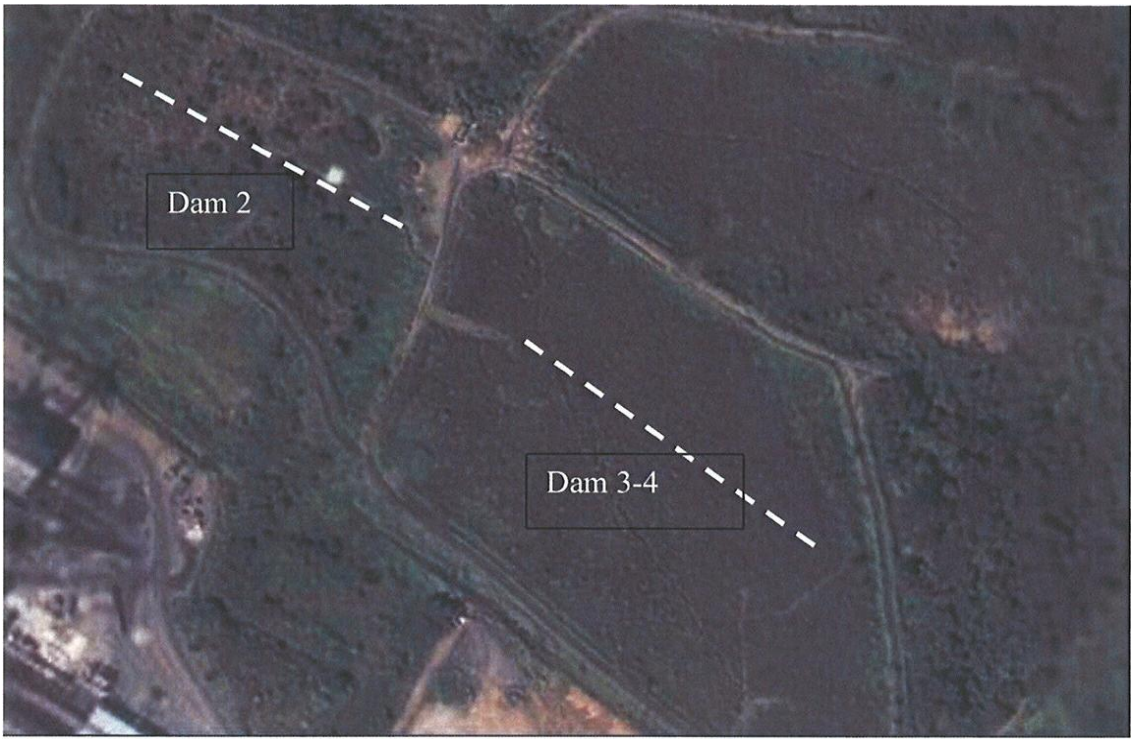

Figure 8.16 Electrical Resistivity Tomography survey lines depicting the respective transect across Dam 2 and across Dam 3-4.

ERT measurements are conducted by inserting multiple probes and directing electrical current into the ground through multiple electrodes and measuring the resulting voltage difference. Clay material will have a resistivity range of 1-100 ohm.m and are further lowered by the water in the material (Dahlin and Loke, 1998). Thus the material with high water content has a lower resistivity, blue, and dryer material has a higher resistivity, red as illustrated in (Figure 8.17). Analysis of the ERT transect across Dam 2, reveals that near surface (top 2 m) of the material is very dry, illustrated in (Figure 8.17). The material does; however, seem to increase in water content with increasing depth of the material. The transect also shows that the north west half of the material is drier than the south east side. Dam 2, where this transect of the survey was performed, has very dense vegetation with more trees and thick grasses in the north west. The south east of the transect is not as densely vegetated, thus explaining the distribution of water below the surface of the material. A very wet patch is evident in the centre of the transect survey and this could be as a result of the way the dam was deposited.

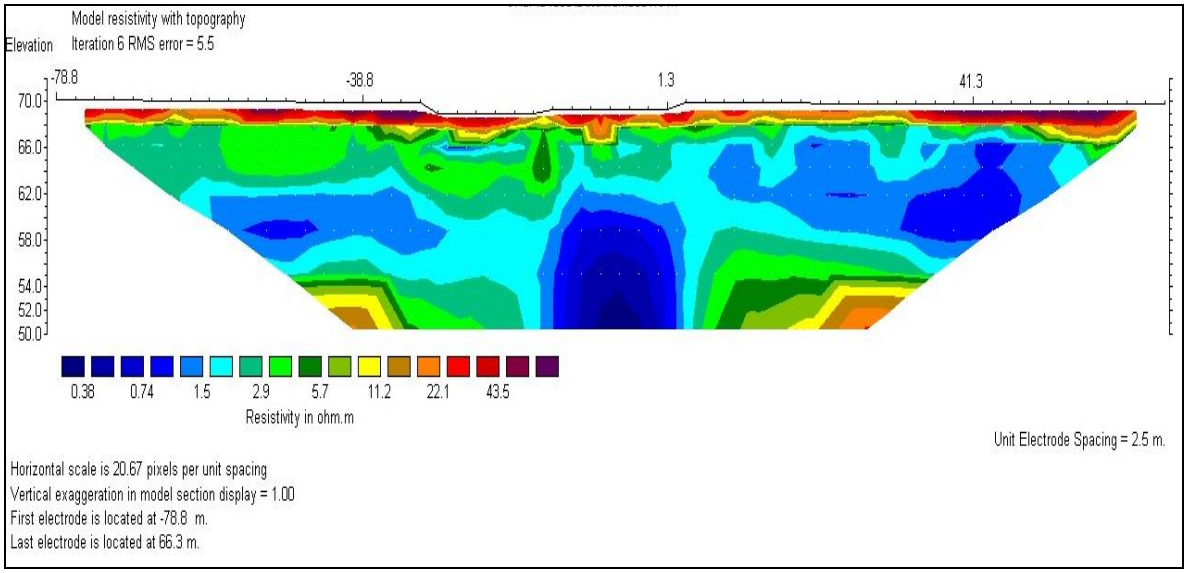

Figure 8.17 Electrical Resistivity Tomography survey of Dam 2.

Analysis of the ERT survey across transect on Dam 3-4, illustrated in (Figure 8.18), reveals a much wetter surface compared to the survey of Dam 2. This is due to Dam 2 having mature and far denser vegetation than that of Dam 3-4 (refer to aerial view in introduction Figure 4.1). The transect shows the distribution of water (low resistivity) to be approximately between 2 and 12 m below the surface. This water distribution is evenly spread across the transect. Further assessment of the survey also reveals a horizontal layering of the material distribution or water content at the bottom of the Dam. The layered material distribution may be the result of different deposits of materials when the Dam was formed.

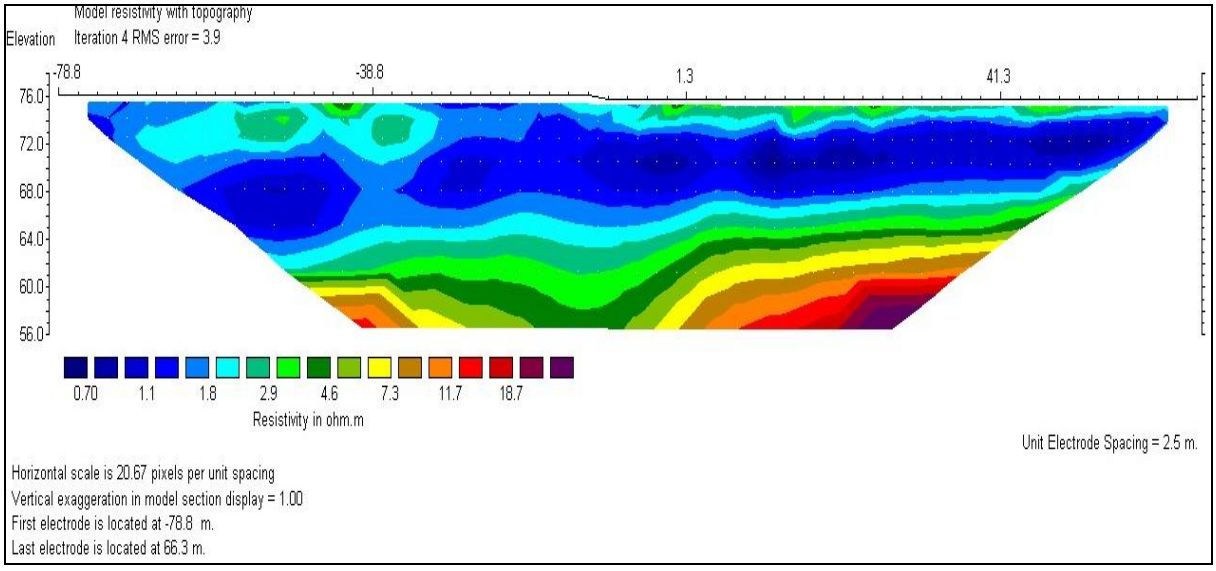

Figure 8.18 Electrical Resistivity Tomography survey of Dam 3-4.

Groundwater recharge could be considered a means of monitoring and determining seepage levels for the Dams. The results of the groundwater could determine whether the aquifers are part of the larger aquifers that extend beyond the Dams. Thus, comparison with the simulated seepages against the piezometric levels would gives estimates of the aquifer boundaries extending beyond the Dams.

8.5 Groundwater Recharge

Groundwater recharge can be estimated for events using near-continuous monitoring data of water table height (episodic recharge). This work has examined technical bases for estimating groundwater recharge at the Fig tree site on Dam 2. Piezometers provide high-frequency data of piezometric levels to build confidence in the estimates made for groundwater recharge in a system with known boundary conditions. A schematic diagram of how the piezometer is placed in the ground is illustrated in (Figure 8.19). Piezometers are designed to be placed in a PVC casing which extends below the groundwater level. The PVC casing is designed to allow water into the casing, which would allow a column of water to be formed in the casing. A transducer is then positioned within the PVC casing ensuring it is submerged below the water column that is formed in the casing, thus allowing measurements of the height of water above it. The height of water above the transducer produces a voltage that is logged over time. Thus the changes in the groundwater level can be interpreted from the measured voltages, which would be associated with the changes of height of the water in the PVC casing.

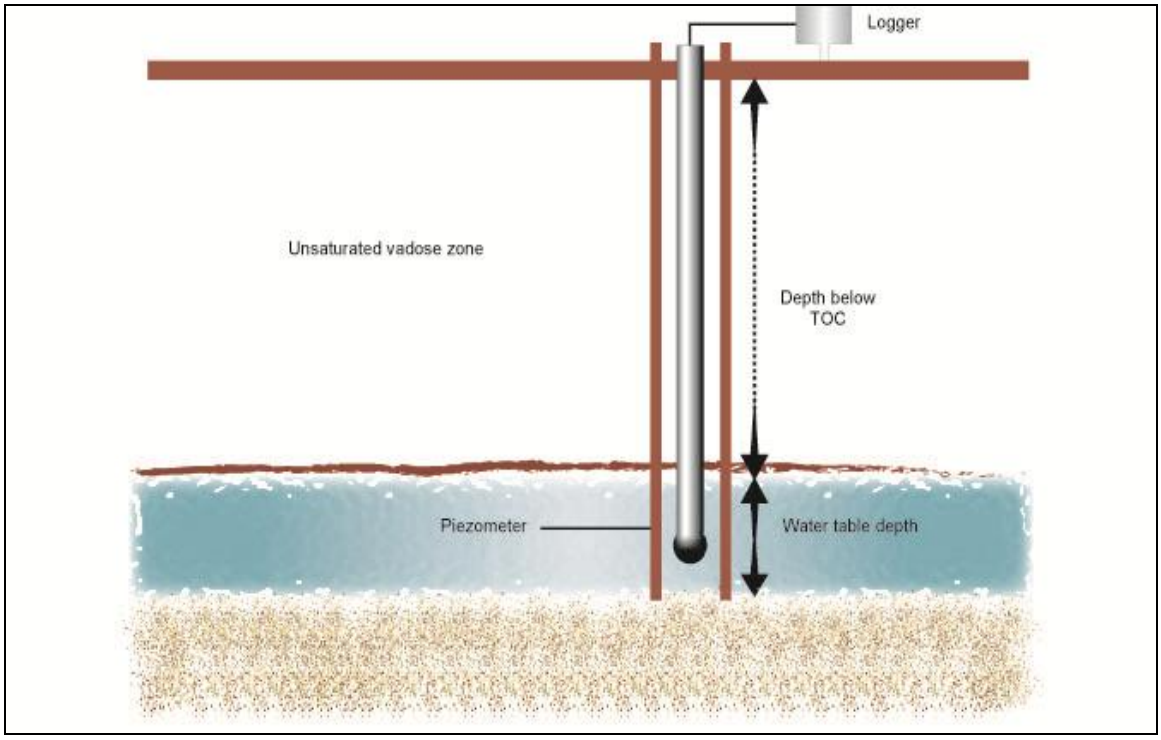

Figure 8.19 Schematic diagram of the piezometer.

Two holes were drilled next to each other at respective depths of 17.5 m and 35 m below the top of the cover (TOC) on Dam 2. PVC casings were placed to these depths. These depths would ensure that the groundwater levels of Dam 2 would be measured with the 17.5 m hole and the 35 m hole would measure groundwater levels of the Dwyka Tillite formation. Pressure transducers were installed to record automatically, the water table height at one hour intervals, providing a continuous piezometric head. Manual groundwater readings were also performed at each site visit to confirm the reliability of the automatic reading. Data of water levels at the time of installation indicated two separate water tables. Data were measured for a period of two years (August 2003 – November 2005), although automatic readings did fail at times. Data for the water levels below the TOC are illustrated in (Figure 8.20) for the 17. 5 m hole and in (Figure 8.21) for the 35 m hole. The data are summarised as:

- The initial reading for the 06 August 2003 indicated the levels of the groundwater to be at a depth 8 140 m below the TOC, while for the groundwater level of the Dwkya Tillite the groundwater level was measured at 16 330 m below the TOC. It is important to note that the water level in the Dam 2 did take one week to equilibrate to a level approximately 13 800 m

below TOC. This indicates the slow movement of water within the Dam 2 material.

- Extreme events did have an impact on groundwater levels. The recharge response levels for Dam 2 are seen later than that of the deeper water table. Again due to the slow movement of water through the material. The movement of the deeper water in the Dwyka Tillite is more rapid, this being the result of the aquifer being far bigger than that over the Dams Area.
- The extreme event for January 2004 increased water levels for the Dam 2 aquifer to 11 700 m below TOC, thus increased the water levels by approximately 2.5 m. This extreme event impacted the deeper aquifer to 15 400 m, thus increased water levels by approximately 3.0 m.

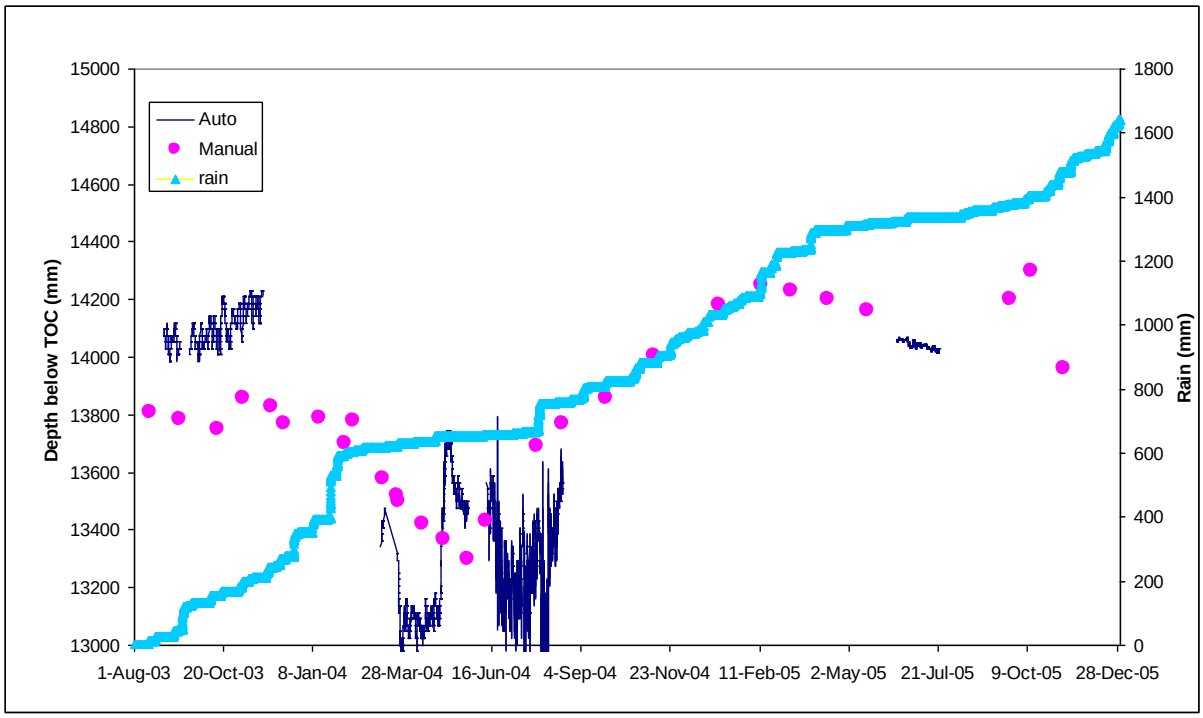

Figure 8.20 Water level depth data for the 17.5 m deep piezometer.

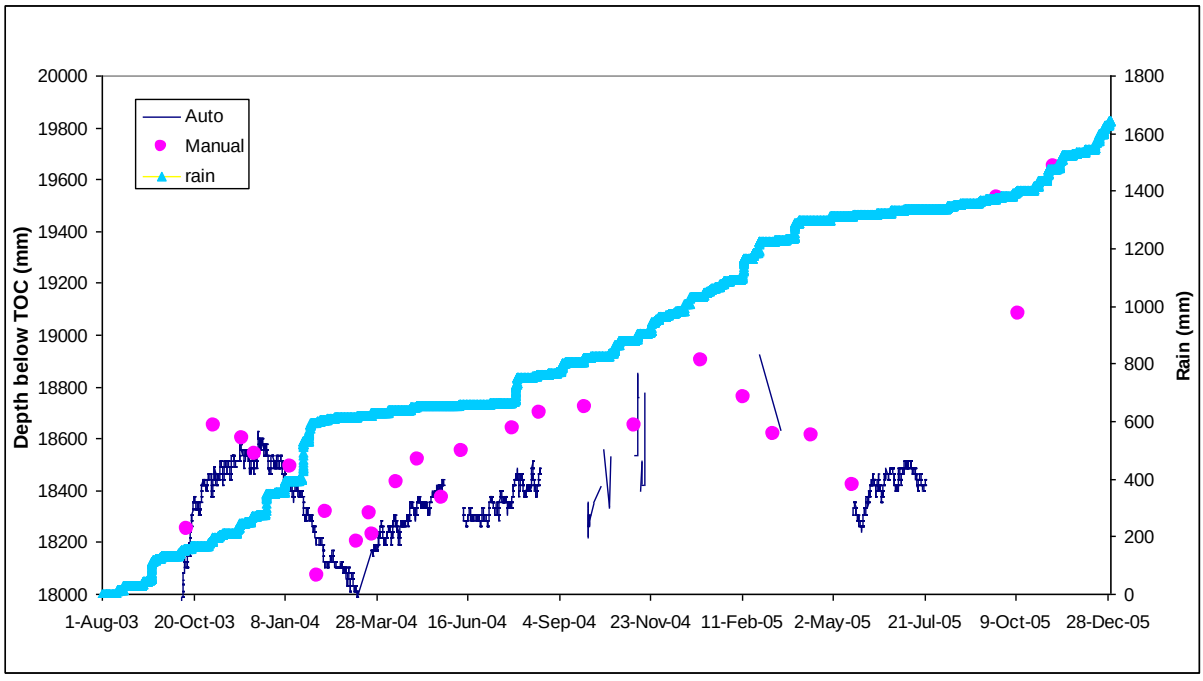

Figure 8.21 Water level depth data for the 35 m deep piezometer.

In this chapter simulations were presented that provide evidence for the ability of a vegetation cover to limit the effluent leaching from the waste impoundment. The chapter provides simulated comparisons of the climatic fluxes, base fluxes for the material, seepage and seepage rates and storage at the different sites. The estimates of simulated results were verified by assessment of the groundwater recharge and investigations of the electrical resistivity tomography survey results. The following chapter contains the discussion, conclusions and recommendation to conclude this study.

9. CONCLUSION AND RECOMMENDATIONS

The overall object of this research was to answer the hypothesis as to whether a vegetated cover is able to limit effluent leaching from a waste impoundment. The advantage of the vegetation over the traditional final cover system, is that it acts with nature and if appropriately and entirely assessed can act to its highest potential. The study set to determine the climatic input and output to the vegetated final cover system. The study utilized weather station data, which was installed on the waste impoundment and this data, were used in the calculation of the empirical Penman-Monteith evaporation equation. The measured parameters on the Dams compared relatively well with the parameters from the Durban International Airport. The estimated potential evaporation was used in the calculation of the actual evaporation, which compared well against the actual measured evapotranspiration of the Bowen ratio experiments on Dam 3-4.

A hand held auger was used to recover material samples from the Dams at various sites and at various depths in order to characterise the material. Characterisation consisted of the textural analysis and particle size distribution. Assessment of the waste revealed the material to range from silt to clay, although it is actually a fine ash. The hydraulic properties and the ability of the porous media to retain and transmit water were required in order to model transport of water in the material. The ability of a porous media to retain and transmit water was characterized by the relationships between water content,(θ), matric pressure head, (h), and the hydraulic conductivity, (K). The material water retention characteristics were derived using experiments of an outflow cell and pressure pot techniques to define the desorption characteristics. These characteristics were done with analysis in the laboratory, however actual field experiments were also undertaken to determine the infiltration into the materials. All these characteristics were assessed for the modelling of the material profile.

A large part of the study was to determine the success from the monitoring of the tensions and determine the fluxes in the waste material. This was done with tensiometers within the root-zone of the material. Comparison of the different sites proved the very presence of a tree or any vegetation provides a so-called outlet for

water to be removed from the material profile. The very fact that roots are capable of evaporating water creates a deficit in the material profile that far exceeds the water content in the material when there is no vegetation. The study of the advanced tensiometers was to large degree the testimony that vegetation reduced seepage in the deeper profile.

The monitoring of the materials results were verified by simulation done with the HYDRUS-2D model. Although conservative estimates of the parameters were used in the modelling, the overall conclusion is that the simulated results from the Fig tree supersede that of Nest 9 and more over that of the Bare site with regard to reducing baseflow from the impoundment. The sensitivity analysis of the HYDRUS–2D model revealed that the saturated hydraulic conductivity, alpha (inverse of air entry pressure), pore size distribution index and macropore flow was most influential on the matric pressure head.

The overall conclusions that prove a vegetated cover is able to control effluent leaching from a waste impoundment were confirmed in the comparison of the simulated seepages from the respective sites. The results clearly show roots of the vegetation provide an outlet besides seepage from the waste impoundment. The study also confirms the importance of material characteristics for such a study. The material having properties of very high water retention capacity, allow roots the ability to ‘suck’ up water from the material. The properties related to the holding capacity when the materials are drier prove to be an advantage in this study. These results proved with a large rainfall event that should be detrimental with regard to leachate, the vegetation cover can limit and even reverse the movement of water that has entered the waste impoundment. The simulations in this study were conservative, as alternative water pathways such as lateral flows were not accounted for and could reduce seepage. The effectiveness of the vegetation can only be expected to improve. The overall conclusion of the study is that vegetation is capable of limiting the leachate on this waste impoundment.

The following work is recommended in order to close gaps in the study.

- Analysis of the materials for Dam 3-4 to assess the hydraulic characteristics for these material properties, since they were superimposed from Dam 2.
- Improved methods such as a scintillometer to measure and improve the estimates of actual evapotranspiration
- For the complete closure of Vumbuka reserve it is imperative a monitoring program is initiated for assessing the success of the ET cover over a longer time period. This will be considered the final process for the DWAF to consider the waste impoundment legally closed. The monitoring programme should be in operation for a period of approximately 3 year to give complete assurance. Basic issues that will be associated with the monitoring program will be:
    - ability to maintaining the integrity of the reserve;
    - surface and groundwater quality – continuous sampling and laboratory analysis to determine and assess the phytoremediation capacity;
    - water levels – monitoring of groundwater levels with boreholes simultaneously determining the phreatic levels with piezometers;
    - performance of the ET cover – monitoring of water fluxes within the root zone and at deeper levels; and
    - monitoring of near base seepage – strongly recommended that results from lysimeters are required for determining the seepage through the waste impoundment.

10. REFERENCES

Allen, R., G, Pereira, L. S., Raes, D., Smith, M.,. 1998. Guidelines for Predicting Crop Water Requirements. Food and Agriculture Organisation of the United Nations, FAO Irrigation and Drainage Paper 56, Rome.

Ankeny, M.D., Ahmed, M., Kaspar, T.C. and Horton, R. 1991. Simple Field Method for Determining Unsaturated Hydraulic Conductivity. Soil Science Society American Journal, 55: 467-470.

Berti, W.R. and Cunningham, S.D. 2000. Phytostabilisation of Metals. In: I. Raskin and B.D. Ensley (Editors), Phytormediation of Toxic Metals: Using Plants to Clean Up the Environment. New York, John Wiley and Sons, Inc, pp. 71-89.

Blaylock, M.J. and Huang, J.W. 2000. Phytoextraction of Metals. In: I. Raskin and B.D. Ensley (Editors), Phytoremediation of Toxic Metals: Using Plants to Clean Up the Environment. New York, John Wiley and Sons, Inc., pp. 53-71.

Blight, G.E. 2002. Measuring evaporation form soil surfaces for environmental and geotechnical purposes. Water SA, 287(4): 381-393.

Bosman, H.H. 1990. Methods to convert American Class A-pan and Symon's tank evaporation to that of the representative environment. Water SA, 16: 227-236.

Caldwell, J.A. and Reith, C.C. 1993. Principles and practice of Waste Encapsulation, Lewis Publishers, Boca Raton.

Clark, G.A., Smajstrla, A.G. and Zazueta, F.S. 1989. Atmospheric Parameters Which Affect Evapotranspiration. University of Florida, Florida.

Dahlin, T. and Loke, M.H. 1998. Resolution of 2D Wenner resistivity imaging as assessd by numerical modelling. Journal of Applied Geophysics, 38: 237-249.

Druzynski, A. and Duthe, D. 2003, Assessment of the Effectiveness of Hydraulic Containment Using Groundwater Modelling. SRK Consulting.
Report No. 277286

Duthe, D. and Cameron-Clarke, I. 2004. Waste Classification and Evironmental Risk Assessment. SRK Consulting. Report No.311081.

DWAF. 1998a. Waste Management Series. Minimum Requirements for Waste Disposal by Landfills. 2nd Edition.

DWAF. 1998b. Minimum Requirement for the Handling, Classification and Disposal of Hazardous Waste. 2nd Edition.

Dye, P. 2003. Tree Transpiration Measurements at AECI Umbogintwini Slimes Dam 2, Environmentek, CSIR, C/O Agrometeorology School of Applied Environmental Sciences, University of Natal

Ensley, B.D. 2000. Rationale for the use of phytoremediation. In: I. Raskin and B.D. Ensley (Editors), Phytoremediation of Toxic Metals: Using Plants to Clean the Environment. New York, John Wiley and Sons, Inc, pp. 3-13.

EPA. 1983. Standards for Owners and Operators of Hazardous Waste Treatment, Storage, and Disposal Facilities. Environmental Protection Agency, Washington, D.C. 40 CFR 264.

EPA. 1991. Design and Construction of RCRA/CERCLA. Environmental Protection Agency, Seminar Publication. EPA/625/4-91/025.

EPA. 2000. Introduction to phytoremediation. U. S. Environmental Protection Agency, Cincinnati, Ohio. Report No. EPA/600/R-99/107.

EPA. 2003. Evapotranspiration Landfill Cover Systems Fact Sheet. U. S. Environmental Protection Agency. EPA/542/F-03/015.

Everson, 2003.Bowen Ratio Experiments, Environmentek, CSIR, C/O Agrometeorology, School of Applied Environmental Sciences, University of Natal

Feddes, R.A., Kowalik, P.J. and Zaradny, H. 1978. Simulation of field water use and crop yield. Pudoc: Wageningen.

Gee, G.W. and Or, D. 2002. Particle-size distribution. In: J. Dane and G. Topp (Editors), Methods of Soil Analysis, Part 4, Physical Methods. Madison, WI, Soil Science Society of America, pp. 255-293.

Hauser, V.L., Weand, B.L. and Gill, M.D. 2001. Alternative Landfill Covers. Air Force for Environmental Excellence Technology Tranfer Division. TX 78235-5363.

Hillel, D. 1998. Environmental soil physics. San Diego, California: Academic Press.

Hubbell, J.M. and Sisson, J.B. 1998. Advance tensiometer for shallow or deep soil-water pressure measurements. Soil Science, 163: 271-277.

ITRC. 1999. Decision Tree: Phytoremediation. Interstate Technology and Regulatory Cooperation Work Group Phytoremediation Work Team.1-9 pp.

ITRC. 2003. Technical and Regulatory Guidance for Design, Installation and Monitoring of Alternative Final Landfill Covers. Interstate Technology and Regulatory Council Alternative Landfill Technologies Team.

Jordahl, J.L., Foster, L., Schnoor, J.L. and Alvarez, P.J. 1997. Effect of hybrid popular trees on microbial populations important to hazardous waste bioremediation. Environmental Toxicology and Chemistry, 16(6): 1318-1321.

Leij, F.J. and van Genuchten, M., Th. 1997. Characterization and Measurement of the Hydraulic Properties of Unsaturated Porous Media. In: M.T. van Genuchten, Leiji, F, J. (Editor), Proceedings of the International Workshop on Characterization and Measurement of the Hydraulic Properties of Unsaturated Porous Media. University of California, Riverside, California, pp. 1-13.

Lorentz, S. 2001. Subsurface Water Balance at AECI, Umbogintwini Slimes Dam 2. University of KwaZulu Natal, Pietermaritzburg.

Lorentz, S. 2003. Proposed Evapo-Transpiration (ET) Cap for the North West Waste Site (NWWS) at the Umbogintwini Industrial Complex: Water Balance Study. School of Bioresources Engineering and Environmental Hydrology, University of Natal, Pietermaritzburg. Report to Umbogintwini Industrial Complex: Land Remediation.

Lorentz, S., Goba, P. and Pretorius, J. 2001. Hydrological Process Research: Experiments and Measurements of the Soil Hydraulic Characteristics. School of Bioresources Engineering and Environmental Hydrology, Pietermaritzburg. WRC Report No : 744/1/1.

Lorentz, S. and Morgan, G. 2006. Determination of the efficiency of an evapo-transpiration cover as an alternative to conventional capping of contaminated land (Interim Report). School of Bioresource Engineering and Environmental Hydrology, University of KwaZulu-Natal, Pietermaritzburg.

Lui, Z. and Dickmann, D.I. 1992. Response of two hybrid Populus clones to flooding, drought and nitrogen availability. Canadian Journal of Botany, 70: p2265-2270.

Lyman, W.J., Reidy, P.J. and Levy, B. 1992. Mobility and Degradation of Organic Contaminants in Subsurface Environments. Michigan, Chelsea: C. K. Smoley, Inc.

McNaughton, K.G. and Jarvis, P.G. 1983. Predicting effects of vegetation changes on transpiration and evaporation. In.Water deficits and plant growth: Additional woody crop plants, Vol. 2. New York: Academic Press, 1-47 pp.

Mualem, Y. 1976. A New Model for Predicting the Hydraulic Conductivity of Unsaturated Porous Media. Water Resources Research, 12(3): 513(10).

Mulder, J.H. and Haven, E.L. 1995. Solid Waste Assessment Test "SWAT" Program. Report to the Integrated Waste Management Board, Division of Clean Water, Environmental Protection Agency, California. 96-1CWP.

Newman, L.A., Strand, S.E., Choe, N., Duffy, J., Ekuan, G., Ruszaj, M., Shurtleff, B.B., Wilmoth, J., Heilman, P. and Gordan, M.P. 1997. Uptake and Bioremediation of Trichloroethylene by Hybrid Populars. Environmental Science Technology, 31: 1062-1067.

Perroux, K.M. and White, I. 1988. Designs for disc permeameters. Soil Science Society American Journal, 52: 1205-1215.

Pivetz, B.E. 2001. Phytoremediation of Contaminated Soil and Groundwater at Hazardous Waste Sites. U. S. Environmetal Protection Agency, Washington, DC. EPA/540/S-01/500.

Schnoor, J.L. and Dee, P.E. 1997. Phytoremediation. Groundwater Remediation Technologies Analysis Centre, Pittsburgh. Report No. TE -98-01.

Schulze, R.E. and Maharaj, M. 2004 Development of a Database of Gridded Daily Temperatures for Southern Africa. Water Research Commision, Pretoria, RSA, WRC Report 1156/2/04.

Schulze, R.E., Lecler, N.L. and Hohls, B.C. 1994. Land Cover and Treatment. In. Schulze, R.E. Hydrology and Agrohydrology: A Text to Accompany the ACRU 3.00 Agrohydrological Modelling System. Water Research Commision, Pretoria. Report TT69-95, AT6-1 to AT6-32 pp.

Šimunek, J., Šejna, M. and van Genuchten, M.T. 1999. The HYDRUS-2D software package for simulating the two-dimensional movement of water, heat and multiple solutes in variably saturated media. U.S. Salinity Laboratory Agricultural Research Service, U.S Department of Agriculture, Riverside, CA.

Smith, M., Allen, R., Monteith, J. L., Perrier, A., Pereira, L. and Segeren, A. 1992. Expert Consultation of Revision of FAO Methodologies for Crop Water

Requirements.Food and Agriculture Organisation of the United Nations (Land and Water Development Division), Rome. 60pp.

Suter, G.W., Luxmoore, R.J. and Smith, E.D. 1993. Compacted Soil Barriers at Abandoned Landfill Sites. Journal of Environmental Quality, 22(2): 217 - 226.

Stormont, J.C. 1997. Incorporating Capillary Barriers in Subsurface Cover Systems, pp. 39-51. In: R.T. D and R.C. Morris (Editors), in *Landfill Capping in the Semi-Arid West: Problems, Perspectives and Solutions*. Idaho Fall, Id., Environmental Science and Research Foundation.

van Genuchten, M.T. 1980. A closed-form equation for predicting the hydraulic properties of unsaturated soils. Soil Science Society American Journal, 44: 892-898.

Weand, B.L., Horin, J.D., Hauser, V.L., Gimon, D.M., Gill, M.D., Mehta, M. and Casagrande, D.J. 1999. Landfill Covers for Use at Air Force Installations. Air Force Centre for Environmental Excellence Technology Transfer Division, Brooks AFB. TX 78235-5363.

Wooding, R.A. 1968. Steady infiltration from a shallow circular pond. Water Resources Research, 4: 1259-1273.

APPENDIX A

TEXTURAL ANALYSIS

Table A.1 Textural analysis for the respective sites and depths

Sample	Depth	Vol	CR	M(Pd)	M(Pd+Sw)	M(Pd+Sd)	Vol WC	Bulk Dens	w	Porosity
	m	cm3	g	g	g	g		g/cm3	(g/g)	
Bare	1	167.83	140.16	6.39	309.96	228.37	0.49	0.49	0.997	0.816
Bare	2.5	164.06	146.64	6.34	364.97	244.90	0.73	0.56	1.306	0.789
Bare	4	182.92	151.69	6.49	405.26	252.72	0.83	0.52	1.613	0.805
Bare	4.5	164.06	139.72	6.38	323.29	221.98	0.62	0.46	1.335	0.825
Bare	5	184.80	146.64	6.39	381.41	233.61	0.80	0.44	1.834	0.835
Bare	6	184.80	139.43	6.38	364.39	218.05	0.79	0.39	2.026	0.852
Bug	0.5	92.40	72.56	6.37	139.14	133.96	0.06	0.60	0.094	0.775
Bug	2	92.40	75.24	6.34	180.52	119.39	0.66	0.41	1.617	0.846
Bug	5	92.40	75.07	6.39	177.40	126.30	0.55	0.49	1.140	0.817
Bug	5.5	92.40	76.56	6.47	182.30	117.63	0.70	0.37	1.869	0.859
Bug	6	92.40	76.42	6.40	173.25	114.53	0.64	0.34	1.852	0.870
Bug	6.5	92.40	74.33	6.39	180.79	111.58	0.75	0.33	2.243	0.874
Bug	7	92.40	75.48	6.38	188.59	130.34	0.63	0.52	1.202	0.802
Bug	7.3	92.40	71.41	6.40	167.28	124.31	0.47	0.50	0.924	0.810
Bug	7.5	92.40	75.44	6.39	183.77	121.62	0.67	0.43	1.562	0.838
Bug	9	92.40	80.69	6.39	189.59	123.46	0.72	0.39	1.818	0.851
Bug	9.5	92.40	80.31	6.42	203.78	133.96	0.76	0.51	1.478	0.807
Bug	10	92.40	77.73	6.45	186.36	126.48	0.65	0.46	1.416	0.827
Bug	11.5	169.72	114.15	6.38	322.12	240.81	0.48	0.71	0.676	0.733
Fig	2	92.40	71.48	6.33	181.27	121.35	0.65	0.47	1.376	0.822
Fig	3	92.40	73.95	6.39	185.78	119.99	0.71	0.43	1.659	0.838
Fig	4	92.40	70.94	6.38	159.21	111.53	0.52	0.37	1.394	0.860
Fig	7	182.92	140.02	6.38	365.85	220.94	0.79	0.41	1.944	0.846
Fig	7.5	160.29	141.81	6.33	348.21	232.42	0.72	0.53	1.374	0.802
Fig	8.5	141.43	140.84	6.36	333.95	227.39	0.75	0.57	1.329	0.786
Fig	9	184.80	142.36	6.37	377.60	224.53	0.83	0.41	2.019	0.845
Fig	10	105.60	139.17	6.38	293.71	204.47	0.85	0.56	1.515	0.789
Fig	10.5	171.60	140.23	6.41	399.68	264.54	0.79	0.69	1.146	0.741
Fig	11	169.72	145.61	6.39	378.92	225.43	0.90	0.43	2.090	0.837
Fig	12	169.72	146.05	6.39	388.84	228.51	0.94	0.45	2.108	0.831

Where Pd is the pie dish

Sw is the wet soil

Sd is the dry soil

WC is the volumetric content

APPENDIX B

PARTICLE SIZE DISTRIBUTION

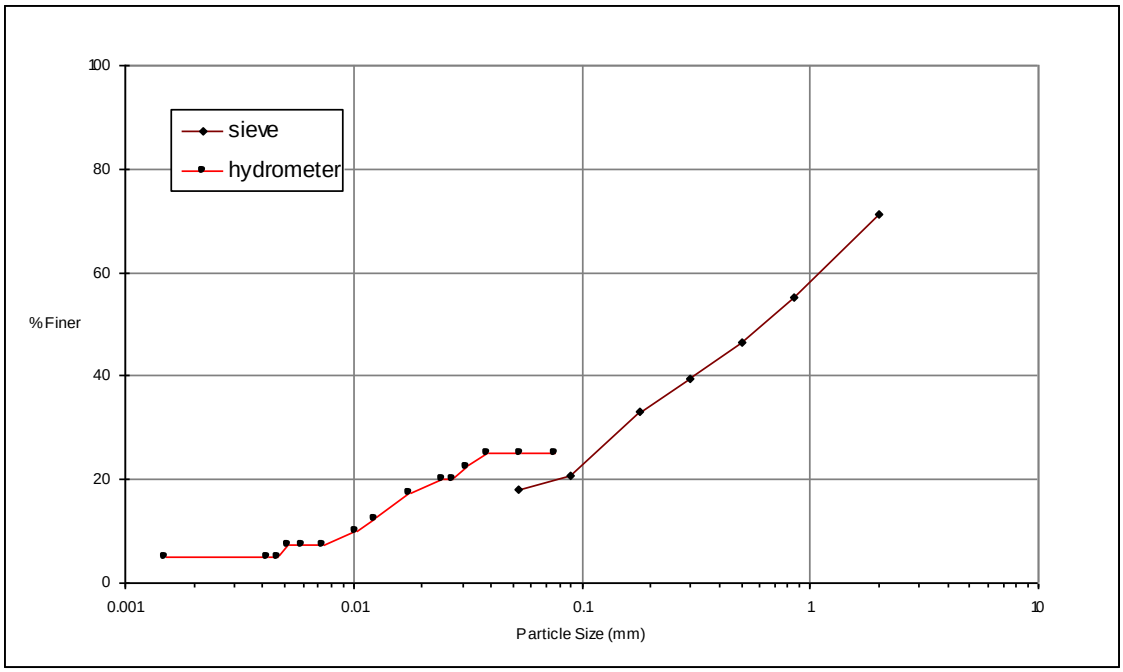

Figure B.1 Particle size distribution for the Bugweed site at 500 mm

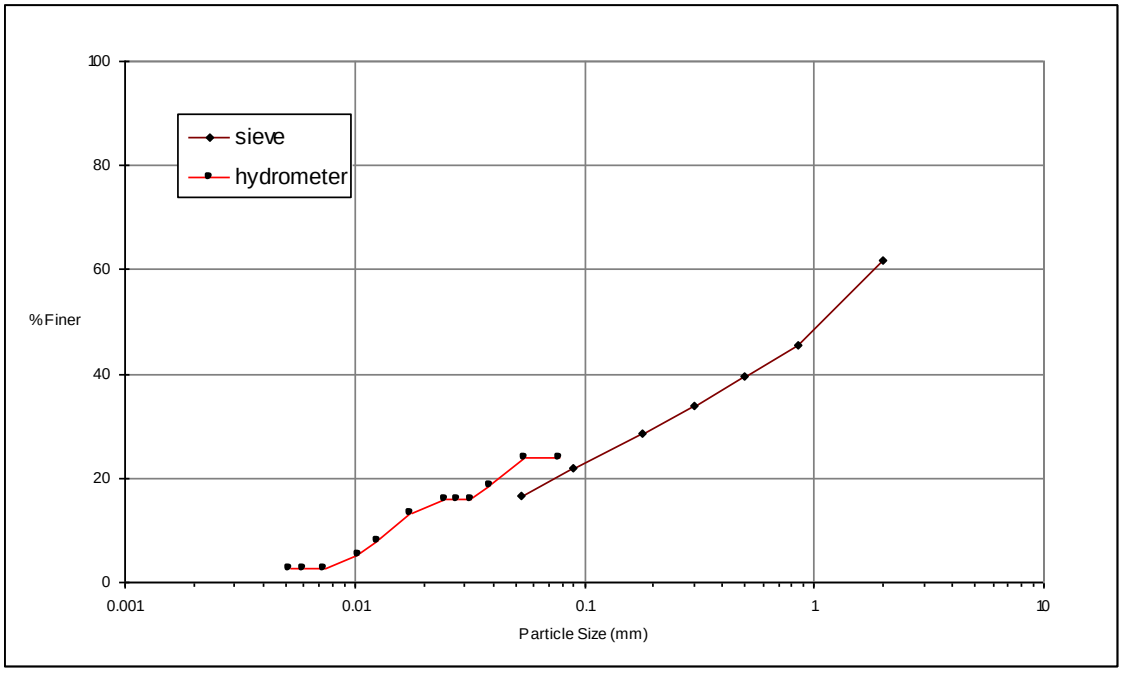

Figure B.2 Particle size distribution for the Bugweed site at 2000 mm

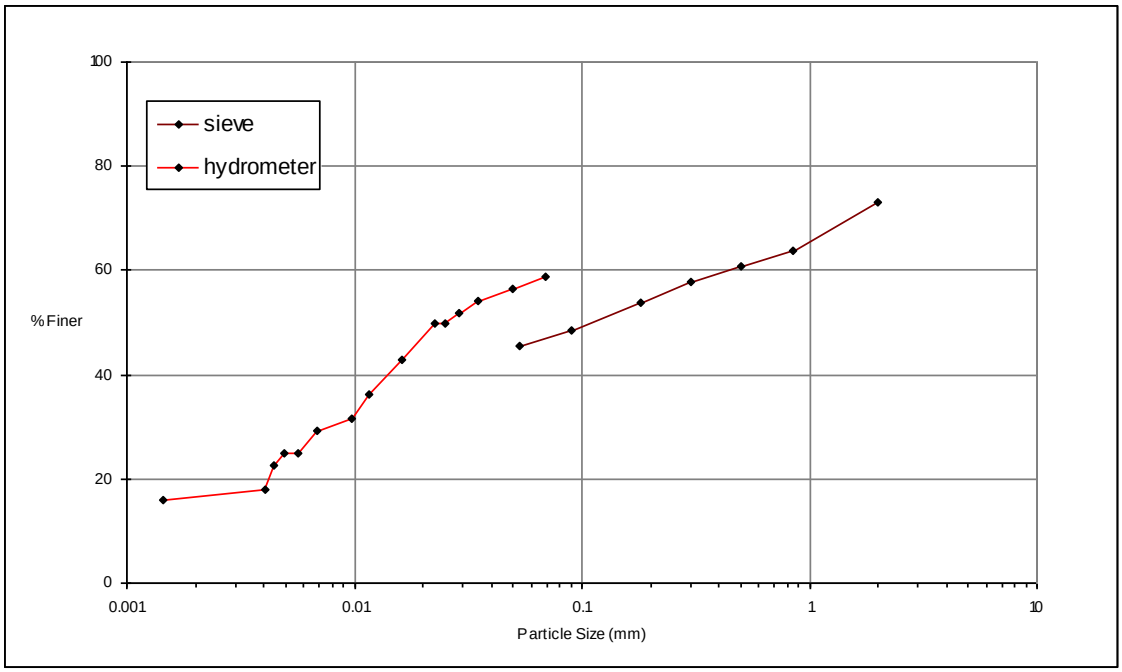

Figure B.3 Particle size distribution for the Bugweed site at 5000 mm

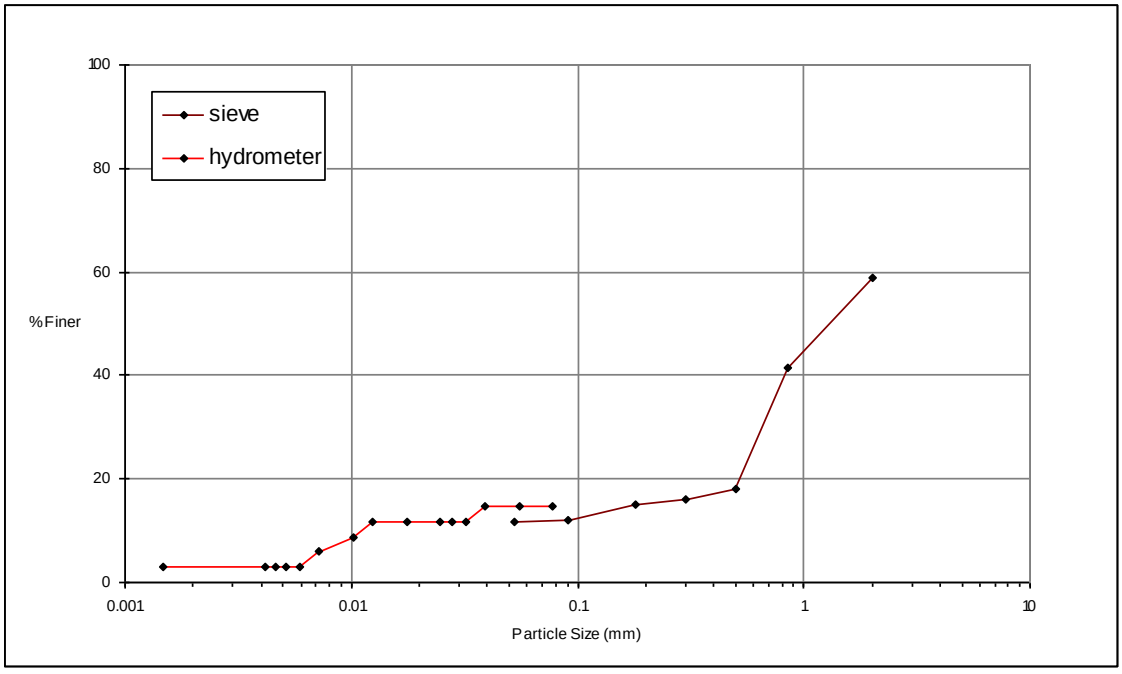

Figure B.4 Particle size distribution for the Bugweed site at 5500 mm

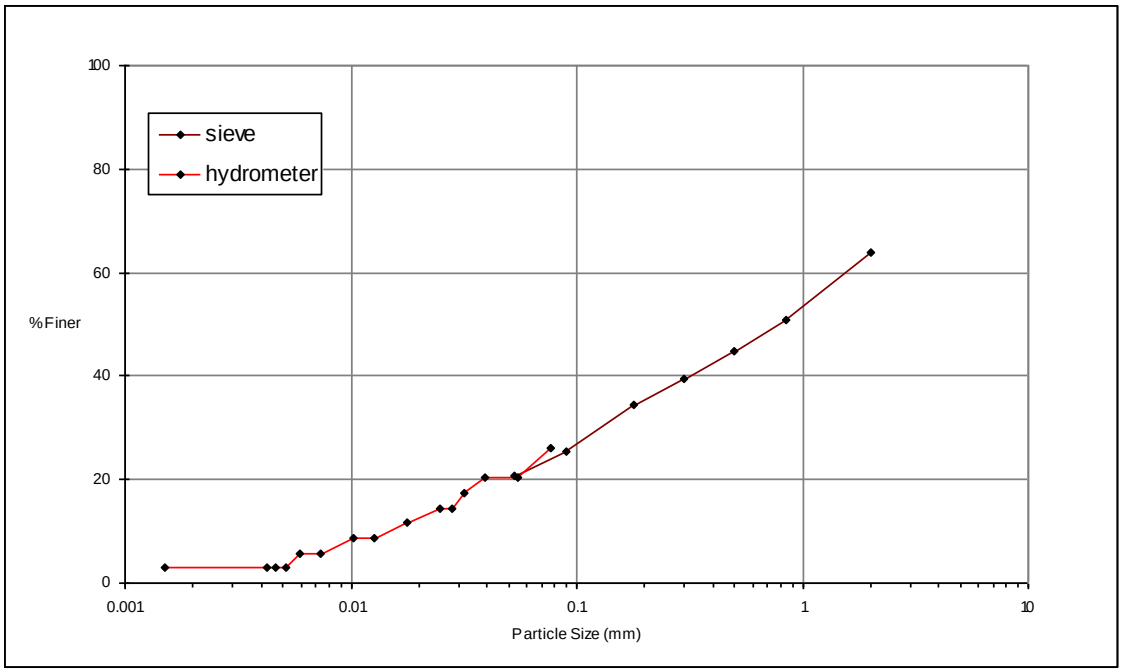

Figure B.5 Particle size distribution for the Bugweed site at 6000 mm

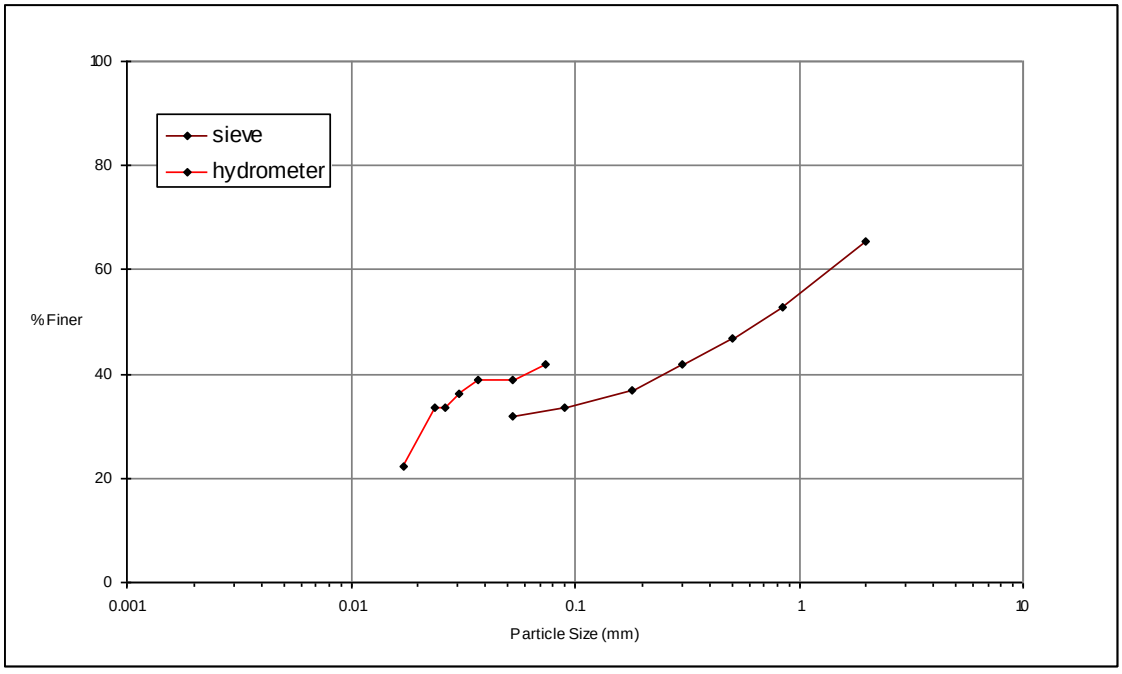

Figure B.6 Particle size distribution for the Bugweed site at 6500 mm

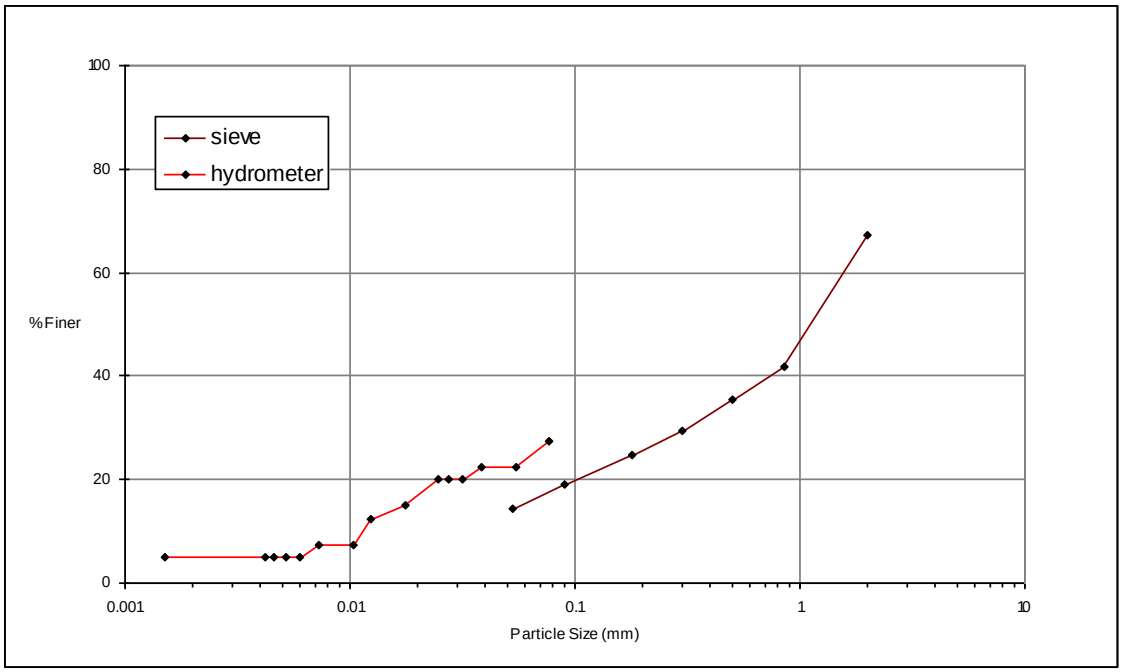

Figure B.7 Particle size distribution for the Bugweed site at 7000 mm

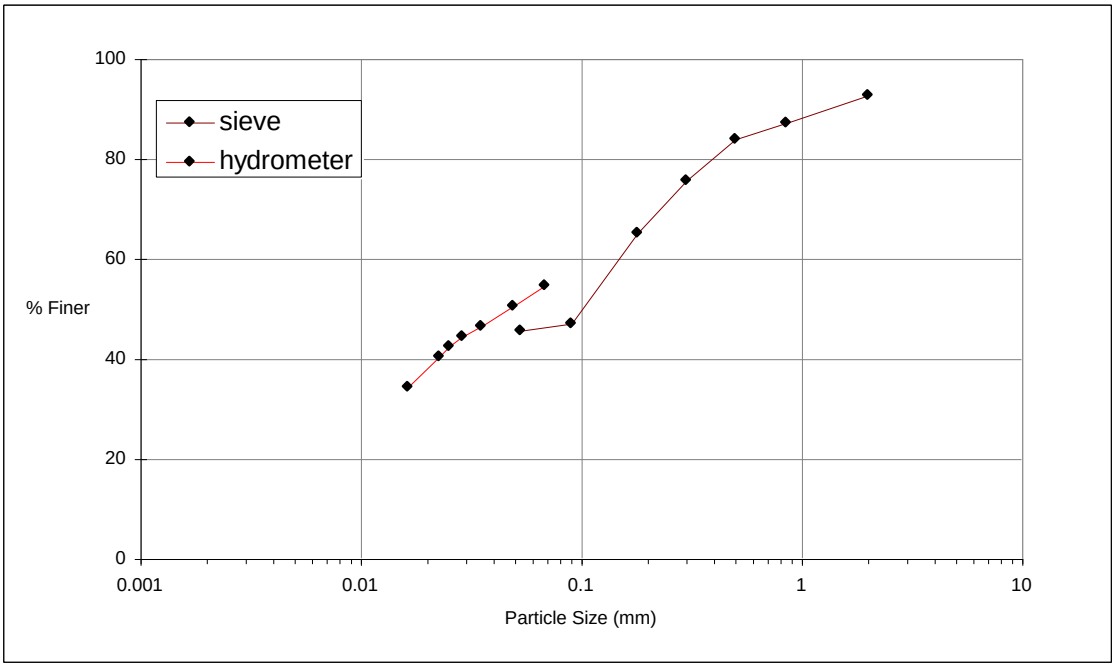

Figure B.8 Particle size distribution for the Bugweed site at 7500 mm

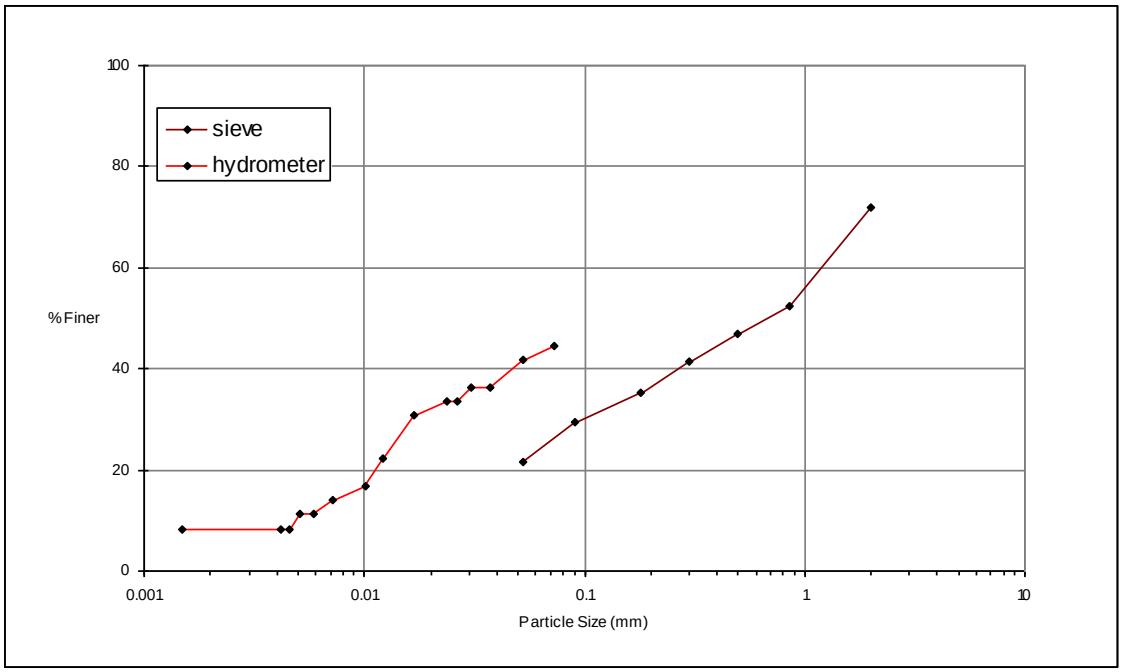

Figure B.9 Particle size distribution of the Bugweed site at 9000 mm

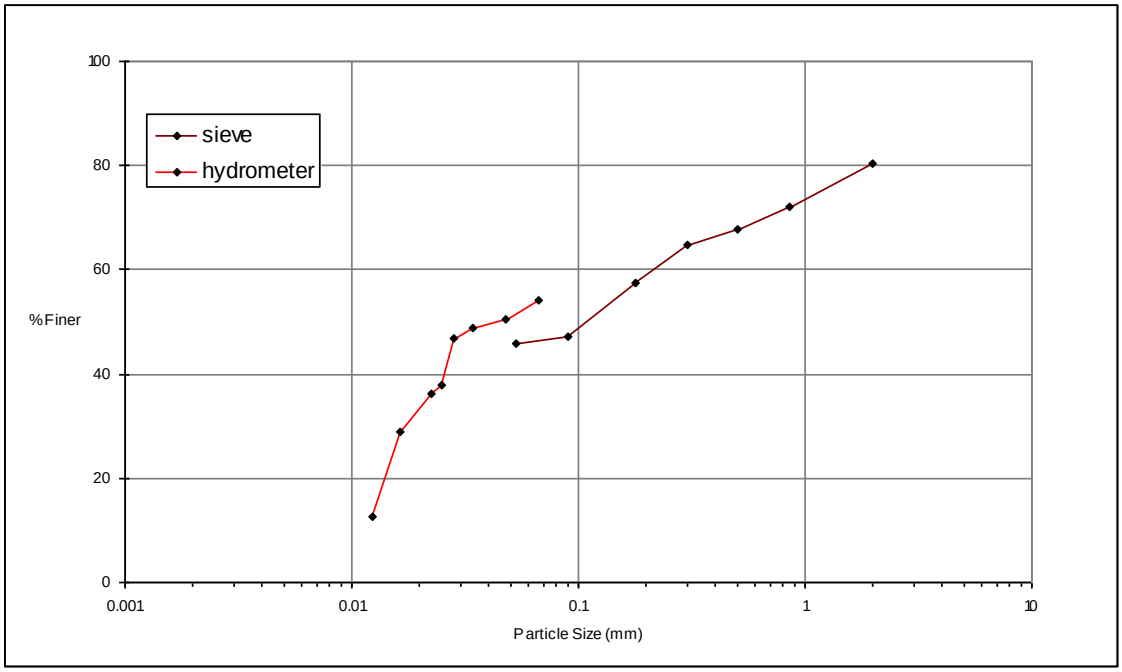

Figure B.10 Particle size distribution for the Bugweed site at 9500 mm

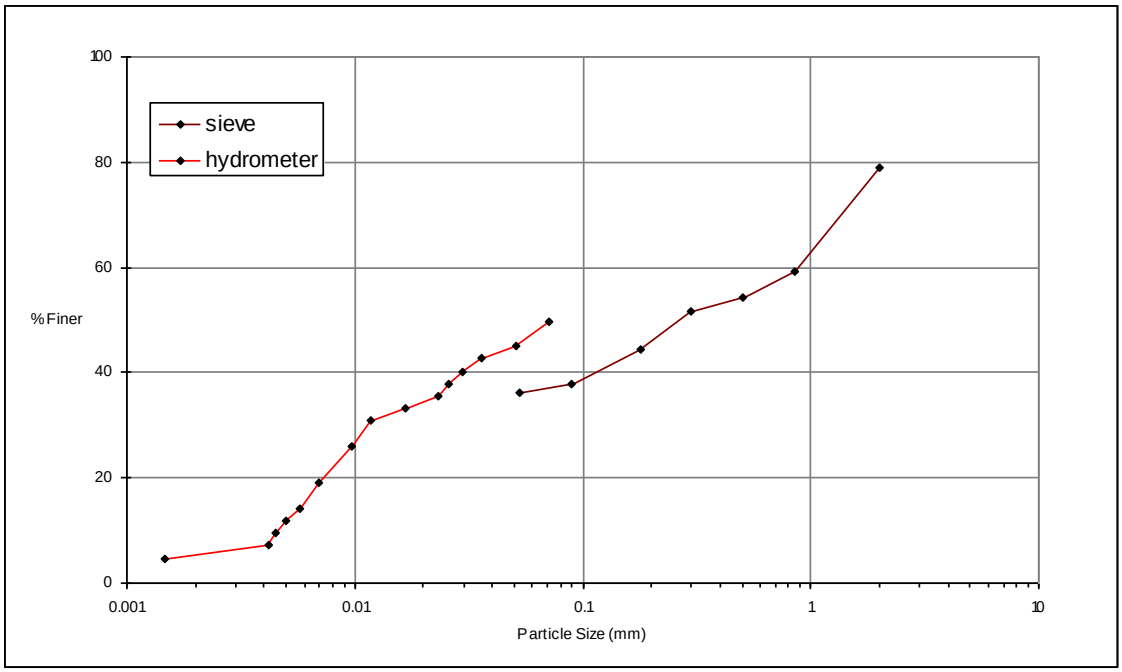

Figure B.11 Particle size distribution for the Bugweed site at 10000 mm

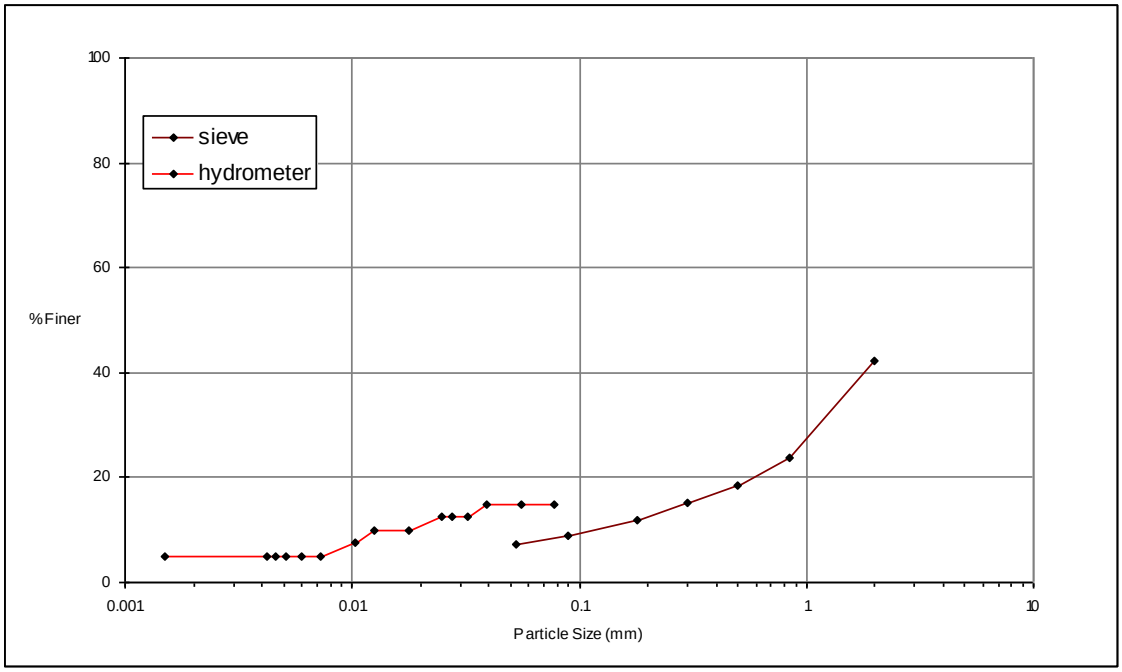

Figure B.12 Particle size distribution for the Bugweed site at 11500 mm

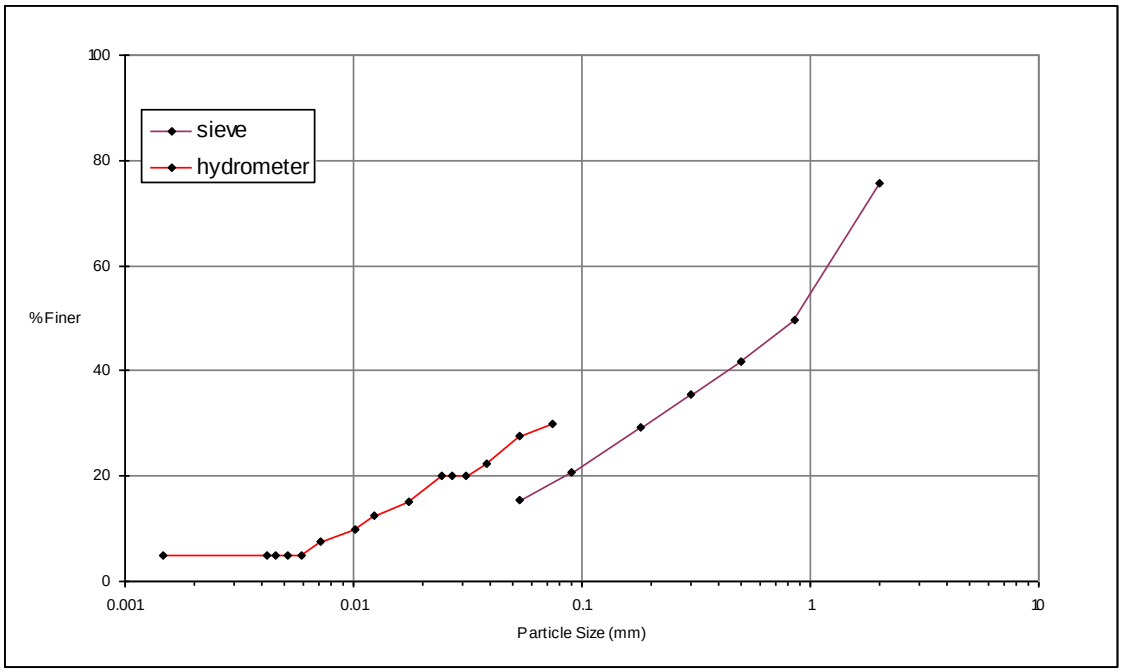

Figure B.13 Particle size distribution for the Fig tree site at 500 mm

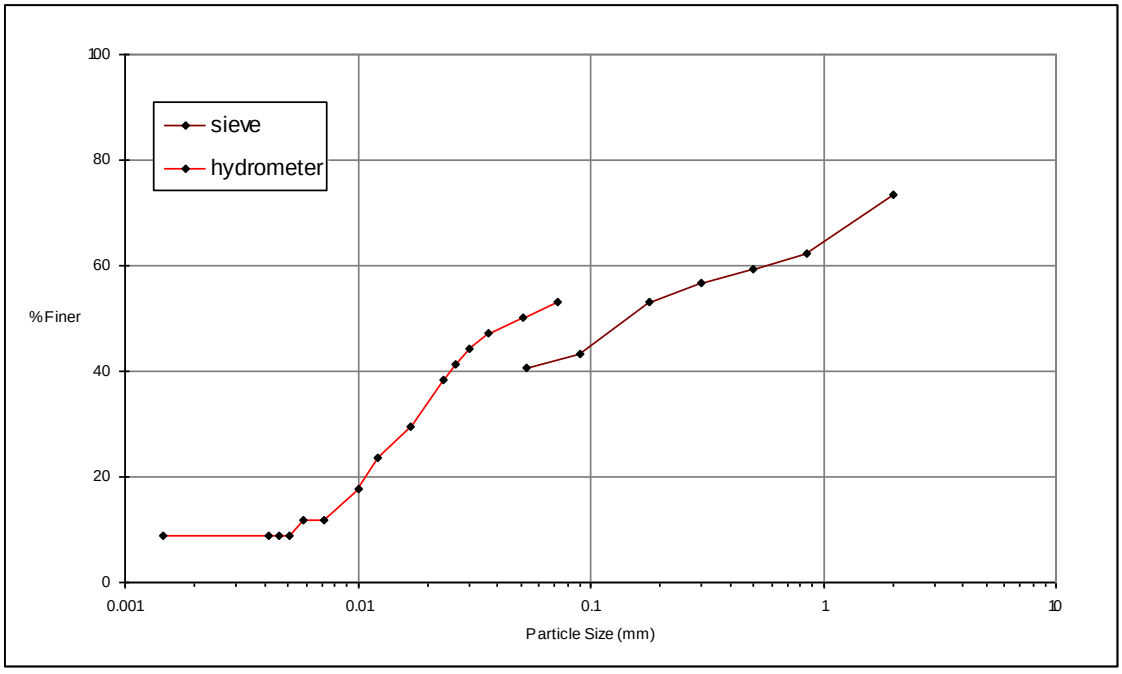

Figure B.14 Particle size distribution for the Fig tree site at 2000 mm

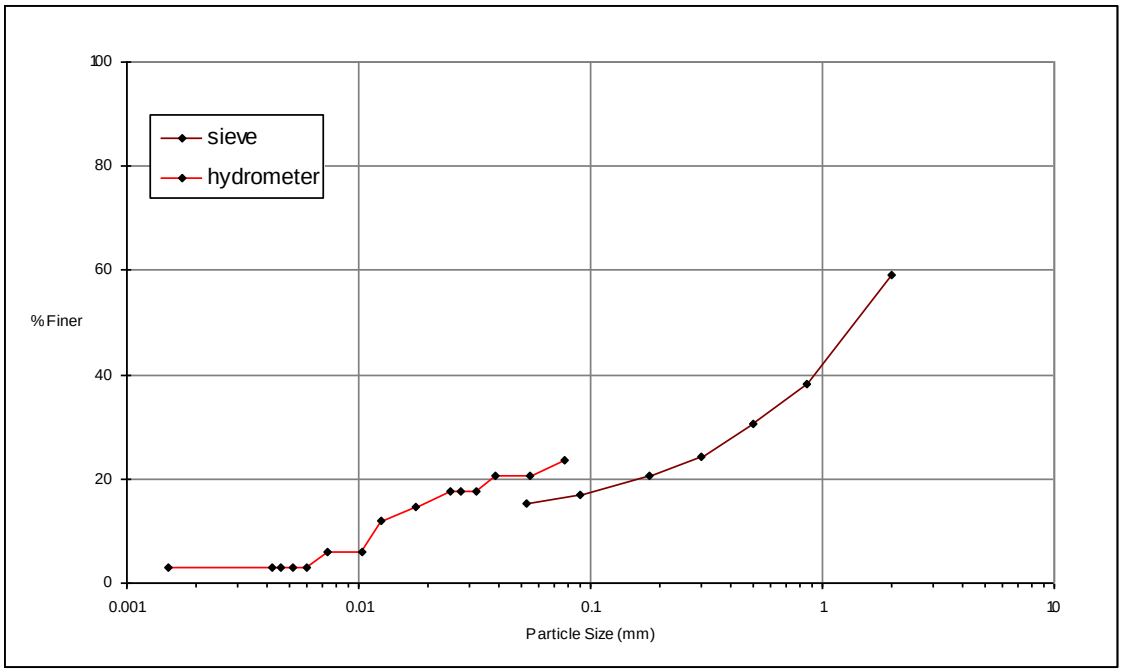

Figure B.15 Particle size distribution for the Fig tree site at 4000 mm

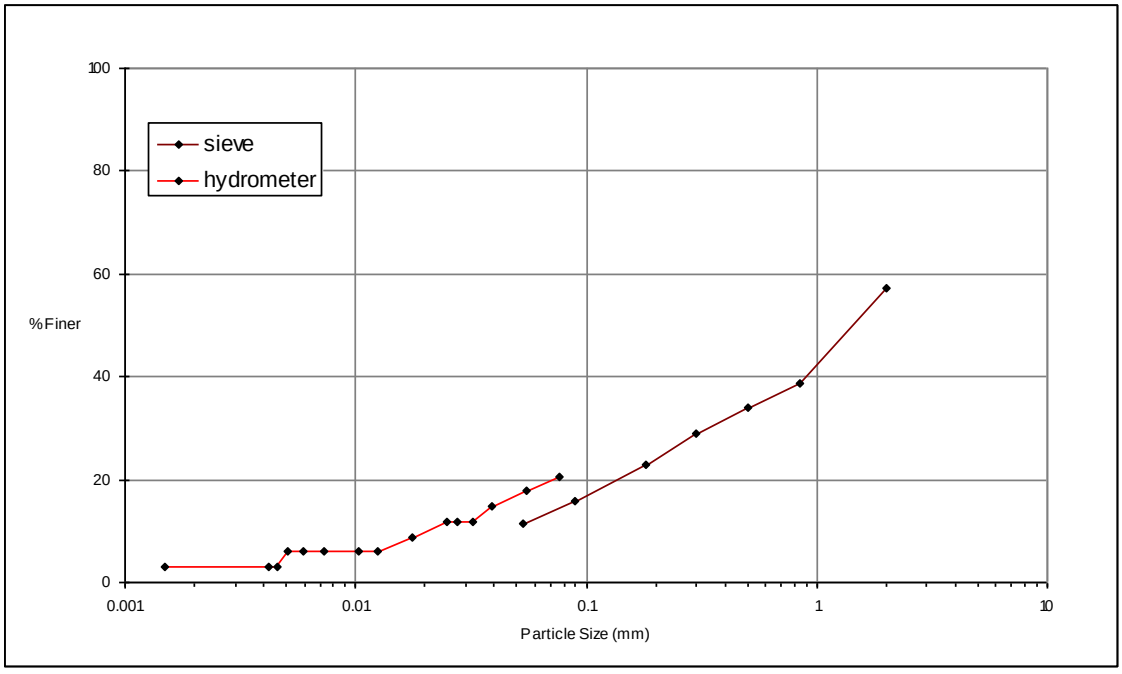

Figure B.16 Particle size distribution for the Fig tree site at 7300 mm

APPENDIX C

WATER RETENTION CHARACTERISTICS

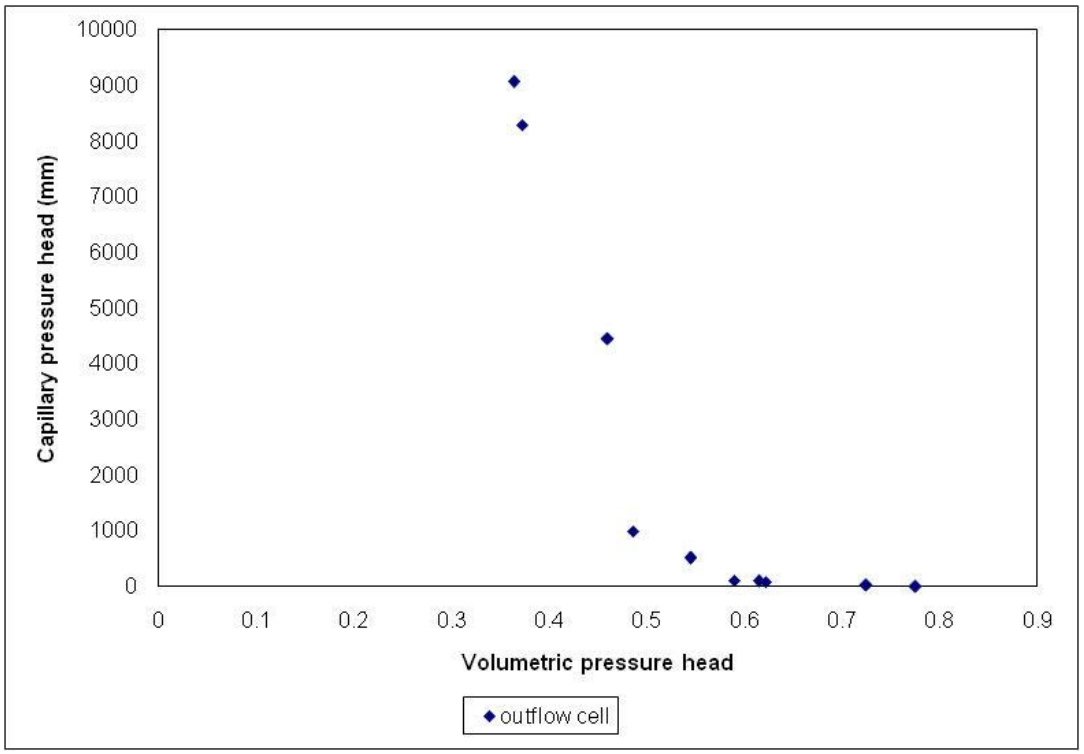

Figure C.1.1 Water retention characteristics of the Fig tree site at depth 0 mm.

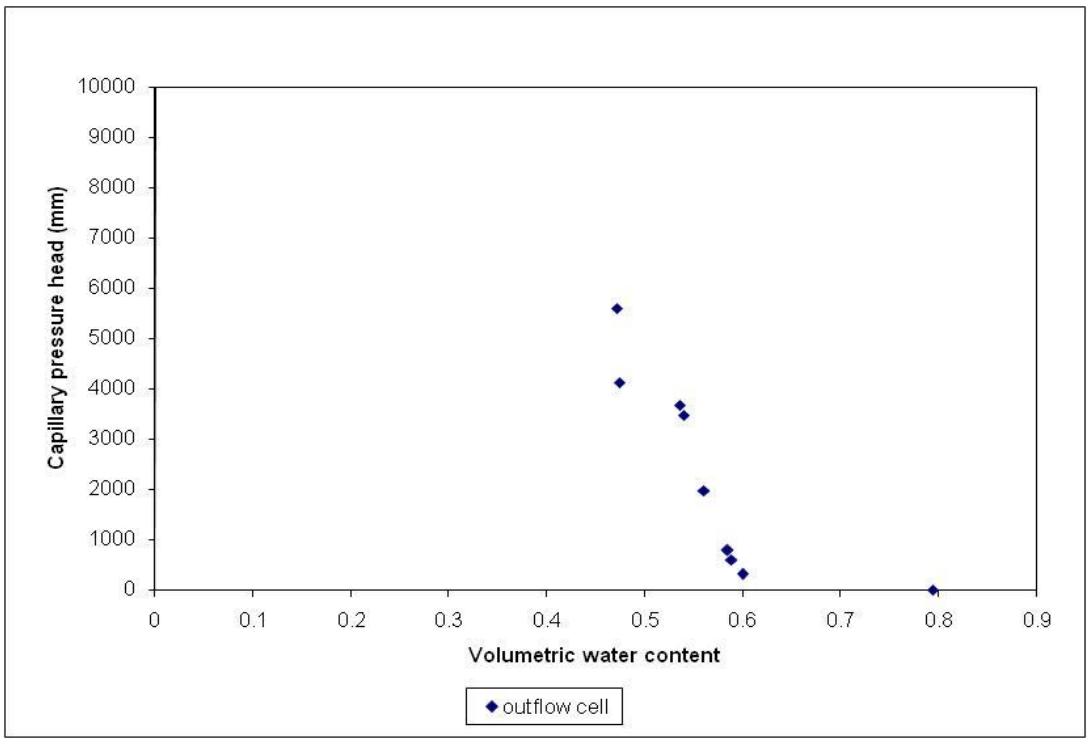

Figure C.1.2 Water retention characteristics of the Fig tree site at depth 250 mm.

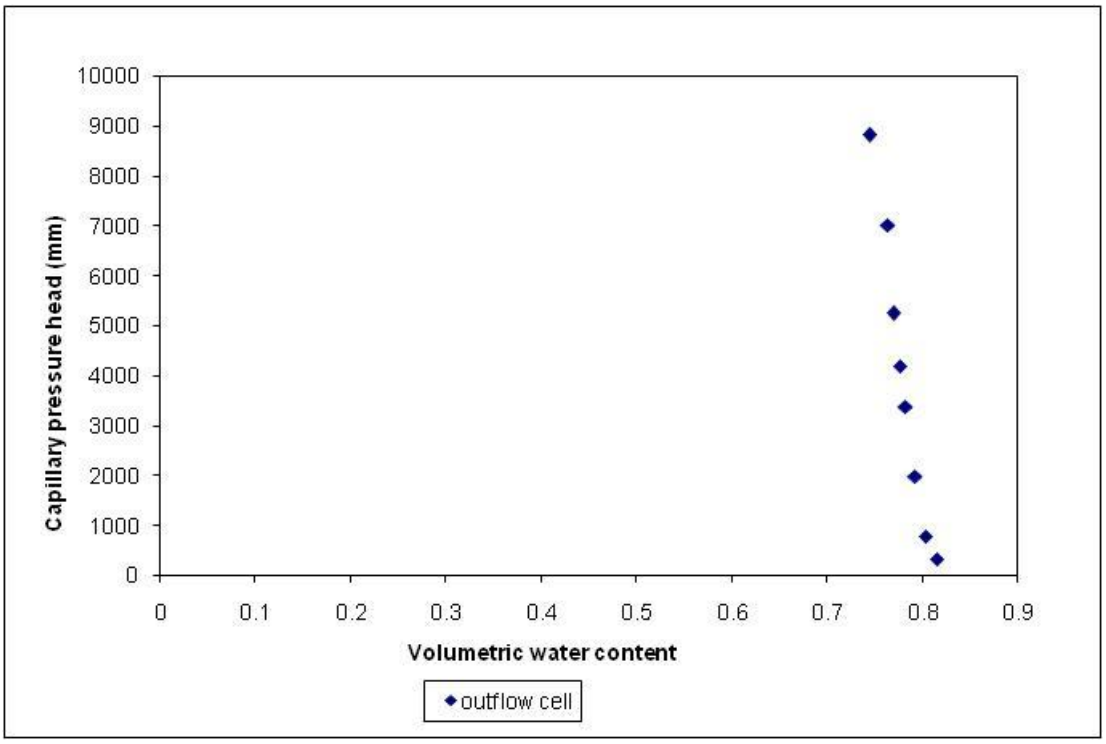

Figure C.1.3 Water retention characteristics of the Fig tree site at depth 1000 mm.

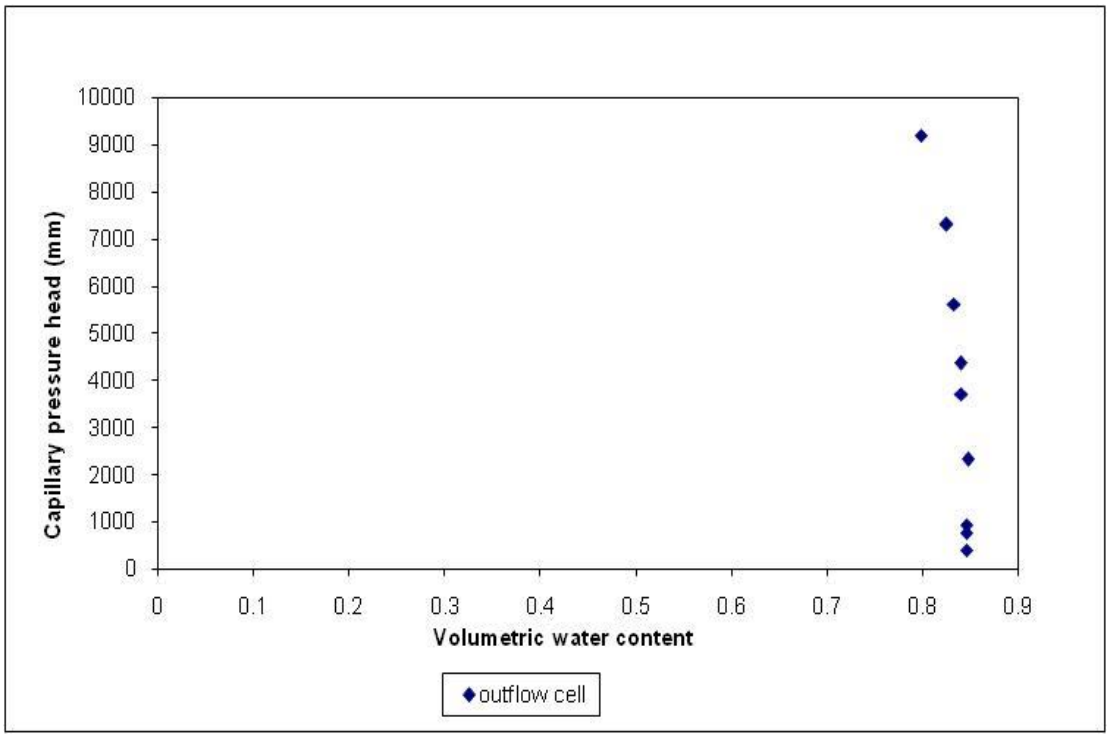

Figure C.1.4 Water retention characteristics of the Fig tree site at depth 2000 mm.

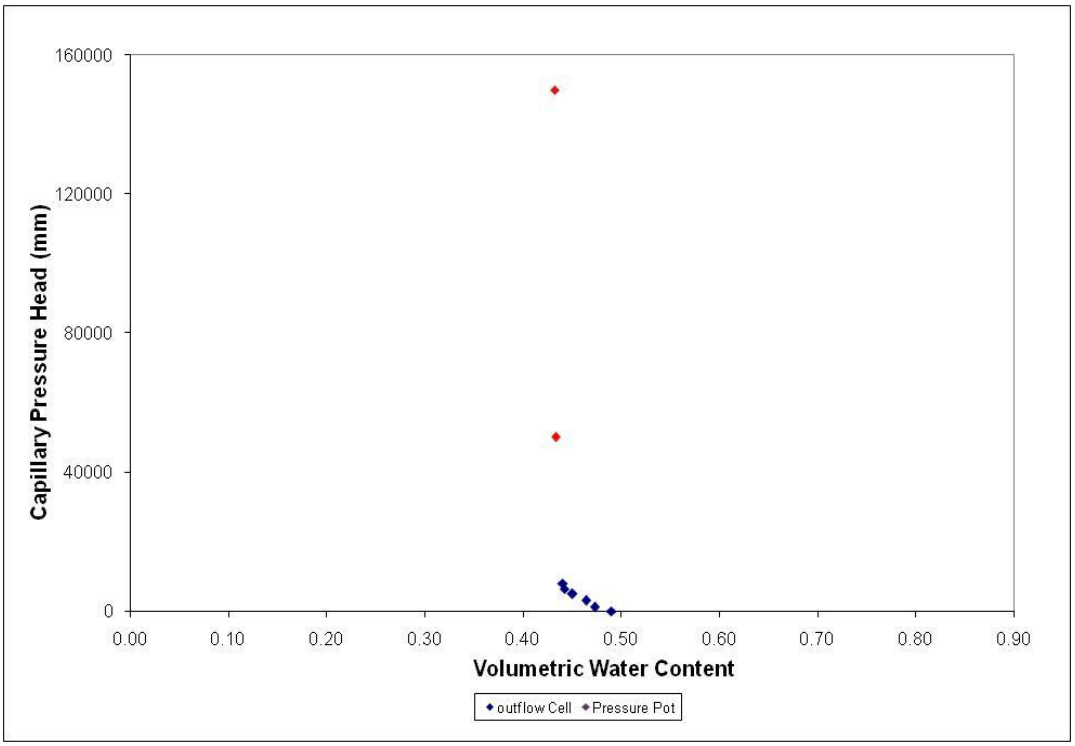

Figure C.1.5 Water retention characteristics of the Fig tree site at depth 3500 mm.

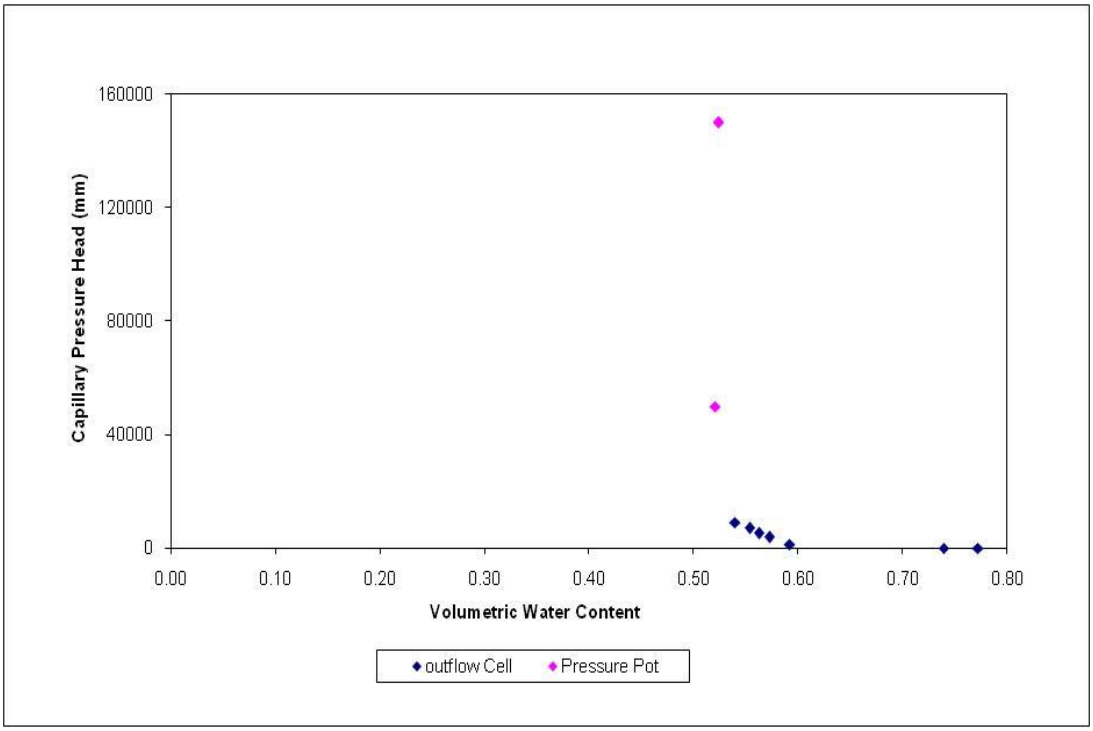

Figure C.1.6 Water retention characteristics of the Fig tree site at depth 4500 mm.

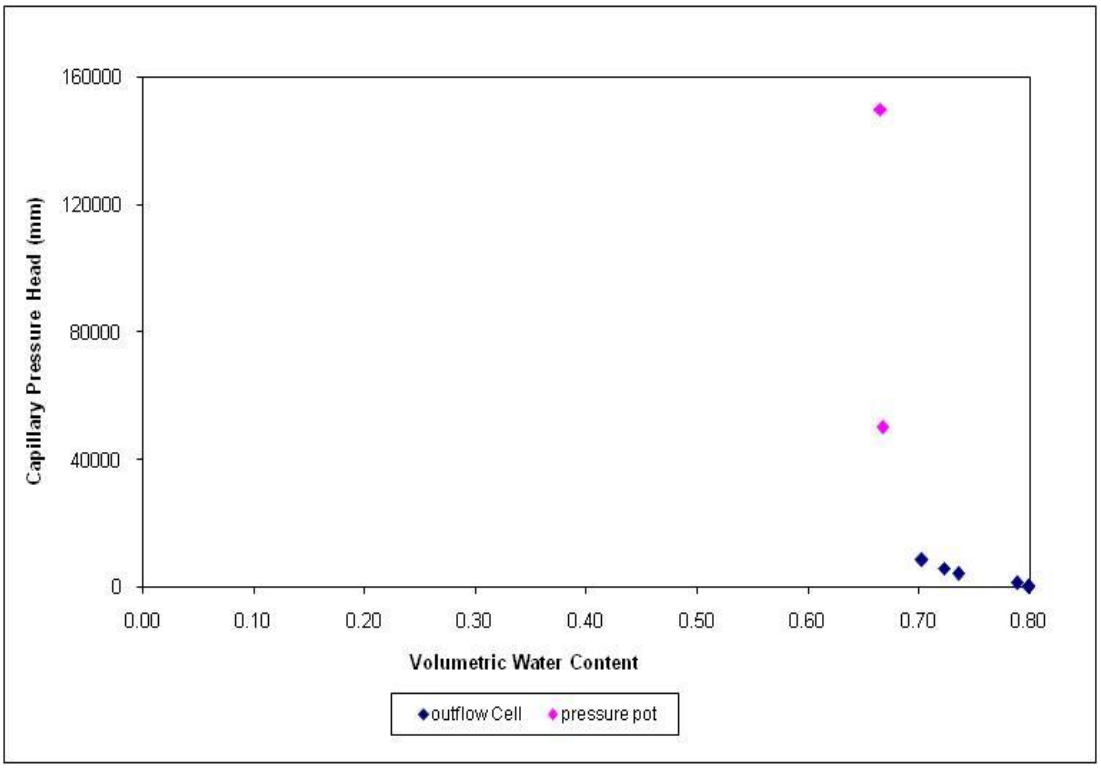

Figure C.1.7 Water retention characteristics of the Fig tree site at depth 6500 mm.

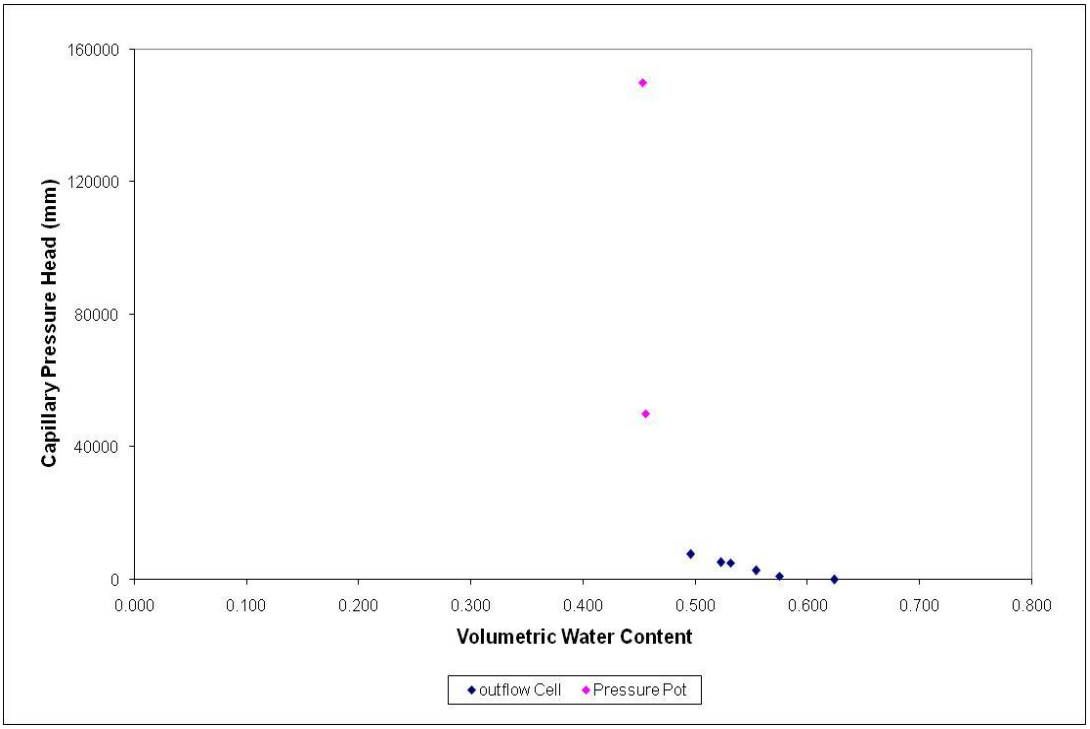

Figure C.1.8 Water retention characteristics of the Fig tree site at depth 8000 mm.

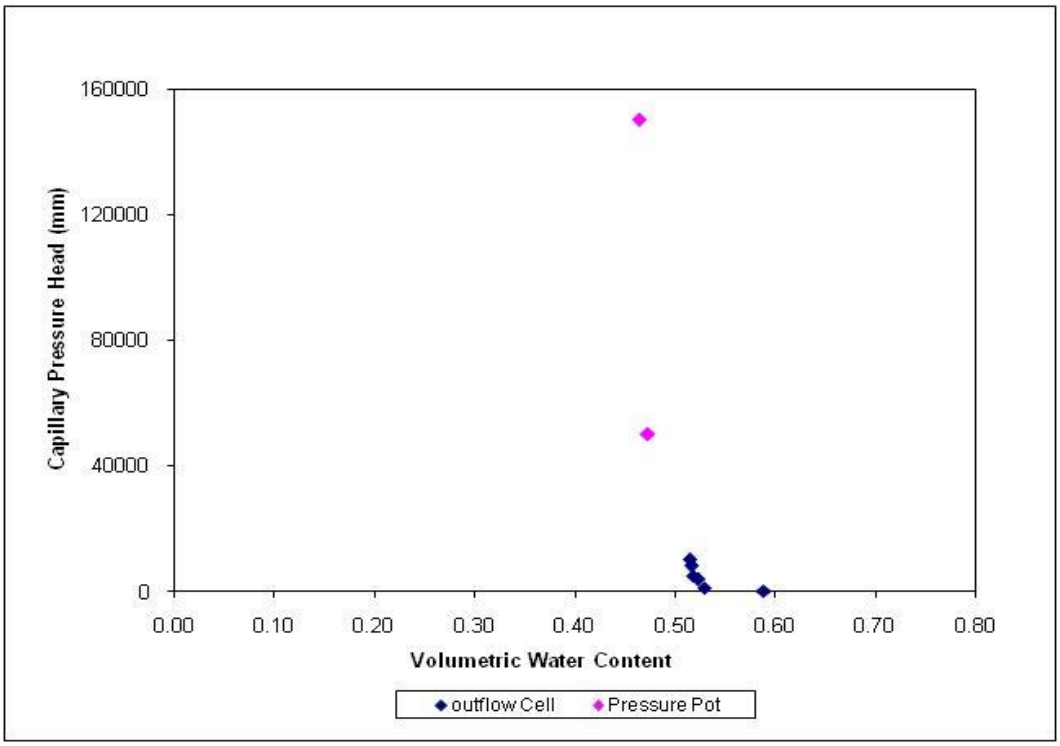

Figure C.1.9 Water retention characteristics of the Fig tree site at depth 11500 mm.

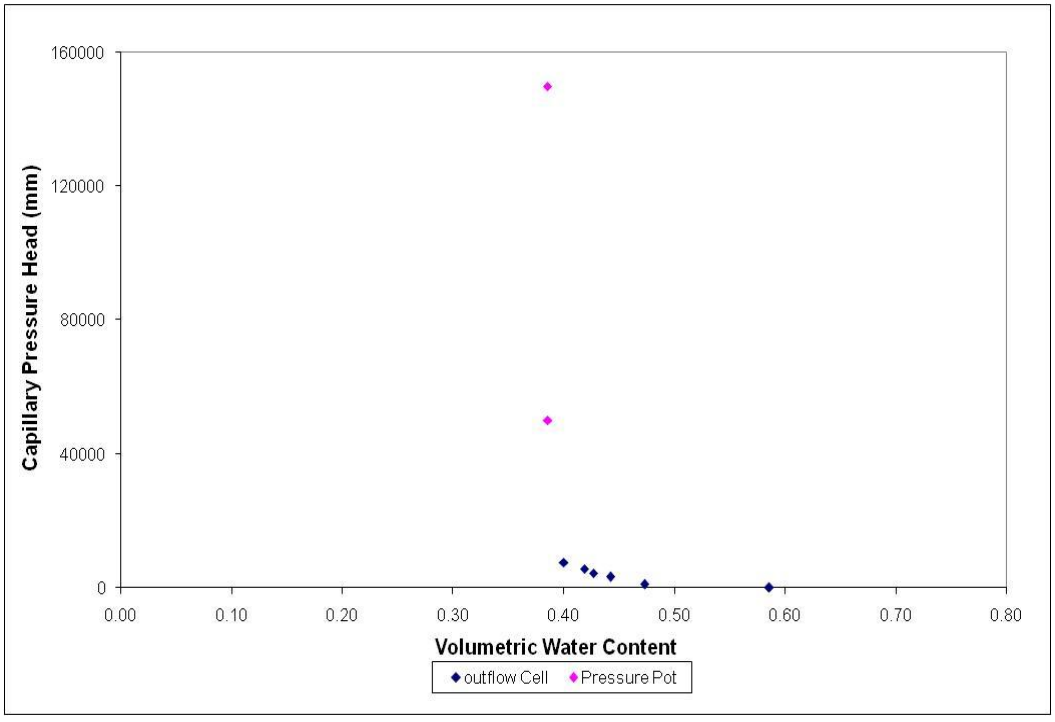

Figure C.1.10 Water retention characteristics of the Fig tree site at depth 12500 mm.

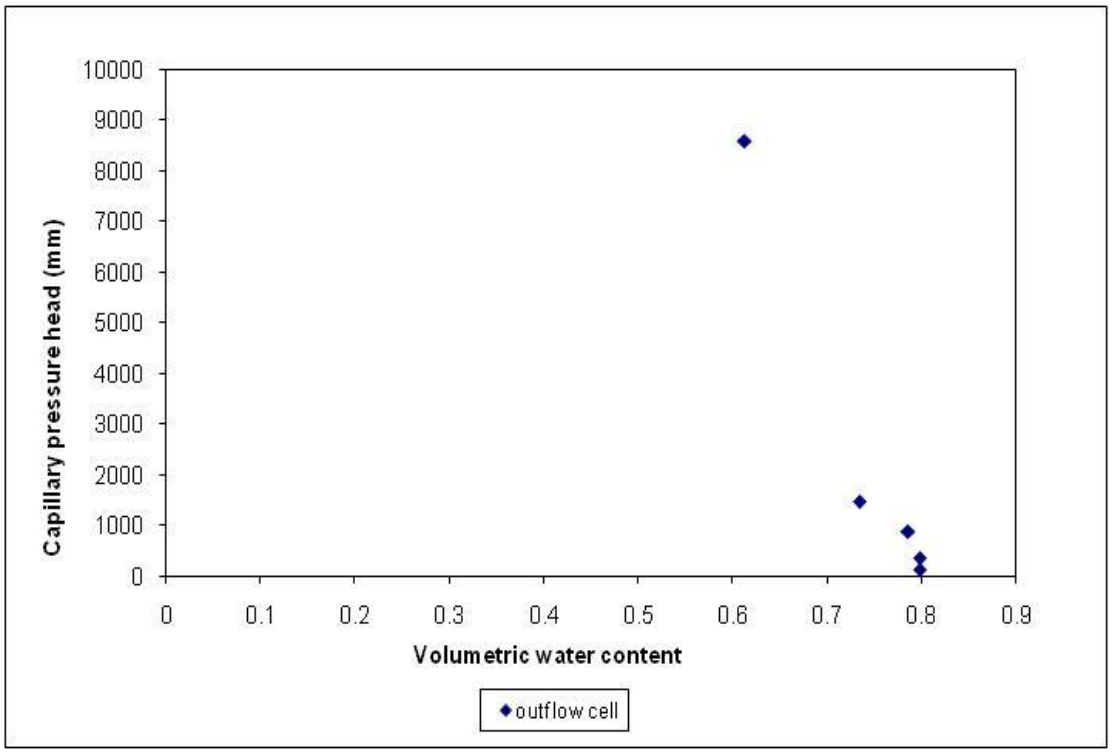

Figure C.2.1 Water retention characteristics of the Grass site at depth 0 mm.

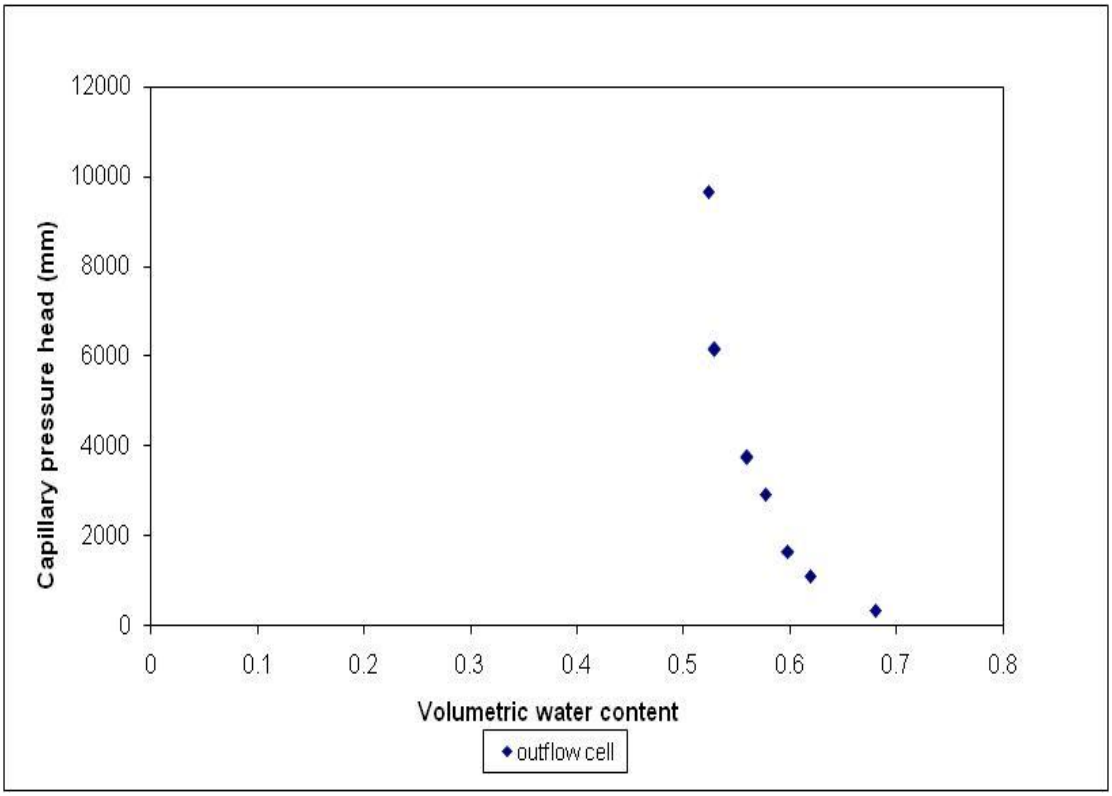

Figure C.2.2 Water retention characteristics of the Grass site at depth 250 mm.

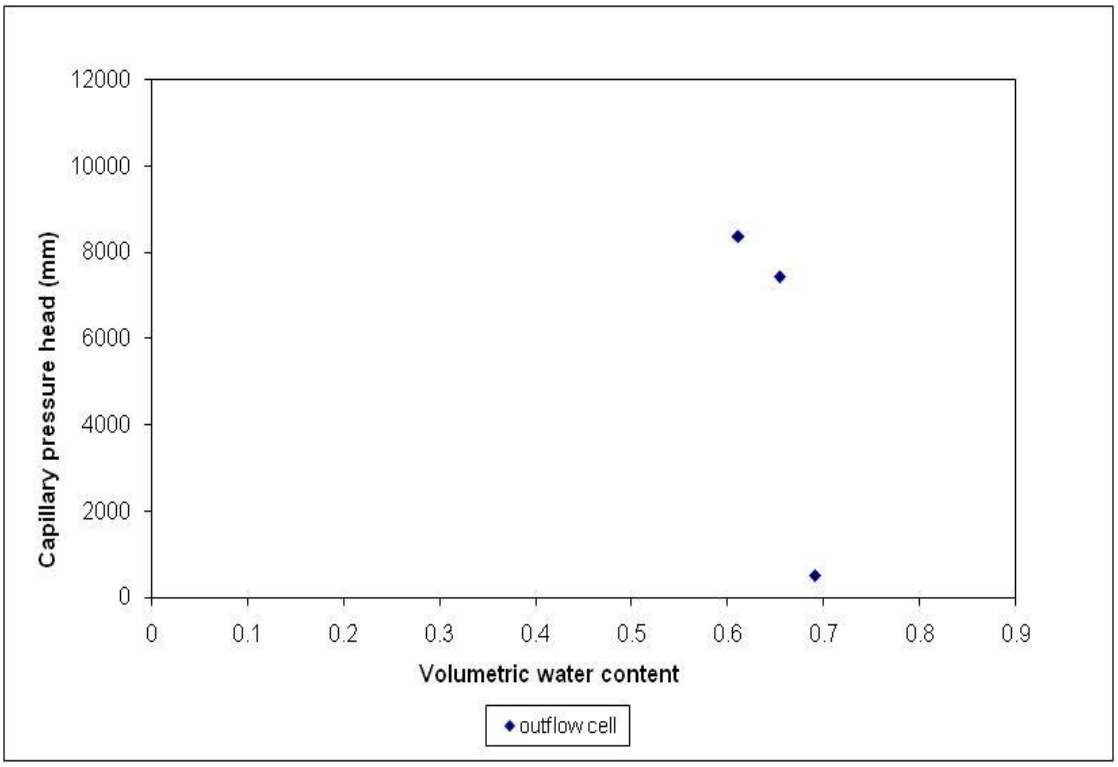

Figure C.2.3 Water retention characteristics of the Grass site at depth 500 mm.

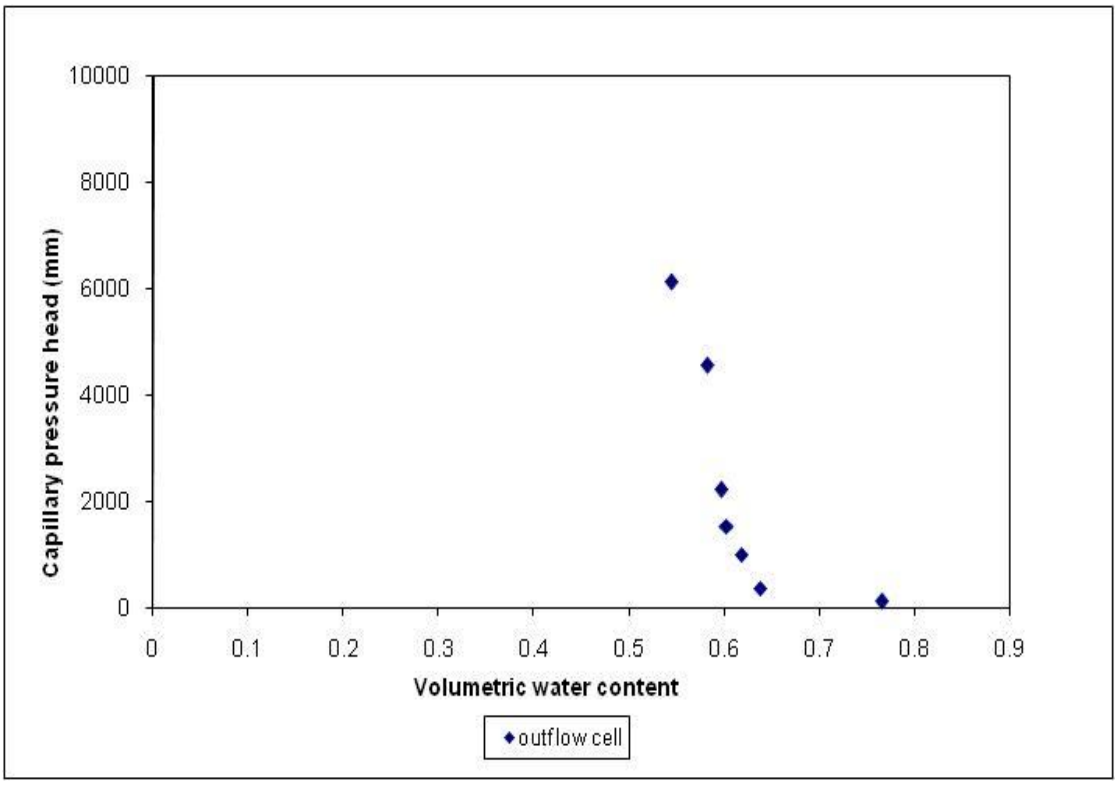

Figure C.2.4 Water retention characteristics of the Grass site at depth 1000 mm.

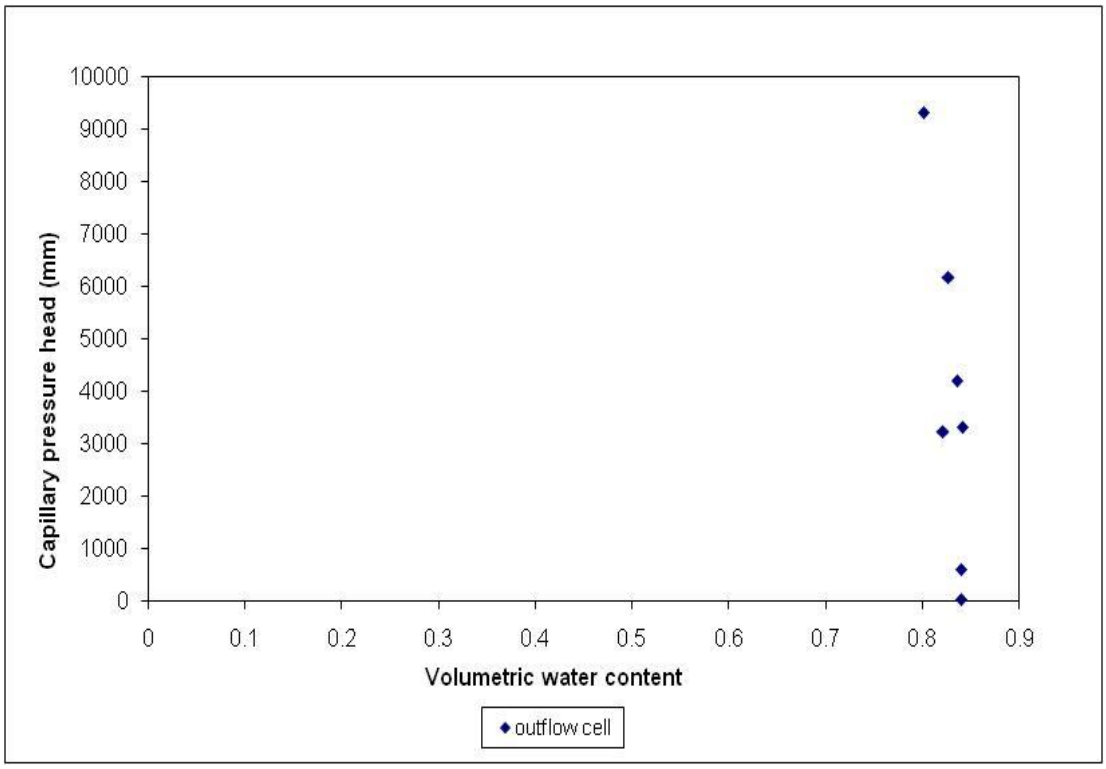

Figure C.2.5 Water retention characteristics of the Grass site at depth 2000 mm.

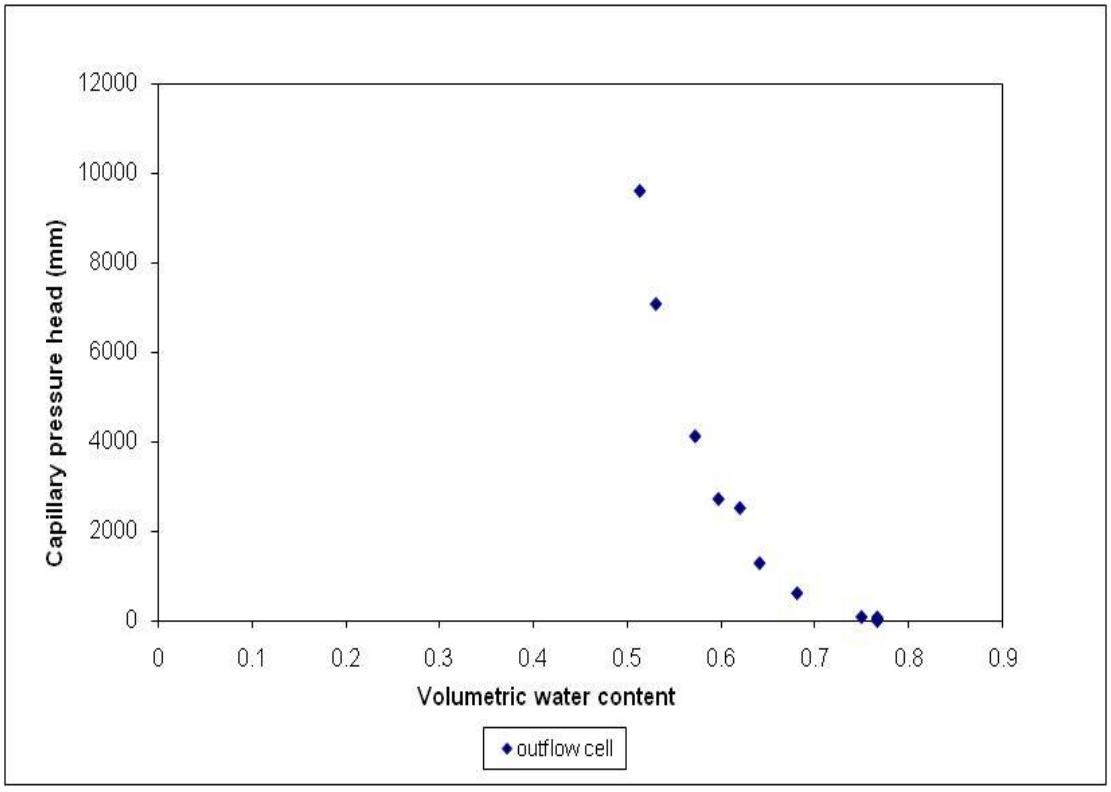

Figure C.2.6 Water retention characteristics of the Grass site at depth 2500 mm.

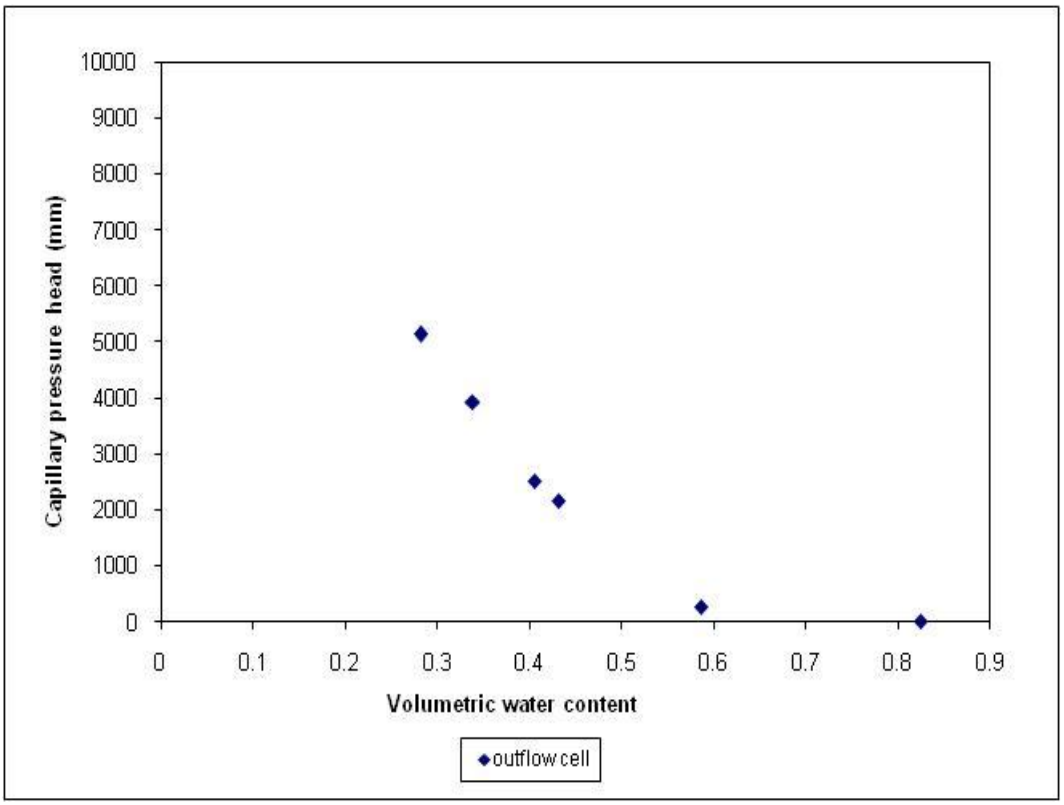

Figure C.3.1 Water retention characteristics of the Bugweed site at depth 0 mm.

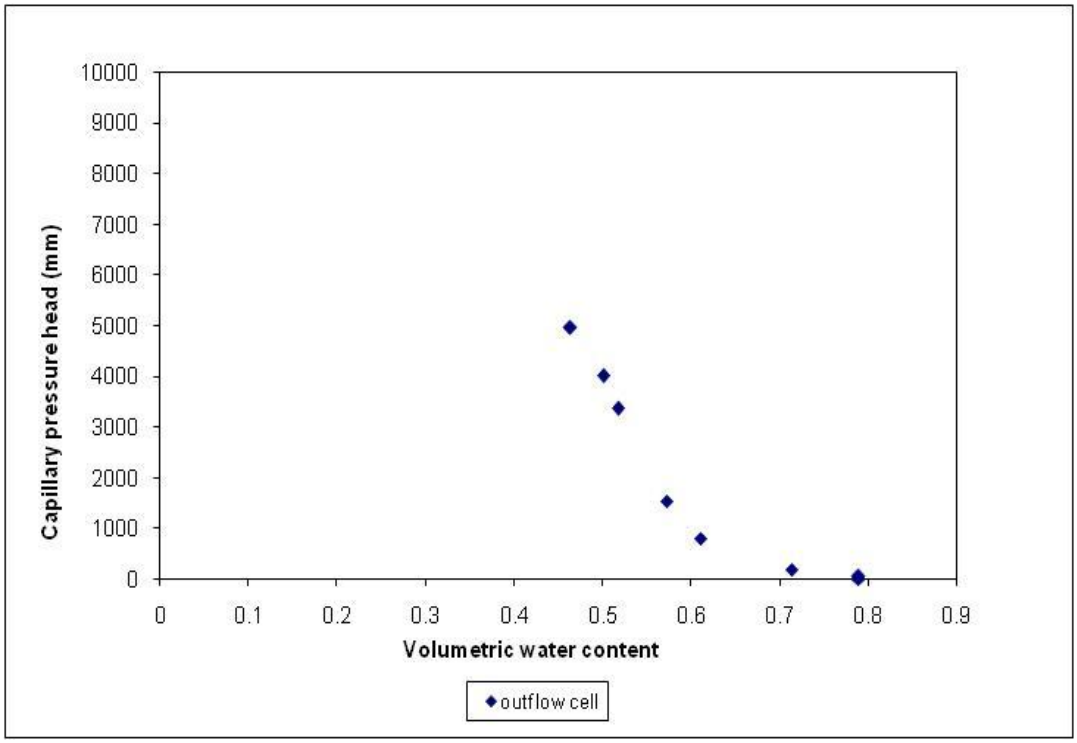

Figure C.3.2 Water retention characteristics of the Bugweed site at depth 500 mm.

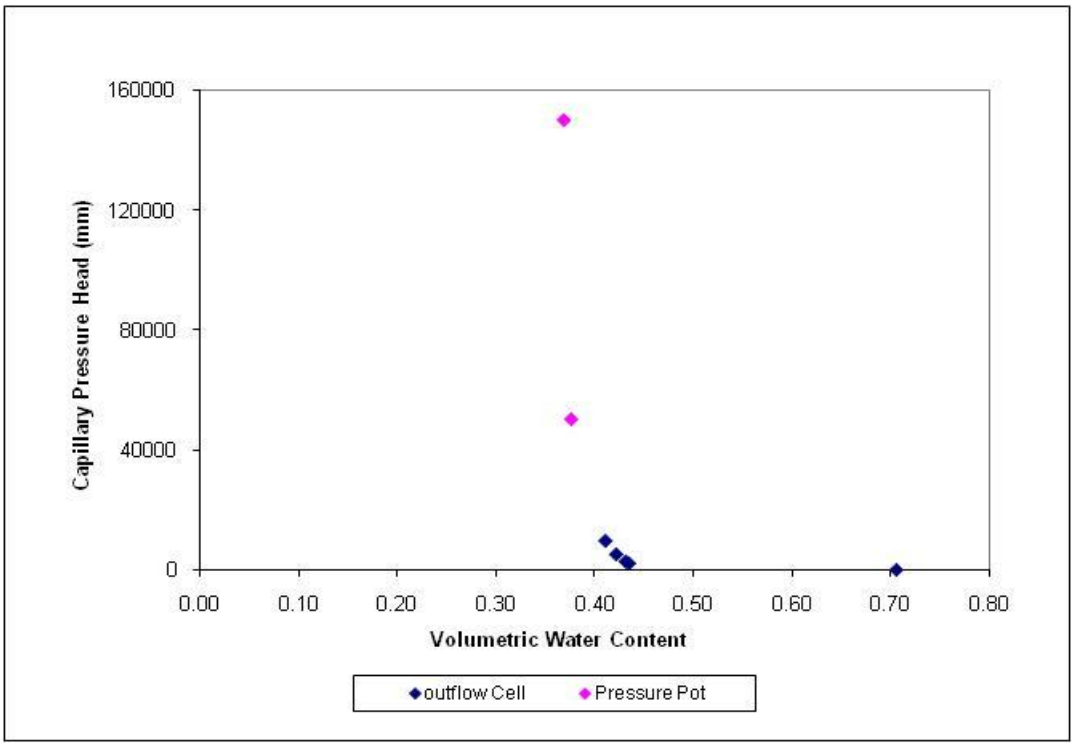

Figure C.3.3 Water retention characteristics of the Bugweed site at depth 1500 mm.

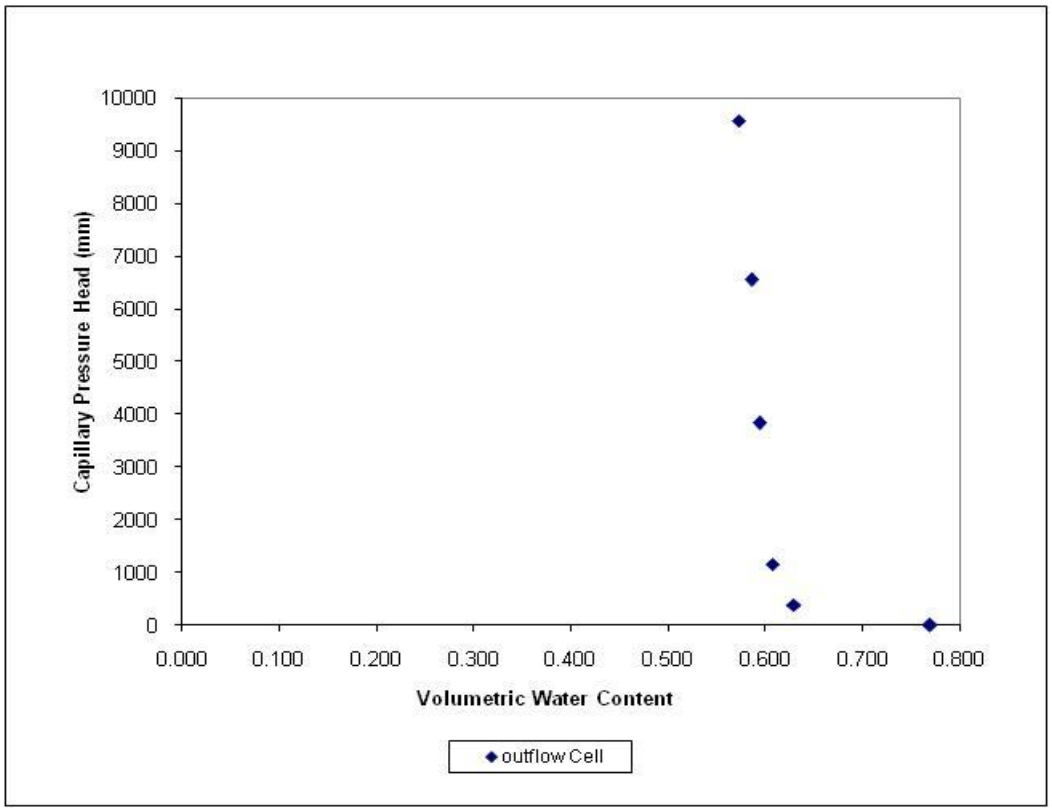

Figure C.3.4 Water retention characteristics of the Bugweed site at depth 2500 mm.

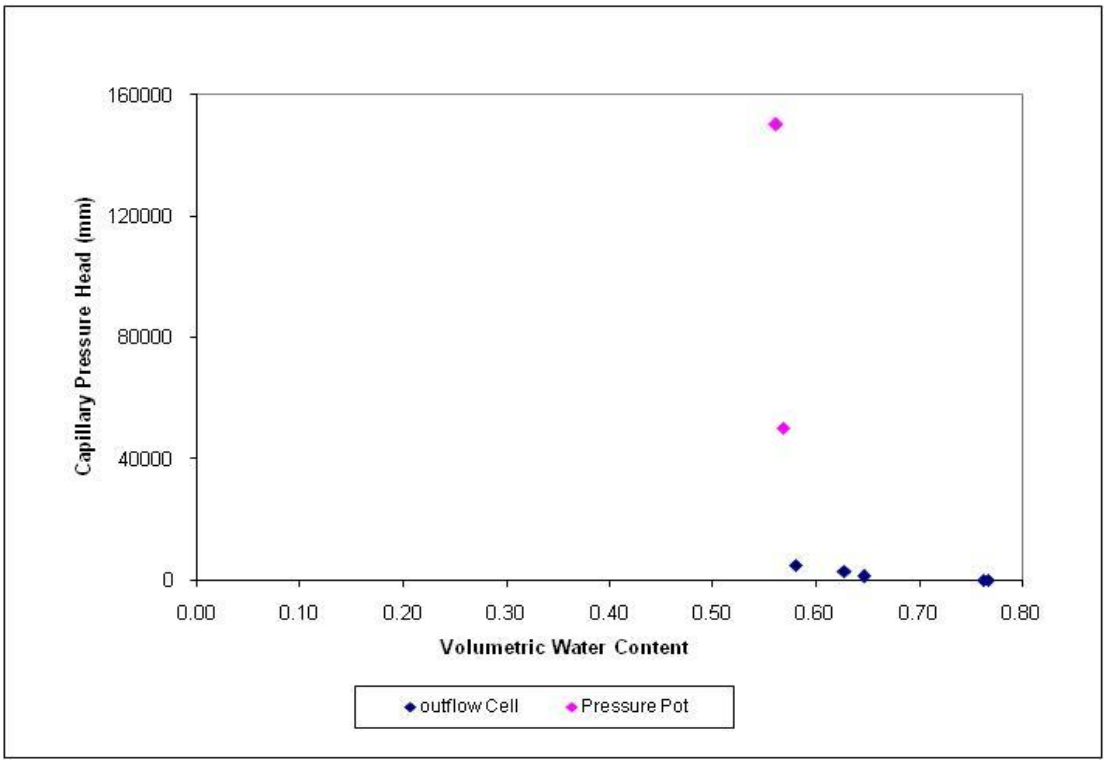

Figure C.3.5 Water retention characteristics of the Bugweed site at depth 3000 mm.

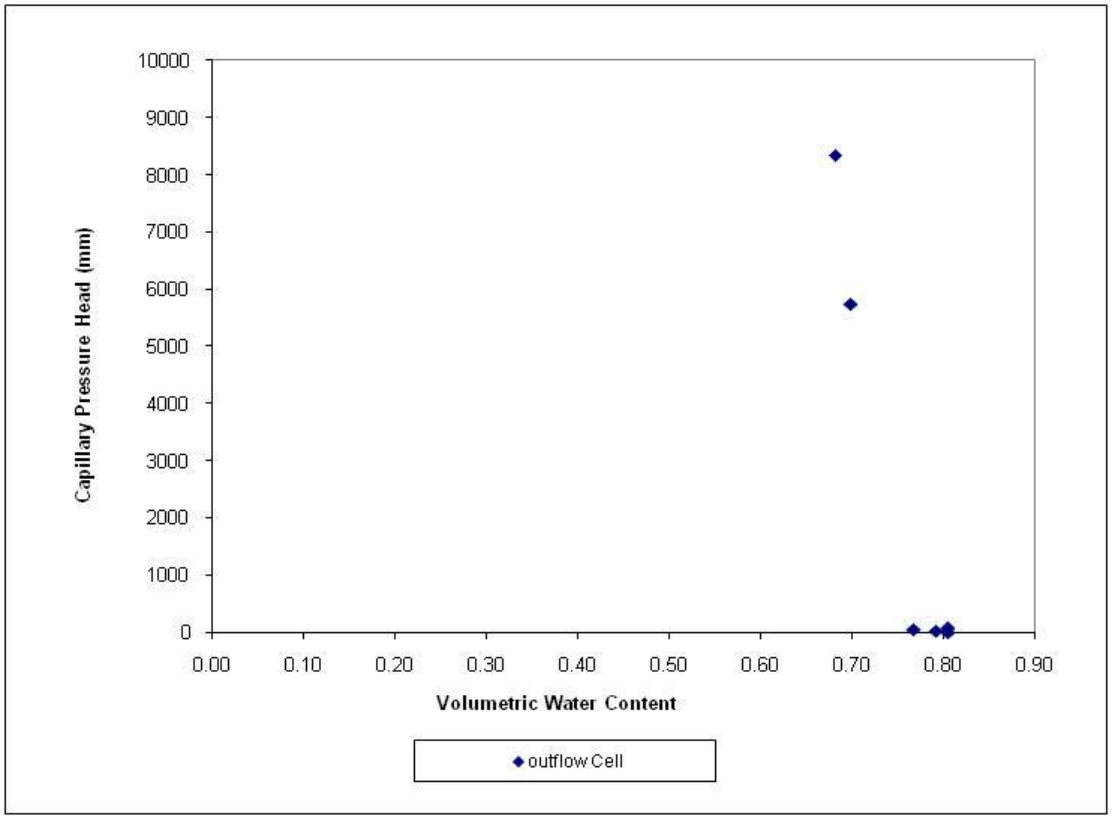

Figure C.3.6 Water retention characteristics of the Bugweed site at depth 4000 mm.

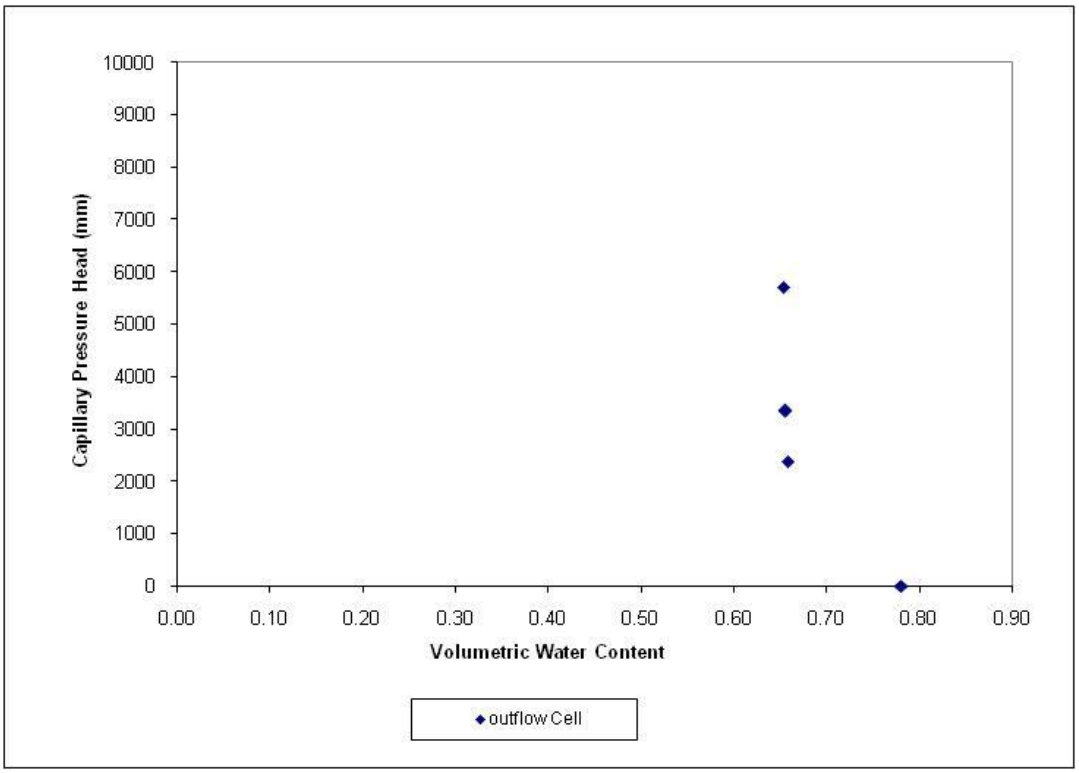

Figure C.3.7 Water retention characteristics of the Bugweed site at depth 4500 mm.

APPENDIX D

HYDRUS 2-D MODEL INPUT PARAMETERS

Simulation	Bare	Nest 9	Fig
Main Processes	Water Flow	Water Flow Root Water Uptake	Water Flow Root Water Uptake
Geometry Information			
Length Units	mm	mm	mm
Number of Soil Materials	3	3	3
Type of flow	vertical	vertical	vertical
Time Information			
Time Units	Hours	Hours	Hours
Initial Time	0	0	0
Final Time	34266	29461	34266
Initial Time Step	1	1	1
Minimum Time Step	2.4e-0.05	2.4e-0.05	2.4e-0.05
Maximum Time Step	20	20	20
Number of Time Variable Records	7964	6876	7964
Iteration Criteria			
Maximum Number of Iterations	20	20	20
Water Content Tolerance	0.0005	0.0005	0.0005
Pressure Head Tolerance	500	50	50
Lower Optimal Iteration Range	3	3	3
Upper Optimal Iteration Range	7	7	7
Lower Time Step Multi. Fac.	1.3	1.3	1.3
Upper Time Step Multi. Fac.	0.3	0.3	0.3
Lower Limit of the Tension Int.	0.01	0.001	0.001
Upper Limit of the Tension Int.	1e+008	1e+007	1e+007
Initial Condition	Pressure head	Pressure head	Pressure head
Soil Hydraulic Model			
	Modified van Genuchten No Hysteresis		
Water Flow Parameters			
Layer 1			
θ_r	0.25	0.25	0.25
θ_s	0.77	0.77	0.58
α	0.005	0.005	0.005
n	1.2	1.2	1.2
K_s	80	80	80
I	0.5	0.5	0.5
Q_m	0.773	0.773	0.59
Q_a	0.25	0.25	0.25
Q_k	0.767	0.767	0.58

K_k	78	78	78
Layer 2			
θ_r	0.38	0.38	0.38
θ_s	0.68	0.68	0.60
α	0.004	0.004	0.007
n	1.2	1.2	1.1
K_s	60	60	60
I	0.5	0.5	0.5
Q_m	0.68	0.68	0.605
Q_a	0.38	0.38	0.38
Q_k	0.68	0.68	0.595
K_k	59	59	58
Layer 3			
θ_r	0.42	0.42	0.40
θ_s	0.58	0.58	0.60
α	0.006	0.006	0.007
n	1.1	1.1	1.1
K_s	35	35	50
I	0.5	0.5	0.5
Q_m	0.58	0.58	0.6
Q_a	0.52	0.42	0.4
Q_k	0.58	0.58	0.6
K_k	35	35	50
Root Water Uptake Model			
Water Uptake Reduction Model		Feddes	Feddes
Solute Stress Model		No	No
Root Water Uptake Parameters			
P0		-100	-10
P0pt		-500	-25
P2H		-3000	-10000
P2L		-10000	-10000
P3		-80000	-15000
r2H		0.5	0.5
r2L		0.1	0.1
Boundary Condition Editor			
Material Distribution			
1	0-165	165-3350	3350-15000
2	0-165	165-3350	3350-15000
3	0-165	165-3350	3350-15000
Upper Boundary Conditions		Atmospheric boundary conditions	

Lower Boundary Conditions	Constant boundary conditions	
Maximum Rooting Depth	300	2000

APPENDIX E

SIMULATED VERSUS OBSERVED TENSIONS

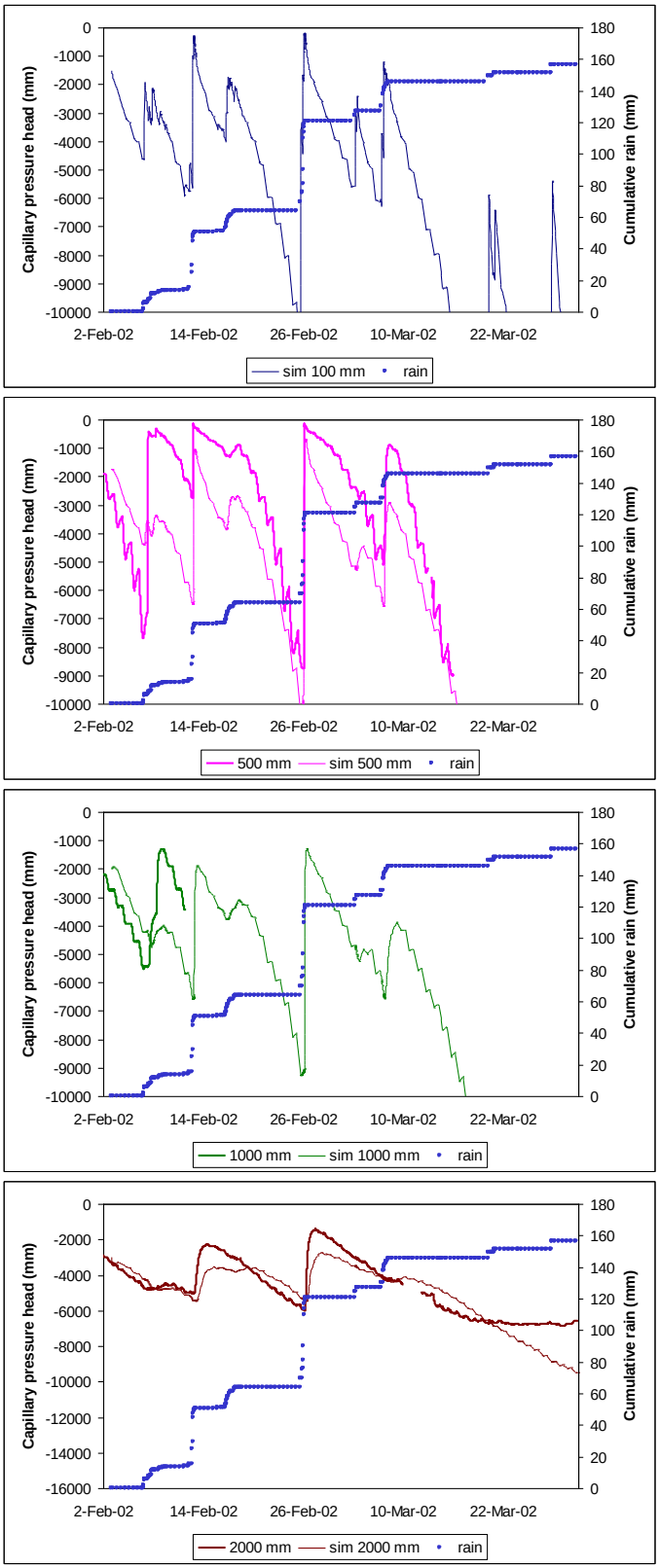

Figure E.1.1. Observed (bold) and simulated (light) tensions at the Fig Tree site at (from top) 100mm, 500mm, 1000mm and 2000mm below surface with cumulative rainfall (circles)from 2 February 2002 to 1 April 2002.

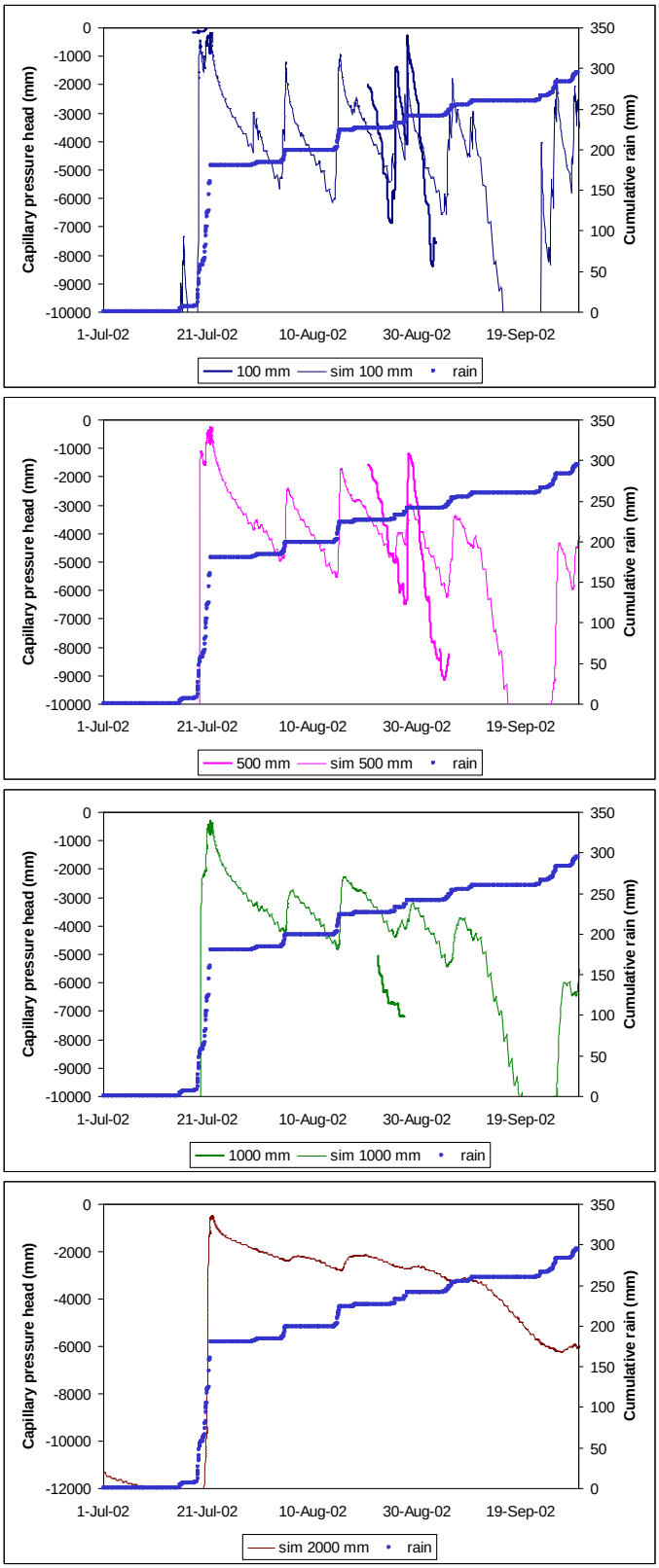

Figure E.1.2. Observed (bold) and simulated (light) tensions at the Fig Tree site at (from top) 100mm, 500mm, 1000mm and 2000mm below surface with cumulative rainfall (circles)from 1 July 2002 to 7 September 2002

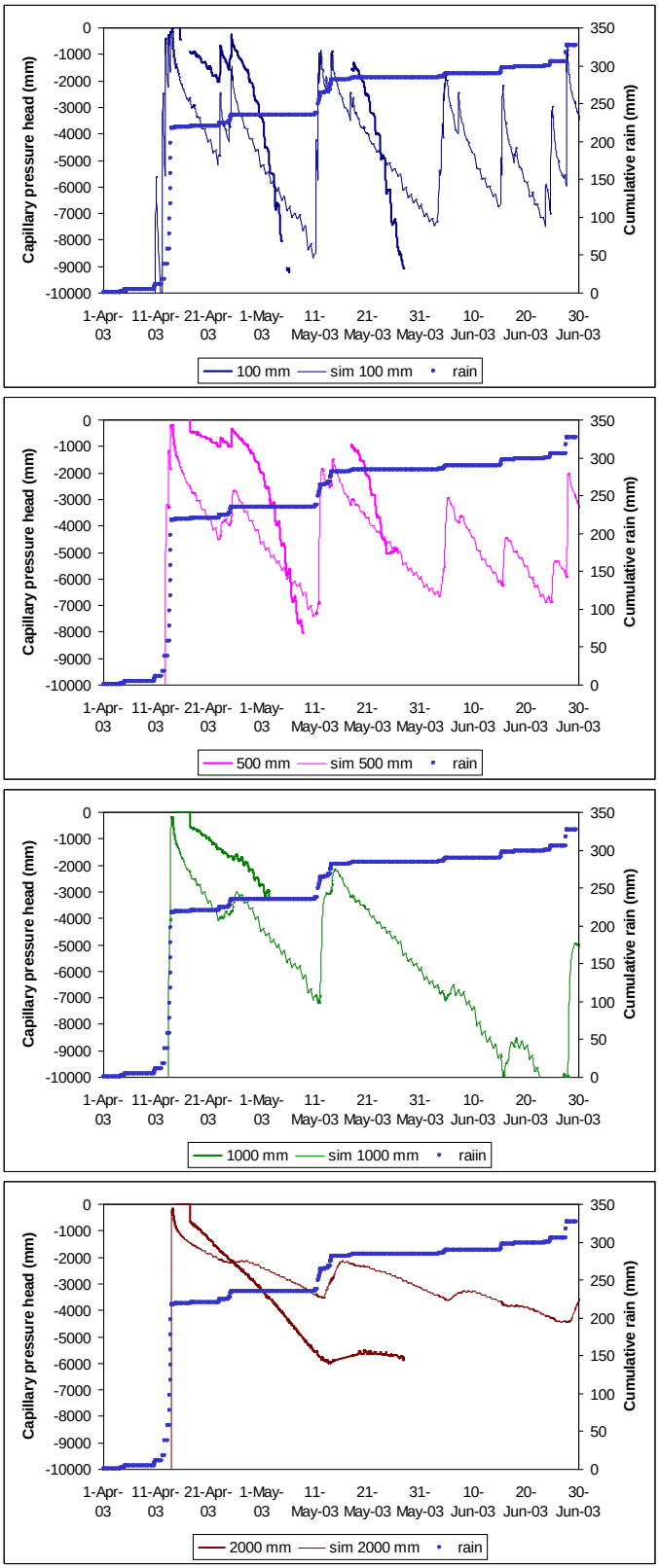

Figure E.1.3. Observed (bold) and simulated (light) tensions at the Fig Tree site at (from top) 100mm, 500mm, 1000mm and 2000mm below surface with cumulative rainfall (circles)from 1 April 2003 to 30 June 2003

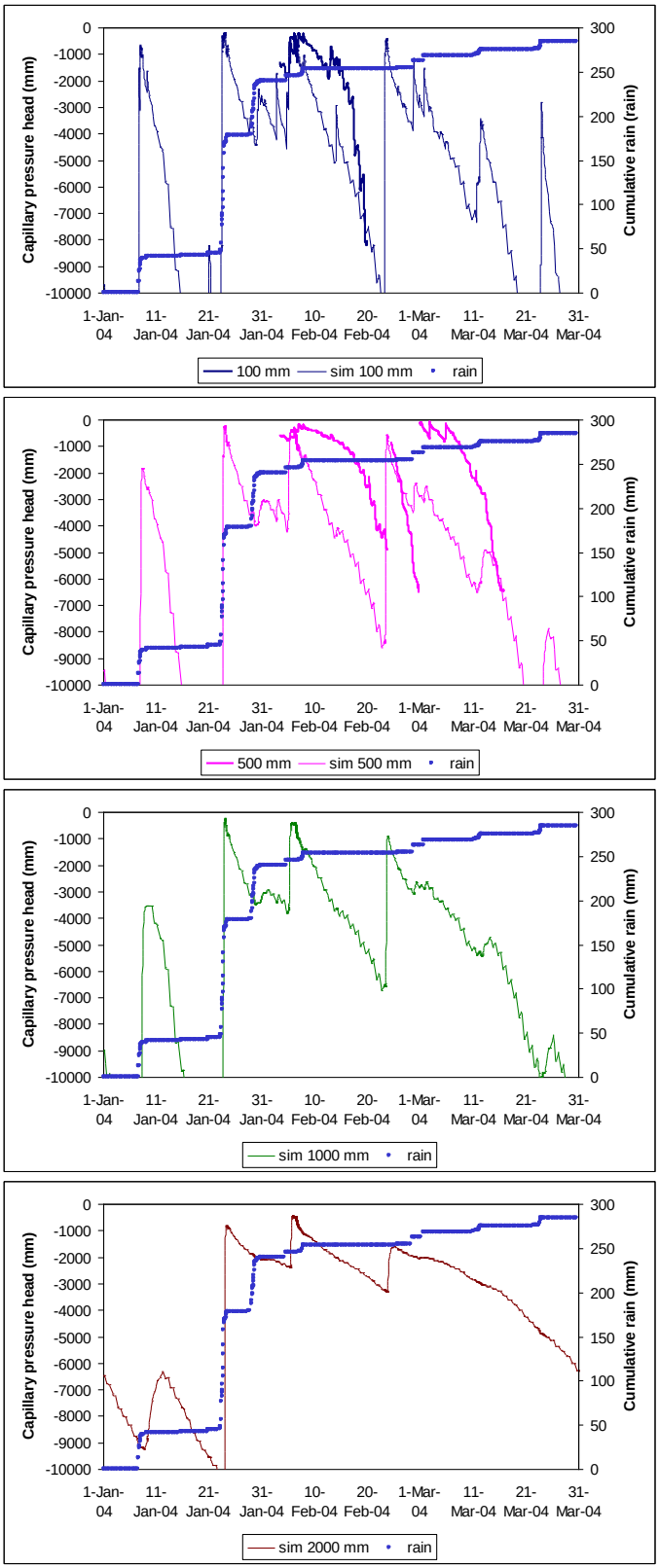

Figure E.1.4. Observed (bold) and simulated (light) tensions at the Fig Tree site at (from top) 100mm, 500mm, 1000mm and 2000mm below surface with cumulative rainfall (circles) from 1 January 2004 to 31 March 2004.

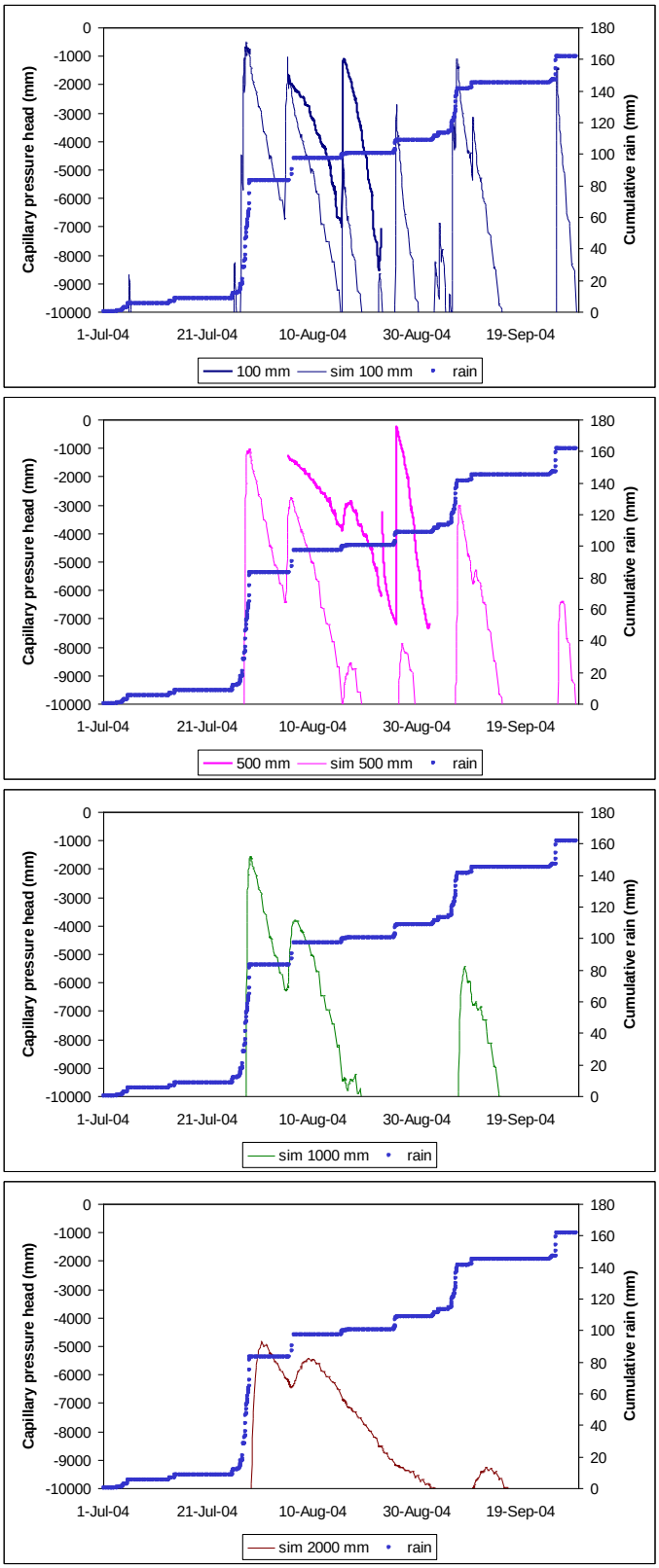

Figure E.1.5. Observed (bold) and simulated (light) tensions at the Fig Tree site at (from top) 100mm, 500mm, 1000mm and 2000mm below surface with cumulative rainfall (circles) from 1 July 2004 to 30 September 2004.

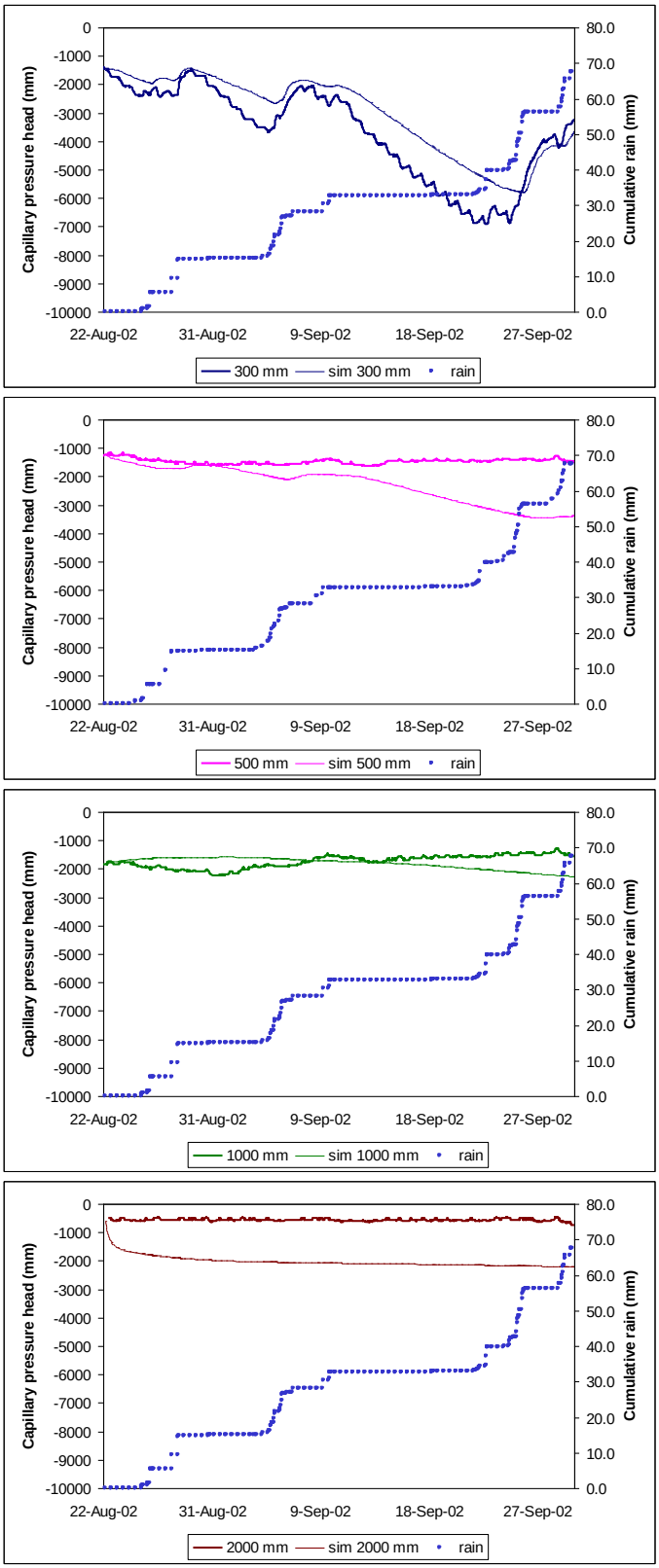

Figure E.2.1. Observed (bold) and simulated (light) tensions at Nest9 site at (from top) 100mm, 500mm, 1000mm and 2000mm below surface with cumulative rainfall (circles) from 22 August 2002 to 30 September 2002.

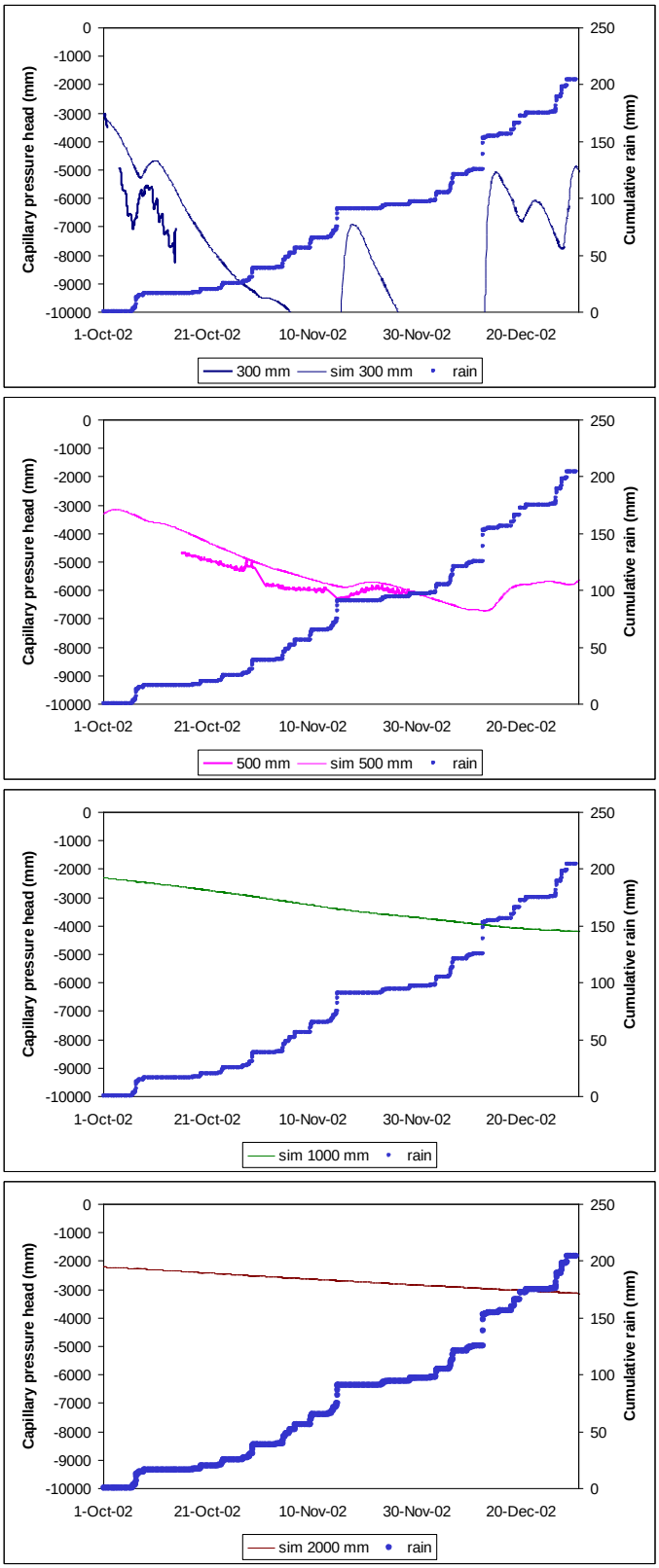

Figure E.2.2. Observed (bold) and simulated (light) tensions at Nest9 site at (from top) 100mm, 500mm, 1000mm and 2000mm below surface with cumulative rainfall (circles) from 1 October 2002 to 31 December 2002.

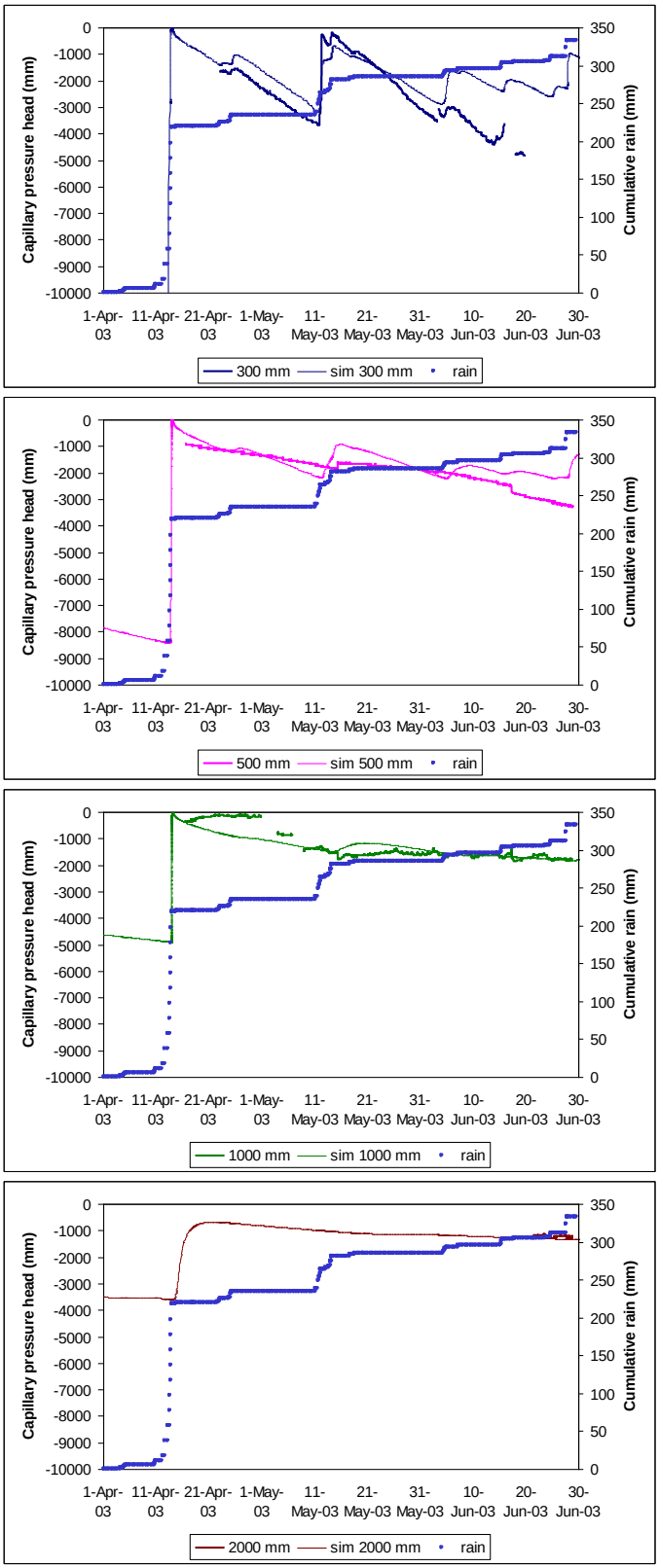

Figure E.2.3. Observed (bold) and simulated (light) tensions at Nest9 site at (from top) 100mm, 500mm, 1000mm and 2000mm below surface with cumulative rainfall (circles) from 1 April 2003 to 30 June 2003.

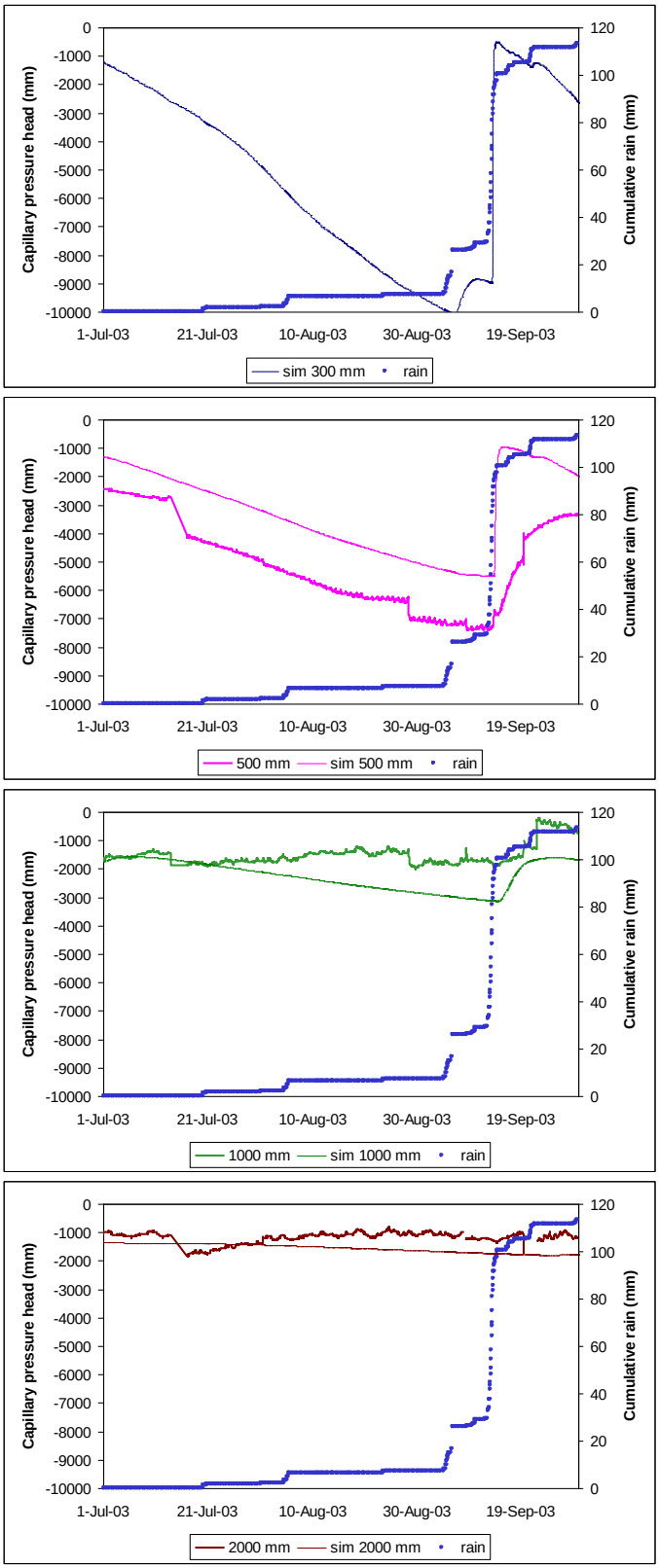

Figure E.2.4. Observed (bold) and simulated (light) tensions at Nest9 site at (from top) 100mm, 500mm, 1000mm and 2000mm below surface with cumulative rainfall (circles) from 1 July 2003 to 30 September 2003.

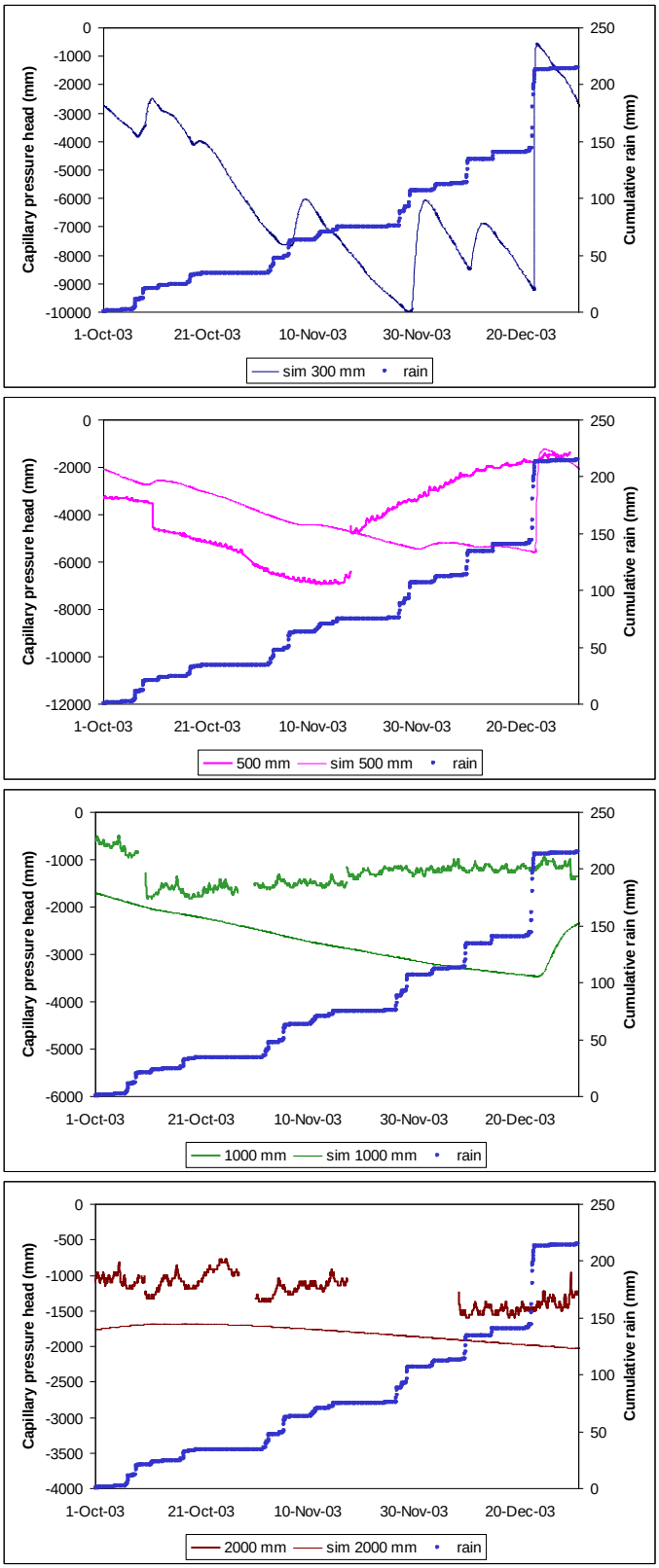

Figure E.2.5. Observed (bold) and simulated (light) tensions at Nest9 site at (from top) 100mm, 500mm, 1000mm and 2000mm below surface with cumulative rainfall (circles) from 1 October 2003 to 31 December 2003.

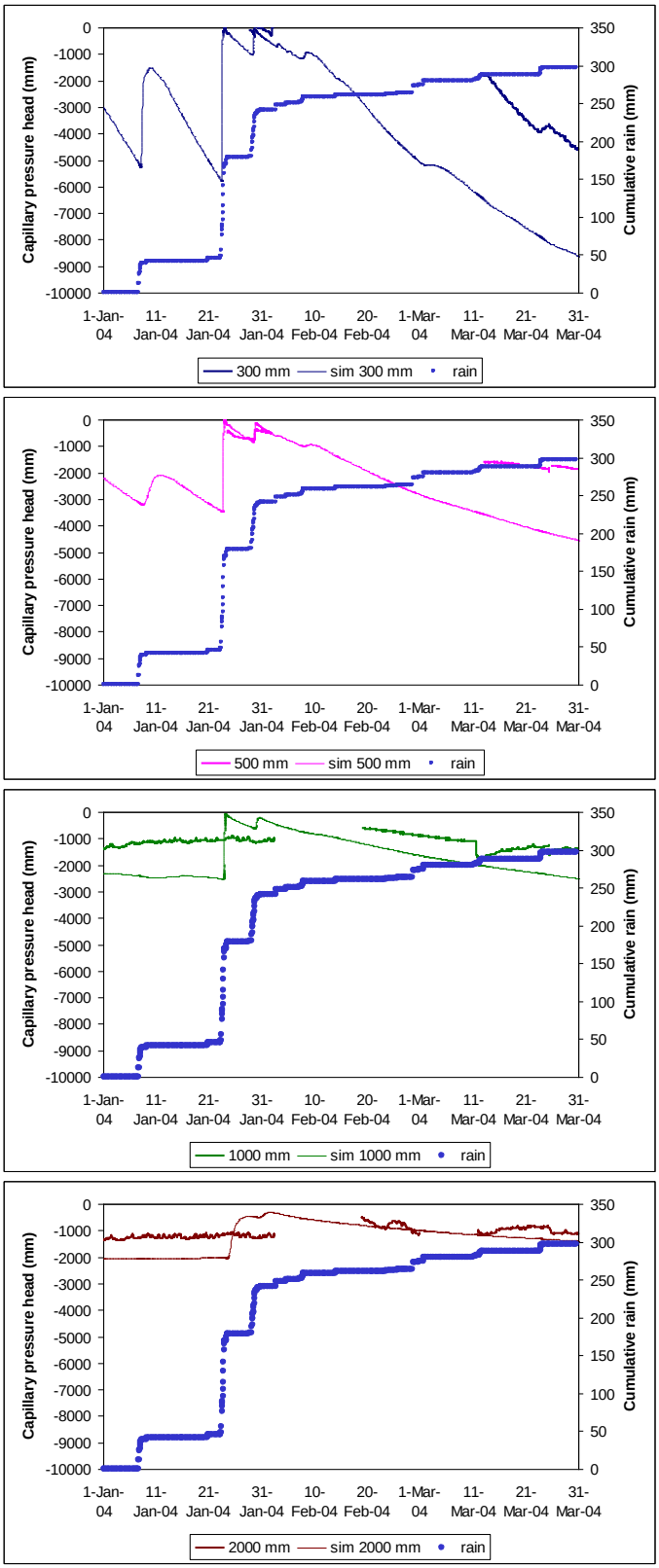

Figure E.2.6. Observed (bold) and simulated (light) tensions at Nest9 site at (from top) 100mm, 500mm, 1000mm and 2000mm below surface with cumulative rainfall (circles) from 1 January 2004 to 31 March 2004.

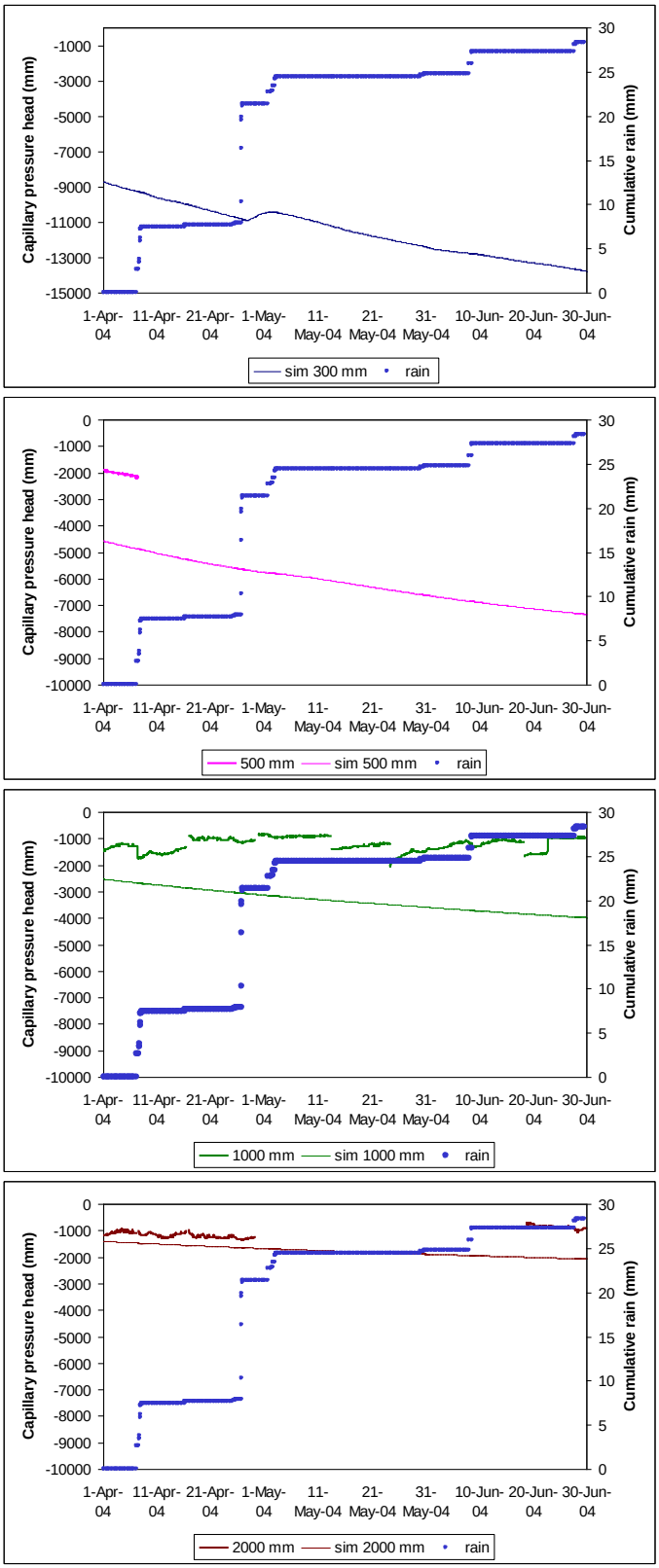

Figure E.2.7. Observed (bold) and simulated (light) tensions at Nest9 site at (from top) 100mm, 500mm, 1000mm and 2000mm below surface with cumulative rainfall (circles) from 1 April 2004 to 30 June 2004.

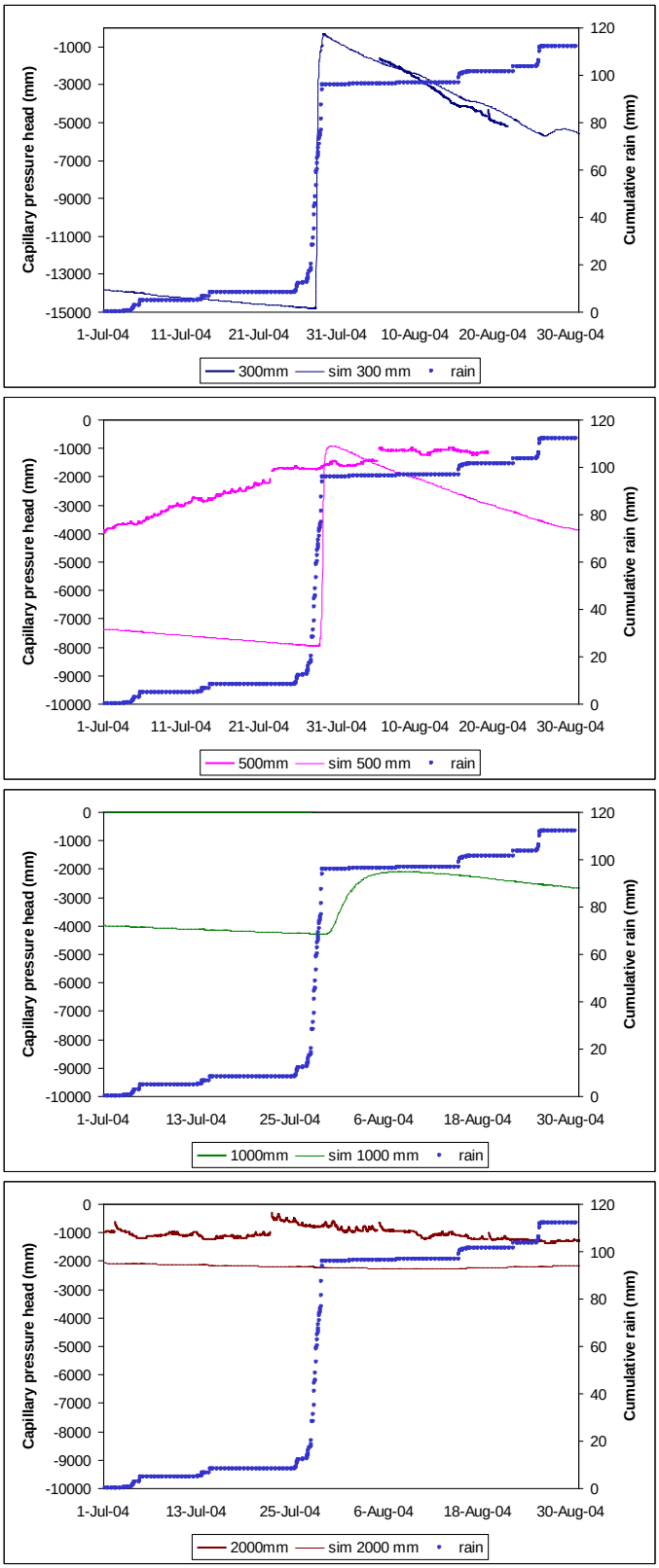

Figure E.2.8. Observed (bold) and simulated (light) tensions at Nest9 site at (from top) 100mm, 500mm, 1000mm and 2000mm below surface with cumulative rainfall (circles) from 1 July 2004 to 31 August 2004.

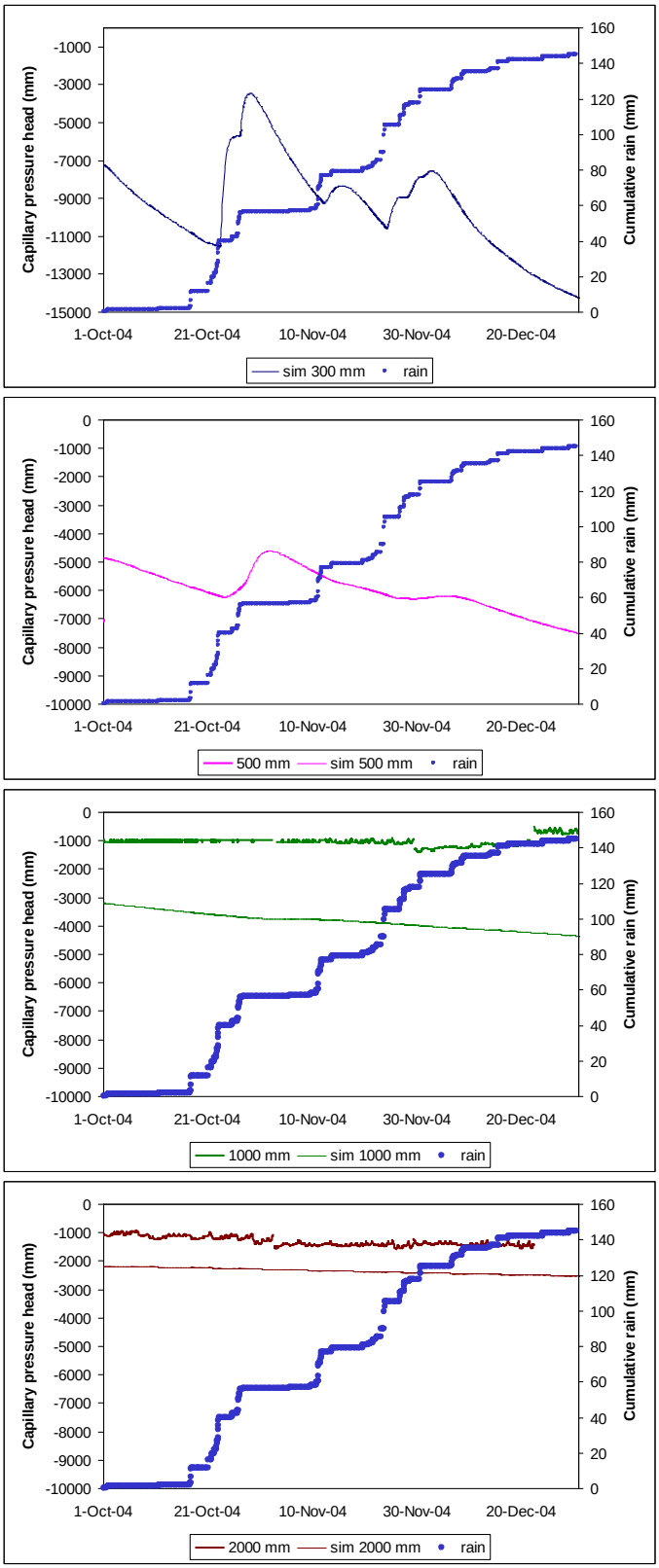

Figure E.2.9. Observed (bold) and simulated (light) tensions at Nest9 site at (from top) 100mm, 500mm, 1000mm and 2000mm below surface with cumulative rainfall (circles) from 1 October 2004 to 31 December 2004.

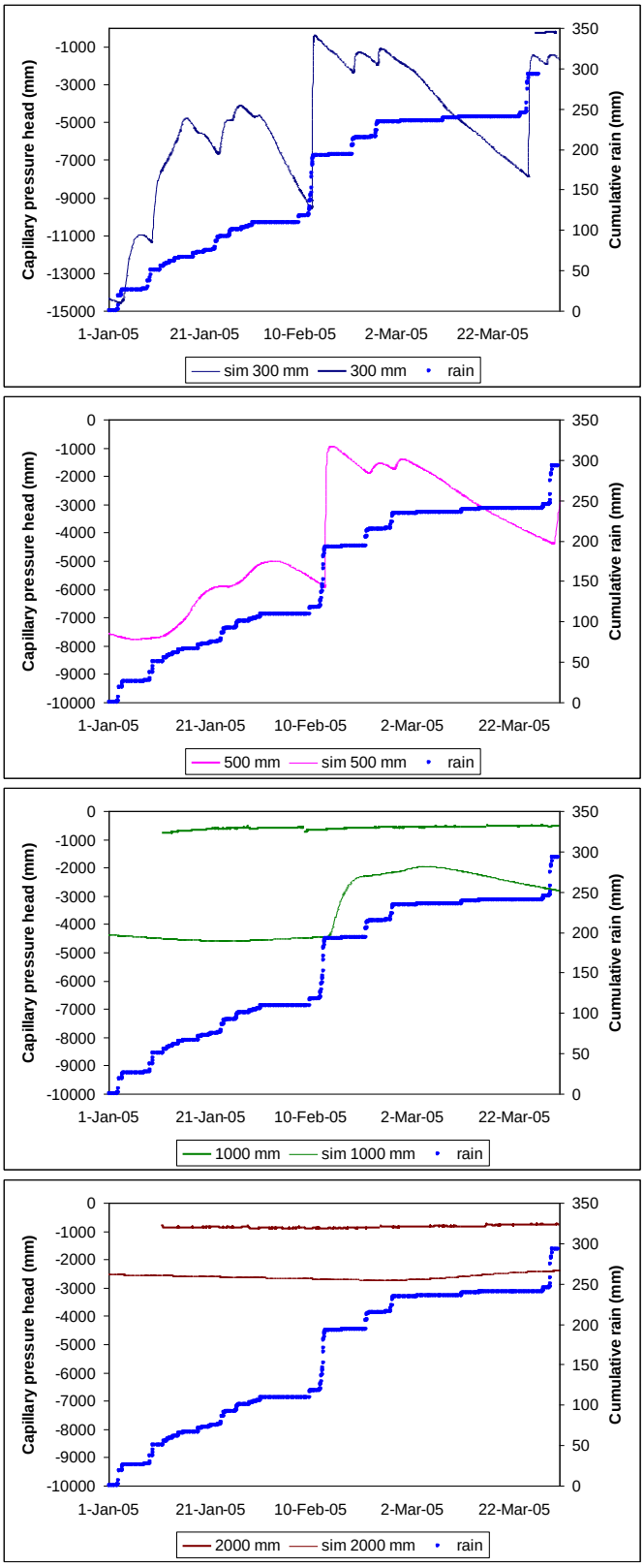

Figure E.2.10. Observed (bold) and simulated (light) tensions at Nest9 site at (from top) 100mm, 500mm, 1000mm and 2000mm below surface with cumulative rainfall (circles) from 1 January 2005 to 5 April 2005.

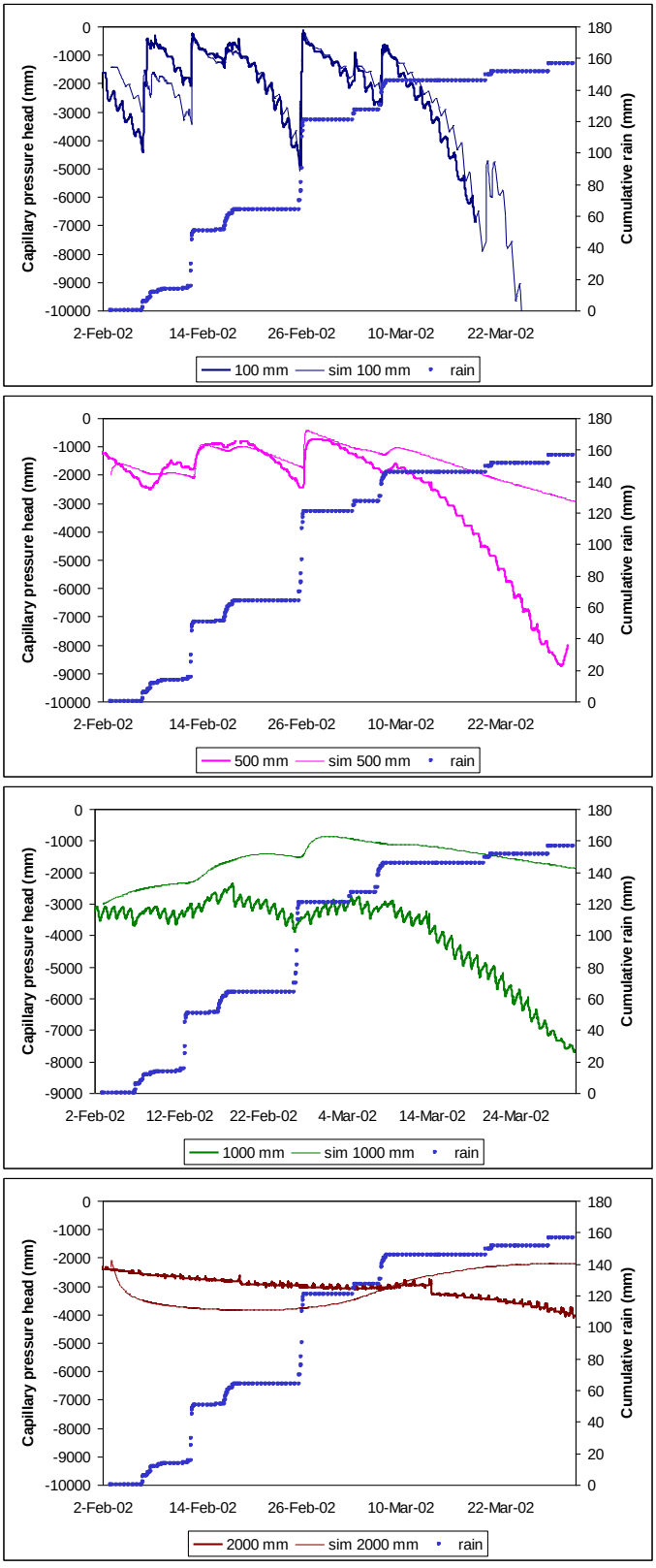

Figure E.3.1. Observed (bold) and simulated (light) tensions at the Bare site at (from top) 100mm, 500mm, 1000mm and 2000mm below surface with cumulative rainfall (circles) from 2 February 2002 to 31 March 2002.

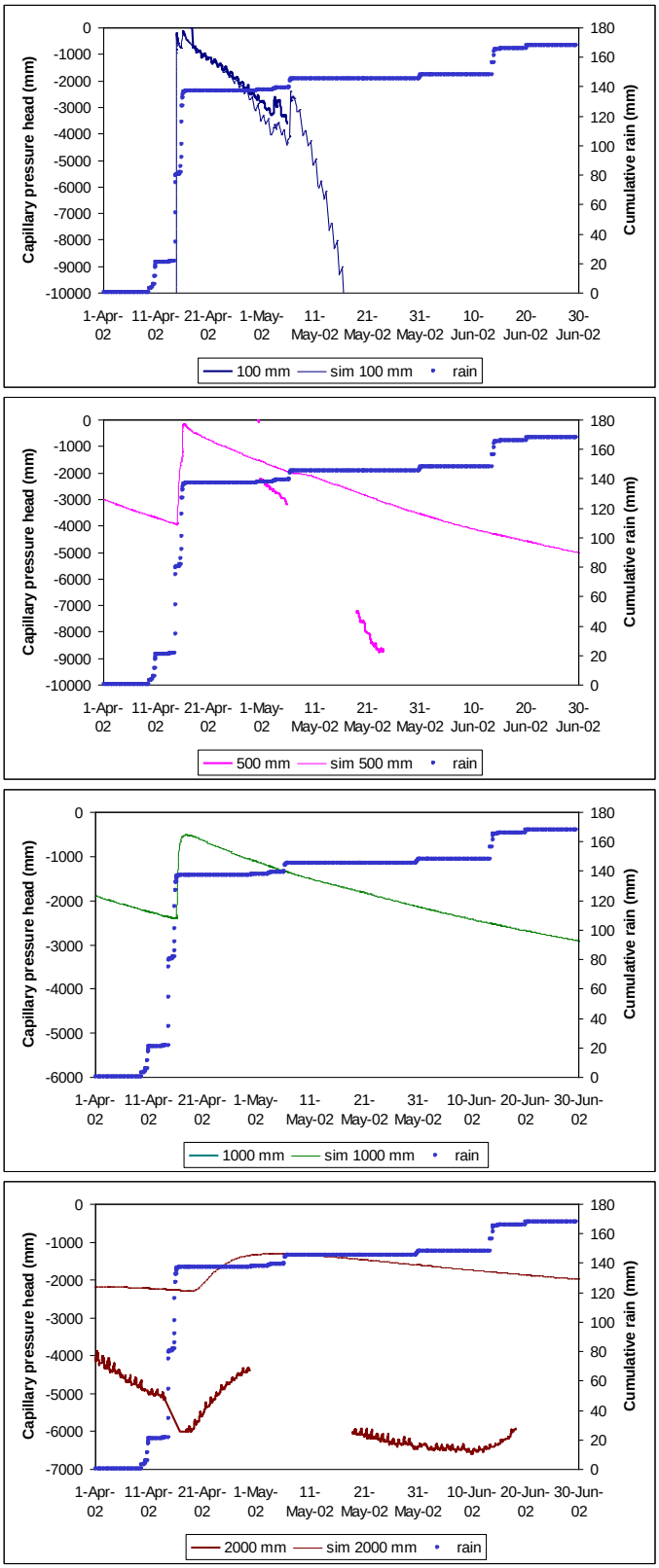

Figure E.3.2. Observed (bold) and simulated (light) tensions at the Bare site at (from top) 100mm, 500mm, 1000mm and 2000mm below surface with cumulative rainfall (circles) from 1 April 2002 to 30 June 2002.

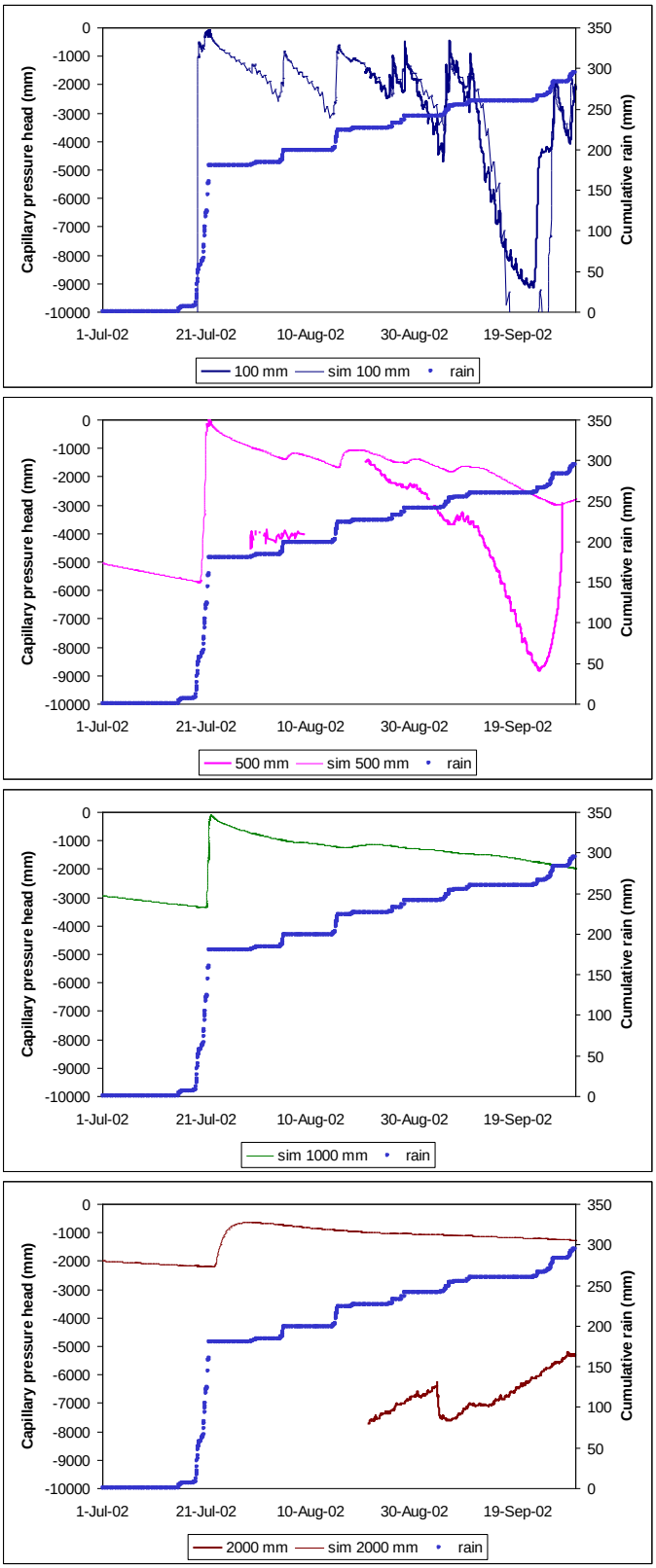

Figure E.3.3. Observed (bold) and simulated (light) tensions at the Bare site at (from top) 100mm, 500mm, 1000mm and 2000mm below surface with cumulative rainfall (circles) from 1 July 2002 to 30 September 2002.

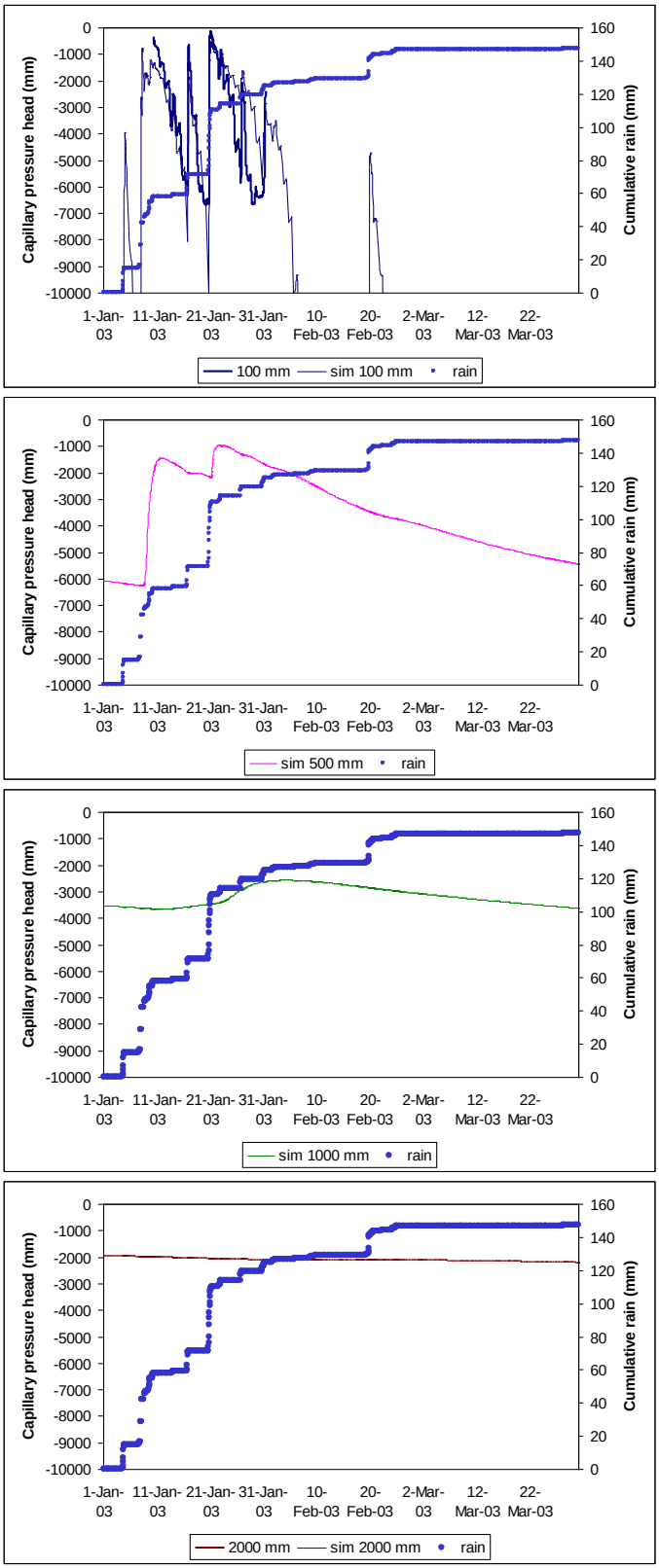

Figure E.3.4. Observed (bold) and simulated (light) tensions at the Bare site at (from top) 100mm, 500mm, 1000mm and 2000mm below surface with cumulative rainfall (circles) from 1 January 2003 to 31 March 2003.

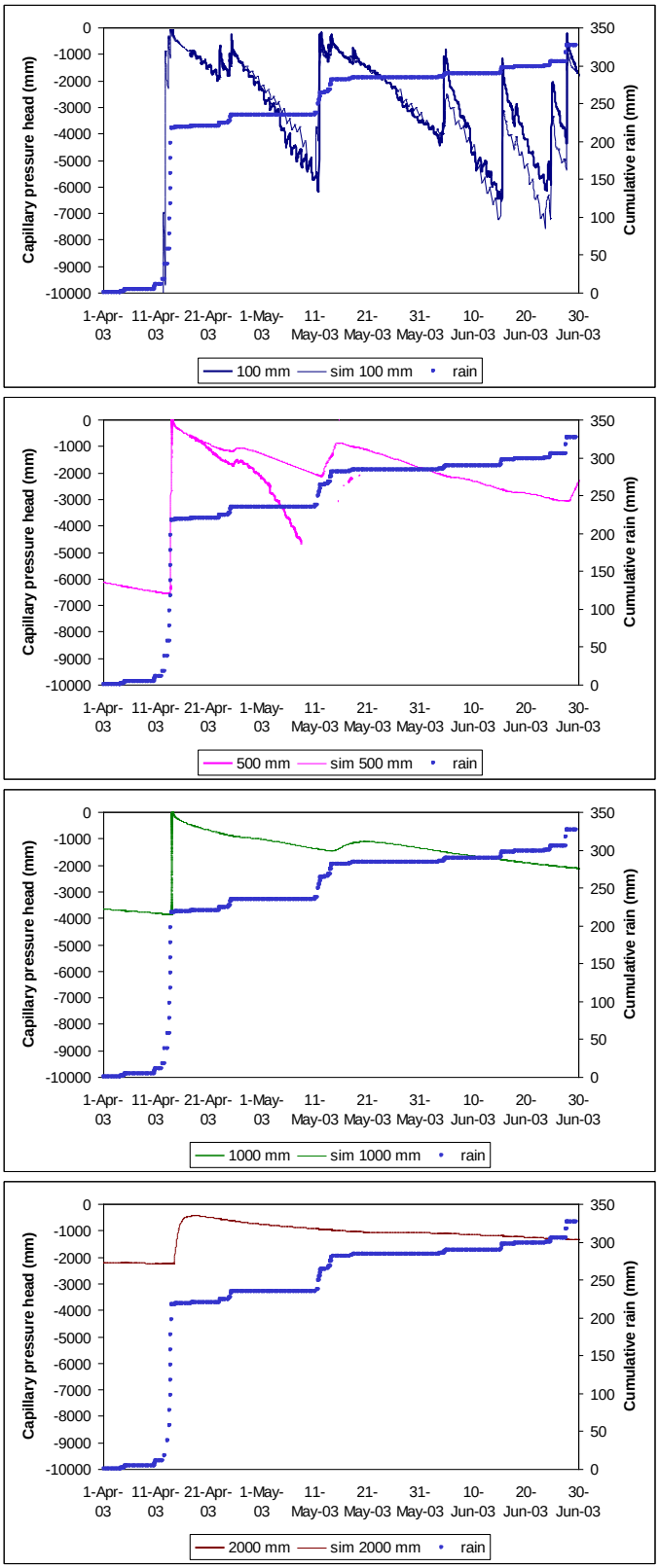

Figure E.3.5. Observed (bold) and simulated (light) tensions at the Bare site at (from top) 100mm, 500mm, 1000mm and 2000mm below surface with cumulative rainfall (circles) from 1 April 2003 to 30 June 2003.

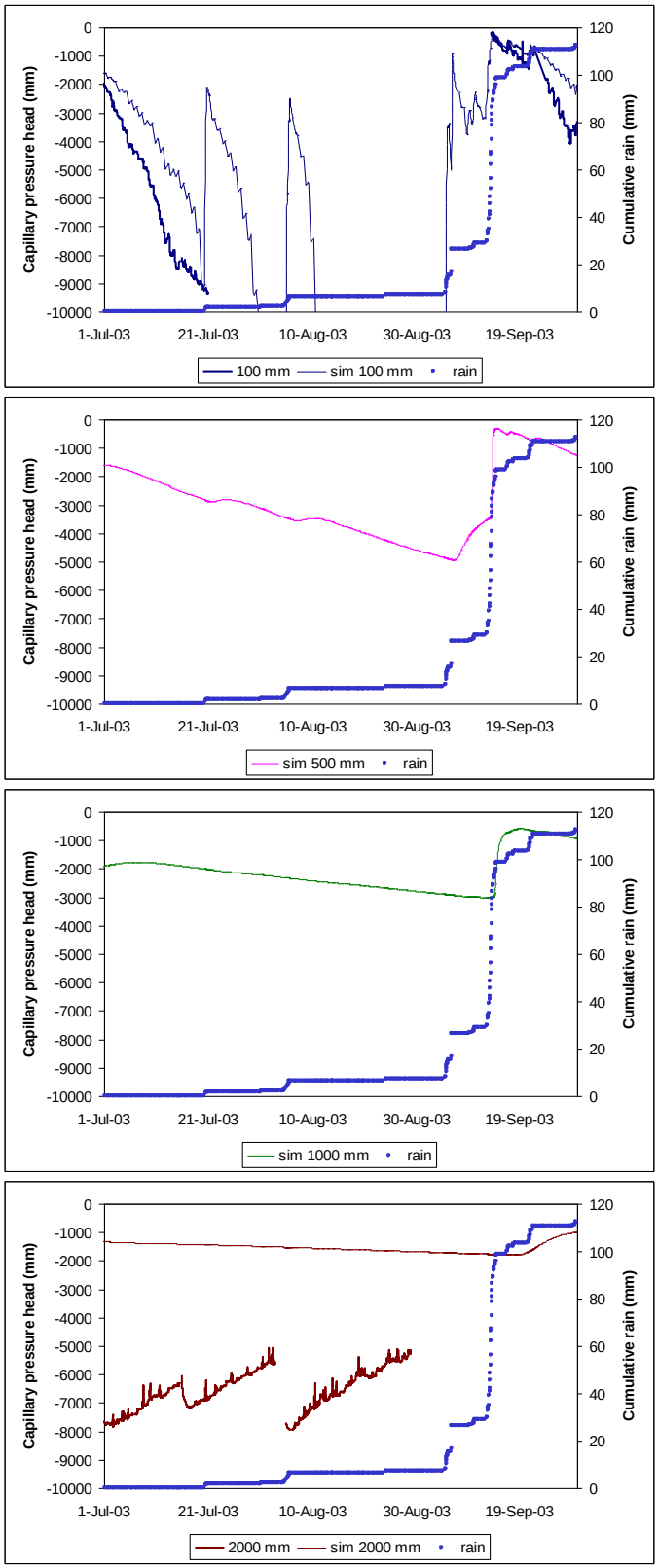

Figure E.3.6. Observed (bold) and simulated (light) tensions at the Bare site at (from top) 100mm, 500mm, 1000mm and 2000mm below surface with cumulative rainfall (circles) from 1 July 2003 to 30 September 2003.

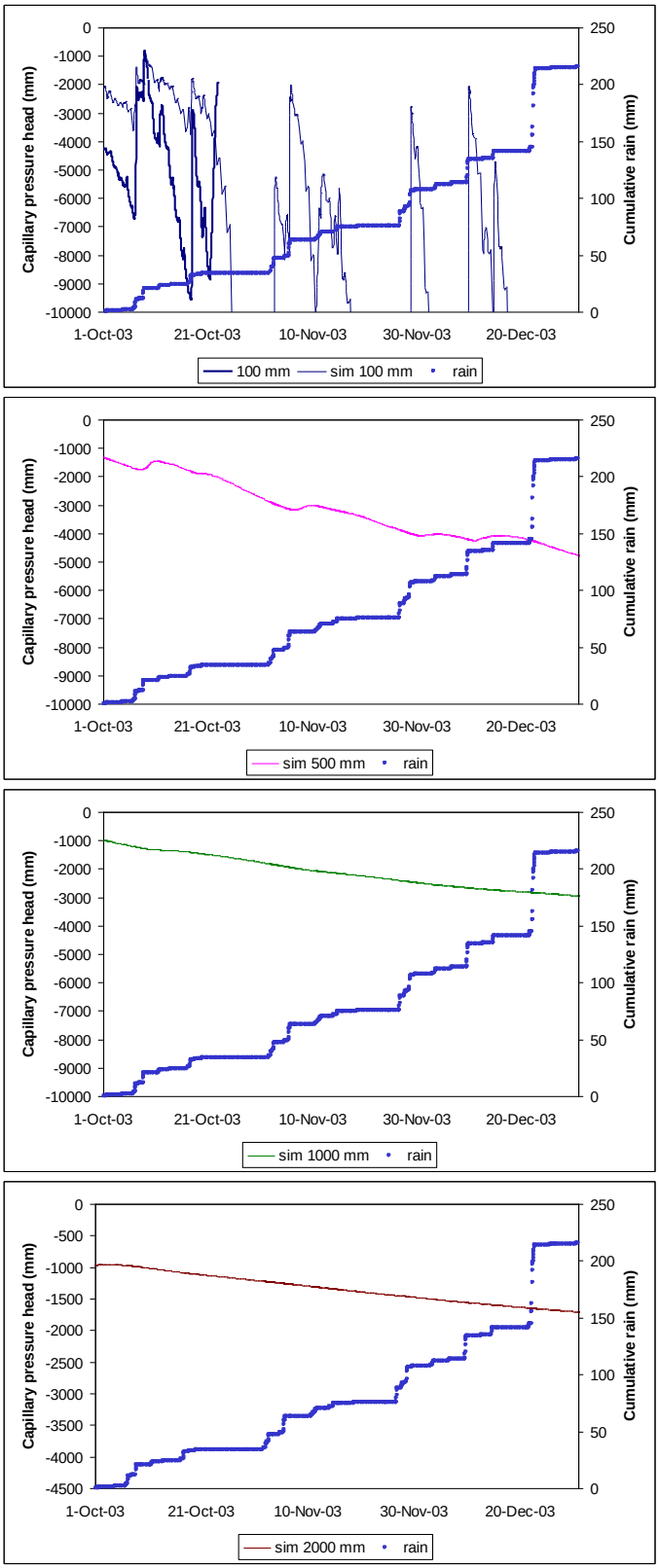

Figure E.3.7. Observed (bold) and simulated (light) tensions at the Bare site at (from top) 100mm, 500mm, 1000mm and 2000mm below surface with cumulative rainfall (circles) from 1 October 2003 to 31 December 2003.

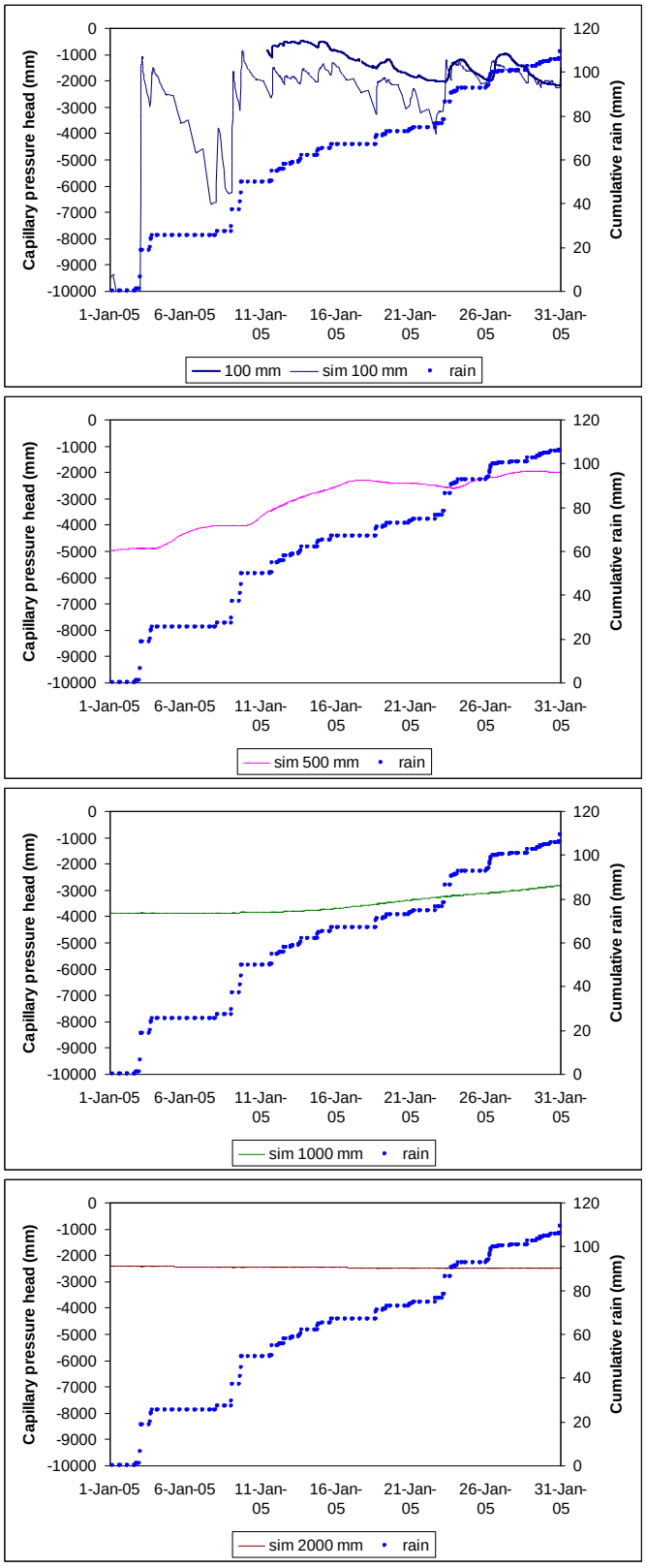

Figure E.3.8. Observed (bold) and simulated (light) tensions at the Bare site at (from top) 100mm, 500mm, 1000mm and 2000mm below surface with cumulative rainfall (circles) from 1 January 2005 to 31 January 2005.